DRAFT

Houston-Galveston-Brazoria Nonattainment Area Ozone Conceptual Model

May 2009

Prepared By: The TCEQ Data Analysis Team

Houston-Galveston-Brazoria Nonattainment Area
Ozone Conceptual Model

May 19, 2009

EXECUTIVE SUMMARY

The Houston-Galveston-Brazoria (HGB) area has made substantial progress in controlling its ozone pollution problem. While much has been accomplished in pursuit of attainment of the 1997 National Ambient Air Quality Standards (NAAQS) of 0.08 ppm, much work remains to achieve this standard, as well as the more stringent 2008 standard of 0.075 ppm. This appendix provides a detailed conceptual model which explains how, when, where, and why ozone forms in the Houston-Galveston-Brazoria area. Beyond that, it documents the large decreases in ozone and its precursors recorded over several years at monitors throughout the region, and then corroborates these findings through trend analyses, detailed investigations of emissions patterns across time and space, and extensive examination of background and transport phenomena.

Local ozone production in the HGB area peaks at the same time of year and for many of the same reasons as in other areas of Texas and the United States. However, the ozone season in Houston lasts longer than in many other areas. The HGB area also has a relatively high frequency of ozone exceedance days compared to the national averages, reflecting the persistent hot, sunny and relatively stagnant conditions associated with high pressure in the Gulf of Mexico during the summer as well as the large number of mobile, area and industrial sources in the area.

Ozone production is generally associated with relatively clear skies, light winds, abundant sunshine, and warm temperatures. Typically, these meteorological conditions are associated with high pressure areas that migrate across the U.S. during the summer season. However, the persistent summertime high pressure area in the Gulf of Mexico, and air mass flow reversals associated with the land/sea breeze phenomenon, make the Houston situation unusual, if not unique, among U.S. metro areas. High pressure areas have two characteristics that encourage ozone formation: light winds and subsidence inversions. Typically, winds circulating around a high pressure system are too weak to ventilate the urban area well, so local emissions tend to accumulate. Subsidence inversions cap the vertical mixing, further aggravating the situation by concentrating local pollutants near the surface.

Ozone formation in the HGB area has been associated with the daytime/nighttime flow reversal of the land/sea breeze, described above, which was identified as a cause during the 1993 Gulf of Mexico Air Quality Study and confirmed by several more recent studies by state and federal researchers. Land/sea breezes are common in coastal areas and have been associated with ozone formation in Athens, Greece and Barcelona, Spain as well as in the Houston area. Land/sea breeze flow reversal requires light synoptic scale forcing associated with high pressure areas, thereby allowing local phenomena to dominate the local circulations. Light winds and the restricted vertical mixing allow high concentrations of pollutants to accumulate during the night and morning hours, and the nocturnal land breeze carries the pollutants out over Galveston Bay and into the Gulf of Mexico. Then, during the afternoon, the sea breeze flow reversal carries the ozone back into the city. In contrast, on low ozone days, the precursor emissions are diluted and carried out of the area by the stronger and more persistent winds.

A number of other specific factors add considerably to the complexity of the HGB area situation. For example, the large cluster of petrochemical industries and other sources in the Houston Ship Channel emit NO_X along with a variety of VOC precursors not typically found in other urban areas. Oak forests near the city emit large amounts of isoprene, which reacts strongly with the NO_X emitted from these industries and numerous other anthropogenic sources in the area. When compared to local sources, background concentrations and transport issues appear to play a secondary, though not insignificant, role in the HGB area. However, transport issues are likely to grow in importance in the future as local emissions reductions continue.

Detailed investigation of these factors establishes the following findings:

The highest ozone concentrations and events in the HGB area appear to be driven by industrial emissions of ozone precursors – NO_X and highly-reactive VOC (HRVOC) – as well as by other local sources and meteorological conditions that facilitate ozone accumulation and transport across the city.

Over time, ozone concentrations in Houston have been decreasing, and, in some cases, substantially. This downward trend is confirmed by various analytical techniques. Collectively, these methods validate the downward trend in ozone over the past decade, and several of the methods provide statistically robust corroboration of these findings. Even when data are adjusted to account for inter-annual variations in meteorology, a statistically significant downward trend in concentrations is observed.

The decline in ozone concentrations is substantiated, in part, by sizeable and significant reductions in emissions of NO_X and HRVOC, in the HGB area. HRVOC concentrations attributable to industrial sources appear to be decreasing substantially. In spite of measured decreases in industrial emissions, industrial regions of the HGB area continue to appear linked to the highest ozone concentrations observed in the city.

While local meteorology plays a substantial role in ozone formation in the HGB area, the reductions observed in both ozone and precursor concentrations cannot be linked to deviations of meteorology from typical historical conditions. None of the predominant meteorological factors – solar radiation, wind speed, temperature, or relative humidity – were found to diverge sufficiently from typically observed ranges to account for the observed reductions in ozone and precursors.

Finally, background ozone concentrations do not appear to have changed in recent years. Studies have found neither an upward nor a downward trend, though more work is needed to fully establish the robustness of this tentative conclusion. Background ozone concentrations entering the HGB area are higher when transport winds are very light and when the transported parcels originate from the northeast. In the former case, recirculation of local emissions and ozone is a strong possibility. In the latter case, the northeasterly winds appear to carry higher levels of background ozone into southeast Texas from the midwest and southeast U.S. However, neither direction nor velocity of transport winds was sufficient to explain the observed decreases in measured local ozone concentrations.

TABLE OF CONTENTS

LIST OF TABLES

LIST OF FIGURES

CHAPTER 1: OZONE FUNDAMENTALS

Ozone formation conceptual models characterize ozone trends, precursors, formation, and transport in a particular geographic area, to explain the dynamics of ozone formation in that area. This information is compiled and developed into a comprehensive picture of not only where and when ozone forms, but also how and why ozone forms in a geographic area. Conceptual models are required by the U.S. Environmental Protection Agency (EPA) to accompany ozone photochemical modeling performed for State Implementation Plans (SIP). This appendix updates the ozone conceptual model for the Houston-Galveston-Brazoria (HGB) nonattainment area.

Conceptual models can be used as tools for selecting representative modeling episodes and for qualitatively evaluating and assessing photochemical modeling results. They are intended to guide modeling efforts conducted in compliance with SIP requirements by presenting the state of the science in terms of our understanding of factors that influence ozone formation and transport. This document begins with a discussion of the fundamentals of ozone photochemistry and meteorology, followed by recent findings in ozone formation, transport and fate in the HGB area, along with results of detailed investigations of trends and patterns in local precursor emissions, meteorological factors, and background ozone transport. All of these investigations point to the same general conclusion: decreasing trends in measured ozone concentrations are largely a result of real, quantifiable reductions in precursor emissions, and are not due to unusual meteorological conditions.

This conceptual model begins with a discussion of the fundamentals of ozone formation photochemistry, followed by more detailed treatment of the characteristics that make the ozone situation in the HGB area unique, and, thus, more intractable. Annually, the HGB area experiences more days on which ozone measured in the ambient air exceeds healthy levels, than any other area in Texas. Ozone formation in the HGB area is extremely complicated due to the variety and magnitude of industrial emissions, the large population, and the complexity of meteorological conditions.

1.1 BASIC OZONE FORMATION PHOTOCHEMISTRY AND METEOROLOGY

Tropospheric, or ground level, ozone pollution is a public health concern in many metropolitan areas throughout the United States (National Academy of Sciences, 1991; Bell, 2004, EPA, 2006). Other studies have linked ozone to damage to vegetation (Heck, 1984; Westenbarger and Frisvold, 1994) and other materials. Ozone production is generally associated with relatively clear skies, light winds, abundant sunshine, and temperatures above 80 to 85 degrees Fahrenheit. Typically, these meteorological conditions are associated with high pressure areas that migrate across the U.S. during the summer season.

Large urban areas are prone to generating elevated levels of ozone in the ambient air because of a confluence of contributing factors: the presence of millions of people, the presence of a vast multitude of emissions sources that serve and employ that population, and meteorological conditions favorable to the formation of ozone from those emissions. Substantial amounts of precursor compounds, chiefly nitrogen oxides (NO_X) and volatile organic compounds (VOC), are emitted by mobile sources, including cars, trucks, ships, planes, locomotives, and construction equipment; area sources, such as gas stations, dry cleaners, fertilizer application, and personal care products; and point sources, notably petrochemical facilities and electricity generation facilities. Other sources include biogenic emitters (mainly trees), and precursor compounds (along with ozone) transported into an urban area from external locations, and the continental background of ozone and precursors.

Ozone consists of a molecule of three oxygen atoms, expressed chemically as O_3, and is created from oxygen, NO_X and VOC in the presence of sunlight. NO_X is a shorthand term for the combination of NO and NO_2 in the atmosphere. The catalytic cycle of ozone formation and destruction is displayed in Figure 1-1. This diagram shows that in the presence of ultraviolet

energy from sunlight, denoted by the term "hν," NO_2 reacts with ordinary oxygen to form ozone and NO. In the absence of sunlight, the process reverses and is known as ozone titration, or "scavenging." NO from the first step feeds into the second step, while NO_2 from the second step feeds back into the first step.

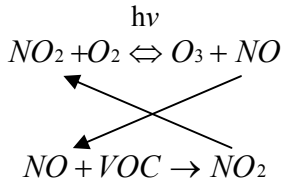

This reaction runs forward in sunlight, and reverses in the dark.

Figure 1-1: Chemical Reactions that Form Ozone
The first reaction usually operates forward in sunlight and reverses in the dark. Note, however, that even in sunlight, it may reverse immediately downwind of a very large NO_X source.

Certain types of highly-reactive VOC (HRVOC), the light alkenes, have been found to play a major role in forming ozone. HRVOC react more quickly with sunlight to form radicals that contain unpaired electrons, which accelerate the ozone formation process (Ryerson et al., 2003; Daum et al., 2003, 2004; Kleinman et al., 2002, 2005; Wert et al., 2003; Czader et al., 2008). HRVOC recycle NO_X, while ordinary VOC recycle radicals. NO_X recycling speeds up the process of ozone formation and accumulation. Figure 1-2 details some types of HRVOC radicals and shows the points in the ozone formation cycle where these radicals participate.

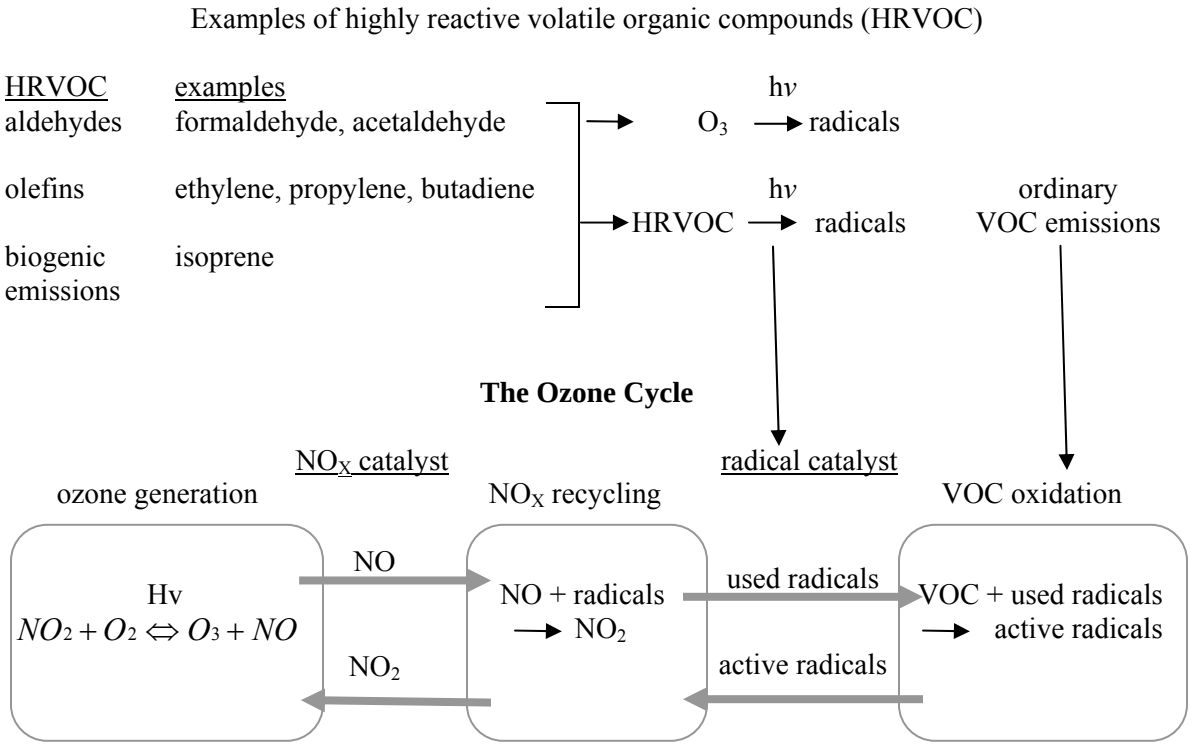

Figure 1-2: The Ozone Cycle with Examples of HRVOC Species
Radicals from HRVOC participate in ozone formation by catalyzing the NO_x cycling process in the presence of sunlight (hν). Ordinary VOC emissions operate through the oxidation process to recharge used radicals that then react with NO to form NO_2.

The chemical reaction that forms ozone stops when it runs out of either of the reactants: NO_X or VOC. If the reactant in short supply is NO_X, the area is said to be "NO_X limited" because no further ozone is created even though excess VOC might remain. Similarly, when the ozone reaction stops due to a lack of VOC, the area is termed "VOC limited." Some areas may be both

NO_X and VOC limited at different times of the day, depending on wind direction and the amounts of NO_X and VOC, both in the ambient air and transported from upwind emissions sources. Winds from one direction may direct emissions from a NO_X source over the area, while winds from a different direction may direct VOC emissions over the area. Therefore, consideration of changes in wind patterns, along with types and locations of emissions sources, is essential in formulating effective policies to control ozone formation and accumulation.

Because precursor compounds, NO_X and VOC, also exist under natural conditions, ozone is created and destroyed on a natural cycle according to atmospheric chemical conditions, even in the absence of additional anthropogenic, or human, precursor sources. This natural ozone formation is known as "background" ozone and is the starting point for measuring the contribution of ozone and precursors attributable to human activity. Within an urban area, not all ozone is necessarily due to emissions produced locally because anthropogenic precursors, along with ozone formed by them, are often transported over long distances. This type of ozone is termed "transport" ozone and is sometimes aggregated with natural background ozone when referring to ozone that is not produced locally.

Figure 1-3 shows that ozone formation occurs in a daily, or diurnal, cycle, starting from low levels before sunrise, increasing during the morning and into the afternoon, then declining to low (background) levels again after nightfall. Each morning, emissions of NO_X and VOC begin to mix with precursors remaining from the previous day. As the sun heats the atmosphere, providing energy in the form of light photons, this mixture begins to form ozone. As the energy of the sun dissipates in the evening, the process slows and finally halts overnight.

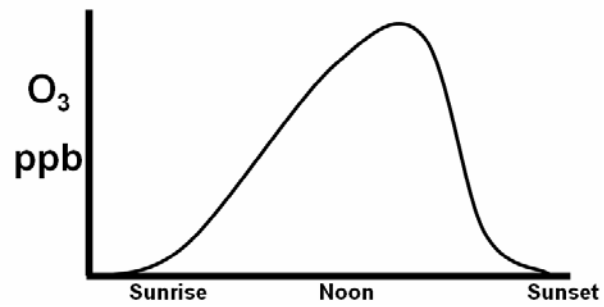

Figure 1-3: Typical Diurnal Ozone Cycle

At locations downwind of a major NO_X source, such as depicted in Figure 1-4, there may be initial scavenging of ozone due to high levels of NO_X, near the source. However, with additional time and sunlight, the NO_X is gradually converted to additional ozone, resulting in even higher ozone concentrations farther downwind from the source (EPA, 2006). In Figure 1-4, note the initial spike in NO_X emissions (blue line) near mile zero and the corresponding drop in ozone (dark red line) soon after. Even though NO_X has dropped precipitously by about mile eight, ozone soon rebounds from its nadir and begins accumulating.

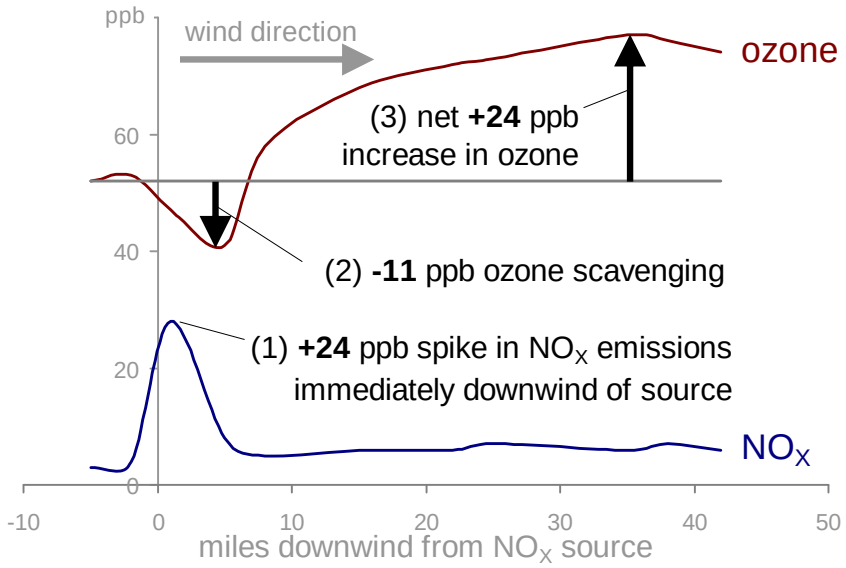

Figure 1-4: Example of Ozone Scavenging Downwind of a NO_X Source
(1) An initial injection of NO_X emissions from a NO_X source quickly (2) reduces ambient ozone through scavenging. This reduction is later offset by (3) greater ozone production further downwind.

Meteorological conditions, such as wind direction and speed, temperature, mixing height, solar radiation and other factors, affect the rates at which ozone formation and scavenging reactions occur. Net reactivity of precursor compounds found in a plume of emissions is affected by the type, as well as the concentration, of precursors present. Concentration is determined by the quantity of emissions and volume of well-mixed air, which in turn is determined by the speed of winds and the mixing height. Mixing height, determined by temperature and other factors, forms an atmospheric "ceiling" on the available volume of air in which mixing can occur (Figure 1-5).

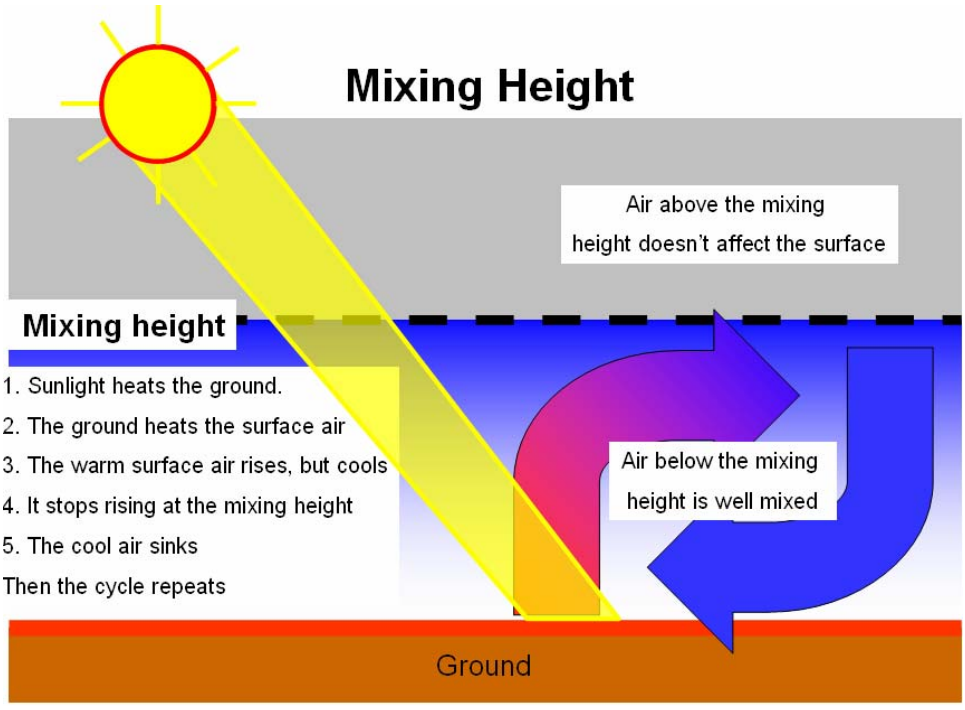

Figure 1-5: Example of Dynamics of Atmospheric Mixing Height
During daylight hours, sunlight heats the ground, which in turn heats surface air. Warm surface air rises and cools until it reaches the mixing height, where the relatively cooler air sinks downward. The cycle repeats until sundown.

For a fixed mass of precursor emissions, a lower mixing height results in a smaller volume of air than does a higher mixing height. This gives a more concentrated, and thus more reactive, air parcel. A higher mixing height dilutes the precursors into a larger volume, thus resulting in a less reactive parcel (Figure 1-6).

Mixing height is known to vary by time of day over land, but is fairly constant over water bodies, such as Galveston Bay and the Gulf of Mexico (Senff, et al., 2002). As temperatures over land rise during the day, the mixing height rises so the volume of air available for diluting precursors and ozone expands. During the afternoon, sea breezes contribute to mixing and transport over land. These breezes are caused by the temperature differentials between the land and water areas that carry cooler maritime air inland over relatively hotter land areas.

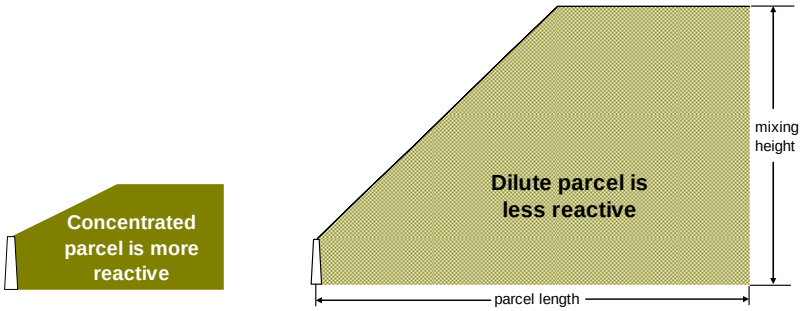

Figure 1-6: Effect of Mixing Height on Parcel Concentration
A lower mixing height maintains a more concentrated parcel of ozone and precursors, while a higher mixing height provides a greater volume of air and a more dilute parcel.

Besides affecting wind patterns, large bodies of water can affect local meteorology by affecting the temperature of the ambient air and, thus, the mixing height of the atmosphere (Nielsen-Gammon, et al., 2007). A low mixing height over water tends to constrain emissions within a smaller volume of air, which keeps them concentrated. Sea breezes can also cause stagnation of air over sources; circular wind patterns can redirect plumes back over sources for additional injections of emissions. The difficulties in measuring and modeling sea breeze direction and timing are considerable.

The interplay of different atmospheric layers due to heating and cooling air influences the behavior of winds at the surface, where most ozone is formed. Warmer air rises, while cooler air sinks. This sinking is known as "subsidence" and it is a driving force in atmospheric dynamics. As cooling air falls, it fans out in multiple directions at the location of the subsidence, which is often hundreds of miles across (Banta et al. 2005). When this occurs at a distance from the region, local wind appears to be a persistent breeze coming from the center of the subsidence.

However, when the subsidence occurs locally, local winds may be propelled in a multitude of directions, depending on the strength of opposing air masses. Locally occurring subsidence often leads to stagnation and mixing that enhances ozone formation.

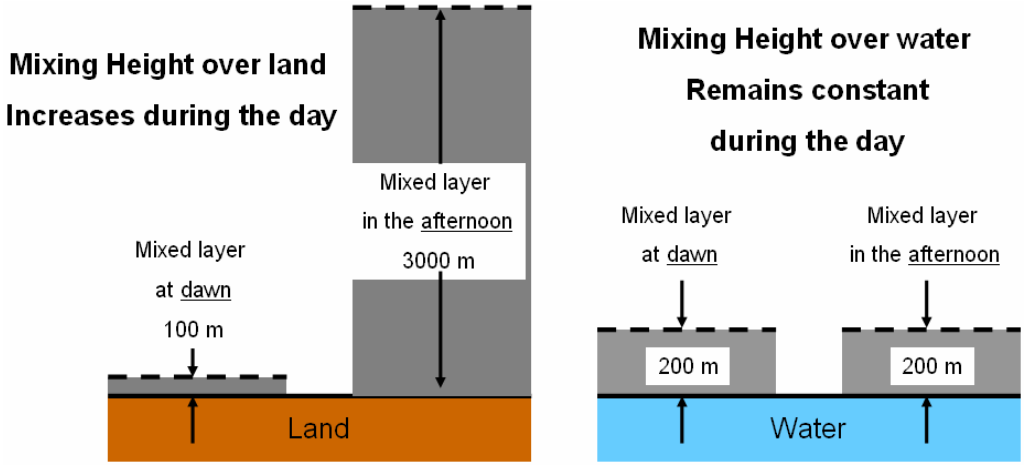

Figure 1-7: Example of Mixing Height Over Land and Water
Mixing height often varies over land (left) but is fairly constant over water (right). This is a general example. Mixing height in the HGB area has been found to be fairly constant at roughly 500 meters.

In coastal zones, wind dynamics are complicated by the additional factor of the water body. Because atmospheric temperatures over water are less variable than over land, the diurnal pattern of rising and falling air masses tends to be more pronounced over land than over water. Figure 1-8 displays this dynamic. As the sun heats the atmosphere over land during the day, convection currents of rising air are generated. This air flows back out over the water body at higher levels in the atmosphere, displacing the air over the water, which is relatively cooler and sinking. The cooler air over water at the surface mobilizes to replace the rising air over land, creating the familiar sea breeze that blows inland.

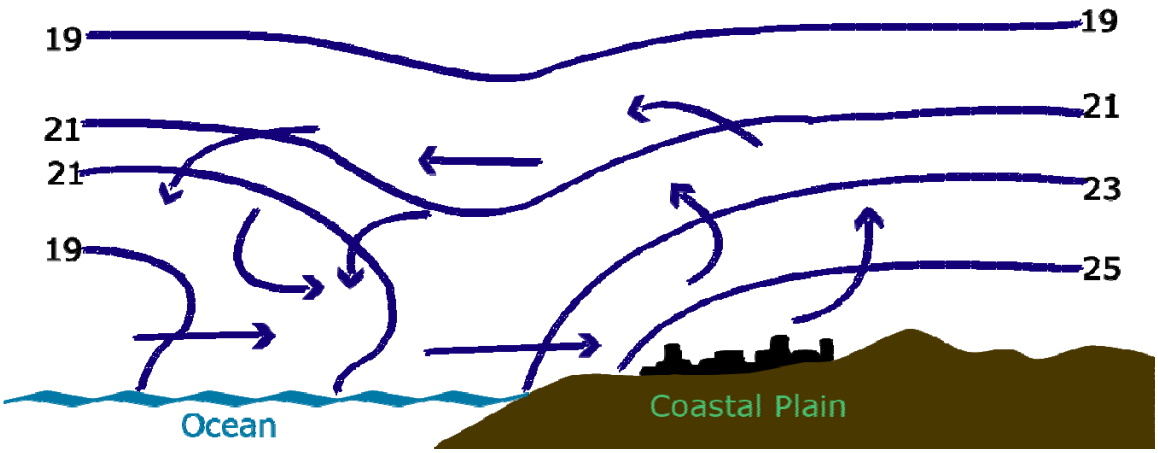

Figure 1-8: Example of Wind Dynamics in a Coastal Zone
Numbered curves denote air temperature isopleths in ^{o}C. Warming air over land rises and is displaced by cooling and sinking air over the water. The sinking air phenomenon is known as "subsidence" and results in a persistent breeze from the water toward the land during the day. In the evening, when the sun sets, this flow reverses as air over land cools faster than air over water.

Daytime subsidence over water reverses during the night, when the subsidence occurs over land because land cools faster than water. The daytime sea breeze tends to be stronger than the nighttime reverse breeze, due to lower friction as air moves over water, compared to friction over land masses. Understanding this land-sea breeze dynamic and flow reversal is important to understanding ozone formation, transport, and fate in the HGB area.

1.2 OZONE FORMATION IN THE HOUSTON-GALVESTON-BRAZORIA AREA

Although ozone in the HGB area peaks at roughly the same time of year as other areas of Texas and the U.S., the ozone season in Houston is of longer duration than most other areas, effectively spanning the entire year (Davis et al., 1998). During the ozone season, and especially in late summer, Houston experiences relatively light winds and persistent hot, humid, and sunny conditions. Late summer peak ozone concentrations in the HGB area also tend to be higher than other areas (Figure 1-9). While the basic factors that contribute to ozone formation are abundant in the HGB area, the area is unusual among U.S. urban areas by virtue of its large population, extensive petrochemical industry, major port facilities, and subtropical coastal meteorology.

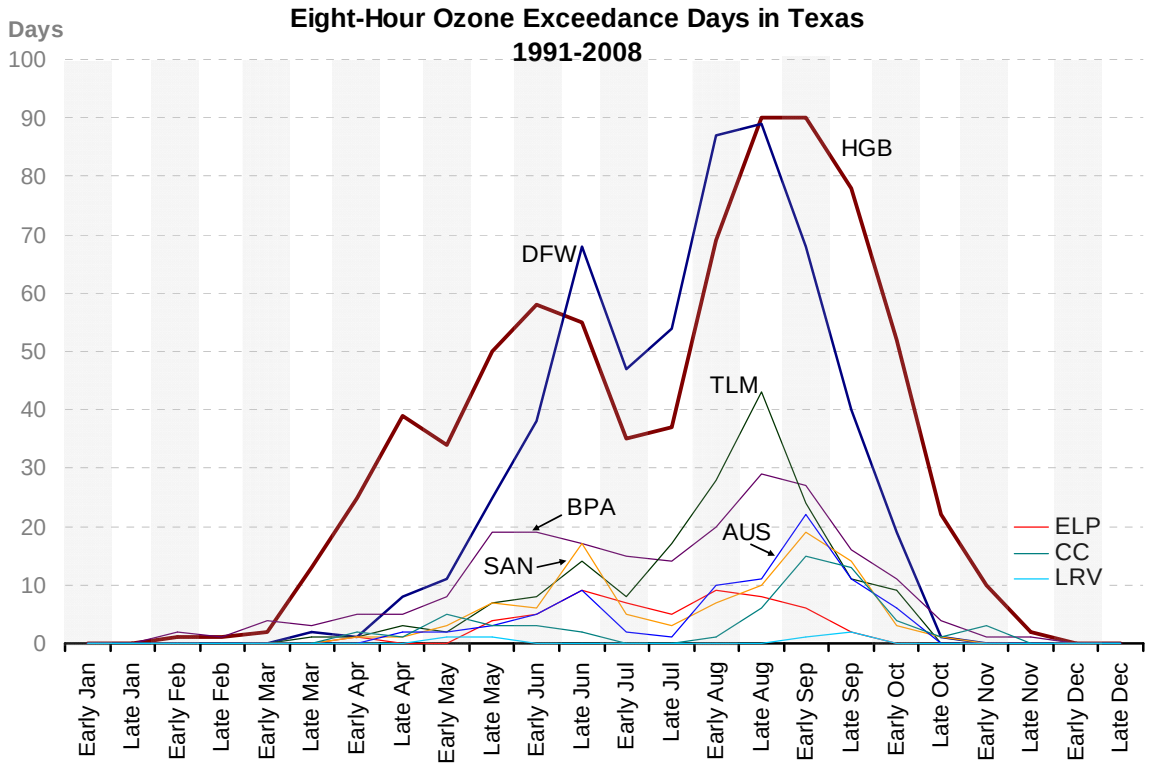

Figure 1-9: Eight-Hour Ozone Exceedance Days in HGB and Other Areas of Texas

An exceedance day is any day when an exceedance of the eight-hour ozone NAAQS is measured in an area. Note that the HGB area experiences more exceedance days throughout the year than any other area of Texas, starting in early March and extending through late November. The ozone season in the HGB area encompasses all twelve months of the year. HGB also records two peaks, one in late spring and another in late summer. AUS = Austin; BPA = Beaumont-Port Arthur; CC = Corpus Christi; DFW = Dallas-Fort Worth; ELP = El Paso; LRV = Lower Rio Grande Valley; SAN = San Antonio; TLM = Tyler-Longview-Marshall.

1.2.1 Emissions Sources

The HGB area is the sixth largest metropolitan area in the U.S., home to nearly 5.6 million residents as of 2007 (U.S. Census Bureau, 2009). These residents own and use motor vehicles, recreational vehicles, lawn and garden equipment, and other emission sources in their daily activities. They work, shop, and recreate at a multitude of commercial, industrial, educational, and recreational sites that contribute emissions from all manner of equipment, including furnaces, compressors, ovens, heaters, and more.

Lying due east of downtown Houston, the Port of Houston is an enormous international trading hub, hosting shipping vessels from all over the world, as well as harbor craft such as barges and tug boats, equipment such as cranes and forklifts that service those ships, and trucks and trains that transport goods to and from the port. These vessels, vehicles, and equipment require vast amounts of motive power, provided by motors and engines that emit sizeable quantities of ozone precursors.

The distinctive history of Texas as a petroleum producing region is evident in the colossal scale of the local petrochemical industry, and its associated refining facilities. These facilities contain a variety of types of processing equipment, such as tanks, catalytic crackers, distillation towers, flares, pumps, and mile upon mile of piping, valves, hatches, flanges, and other apparatus, all of which have the potential to emit ozone precursors, especially if not maintained in satisfactory condition. Although the Houston Ship Channel is among the most, if not the most, comprehensively regulated industrial zones in the world, permitted emissions alone, not to mention upsets and undetected leaks, from an industry of this size would dwarf emissions of many cities.

Even the natural environment of east Texas contributes to degraded air quality in the HGB area. Oak forests and other vegetation located near the city emit large amounts of isoprene and other biogenic compounds. These VOC, react particularly quickly with NO_X to form ozone (TexAQS II RSST, 2006).

Background ozone concentrations in southeast Texas average about 50 ppb, with higher concentrations observed when winds originate from the continental U.S., and much lower concentrations observed when winds originate directly from the Gulf of Mexico (Nielsen-Gammon et al., 2005a). Background and transport appear at this time to play a secondary, though not inconsequential, role in HGB ozone photochemistry, at least when compared to local sources. However, these sources may contribute a greater fraction of the total in the future as local emissions reductions are implemented.

1.2.2 Highly Reactive Volatile Organic Compounds

Elevated emissions of ozone precursor compounds emanate from industrial and petrochemical facilities located throughout the region, but the highest concentrations originate predominantly along the Houston Ship Channel. In this region, distinctive photochemistry is observed. Elevated concentrations of HRVOC are co-emitted with NO_X from industrial facilities. This combination leads to substantial and rapid ozone production in periods as short as one hour. Other urban areas in the U.S. typically observe ozone accumulation over much longer periods, from an entire day up to several days. In fact, the HGB area is marked by some of the highest ozone production rates routinely encountered in the U.S. (Kleinman et al., 2002). The rate of ozone production observed in this area is two to five times greater than other less industrialized cities and can exceed 100 parts per billion (ppb) per hour (Kleinman et al., 2002). Furthermore, ozone production in the HGB area can vary significantly over small spatial scales. Ozone concentrations may vary by 50 ppb or more over distances as small as a few kilometers (Kleinman et al., 2002; Ryerson et al., 2003). The unique ozone formation chemistry in the HGB area atmosphere, specifically in the Houston Ship Channel region, places demands on chemical mechanisms not encountered in other regions.

In areas in and around the Houston Ship Channel, and even farther afield, such as Mont Belvieu, Texas City, and Brazoria County, high concentrations of HRVOC such as propene, ethene, 1,3-butadiene and butenes have been observed (Ryerson et al., 2003; Daum et al., 2003; Daum et al., 2004; Berkowitz et al., 2004; Berkowitz et al., 2005; Kleinman et al., 2002; Kleinman et al., 2005; Jobson et al., 2004; Karl et al., 2003; Buzcu and Fraser, 2006; Xie and Berkowitz, 2006, 2007; Kim et al., 2005). Historical analyses of routinely-collected VOC data indicate that HRVOC compounds are present in high concentrations on a routine basis in the Houston area (Hafner Main et al., 2001; Estes et al., 2002; Brown and Hafner Main, 2002; Brown et al., 2002; Hafner and Brown, 2003; Jolly et al., 2003; Fang and McDowell, 2003; Jolly, 2003; Kim et al., 2005; Buzcu and Fraser, 2006; Xie and Berkowitz, 2006, 2007). Consequently, high HRVOC concentrations observed during the two field study periods in 2000 and 2006 are not anomalously large, and conclusions drawn from those data should be generally applicable to the Houston area.

Field study results from 2000 indicate that industrial emissions of highly-reactive VOC have been under-reported in Houston (Wert et al., 2003; Xie and Berkowitz, 2007; Karl et al., 2004).

Results from more recent studies indicate these emissions are still under-reported (Robinson et al., 2008; Melqvist et al., 2007; Smith and Jarvie, 2008). Source apportionment studies have been performed for VOC observations using TexAQS 2000 data (Karl et al., 2004; Zhao et al., 2003) and routine VOC measurements (Buzcu and Fraser, 2006; Buzcu-Guven and Fraser, 2008; Xie and Berkowitz, 2006; Xie and Berkowitz, 2007; Wittig and Allen, 2008; Kim et al., 2005; Hafner Main et al., 2001; Brown and Hafner Main, 2002; Hafner and Brown, 2003). These studies have verified that observed HRVOC are strongly associated with industrial emissions, and the studies have identified specific areas from which the highest HRVOC emissions are emanating, largely concentrated on the Houston Ship Channel, but including other locations in the area. Research efforts have not yet precisely quantified actual emissions occurring on a long-term basis from under-reported sources. Mellqvist et al. (2007) and Robinson et al. (2008) have had some success in measuring emission fluxes from industrial point sources, but their efforts have been limited to short time frames. Both of these flux studies have verified that industrial point source emissions for the areas studied are under-reported, at least part of the time, by factors approaching an order of magnitude.

Actual emissions from industrial facilities may vary considerably, due to periodic or sporadic changes in processes, variations in control efficiency, and accidental or planned releases. Mellqvist et al. (2007) found that the ethene emission flux in one area near the Houston Ship Channel varied by a factor of 10 within 30 minutes, and smaller variations were common from day to day for propene and total alkanes. However, the exact degree of variation of these emissions, and the quantity, composition, and locations of sporadic emissions, has not been well quantified. They could be a relatively large portion of the total annual emissions, based upon industry-supplied emission reports (Murphy and Allen, 2005; Webster et al., 2007), but since the reported point source inventory is inconsistent with observations, and thus is inadequately quantified, it is difficult to reach a definitive conclusion.

1.2.3 Basic Meteorology

In the absence of accidental releases or spills, whether high concentrations of pollutants form on a given day is controlled mostly by meteorological processes, which may transport the pollutants and either dilute pollutant emissions or allow them to accumulate. Meteorology also affects other key processes, such as chemical reaction rates (Banta, et al., 2005). High ozone concentrations are observed most frequently in the HGB area on days lacking strong synoptic, or large-scale, pressure gradients. When synoptic (large-scale) weather systems move through the region, ozone and precursor emissions tend to be diluted and carried out of the city, rather than concentrated in still, stagnating air, to be heated, reacted and turned into ozone. Days dominated by strong synoptic weather systems tend to experience low ozone levels (Banta, et al., 2005).

Absent dominant synoptic weather systems, smaller-scale local wind patterns govern ozone formation, most notably the complex local coastal and sea breeze oscillations (Rao et al., 1997; Banta et al., 2005; Nielsen-Gammon et al., 2005b). Light to moderate synoptic-scale winds originating from the northeast oppose the direction of the bay breeze arising in the late morning or early afternoon (Banta et al., 2005; Ngan et al., 2008; Darby, 2005). Local wind components, including persistent sea breezes along the coast of the Gulf of Mexico, land-sea breeze flow reversals, and a shoreline convergence zone, combine to form a rotational wind pattern that often re-circulates emissions over ozone precursor sources, amplifying ozone formation dynamics (Banta, et al., 2005; Nielson-Gammon et al., 2005b).

As precursor emissions are advected across the region, they mix with other local emissions, as well as compounds transported into the region, to generate elevated concentrations of ozone. The rotational wind pattern accumulates precursors generated in the morning, along with those remaining from the previous day, which then react during the warmest and sunniest portion of the day. Ozone rich air masses typically begin to form in the center and south of the city. Later in the afternoon, southerly Gulf breezes and the rotational pattern can advect, or horizontally transport, the pool of high ozone over the city toward the west and northwest (Darby, 2005; Banta

et al., 2005).

Studies (Allen, et al., 2005; Allen et al., 2006; Allen, 2006) have found that a few (four to seven) days with unusually high ozone concentrations drive the high ozone design value in the HGB area. Those days are associated with elevated morning emissions of HRVOC in the area of the Houston Ship Channel. Consistent meteorology is exhibited on these days, notably an advection of air parcels from eastern Harris County and the Houston Ship Channel, to the west over urban areas and their associated emissions. These studies also found that on exceptional ozone days the contributions from outlying areas, either perimeter counties of the HGB area or other areas of Texas to the east, were greater than on moderate ozone days. These contributions were estimated to be in the range of one to three parts per billion ozone on days observing unusually high ozone concentrations at certain monitors that tend to determine the HGB area design value, most notably Houston Bayland Park (CAMS 53) (see Chapter 2 for an exhaustive discussion of design values).

Local wind patterns in the HGB area are dominated by a land-sea breeze flow reversal which is driven by atmospheric warming over land and subsidence over the Gulf of Mexico and Galveston Bay (Banta, 2005; Ngan et al., 2008; Darby, 2005). In the HGB area, the convergence zone, where winds in different layers, traveling in opposite directions, meet, mix and often stagnate, frequently occurs near the shoreline of Galveston Bay. This is also, unfortunately, the location of many major industrial sources of precursors, including HRVOC.

While light winds inhibit ventilation, subsidence inversions, which are also typical of high pressure areas like those observed in the Gulf, reduce vertical mixing. This combination encourages ozone formation by concentrating local pollutants near the surface. Areas of elevated ozone concentrations are also found to occur when the mixing height is low, cloud cover is minimal, background ozone levels are high, and widespread convection, or transfer of heat, does not occur until late afternoon or evening (Nielson-Gammon et al., 2005b). Varying wind patterns, the presence or absence of large-scale synoptic weather systems, ambient temperatures, and other factors, influence atmospheric mixing height, which in turn determines the volume of air in which photochemistry acts on the available precursors.

Wind directions on days when eight-hour ozone levels in the HGB area exceed the NAAQS typically show a circular movement throughout the day, rotating continuously over a twenty-four hour period. Very early in the morning, winds originate from the west, with directions gradually shifting to the northwest to north soon after sunrise. During the morning hours, winds continue to shift gradually, coming from the northeast, then from the east a little after noon. Finally, directions shift again, coming from the southeast a little before sunset, and then shifting to the south, while calming, at about midnight.

On days with mild synoptic winds, three patterns of winds, depicted in Figure 1-10, are generally observed in the HGB area. The first pattern, seen in Figure 1-10(a), exhibits a simple northwest-southeast land-sea breeze flow reversal from the city to Galveston Bay, the Houston Ship Channel, and back. This is a special case of the ozone-generating rotational pattern proposed by Nielson-Gammon (2005b), with some, albeit minor, observed rotation. The pattern presented in Figure 1-10(b) includes a stronger rotational element that circulates elevated ozone over multiple precursor sources, including Galveston Bay and the Houston Ship Channel, before transporting it over downtown Houston. Finally, Figure 1-10(c) shows a similar rotational pattern to (b) with elevated ozone traveling to the south of the city, and ending up in west Houston, after passing over the Houston Ship Channel region.

This pattern is evident from resultant wind vectors computed from wind speed and wind direction measurements collected in the HGB area. The loops in Figure 1-11(a) and Figure 1-11(b) are generalized examples of resultant wind vectors observed on (a) high ozone days and (b) low ozone days in the HGB area (TCEQ 2006). Measured wind speeds and directions are averaged

over each hour of the day, resultant wind vectors are computed, and origins of each vector are plotted as the hour of the day, except for midnight ("mid") and noon ("noon"). All vectors terminate at the origin, though the vectors themselves are not displayed here, for clarity. Direction from the origin represents the direction from which the wind originated, on average, during that hour. Distance from the origin represents average wind speed.

(a) (b) (c)

Figure 1-10: Wind Patterns Frequently Observed in the Houston-Galveston-Brazoria Area
Pattern (a) exhibits a simple northwest-southeast land/sea breeze flow reversal from the city to Galveston Bay, the Houston Ship Channel, and back; pattern (b) includes a rotational element that circulates elevated ozone over multiple precursor sources, before transporting it over downtown Houston; pattern (c) shows a similar rotational pattern with elevated ozone traveling to the west and south of the city, instead of downtown, after passing over the Houston Ship Channel region.

Daily average resultant wind vectors are plotted as blue arrows. These aggregate all wind vectors over the 24-hour period. On high ozone days, depicted in Figure 1-11(a), winds from multiple directions cancel out and the average resultant vector is short, meaning that overall air mass movement across the 24-hour period is relatively small. As the arrow indicates, winds on high ozone days, when averaged over the period, are light and from the east. On these days, precursor emissions tend to be blown around within the area, accumulating, concentrating, and reacting to form more ozone. On low ozone days, shown in Figure 1-11(b), the average resultant vector is longer, extending further from the origin, and points in a clear northwest direction, indicating the dominance of winds from the southeast. This, not coincidentally, is the direction of the Gulf of

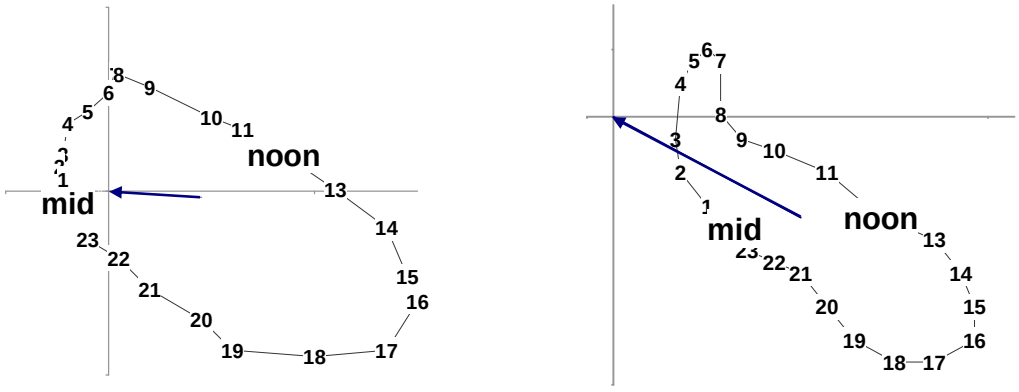

(a) (b)

Figure 1-11: Examples of Hourly Average Resultant Wind Vectors on (a) High Ozone Days and (b) Low Ozone Days
These loops of resultant wind vectors are generalized examples observed on (a) high ozone days and (b) low ozone days in the HGB area. Continuous measurements of wind speeds and directions are averaged over each hour of the day, resultant wind vectors are computed, and origins of each vector are plotted as the hour of the day, except for midnight ("mid") and noon ("noon"). All vectors terminate at the origin. Direction from the origin represents the direction from which the wind originated. Distance from the origin represents average wind speed, in meters per second (m s^{-1}). Blue arrows indicate daily averages of all 24 one-hour vectors.

Mexico and Galveston Bay, two sources of relatively unpolluted air. On these days, precursor emissions tend to be blown out of the region, rather than accumulating, by winds dominated by forces from one direction. Days when this pattern is observed tend to be days when synoptic winds are strong, such as from the semi-permanent high pressure system located in the Gulf of Mexico, or from large scale weather systems moving across the North American continent, reducing or even negating local forcings.

1.3 SUMMARY OF FINDINGS OF THE 2005-2006 TEXAS AIR QUALITY FIELD STUDY

In 2005 and 2006, TCEQ coordinated an 18-month long major field study of formation and accumulation of ozone and particulate matter over the entire eastern portion of Texas, focusing especially on the Houston-Galveston-Brazoria (HGB) area. Findings from this effort provide a very detailed snapshot of meteorological and photochemical mechanisms operating in the region during this period. As such, the field study supports and informs development of the conceptual model, helping shape theoretical and practical approaches.

TexAQS II was a follow-up to a previous, much shorter, field study in 2000, known as the Texas Air Quality Study 2000 (TexAQS 2000). The first field study discovered and documented meteorological and photochemical processes, as well as emissions data that, to that point, had only been inferred from indirect measurements. The 2005-2006 Texas Air Quality Study (TexAQS II) confirmed many of the findings of the earlier study, and included substantially more institutions, scientists, and measuring equipment. Participating organizations included government agencies, universities, and research institutions from across the United States and the globe, with the goal of measuring and assessing emissions, meteorology, photochemistry, emission inventories, and modeling capabilities used to monitor and forecast ozone pollution. The scope of the TexAQS II field research program constitutes one of the most comprehensive air quality studies ever undertaken in the United States. Analyses of the data collected during TexAQS II will continue to inform the science of ozone and particulate matter formation, transport, and fate in the HGB area and elsewhere, for year to come.

TexAQS II included a two month "intensive" study period from mid-August through mid-October 2006, during which a multitude of chemical and meteorological parameters were measured simultaneously by different agencies using different equipment, different platforms, and different methods. The multi-agency and multi-platform perspective strengthens the TexAQS II results by providing corroborative evidence for many of the findings. Among the equipment and platforms co-sampling during the study were several instrumented aircraft, the NOAA (National Oceanic and Atmospheric Administration) research vessel Ronald H. Brown, a network of ground based wind profilers, a mobile Solar Occultation Flux van, several dozen aerometric and meteorological samplers atop the 200 foot tall Moody Tower at the University of Houston, a special rural monitoring network, additional surface chemistry sites, and several NASA (National Aeronautics and Space Administration) satellites. Also, during this time, an extensive network of Continuous Air Monitoring Stations (CAMS), Non-Continuous Air Monitoring Stations (NCAMS), Photochemical Assessment Monitoring Stations (PAMS), National Air Monitoring Stations (NAMS), and State or Local Air Monitoring Stations (SLAMS) continued to collect ambient measurements.

Long before sampling began, scientists and project organizers developed a series of research objectives, posing the detailed questions TexAQS II would be designed to address. Because of the wide variety of participants, funding sources, and interests, there were, not surprisingly, many possible objectives. Participants will likely continue to explore scientific questions, as yet unformulated, for many years. Here, we will discuss only a few of the major preliminary findings that are most relevant for the current State Implementation Plan for the HGB area.

Among the principal findings of TexAQS II is that high ozone concentrations were found to form rapidly in plumes of highly reactive volatile organic compounds (HRVOC) and NO_X co-emitted

from petrochemical facilities. The highest ozone concentrations were measured in plumes originating from sources in the Houston Ship Channel, which were the major contributors of HRVOC ozone precursors observed in the HGB area. Prevailing winds carry these plumes across the region; however, shifting winds produce conditions conducive to transient high ozone events recorded by monitors.

Extensive measurement of the structure of the planetary boundary layer, or mixing height, confirmed its complexity and variability. Further, currently available meteorological models are marginally capable of describing these complexities. The 2000 and 2006 field studies observed a wide range of meteorological conditions, yet each measured high ozone concentrations under markedly different weather phenomena.

Some evidence from TexAQS II indicates that ethene (ethylene) emissions, one of the HRVOC, may have decreased as much as 40 percent from 2000 to 2006. Sources with CEMS (Continuous Emissions Monitoring Systems) were found to report NO_X emissions very accurately. Measurements of emissions fluxes at petrochemical plants suggest the 2004 point source inventory, while improved, still under-accounts for 2006 emissions of certain compounds, such as ethylene, by one to two orders of magnitude (1,000 to 10,000 percent). By comparison, these measurements also suggest that the current NO_X inventories are fairly accurate, having decreased substantially since 2000.

While VOC results may seem alarming, many sources were found to have reduced NO_X emissions since 2000. Speciation of mobile source VOC emissions agreed with findings elsewhere, though agreement with the 1999 National Emissions Inventory (NEI) was less than ideal. Mixed results were obtained for other compounds, such as formaldehyde, ammonia, and mercury.

While the TexAQS II field study has helped answer some questions, it has left others unanswered. For example, while models suggest that the HGB area is at times NO_X limited and at times VOC limited, measurements taken during TexAQS II have been unable to confirm specific sensitivities to these precursors.

The TexAQS II study confirmed that, by themselves, background ozone concentrations in the HGB area can exceed the eight-hour NAAQS, although sometimes this background may include pollutants recirculated from the HGB area. Dust and other aerosols were determined to be advected to the HGB area from as far away as Africa, demonstrating the transcontinental nature of pollutant transport. The study also noted that net ozone fluxes out of the HGB area exacerbate background ozone levels seen in other parts of east Texas. Ozone from the HGB area can be transported to the Dallas-Fort Worth (DFW) region, though elevated ozone concentrations in eastern Texas were the combined result of emissions originating from multiple sources. Transported ozone and locally-produced ozone contributed roughly equally to eight-hour ozone averages in the HGB area. Compounding the situation in the HGB area, evidence from TexAQS II suggests that drastic NO_X controls may be necessary to attain the ozone NAAQS, while drastic VOC controls in the absence of NO_X controls would be insufficient.

With this foundation in ozone formation in the HGB area, the remainder of this Conceptual Model investigates the current state of knowledge regarding ozone, precursors, meteorology, background and transport in the HGB area in greater detail. Trends in ozone and precursors are presented to place current HGB area values in context. Several analyses of different aspects of local ozone formation dynamics are offered, including an investigation of local meteorological phenomena. A discussion of recent findings on the influence of background ozone transported into the HGB area follows. Finally, several areas of future research are discussed.

CHAPTER 2: AIR QUALITY TRENDS IN THE HOUSTON-GALVESTON-BRAZORIA AREA

Trends in ozone and its precursors demonstrate not only the substantial progress the HGB area has made in improving air quality, but also the magnitude of the future challenge in attaining the National Ambient Air Quality Standard (NAAQS) for ozone. Trends are also useful as a first look at how ozone is related to its precursors. Ozone is a secondary pollutant, formed through a photochemical reaction of NO_X and sunlight. VOC can amplify ozone production, causing accumulation in the atmosphere. Decreases in NO_X and VOC demonstrate the effectiveness of policies to reduce emissions; however, due to its dependence on meteorological variables, ozone may not always exhibit trends identical to its precursors. Separating variations in meteorological factors from trends in ozone and its precursors can highlight whether ozone reductions are due to decreases in precursor emissions or are due to year to year variability in local meteorology (Sullivan, et al, 2009, Camalier, et al, 2007). This chapter discusses trends, both temporal and spatial, in ozone and its precursors.

2.1 OZONE TRENDS

A "design value" is a statistic used to compare an area's concentrations of a particular pollutant to the pollutant's NAAQS. Design values are commonly used to characterize ambient ozone concentrations because they summarize the severity of a local ozone problem in a single number. The criteria for attainment of the ozone NAAQS have changed over the past 12 years. Until June 2005, the ozone NAAQS was based upon one-hour average concentrations (EPA, 2009). The now-revoked one-hour ozone standard was 0.12 parts per million (ppm), averaged over one hour; an exceedance occurred when the fourth highest one-hour ozone concentration in a three-year period equaled or exceeded 0.125 ppm. The eight-hour NAAQS for ozone was adopted in 1997, but not implemented until April 2004, and was set at 0.08 ppm averaged over 8 hours. Amonitor exceeds that standard when its design value, three-year average of the fourth highest eight-hour ozone concentration for each year, equals or exceeds 0.085 ppm. The design value for an area is the highest design value recorded at any monitor in the area. In 2008, the eight-hour ozone NAAQS was lowered to 0.075 ppm; the exceedance criteria remain the same, but the concentration threshold is now lower (EPA, 2008).

This section examines the frequency at which all three of the NAAQS for ozone are exceeded, with the understanding that (a) the eight-hour standard of 0.08 ppm is currently being used for control strategy development, (b) the new eight-hour standard of 0.075 ppm will be the target within the next few years, and (c) the one-hour standard is no longer in effect, but it is still a useful benchmark for understanding ozone behavior in the Houston area. While the Federal NAAQS is expressed in units of parts per million, this chapter will use the familiar convention of expressing concentrations in parts per billion (ppb).

Daily peak eight-hour ozone concentrations for the years 1991 to 2008 in the HGB area are shown in Figure 2-1. The majority of days show ozone peaks below 85 ppb, but the highest days, which set the design values, are of particular interest. Annual maximum values, annual fourth highest values, and design values, which are constructed from the fourth highs, have all decreased over the time period. Notable in Figure 2-1 is the decrease in the number of daily peaks exceeding the 85 ppb NAAQS. It is also possible to identify the bi-modal character of the annual ozone cycle in several years. This pattern is most evident in 1998 and 1999. On an annual basis, ozone tends to peak first in spring and then again later in the summer.

The annual cycle of ozone is apparent in the graph, as daily peak ozone tends to increase throughout the spring, into the summer, and then falls as winter approaches, when it reaches a nadir. This cycle follows the annual pattern of temperature, also depicted in the figure, which also rises as summer approaches, peaks, then falls in winter. Temperature is likely acting as a proxy for solar radiation or other meteorological factors known to strongly influence ozone formation.

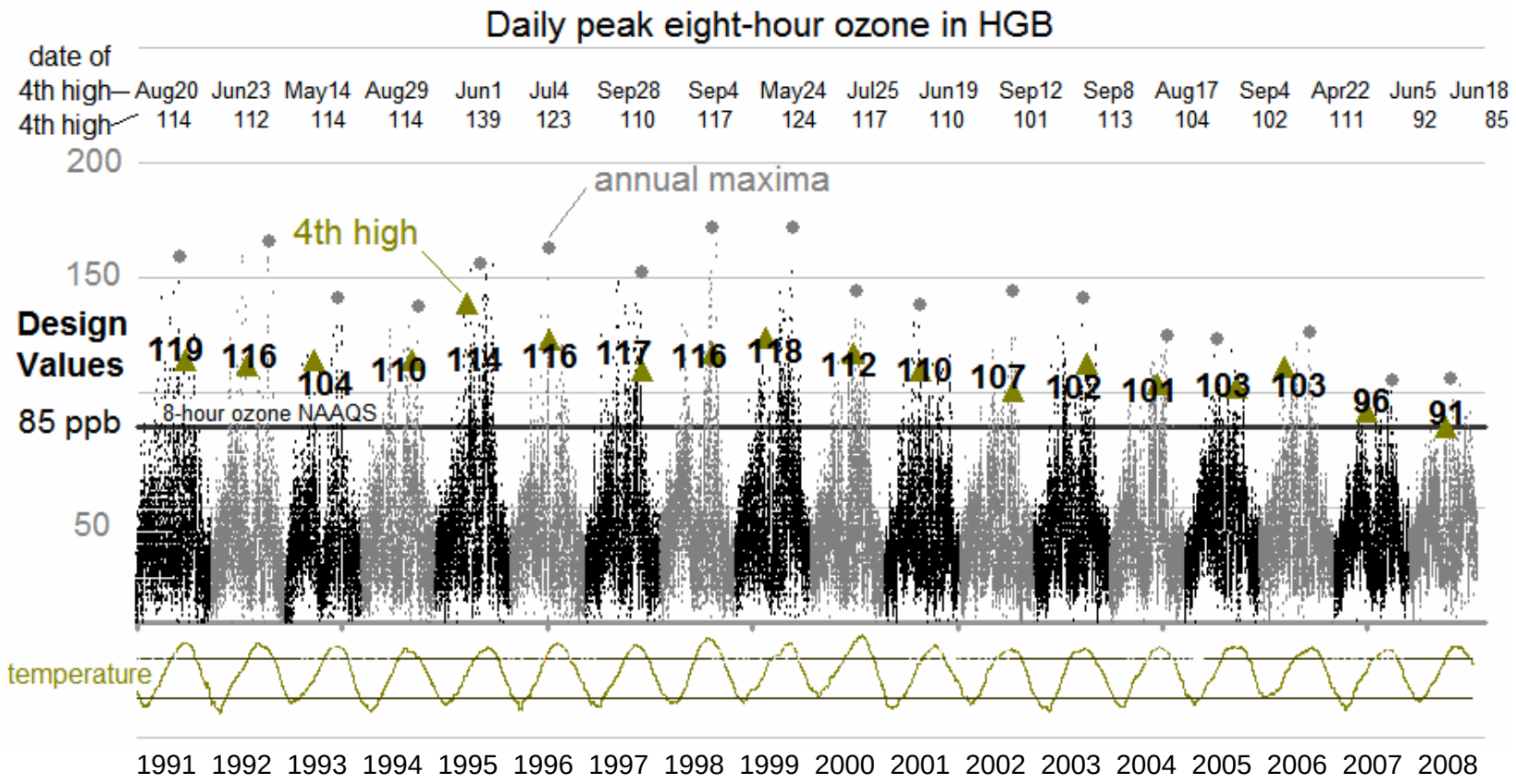

Figure 2-1: Daily Peak Eight-Hour Ozone Values in the Houston-Galveston-Brazoria Area

Maximum values, fourth-highest values, dates of the fourth-highest values, and annual design values are noted. The fourth-highest value for each year is not necessarily from the same monitor. Note the increasing trend during earlier years may be a relic of the expanding monitoring network. Temperature scale at bottom is the 60-day moving average peak daily temperature, with upper and lower bounds at 70ºF and 90ºF.

The seasonal variation in temperature is known to correlate with ozone formation, though temperature variations across years have not been shown to correlate significantly with measures of annual ozone.

The trend in design values is seen more clearly in Figure 2-2. While the HGB area continues to exceed both one-hour and eight-hour ozone standards, one-hour ozone design values have generally decreased over the past seventeen years, and eight-hour ozone design values have decreased over the past nine years. The eight-hour ozone design value in 2008 was 91 ppb, a 24 percent decrease from the 1991 design value of 119 ppb. The 2008 value is approaching the ozone NAAQS of 85 ppb. Work presented in Chapter 3 investigates whether reductions observed from 2006 to 2008 are due to anomalous meteorology or may be expected to continue apace as further emission reductions are achieved. A regression analysis of design value on year estimates that eight-hour ozone design values decreased at the rate of 1.2 ppb per year, which is statistically significant at the 5 percent level ($\alpha = 0.05$). If this trend were to continue at that rate, attainment of the eight-hour standard could be reached in five years, though if the pace of recent years were maintained, it could occur even sooner.

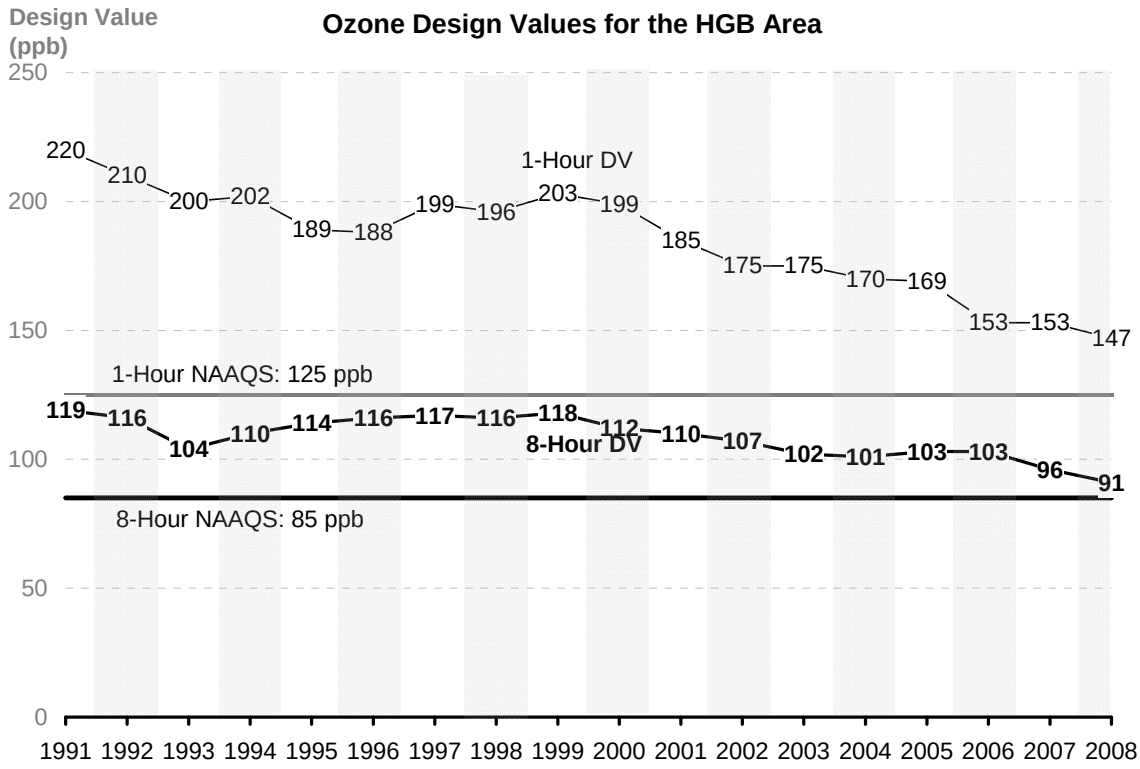

Figure 2-2: Ozone Design Values for the HGB Area
Although the HGB area is not currently in attainment of the NAAQS for either standard, both the one-hour and the eight-hour design values exhibit decreasing trends over the past seventeen years.

The one-hour ozone design value in 2008 was 147 ppb, a 33 percent decrease from the 1991 design value of 220 ppb. Regression of one-hour design values on year shows they decreased at the rate of 3.6 ppb per year, which is faster than the eight-hour ozone design values; the slope is also statistically significant at the 5 percent level ($\alpha = 0.05$).

Table 2-1: Eight-Hour Ozone Design Values by Monitor in the HGB Area

Monitor/CAMS #	1991	1992	1993	1994	1995	1996	1997	1998	1999	2000	2001	2002	2003	2004	2005	2006	2007	2008
Houston Bayland Park C53										111	110	100	102	101	103	103	96	91
Houston Westhollow C410						95	101	95	102	102	104	95	87	87	89	96	92	89
Park Place C416																		89

Houston Deer Park 2 C35/139									108	112	108	103	102	101	100	96	93	87
Manvel Croix Park C84													91	97	97	96	91	85
Northwest Harris Co. C26	98	101	100	110	113	110	106	106	109	108	105	101	100	94	93	91	91	85
Houston Aldine C8/C108/C150	119	116	104	102	103	114	116	116	108	111	108	107	100	95	92	88	84	83
Houston Monroe C406	105	102	96	93	97	102	109	112	113	106	93	90	90	95	97	99	91	81
Houston Croquet C409	117	112	103	96	104	104	117	115	118	110	104	102	99	99	98	94	87	80
Conroe Relocated C78														85	86	85	84	80
Channelview C15/AH115													87	90	89	85	83	80
Houston East C1	104	103	88				86	108	106	102	103	101	100	95	87	83	78	80
Seabrook Friendship Park C45													85	94	92	90	86	79
Houston Texas Avenue C411													88	89	88	84	78	76
Lang C408	105	103	93	95	98	99	100	96	96	96	91	83	78	79	79	80	77	76
Lake Jackson C1016															79	79	76	76
Houston North Wayside C405	114	102	94	91	91	91	96	99	104	105	98	89	86	85	82	78	76	75
Lynchburg Ferry C1015															96	89	82	74
Houston Regional Office C81												95	94	88	88	84	81	74
Clinton C403/C304/AH113	115	109	100	100	106	106	107	100	103	101	97	93	96	96	95	85	79	73
Galveston Airport C34/C109/X152								90	112	108	98	89	89	91	87	83	71	
Clute C11/A111		96	93	91	96	92	92	84	95	93	91	86	87					
Texas City C10	93	82	90	89	114	102	105	91	100	98	91	83	80					
Conroe C65											91							
Houston Crawford C407	105	98	89	89	95	91	97	96	100	100								
Houston Manchester C22	103	104	104	103	106	102	103											
Houston Deer Park C18	107	96	85	89	107	116												

Values are sorted in descending order of design values in 2008, then 2007, 2006, *et cetera*.

The design value in a metropolitan area is the highest design value of all of the area's monitors' individual design values. Because ozone varies spatially, it is also prudent to investigate trends at all monitors in an area. Table 2-1 and Table 2-2 contain the eight-hour and one-hour ozone design values at all regulatory monitors in the HGB area from 1991 to 2008. More monitors operate in the HGB area, but, because the data at those monitors do not meet EPA quality control standards, the design values at those additional monitors are not displayed here.

Table 2-2: One-Hour Ozone Design Values by Monitor in the HGB Area

Monitor/CAMS #	1991	1992	1993	1994	1995	1996	1997	1998	1999	2000	2001	2002	2003	2004	2005	2006	2007	2008
Houston Deer Park 2 C35/139							147	164	203	185	182	168	161	157	153	150	150	147
Houston Bayland Park C53									189	185	173	154	163	148	148	143	142	139
Park Place C416																	136	132
Manvel Croix Park C84												143	132	142	134	138	128	128
Houston Westhollow C410					164	155	164	155	165	150	150	141	141	128	126	131	127	126
Northwest Harris Co. C26	160	160	166	173	172	172	165	164	163	161	157	154	156	148	131	127	127	126
Houston Aldine C8/C108/C150	220	190	197	197	189	173	189	187	187	180	166	166	143	136	139	125	122	122
Channelview C15/AH115												154	141	140	135	134	128	120
Seabrook Friendship Park C45												132	135	135	153	153	153	119
Houston Regional Office C81											185	178	175	170	169	135	131	119
Houston East C1	210	200	200	202		177	182	182	198	180	180	171	171	165	154	137	119	119
Lynchburg Ferry C1015														157	157	152	149	117
Houston Monroe C406	170	170	155	147	154	161	174	196	196	170	143	151	141	141	131	133	131	117
Houston Croquet C409	200	200	178	152	167	167	168	168	167	167	160	157	150	141	136	131	126	117
Conroe Relocated C78												119	137	128	128	128	124	116
Galveston 99th St.																	115	115
Clinton C403/C304/AH113	210	210	176	158	173	173	173	161	183	199	176	157	175	158	158	124	121	111

Houston Texas Avenue C411											146	172	157	157	127	110	110
Lang C408	200	183	158	159	159	159	158	155	155	175	175	149	128	128	127	126	108	108
Houston North Wayside C405	210	190	173	173	155	143	155	158	189	190	168	153	131	138	138	118	100	102
Lake Jackson C1016													119	113	105	99	101
Galveston Airport C34/C109/X152						170	170	176	168		164	133	123	129	129	117	103	97
Texas City C10	150	150	163	163	184	182	182	146	175	172	139	121	116	116	124			
Clute C11/A111	150	150	132	129	144	144	148	134	154	161	154	136	133	136				
Houston Crawford C407	220	190	165	165	165	166	172	172	164	173	173	194						
Conroe C65										145	145	140						
Houston Manchester C22	190	190	180	160	172	170	175	173	176									
Houston Deer Park C18	160	160	150	157	188	188	199	163										
Rosenberg	150	150																
Hempstead	120	120																
Number of Monitors	15	15	13	13	13	14	16	16	16	16	17	22	20	22	21	20	22	22

Values are sorted in descending order of design values in 2008, then 2007, 2006, *et cetera*.

Figure 2-3 and Figure 2-4 display three summary statistics for the eight-hour and one-hour design values, respectively: the maximum, median, and minimum values computed across all monitors in the HGB area. These figures facilitate assessment of the range of design values observed within a year, as well as how these distributions change over time. It appears from the figures that neither eight-hour nor one-hour ozone design values exhibited a noticeable trend until about 1999, when both began falling steadily. Also, whereas previous to 2002, no monitors in the HGB area met either standard, since then, the area has seen a fairly steady increase in the number of monitors attaining the standards. By 2008, over half the monitors in the area attained both standards, as indicated by the median value falling below the NAAQS that year. (The median statistic as used here indicates that half the observed design values are above the median, and half below it.)

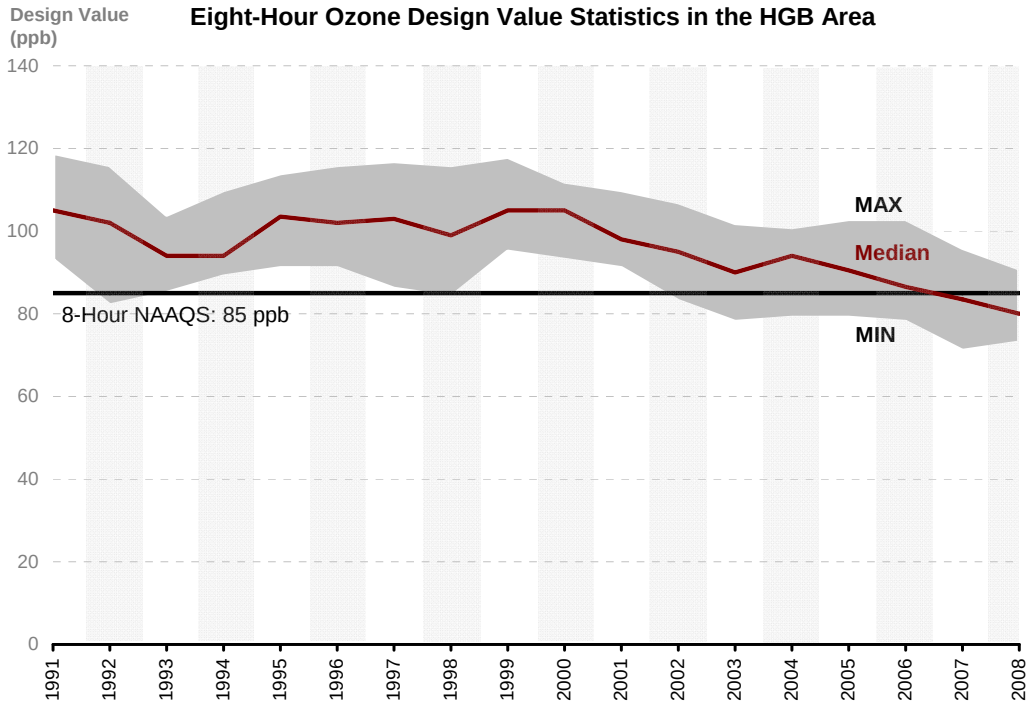

Figure 2-3: Eight-Hour Ozone Design Value Statistics in the HGB Area

Maximum, median, and minimum eight-hour Design Values recorded at all monitors in the HGB area from 1991 to 2008. Trends in all three statistics have decreased since 1999. Note that in 2007 and 2008 over half of the monitors in the HGB area are below the eight-hour ozone NAAQS (half the design values are above the median, and half are below the median).

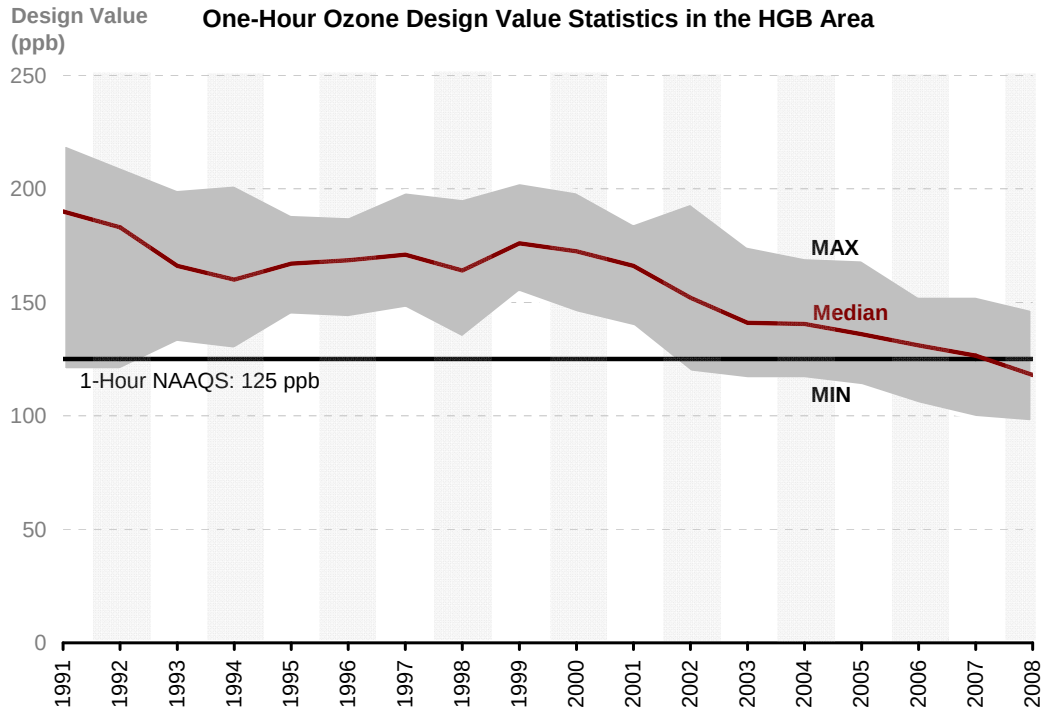

Figure 2-4: One-Hour Ozone Design Value Statistics in the HGB Area

Maximum, median, and minimum one-hour design values recorded at all monitors in the HGB area from 1991 to 2008. Trends in all three statistics have decreased since 1991. The range of observed values (the spread) has also shrunk. Note that in 2008 over half of the monitors in the HGB area are below the one-hour ozone NAAQS (half the design values are above the median and half are below the median).

The Houston Bayland Park (CAMS 53) monitor currently sets the eight-hour design value for the HGB area. Its 2008 design value, 91 ppb, is calculated (like all monitors) by averaging the 2006 through 2008 fourth highest concentrations, and truncating any decimal. At Houston Bayland Park (CAMS 53), these values were 106, 84, and 83 ppb respectively (Table 2-3). Because 2006 will be excluded from the 2009 calculation, Houston Bayland Park (CAMS 53) would need to record a fourth high ozone concentration of 88 ppb or higher in 2009 to violate the NAAQS that year. Of the five other HGB area monitors with 2008 design values of 85 ppb or above, the 2009 fourth high values needed to violate the NAAQS in 2009 all exceed 88 ppb, ranging from 89 to 94 ppb. Among the six, the highest 2008 fourth high was 83 ppb recorded at Houston Bayland Park (CAMS 53), and the lowest was 75 ppb at Manvel Croix Park (CAMS 84).

Table 2-3: Annual Fourth Highest Eight-Hour Ozone Values and Design Values

Monitor	Annual 4th high 2006 *ppb*	2007 *ppb*	2008 *ppb*	2008 design value *ppb*	2009 value needed to violate the NAAQS *ppb*
Houston Bayland Park C53	106	84	83	91	88
Houston Westhollow C410	103	84	82	89	89
Park Place C416	106	85	76	89	94
Houston Deer Park C35	101	86	76	87	93
Northwest Harris Co. C26	90	90	76	85	89
Manvel Croix Park C84	94	86	75	85	94

Monitors are sorted in descending order by 2008 design value, then by 2008 4th high, 2007 4th high, et cetera. The 2008 design value is the average of the 2006 through 2008 4th high values. The Houston Houston Bayland Park (CAMS 53) monitor is highlighted because it is the monitor currently driving the eight-hour ozone design value in the HGB area.

Ozone trends can also be investigated by looking at the number of days an exceedance of the ozone NAAQS was recorded, termed an "exceedance" day. An exceedance day for the eight-hour NAAQS is any day that any monitor in the area measures an eight-hour average ozone concentration greater than or equal to 85 ppb over any eight-hour period. An exceedance day for one-hour ozone is any day that any monitor in the area measures a one-hour average ozone concentration greater than or equal to 125 ppb for at least one hour. Previous research (Savanich, 2006) by the TCEQ has shown that, until 2006, the number of exceedance days was positively correlated with the number of monitors in a particular area. As the number of monitors increases, so does the number of exceedance days recorded, at least until the area has been saturated with monitors or until ozone concentrations truly decrease. Because of this correlation, when examining exceedance day trends, the number of monitors must always be considered. Thus, it is especially noteworthy that Figure 2-5 shows that, despite an increase in the number of monitors, the number of exceedance days for both one-hour and eight-hour ozone has decreased, a decrease that is especially pronounced over the past three years. Since 1999, the number of eight-hour and one-hour ozone exceedance days occurring in the HGB area has fallen 83 percent and 96 percent, respectively. In just the last three years, the number of eight-hour and one-hour ozone exceedance days has fallen 76 percent and 92 percent, respectively.

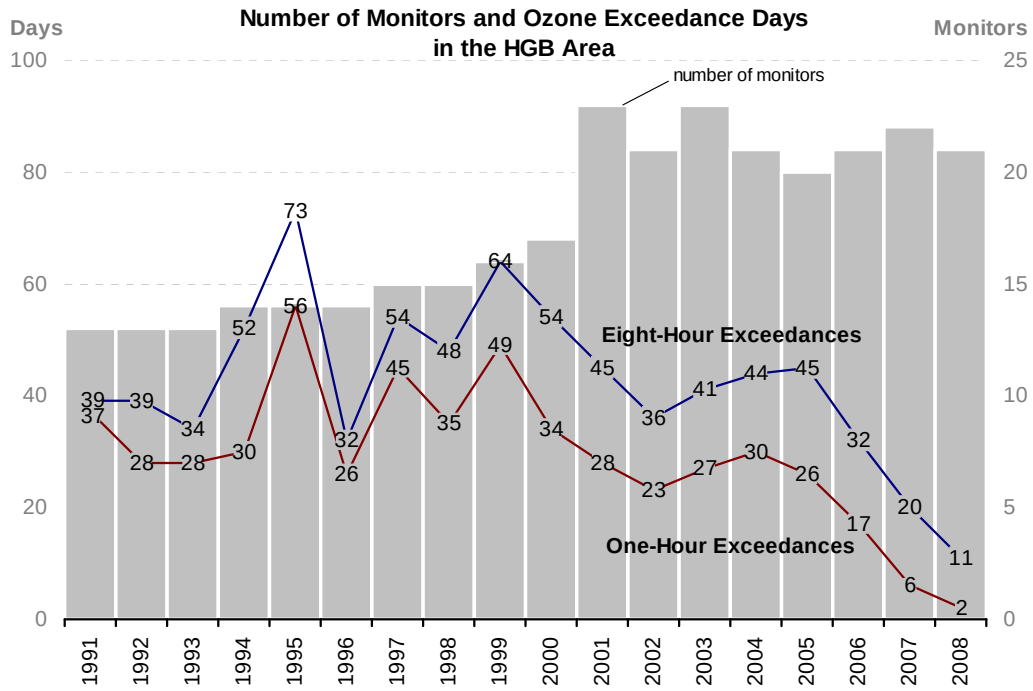

Figure 2-5: Number of Monitors and Ozone Exceedance Days in the HGB Area
The red line represents the number of one-hour ozone exceedance days, the blue line represents the number of eight-hour ozone exceedance days, and the gray bars represent the number of regulatory monitors in the HGB area. The number of both one-hour and eight-hour ozone exceedance days are decreasing despite an increase in the number of monitors.

Results for individual monitors, displayed in **Error! Reference source not found.** and **Error! Reference source not found.**, support this conclusion: the number of exceedance days at individual monitors also appears to be decreasing. Figure 2-6 highlights two monitors, Houston Aldine (CAMS 8) (red line) and Houston Bayland Park (CAMS 53) (blue line), that recorded the most eight-hour ozone exceedances in the past. Since recent peaks in 1999 (at Houston Bayland Park (CAMS 53)) and in 2000 (Houston Aldine (CAMS 8)), neither monitor, in any year, has come within 60 percent of these peaks; in 2008 and 2009, both monitors experienced at least an 85% reduction from the recent peaks. While results for other monitors are less impressive, overall, the trend in ozone exceedance days at monitors throughout the HGB area is clearly downward. Due to the large number of monitors in the HGB area, data from Figure 2-6 and Figure 2-7 are presented in Table 2-4 and Table 2-5 for detailed inspection.

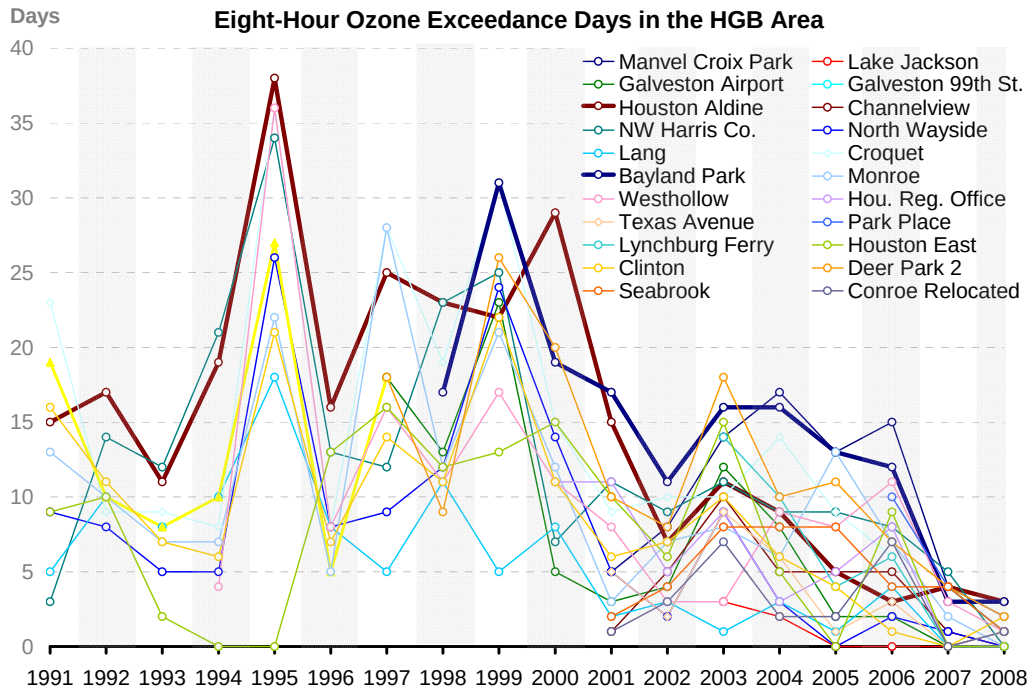

Figure 2-6: Number of Eight-Hour Ozone Exceedance Days by Monitor

Exceedance days in the HGB area from 1991 to 2008. The Houston Aldine (CAMS 8) monitor (dark red) and the Houston Bayland Park (CAMS 53) monitor (blue) are highlighted. In the past, these two monitors observed a large number of eight-hour ozone exceedance days. Recently, eight-hour ozone exceedance days at these two monitors have been reduced to fewer than five per year. Note also that Houston Bayland Park (CAMS 53) has the highest eight-hour ozone design value in the HGB area for 2008.

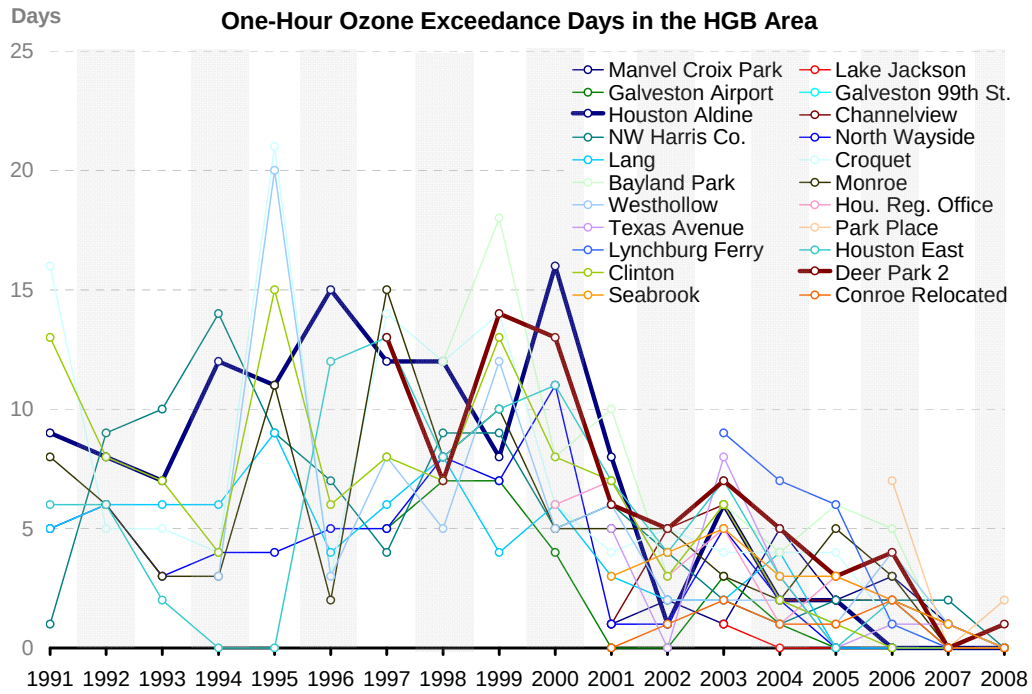

Figure 2-7: Number of One-Hour Ozone Exceedance Days by Monitor

Number of Exceedance days in the HGB area from 1991 to 2008. The Houston Deer Park (CAMS 35) monitor (dark red) and Houston Aldine (CAMS 8) monitor (blue) are highlighted. In the past, these two monitors observed a large number of one-hour ozone exceedance days. Recently, one-hour ozone exceedance days at these two monitors have been reduced to fewer than five per year, or eliminated entirely. Houston Aldine (CAMS 8) did not observe an exceedance of the one-hour NAAQS in either 2007 or 2008.

The progress achieved in recent years in reducing eight-hour and one-hour ozone concentrations in the HGB area is evident in Table 2-4 and Table 2-5. Table 2-4 shows that the total number of eight-hour exceedance days, when this metric is altered so that a single date's value represents the total number of monitors in exceedance on that date, fell from a high of 340 in 1995 to 39 in 2007 and just 19 in 2008. Prior to 2007, that number was never below 100, except for one year, 1993, when it was 94. The number of monitors recording an exceedance of the eight-hour ozone standard has fallen by half, from a maximum of 23 in 2003 to only 12 in 2008.

A similar pattern is apparent with the number of exceedances of the one-hour ozone NAAQS presented in Table 2-5. The table shows that the total number of one-hour ozone exceedance days, as defined in the previous paragraph, fell from a high of 165 in 1995 to just three in 2008. Prior to 2005, the number of one-hour exceedances was never below 50. The three exceedances in 2008 occurred at only two monitors. As recently as 2006, a total of 15 monitors recorded at least one exceedance. This is remarkable progress and has occurred in a fairly short amount of time in an area well known for its air quality challenges.

Table 2-4: Number of Days with an Eight-Hour Ozone Exceedance

Monitor	1991	1992	1993	1994	1995	1996	1997	1998	1999	2000	2001	2002	2003	2004	2005	2006	2007	2008
Houston Bayland Park (CAMS 53)								17	31	19	17	11	16	16	13	12	3	3
Houston Aldine C8/C108/C150	15	17	11	19	38	16	25	23	22	29	15	7	11	9	5	3	4	3
Clinton C403/C304/AH113	16	11	7	6	21	7	14	11	22	11	6	7	10	6	4	1	0	2
Houston Deer Park 2 C35							18	9	26	20	10	8	18	10	11	7	4	2
Park Place C416																10	4	2
Lake Jackson C1016													3	2	0	0	0	1
Houston Croquet C409	23	9	9	8	36	8	28	19	31	15	9	10	10	14	9	6	0	1
Conroe Relocated C78											1	3	7	2	2	7	0	1
Houston Westhollow C410				4	36	8	16	11	17	11	8	3	3	9	8	11	3	1
Seabrook											2	4	8	8	8	4	4	1
Manvel Croix Park C84											5	8	14	17	13	15	4	1
Galveston 99th St.																	4	1
Houston Texas Avenue C411											5	2	9	6	1	3	0	0
Lang C408	5	10	8	10	18	8	5	11	5	8	2	3	1	3	1	4	0	0
Lynchburg Ferry C1015													14	10	4	6	0	0
Houston Regional Office C81										11	11	5	9	3	5	8	0	0
Houston East C1	9	10	2	0	0	13	16	12	13	15	10	6	15	5	0	9	0	0
Houston North Wayside C405	9	8	5	5	26	8	9	12	24	14	5	2	9	3	0	2	1	0
Channelview C15/AH115											1	5	10	5	5	5	1	0
Houston Monroe C406	13	10	7	7	22	5	28	12	21	12	3	7	8	6	13	7	2	0
Northwest Harris Co. C26	3	14	12	21	34	13	12	23	25	7	11	9	11	9	9	8	5	0
Galveston Airport C34/C109/X152							18	13	23	5	3	4	12	8	2	2	0	
Clute C11/A111	8	10	6	5	15	3	4	5	9	2	3	6	3					
Texas City C10	6	1	9	7	25	1	10	10	11	6	1	3	3	0				
Houston Manchester C22	19	10	8	10	27	5	18											
Houston Deer Park C18	8	4	3	18	27	12												
Houston Crawford C407	5	6	7	4	15	3	16	10	11	8	0							
San Jacinto Monument											0	5	1					
Conroe C65									4	17	6							
Number of Monitors	13	13	13	14	14	14	15	15	16	17	23	21	23	21	20	21	22	21

Monitors are sorted in descending order by the number of eight-hour ozone exceedance days recorded in 2008, then 2007, 2006, *et cetera*.

Table 2-5: Number of Days with a One-Hour Ozone Exceedance

Monitor	1991	1992	1993	1994	1995	1996	1997	1998	1999	2000	2001	2002	2003	2004	2005	2006	2007	2008
Park Place C416																7	0	2
Houston Deer Park 2 C35							13	7	14	13	6	5	7	5	3	4	0	1
Northwest Harris Co. C26	1	9	10	14	9	7	4	9	9	5	6	4	2	1	2	2	2	0
Houston Westhollow C410				3	20	3	8	5	12	5	6	2	2	2	1	4	1	0
Manvel Croix Park C84											1	2	1	5	2	3	1	0
Seabrook											3	4	5	3	3	2	1	0
Channelview C15/AH115											1	5	6	2	2	2	1	0
Houston Texas Avenue C411											5	0	8	3	0	1	1	0
Houston Bayland Park (CAMS 53)								12	18	8	10	3	6	4	6	5	0	0
Houston Monroe C406	8	6	3	3	11	2	15	8	10	5	5	5	3	2	5	3	0	0
Houston Regional Office C81										6	7	3	5	1	3	2	0	0
Conroe Relocated C78											0	1	2	1	1	2	0	0
Houston East C1	6	6	2	0	0	12	13	8	10	11	7	4	7	3	0	2	0	0
Lynchburg Ferry C1015													9	7	6	1	0	0
Houston Croquet C409	16	5	5	4	21	3	14	12	14	6	4	5	4	4	4	1	0	0
Houston Aldine C8/C108/C150	9	8	7	12	11	15	12	12	8	16	8	1	6	2	2	0	0	0
Clinton C403/C304/AH113	13	8	7	4	15	6	8	7	13	8	7	3	6	2	1	0	0	0
Lang C408	5	6	6	6	9	4	6	8	4	6	3	2	2	4	0	0	0	0
Houston North Wayside C405	5	6	3	4	4	5	5	8	7	11	1	1	5	2	0	0	0	0
Lake Jackson C1016													1	0	0	0	0	0
Galveston 99th St.																	0	0
Galveston Airport C34/C109/X152							5	7	7	4	0	0	3	1	0	0	0	
Clute C11/A111	3	3	2	0	6	1	3	1	4	2	0	2	1					
Texas City C10	4	1	7	2	14	0	3	3	7	3	0	0	1	0				
San Jacinto Monument											0	2	0					
Conroe C65									1	5	2							
Houston Crawford C407	5	4	5	3	9	4	11	12	5	8	0							
Houston Manchester C22	11	7	7	7	18	4	10											
Houston Deer Park C18	6	2	1	6	18	4												
Number of Monitors	13	13	13	14	14	14	15	15	16	17	23	21	23	21	20	21	22	21

Monitors are sorted in descending order by the number of one-hour ozone exceedance days recorded in 2008, then 2007, 2006, *et cetera*.

The ozone season spans the entire year in the HGB area; however, the period when elevated ozone concentrations are observed varies from year to year. **Error! Reference source not found.** shows the frequency of, and variation in, the number of eight-hour ozone exceedance days in the HGB area by month and year. While the ozone season does vary from year to year, in the past few years the HGB area has experienced fewer ozone exceedance days over fewer months. The darker areas in the figure show that peak ozone season in the HGB area typically occurs from August to September, with a smaller, secondary peak occurring earlier, roughly in June. Recently, however, the peak ozone season appears to be delayed, occurring in September and October, though confirmation of a trend must await more data.

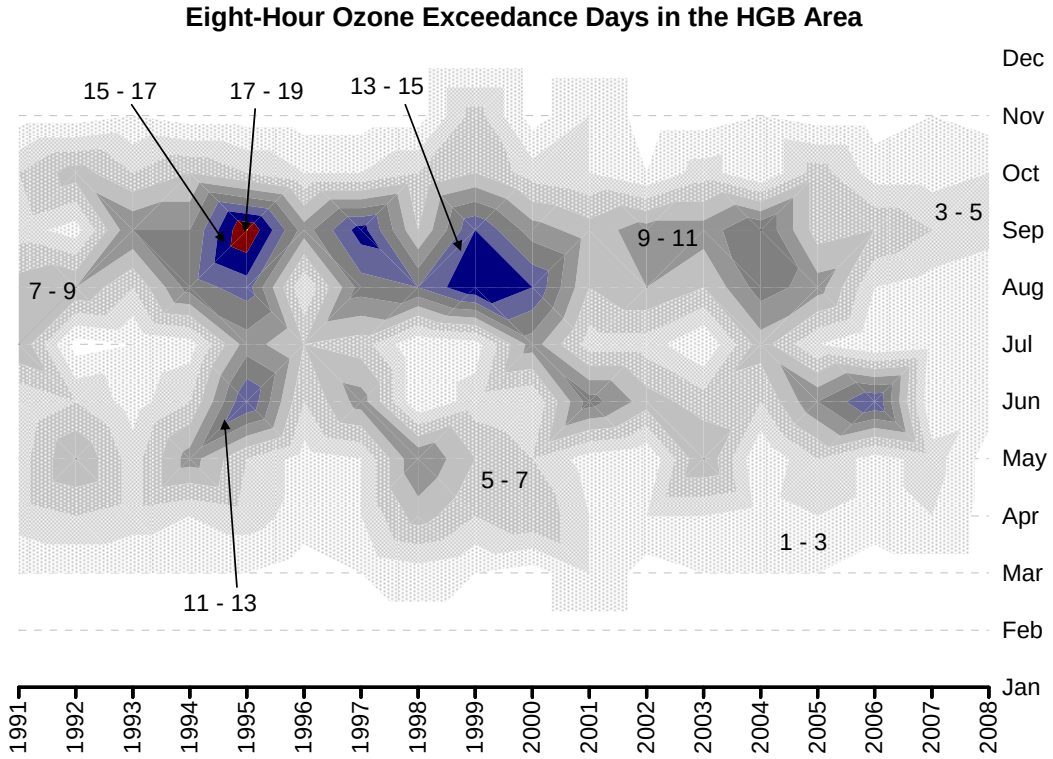

Figure 2-8: Eight-Hour Ozone Exceedance Days in the HGB Area
Darker colors indicate more exceedance days. Note that, historically, the ozone season peaks once in late spring/early summer and again in the late summer; however, the severity of those peaks has been decreasing in recent years and has shifted slightly later in the year.

Hurricane Ike made landfall in Galveston on September 13, 2008. A number of monitors in the area were shut down for several weeks as a result. Despite the lack of monitors operating, September experienced the largest number of eight-hour ozone exceedance days in 2008 (4 days), but the lowest number of eight-hour ozone exceedance days in September since 1992. Prior to Hurricane Ike, the HGB area had the lowest number of exceedance days in the month of August compared to all years back to 1991.

A variety of methods has been presented for understanding ozone trends in the HGB area. These methods generally agree that ozone concentrations have been decreasing. However, the area still faces challenges in achieving attainment of the 1997 ozone NAAQS. Because ozone formation depends on a multitude of factors, these factors must be investigated in detail before conclusions as to causes of the observed decreases can be reached.

2.2 NITROGEN OXIDE TRENDS

Nitrogen oxide (NO_X), a precursor to ozone formation, is a variable mixture of nitric oxide (NO) and nitrogen dioxide (NO_2). NO_X is primarily emitted by fossil fuel combustion, lightning, biomass burning, and soil. (Martin, et.al., 2006) Examples of common NO_X emission sources, which occur in all urban areas, are automobile, diesel, and small engines; residential water heaters; industrial heaters and flares; and industrial and commercial boilers. Mobile, residential, and commercial NO_X sources are usually numerous, smaller sources distributed over a large geographic area, while industrial sources are usually large point sources, or numerous small sources, clustered in a small geographic area. Because of the large number of NO_X sources, high ambient NO_X concentrations can occur throughout the HGB area.

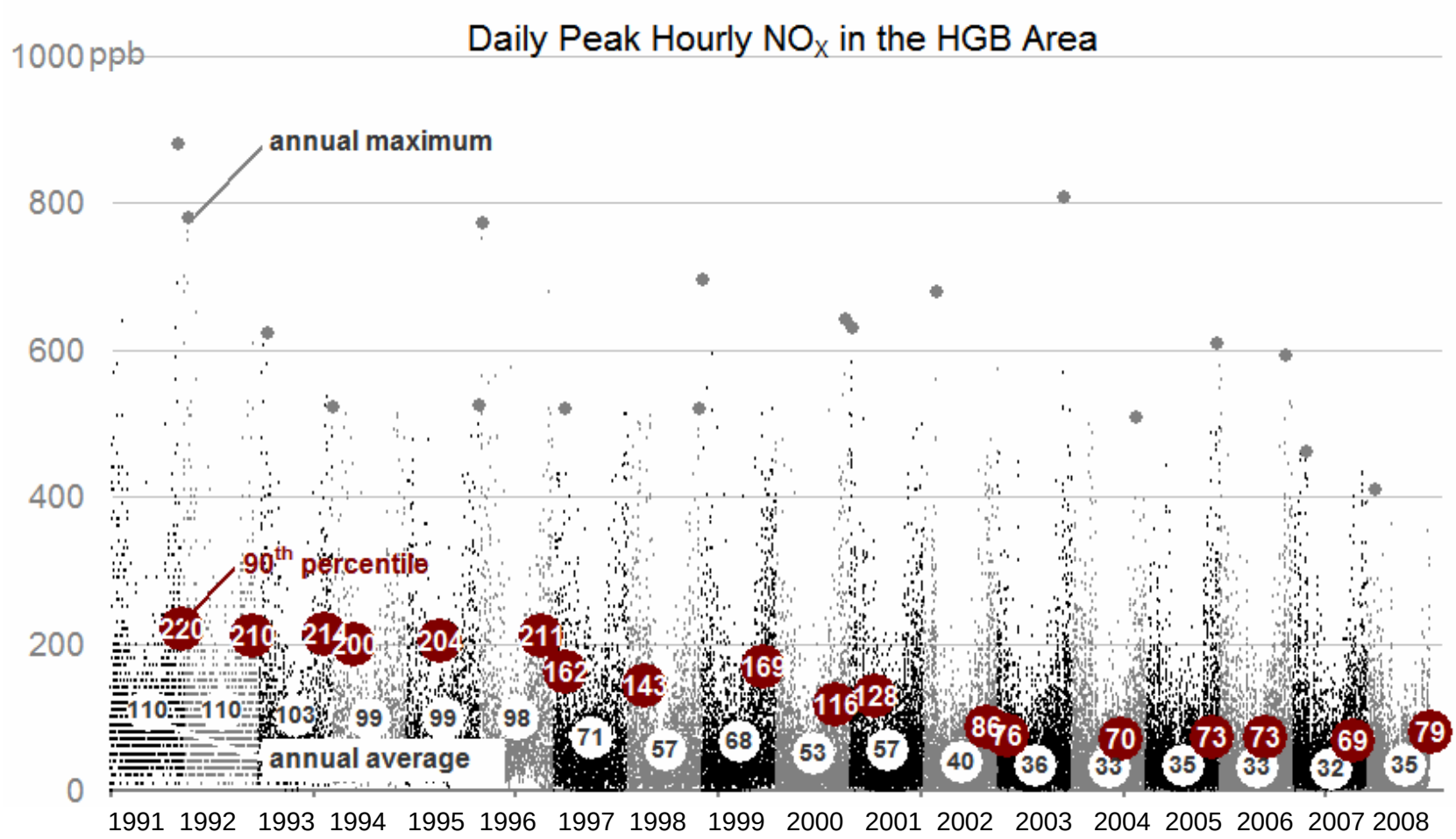

Date of 90th percentile:

1991	1992	1993	1994	1995	1996	1997	1998	1999	2000	2001	2002	2003	2004	2005	2006	2007	2008
Oct 22	Dec 15	Dec 25	Oct 30	Nov 22	Dec 12	Nov 19	Feb 24	Nov 12	Sep 5	Apr 27	Dec 15	Dec 19	Apr 28	Dec 1	Nov 16	Nov 14	Oct 22

Figure 2-9: Daily Peak Hourly NO_X in the HGB Area

Note maximum NO_X values tend to occur in winter. Annual maximum NO_X has been variable but has fallen overall by 54 percent since 1991, and 41 percent since 1999, excepting one anomalous extreme value in 2003. Annual average NO_X has decreased 62 and 53 percent over the same periods. Annual ninetieth percentile NO_X value has fallen 64 and 53 percent over those periods.

Other sources of NO_X that are important to air quality in the HGB area are large electric generation units (EGU) in rural areas near Houston and in East Texas. These produce large concentrated plumes of emissions that can enhance ozone generation. Analyses done by the Rapid Science Synthesis Team of the 2005-2006 Texas Air Quality Study (TexAQS II) indicate that NO_X emissions at several EGUs have decreased by factors ranging from two to four between 2000 and 2006. These reductions were seen at EGUs that implemented NO_X control features, such as Selective Catalytic Reduction (SCR), between 2000 and 2006, suggesting these control strategies are working.

The *Rapid Science Synthesis Report*, summarizing findings from TexAQS II, confirms that the largest ozone concentrations in the HGB area tend to form in narrow NO_X and VOC rich plumes emitted from petrochemical facilities. Previous analyses performed using aircraft measurements and emission inventories obtained during TexAQS 2000 and TexAQS II indicate that NO_X emissions in the Houston Ship Channel area have decreased between 2000 and 2006. Furthermore, aircraft data obtained during the two field studies were in agreement with data measured by Continuous Emission Monitoring Systems (CEMS) located at the facilities. Constant NO_X emissions, however, can result in widely varying ambient monitored NO_X concentrations due to changes in meteorological conditions (Blanchard, et al., 2007). This section corroborates the TexAQS 2000 and TexAQS II analysis by investigating long term trends in NO_X concentrations.

Daily peak one-hour NO_X from all monitors in the HGB area from 1991 to 2008 is plotted in Figure 2-9. The increasing density of NO_X data points shows that the NO_X monitoring network has increased greatly in the HGB area since 1991. Annual ninetieth percentile and annual average NO_X values are also plotted in the figure. Both these measures have decreased markedly over the 1991 to 2008 period, falling 64 percent and 68 percent, respectively. Even more remarkable may be the 53 percent and 48 percent declines since 1999.

Table 2-6: NO_X Values in the HGB Area by Year

year	annual maximum NO_X *ppb*	annual average NO_X *ppb*
1991	880	110
1992	780	110
1993	622	103
1994	523	99
1995	524	99
1996	773	98
1997	521	75
1998	520	67
1999	696	75
2000	641	57
2001	629	66
2002	678	52
2003	809	53
2004	509	49
2005	609	49
2006	593	49
2007	461	48
2008	409	35

overall decrease through 2008 since:

1991	53.5%	67.7%
1999	41.2%	53.0%

annual decrease through 2008 since:

1991	4.4%	6.4%
1999	5.7%	8.0%

Annual decreases are computed as compound annual rates.

Though highly variable from season to season, daily peak hourly NO_X also shows a general decreasing trend since 1991. Maximum NO_X concentrations typically occur in winter, and, while erratic, have decreased overall by 41 percent, to 409 ppb, since 1999, though one anomalous extreme value, 809 ppb, occurred in 2003. This is an average of roughly 32 ppb per year, or nearly 6 percent. The drop since the 1991 high of 880 ppb is 54 percent, or over 4 percent annually.

Average daily peak hourly NO_X has dropped even more precipitously, falling 53 percent, or 8 percent per year, from 75 ppb to 35 ppb, since 1999. Since 1991, average hourly NO_X has dropped 68 percent, or over 6 percent per year, from the series high of 110 ppb. Notice that in 2008, both the NO_2 design value and maximum daily peak NO_X recorded the lowest values of any previous year back to 1991.

While the highest NO_X values occur in the winter, it is the NO_X values during the summer months, when ozone production is the highest, that are of particular interest. Trends in median hourly NO_X concentrations at individual monitors in the HGB area from May to October, 1998 to 2008, are shown in Figure 2-10. Four monitors of particular interest, Housotn Texas Avenue (CAMS 411), Lang (CAMS 408), Clinton (CAMS 403), and Houston Bayland Park (CAMS 53), are highlighted in Figure 2-10. Sites with less than 75 percent complete data for a year were not plotted for that year; for example, Clinton (CAMS 403) had less than 75 percent complete data in 2008, and therefore was not plotted.

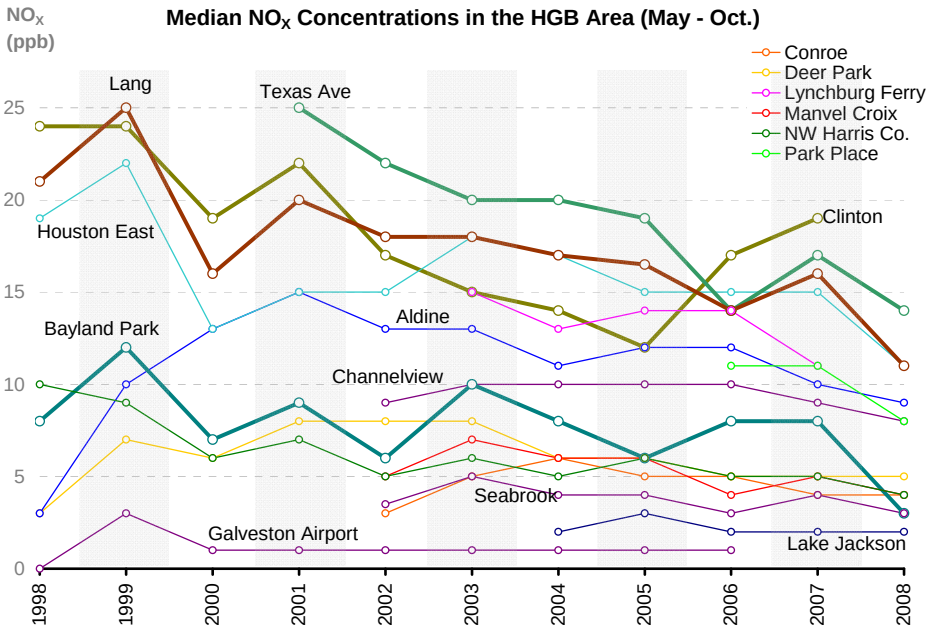

Figure 2-10: Median NO_X Concentrations in the HGB Area

Median hourly NO_X concentrations, May to October, 1998 to 2008. Highlighted monitors, Houston Texas Avenue (CAMS 411), Lang (CAMS 408), and Houston Bayland Park (CAMS 53), represent some of the larger NO_X decreases. Sites with less than 75 percent complete data for a year were not plotted for that year; for example, Clinton (CAMS 403) had less than 75 percent complete data in 2008, and therefore was not plotted.

Table 2-7: Median and 90th Percentile Hourly NO_X Values

	median				90th percentile			
monitor	1998	2007	2008	% change 1998-2008*	1998	2007	2008	% change 1998-2008*
	ppb	*ppb*	*ppb*	*%*	*ppb*	*ppb*	*ppb*	*%*
monitors with decreasing trends								
Houston Bayland Park (CAMS 53)	19	-42	8	8	3	-63	33	30
Northwest Harris Co. C26	10	-43	5	4	-60	21	12	12
Lang C408	21	16	11	-48	65	48	35	-46
Houston East C1	19	15	11	-42	56	46	37	-34
Clinton C403/C304/AH113	*	24	19	-	-21	56	47	-
	-16							
monitors with increasing trends								
Houston Aldine C8/C108/C150	3	0	10	9	200	30	32	30
Houston Deer Park 2 C35	3	-28	5	5	67	25	21	18
monitors with indeterminate trends								
Channelview C15/AH115		20	-	9	8		-	24
Conroe C65		-	4	4		-	10	10
Galveston Airport C34/C109/X152		-	0	-	-		1	-
Texas Avenue	-	17	14		-	53	37	
Lake Jackson C1016	-	2	2		-	7	6	
Lynchburg Ferry C1015	-	11	-		-	33	-	
Manvel Croix Park C84	-	5	4		-	17	15	
Park Place C416	-	11	8		-	47	32	
Seabrook	-	4	3		-	12	12	

* Percentage changes computed from 1998 to 2007 for years missing 2008 data, due to incomplete data. Monitors are sorted in increasing order by percentage change in median values. Monitors with indeterminate trends began operating after 1998.

Median NO_X values tend to vary from year to year, but most monitors show overall decreases in median NO_X since 1998. Monitors that show the smallest decreases or show no change are at sites that have traditionally had lower NO_X concentrations. Some of the largest median NO_X concentrations were measured at the Lang (CAMS 408) monitor, which is in close proximity to Highway 290, and at the Texas Avenue monitor in downtown Houston. These monitors are both near major roadways and their similar trends suggest they may be measuring decreases in NO_X emissions from mobile sources. The lowest median NO_X concentrations were measured by monitors closest to the coast, at Galveston Airport (CAMS 34), Seabrook (CAMS), and Lake Jackson (CAMS 1016).

Note that sites recording among the highest ozone design values, for example, Houston Bayland Park (CAMS 53) and Park Place (CAMS 416), are not necessarily the sites with the highest median NO_X concentrations. The previous section showed that Houston Bayland Park (CAMS 53) has the highest eight-hour ozone design value in the HGB area of 91 ppb, yet it has a lower median NO_X concentration than many other sites in the area.

For a more robust examination of the distribution of hourly NO_X concentrations, the 90th percentile was also analyzed. Although there is less variability in 90th percentile NO_X concentrations compared to medians, all sites appear to exhibit a slight decrease. Houston Bayland Park (CAMS 53), Houston East (CAMS 1), Clinton (CAMS 403), Houston Texas Avenue (CAMS 411), Lang (CAMS 408), and Park Place (CAMS 416) monitors exhibited particularly sharp decreases in 90th percentile NO_X concentrations from 2007 to 2008 compared with other monitors in the HGB area.

The largest decreases since 1998 (Table 2-7) were observed at monitors primarily influenced by mobile source emissions, rather than industrial sources. Clinton (CAMS 403) and Houston East (CAMS 1), both located near industrial sources, have seen larger decreases in median NO_X values than in 90th percentile values since 1998. At Houston East (CAMS 1), the 90th percentile value decreased 34 percent, while the median decreased 42 percent between 1998 and 2008. The Clinton (CAMS 403) monitor experienced a drop of 16 percent in the 90th percentile, with a 21 percent decrease in the median between 1998 and 2007 (2008 was not used due to incomplete data), though these measures have increased in recent years.

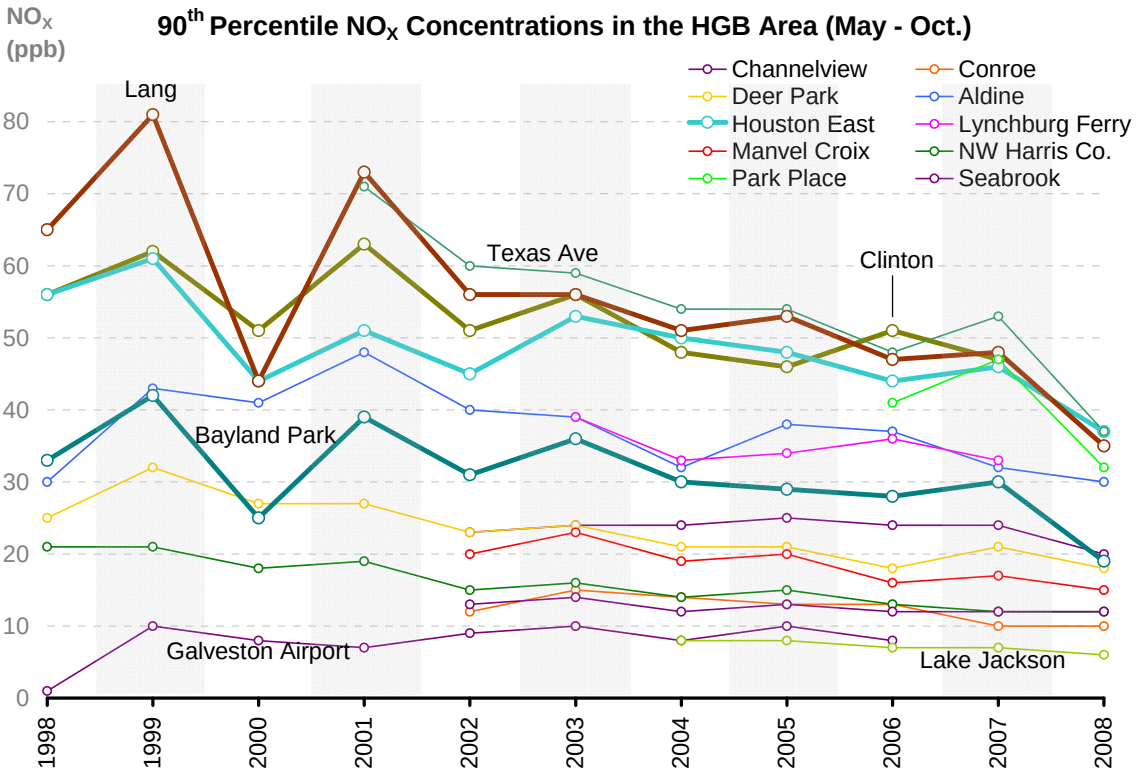

Figure 2-11: 90th Percentile NO_X Concentrations in the HGB Area
90th percentile NO_X concentrations, May to October, 2000 to 2008. Note that highlighted monitors represent some of the larger decreases in 90th percentile NO_X concentrations.

Though the 2007 median value at Clinton (CAMS 403) is lower than at the beginning of the period, it is higher than all recent years back to 2001. The 42 percent jump in median NO_X concentration measured at Clinton (CAMS 403) from 2005 to 2006, is anomalous compared to all other HGB area monitors, save Houston Bayland Park (CAMS 53), the only other monitor also recording an increase (33 percent) from 2005 to 2006. Further work is necessary to confirm whether these trends are statistically significant.

While several monitors recorded large decreases from 2007 to 2008, most others observed only minimal changes over that same period. These large disparities in patterns of ambient NO_X concentrations across the region are appropriate for further investigation, suggesting that larger decreases are not due solely to variations in meteorological conditions, which would be expected

to influence all monitors similarly, though not identically. The differences seem to be related to the relative magnitudes of the overall concentrations: sites with the highest concentrations, which tend to be urban sites, showed the most decrease. More rural sites like Lake Jackson (CAMS 1016) and Conroe (CAMS 65) may reflect slight changes in background values, while more urban sites may reflect actual emission changes.

Similar to ozone, NO_X concentrations in the HGB area appear to be decreasing over time, in large measure the result of the comprehensive suite of NO_X-targeted controls implemented since 2000. Stringent point source NO_X standards have been adopted along with numerous factors affecting mobile source NO_X emissions. Besides normal fleet turnover, as older vehicles are replaced by newer, less polluting ones in the on-road fleet, mobile source NO_X reductions since 2000 could also be due to improvements in the Air Check Texas motor vehicle inspection and maintenance program, expansion of the Low Income Vehicle Repair and Replacement Assistance Program, and expansion of the Texas Emission Reduction Program for diesel trucks and heavy equipment. NO_X concentrations have shown larger decreases in recent years, especially 2008, a year that also recorded some of the lowest ozone concentrations. Ozone formation, however, is not only dependent on NO_X, but also on VOC, whose trends will be investigated in the next section.

2.3 VOLATILE ORGANOC COMPOUNDS TRENDS

Volatile organic compounds (VOC) play a central role in ozone production by oxidizing radicals. This section examines trends in ambient VOC measurements, specifically VOC classified as non-methane hydrocarbons. While methane is an organic compound, total non-methane hydrocarbons (TNMHC) is commonly used to distinguish the more reactive species of organic compounds from methane, which is naturally more pervasive in the atmosphere, less reactive in the ozone formation process, and thus less appealing as a measure of precursor patterns. Trends in TNMHC concentrations, as a proxy for VOC, provide insight into variation in VOC levels in the HGB area over time.

Like most other pollutants described in this paper, TNMHC concentrations shown here are hourly values. Each day's peak hourly value at each automated gas chromatograph (auto-GC) monitor in the HGB area is displayed in Figure 2-12. These daily peaks exhibit large variability and range from less than 100 to more than 10,000 ppbC (parts per billion, carbon). Because TNMHC measurements are characterized by a small number of extremely high values, combined with a large number of low and moderate values, plotting TNMHC on a logarithmic scale is necessary to distinguish trends. The increasing density of the plotted points from earlier to more recent years reflects the deployment of additional auto-GC monitors over time. Unlike NO_X or ozone data, TNMHC peaks do not exhibit a clear seasonal pattern, with maximum TNMHC occurring during various times of the year throughout the eleven-year period. Daily peak TNMHC concentrations do not appear to display any trend, with maximum values appearing to be flat or slightly increasing from 1997 to 2008.

The 90^{th} percentile and median hourly TNMHC concentrations, by year, are plotted on Figure 2-12, and demonstrate a more general picture of VOC trends in the HGB area. Note that the 90^{th} percentile and the median TNMHC are plotted on a separate, linear scale. These statistics were calculated for each year using valid data from all available auto-GC monitors. Unlike the daily peak TNMHC, both the median and the 90^{th} percentile TNMHC show decreasing trends. The 90^{th} percentile TNMHC has exhibited a sizeable decrease, from 433 ppbC to 258 ppbC, or roughly 5 percent annually, over the 1997 to 2008 period, but the decline is even sharper, over 8 percent annually, after 2001. Interestingly, in 2008 both the median and the 90^{th} percentile TNMHC are at the lowest levels compared to all other years of data.

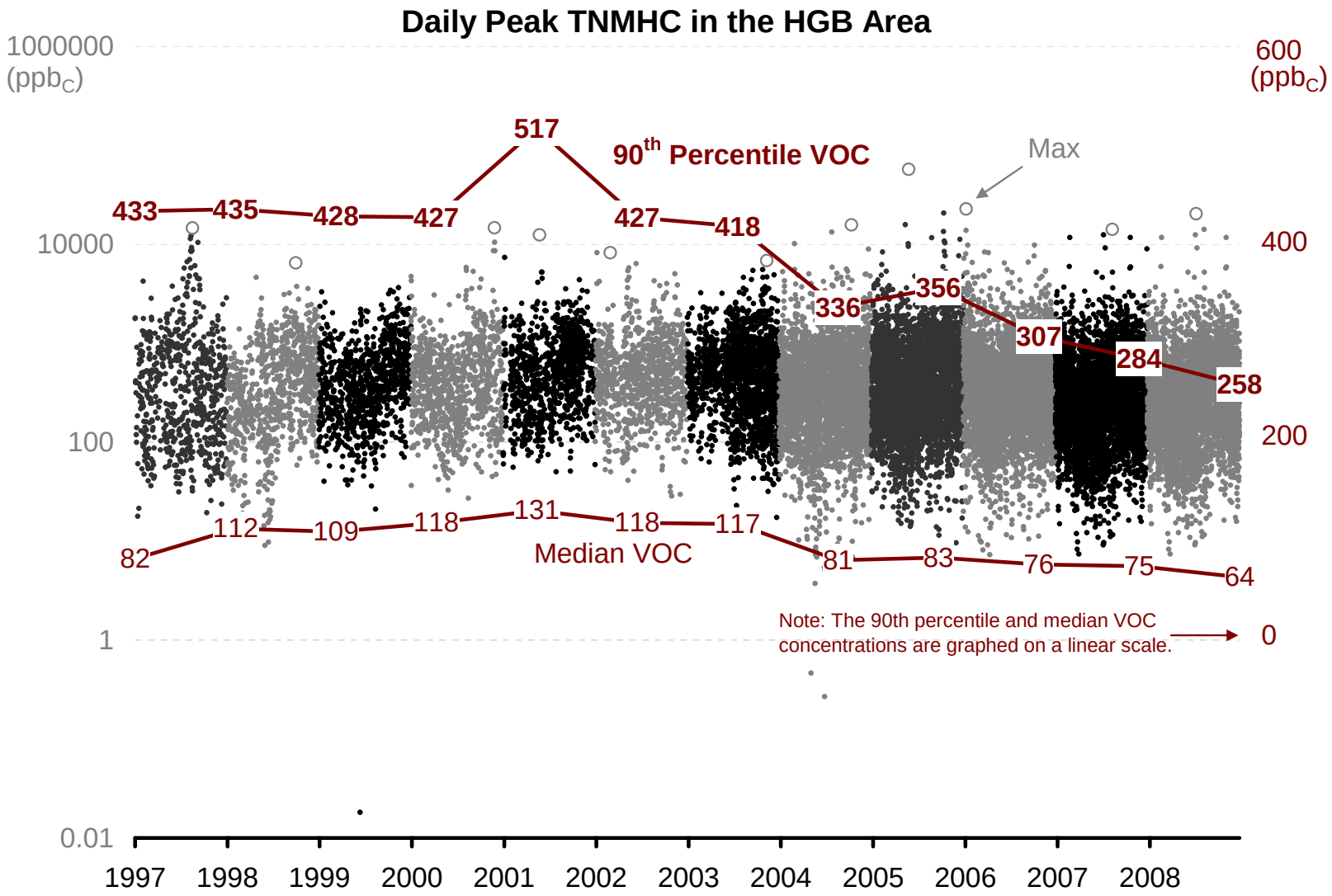

Figure 2-12: Daily Peak TNMHC in the HGB Area

All valid TNMHC data available at the auto-GC monitors was used. Note that the daily peak hourlyTNMHC is plotted on a logarithmic scale and that the daily peaks were calculated at each monitor site for each day. The maximum hourly TNMHC value for each year is marked as a hollow circle. Median and 90th percentile VOC concentrations are for all available monitors and are plotted on a separate linear scale, shown in dark red.

Because VOC concentrations are highly variable spatially, and to better assess trends at individual monitors, 90th percentile TNHMC concentrations at each auto-GC monitor were calculated, and are shown in Figure 2-13. Like overall 90th percentile TNMHC, 90th percentile TNMHC is decreasing at most individual monitors. Smaller decreases are evident at Wallisville Road (CAMS 617), Channelview (CAMS 15), Lake Jackson (CAMS 1016), Mustang Bayou (CAMS 619), and Danciger (CAMS 618), while larger decreases are observed primarily at monitors closer to the Houston Ship Channel. These decreases will be discussed in greater detail in Chapter 3. Note that monitors in Brazoria County (Danciger (CAMS 618), Lake Jackson (CAMS 1016), and Mustang Bayou (CAMS 619)) and Galveston County (Texas City (CAMS 10), Texas City 34th St. (CAMS 620)) tend to report lower 90th percentile TNMHC than monitors located in Harris County. In the past, Clinton (CAMS 403) has recorded the highest TNMHC concentrations, but since 2006, Channelview (CAMS 15) has taken the top spot.

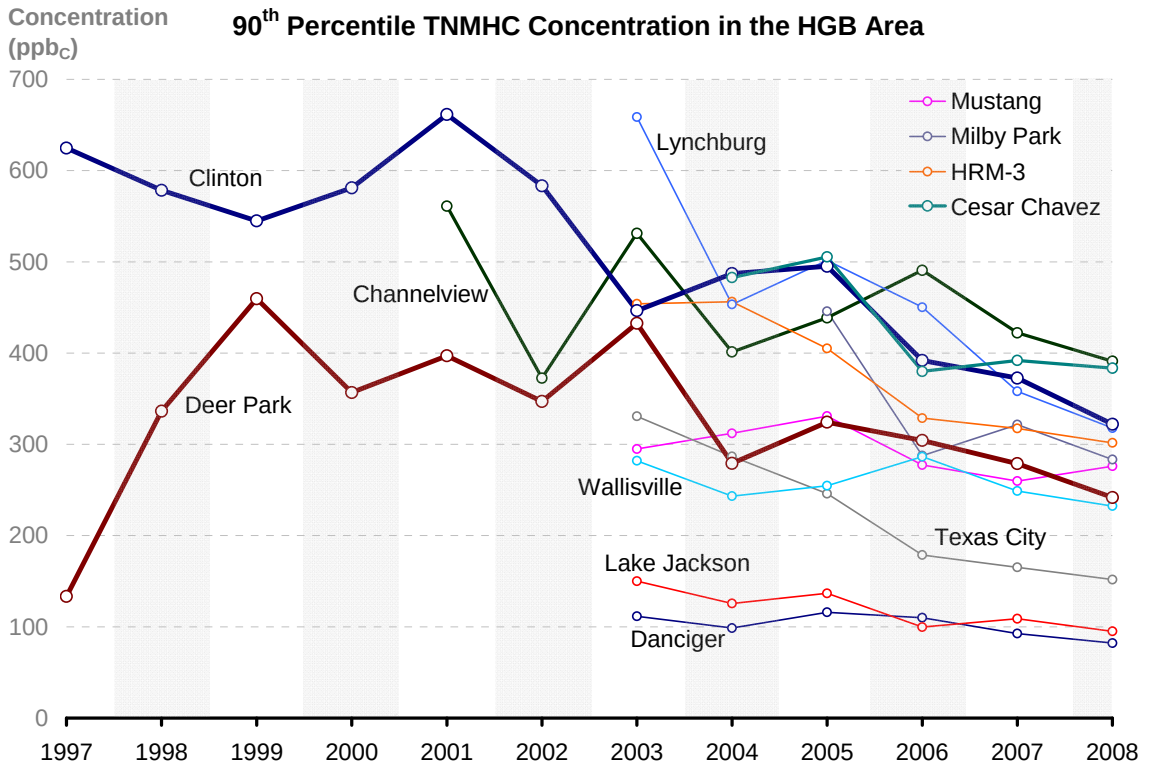

Figure 2-13: 90th Percentile TNMHC Concentration in the HGB Area
TNMHC concentrations calculated at each individual auto-GC monitor. Houston Deer Park (CAMS 35) and Clinton (CAMS 403) are highlighted because they demonstrate long-term trends.

While maximum VOC in the HGB area may not be demonstrating a trend (Figure 2-12), the highest TNMHC concentrations are showing a decline. Further, portions of HGB that typically show the highest VOC concentrations have recently seen a decline in TNMHC. Although it is the highly reactive species of VOC that are most important to ozone formation, it is encouraging to see a drop in total VOC concentrations. The next chapter will provide a more detailed look at these HRVOC concentrations and trends in the HGB Area.

2.4 SUMMARY OF TRENDS IN OZONE AND OZONE PRECURSORS

Identifying and assessing trends in ozone and its precursors provide an initial appraisal of the current ozone situation in the HGB area, the magnitude of progress made to date, and the scale of future challenges. Examination of ozone trends has shown that ozone design values, the statistics used to compare observed ambient ozone levels to the NAAQS, have decreased in the HGB area over the past seventeen years. The eight-hour ozone design value in 2008 was 91 ppb, a 24 percent decrease from the 1991 design value of 119 ppb. The 2008 value is approaching the ozone NAAQS of 85 ppb. A regression analysis of design value on year estimates that eight-hour

ozone design values decreased at the rate of 1.2 ppb per year, which is statistically significant at the 5 percent level ($\alpha = 0.05$). The one-hour ozone design value in 2008 was 147 ppb, a 33 percent decrease from the 1991 design value of 220 ppb. Regression of one-hour design values on year show they decreased at the rate of 3.6 ppb per year, which is even faster than the eight-hour ozone design values.

Examination of design values at individual monitors corroborates these decreases, with over half of those monitors at levels below both the eight-hour standard and the vacated one-hour standard by 2008. Since 1999, the number of eight-hour and one-hour ozone exceedance days occurring in the HGB area has fallen 83 percent and 96 percent, respectively. In just the last three years, the number of eight-hour and one-hour ozone exceedance days has fallen 76 percent and 92 percent, respectively. Decreases in exceedance days are apparent despite an increase in the number of monitors located throughout the HGB area. The ozone season was also determined to be less severe, and to peak at a later date, in recent years.

The total number of eight-hour exceedance days, including multiple counting of days when more than one monitor may have exceeded the standard, fell from a high of 340 in 1995 to 39 in 2007 and just 19 in 2008. Prior to 2007, that number was never below 100, except for one year, 1993, when it was 94. The number of monitors recording an exceedance of the eight-hour ozone standard has fallen by half, from a maximum of 23 in 2003 to only 12 in 2008.

A similar pattern is apparent with the number of exceedances of the one-hour ozone NAAQS. The total number of one-hour ozone exceedance days, including multiple counting of days when more than one monitor may have exceeded the standard, fell from a high of 165 in 1995, to just three in 2008. Those three exceedances occurred at only two monitors. Prior to 2005, the number was never below 50. As recently as 2006, a total of 15 monitors recorded at least one exceedance. This is remarkable progress and has occurred in a fairly short amount of time in an area well known for its air quality challenges.

A variety of methods has been presented for understanding ozone trends in the HGB area. These methods generally agree that ozone concentrations have been decreasing. However, the area still faces challenges in achieving attainment of the 1997 ozone NAAQS. Because ozone formation depends on a multitude of factors, these factors must be investigated and understood in detail before conclusions as to the causes of the observed decreases can be reached.

Similar to ozone, NO_X concentrations in the HGB area are decreasing over time. NO_X concentrations have shown larger decreases in recent years, especially 2008, a year that also recorded some of the lowest ozone concentrations. Though highly variable from season to season, daily peak hourly NO_X also shows a general decreasing trend since 1991. Maximum NO_X concentrations typically occur in winter, and, while erratic, have decreased overall by 41 percent, to 409 ppb, since 1999, though one anomalous extreme value, 809 ppb, occurred in 2003. This is an average of roughly 32 ppb per year, or nearly 6 percent. The drop since the 1991 high of 880 ppb is 54 percent, or over 4 percent annually.

Average daily peak hourly NO_X has dropped even more precipitously, falling 53 percent, or 8 percent per year, from 75 ppb to 35 ppb, since 1999. Since 1991, average NO_X has dropped 68 percent, or over 6 percent per year, from the series high of 110 ppb. Daily peak hourly NO_X also demonstrates a general decreasing trend since 1991. The maximum NO_X concentration typically occurs in the winter, and, while variable, has shown large decreases, especially since 2003. In 2008, maximum daily peak NO_X recorded the lowest value of any previous year back to 1991.
Among individual monitors, favorable trends were noted at Houston East (CAMS 1), where the 90^{th} percentile NO_X concentration decreased 34 percent, and the median decreased 42 percent, between 1998 and 2008. The Clinton (CAMS 403) monitor experienced a drop of 16 percent in the 90^{th} percentile, with a 21 percent decrease in the median between 1998 and 2007 (due to incomplete data in 2008).

Regarding VOC, the 90th percentile hourly TNMHC concentration has exhibited a sizeable decrease, from 433 ppbC to 258 ppbC, or roughly 5 percent annually, over the 1997 to 2008 period, but the decline is even sharper, over 8 percent annually, after 2001. Interestingly, in 2008 both the median and the 90th percentile TNMHC are at the lowest levels compared to all other years of data.

NO_X trends from 1991 to 2008, and VOC trends from 1997 to 2008, show that most monitors in the HGB area experienced decreases in both median and 90th percentile concentrations of these pollutants. Most strikingly, 2008 experienced not only some of the lowest ozone design values in seventeen years, but also some of the lowest NO_X and VOC values. Note that while NO_X and VOC are precursors to ozone formation, meteorology can play an important, if not more significant, role in ozone concentration and precursor trends. The next chapter will take a closer look at local variables that contribute to ozone formation in the HGB area, including meteorology.

CHAPTER 3: RECENT FINDINGS IN LOCAL OZONE DYNAMICS IN THE HOUSTON-GALVESTON-BRAZORIA AREA

Analyses of ozone trends in the HGB area demonstrate that ozone and its precursors in the HGB area have steadily decreased over the past several years. The complexity of ozone formation, however, requires a comprehensive examination of contributing factors. Observed ozone is the aggregate of background ozone and locally produced ozone. Background ozone is either formed by naturally occurring processes, or generated elsewhere and transported into a region. This type of ozone is largely outside the purview of state and local air control authorities. Even much ozone produced locally is difficult, if not impossible, for state and local authorities to control.

This chapter examines patterns of local precursor emissions, local ozone formation and transport, and local meteorology, beginning with a detailed look at spatial and temporal patterns of ozone variability across the region. This is followed by a presentation of recent findings in local patterns of NO_X and VOC emissions, including discussion of emission variability by day of the week. Finally, we explore local meteorological factors and their contribution to local ozone formation. The findings presented here all support the conclusion that reductions in ozone observed in the HGB area over the previous decade are due in large part to real, quantifiable reductions in precursors, rather than anomalous meteorological conditions that are unlikely to recur.

3.1 LOCAL VARIATION IN OZONE

The previous chapter showed that ozone concentrations can vary by monitor and location. Taking this finding one step further, this section employs a spatial interpolation method borrowed from the field of geology to identify which specific parts of the HGB area experience higher or lower ozone concentrations. These patterns guide a more detailed examination of variability in the factors contributing to ozone formation, both across time and space.

Annual eight-hour ozone design values at each monitor in the HGB area were interpolated onto a two dimensional grid using the kriging procedure, a spatial estimation technique. The eight-hour ozone design value is the three-year average of the fourth highest values recorded at a monitor. The kriging procedure uses an inverse distance weighting algorithm to interpolate values for grid cells from nearby monitors, taking into account distances and directions of the monitors. It is most robust where a monitoring network is most dense. Kriging produces estimates of design values at locations that lack monitors. Performing this procedure for multiple years provides additional corroboration of the decreasing temporal trends identified previously. Three years, 2000, 2005 and 2008, were selected for analysis; data was restricted to monitors providing the highest quality measurements, those used for regulatory purposes.

The eight-hour ozone design values for each monitor in the HGB area for the selected years are displayed in Figure 3-1. The highest eight-hour ozone design values in 2000 exceeded 109 ppb and occurred north of downtown Houston at Houston Aldine (CAMS 8), east of downtown at Houston Deer Park (CAMS 35), and west of downtown at Houston Bayland Park (CAMS 53) and Houston Croquet (CAMS 409). The lowest eight-hour ozone design values in 2000 occurred northwest of downtown Houston at Lang (CAMS 408), and to the south at Clute (CAMS 11). Note that even the minimum eight-hour ozone design values in 2000 were above the 85 ppb eight-hour ozone NAAQS.

By 2005, eight-hour ozone design values had dropped across the region. While the highest concentrations still occurred at Houston Bayland Park (CAMS 53) and Houston Deer Park (CAMS 35), they were no longer observed in the Houston Aldine (CAMS 8) area. Further, the 2005 peaks are much lower, between 100 and 103 ppb. The minimum eight-hour ozone concentration is still observed at Lang (CAMS 408), but low ozone also occurs to the northeast at Houston North Wayside (CAMS 405), to the north at Conroe (CAMS 65), and to the south at Galveston. The minimum eight-hour ozone concentration in 2005 is below the NAAQS.

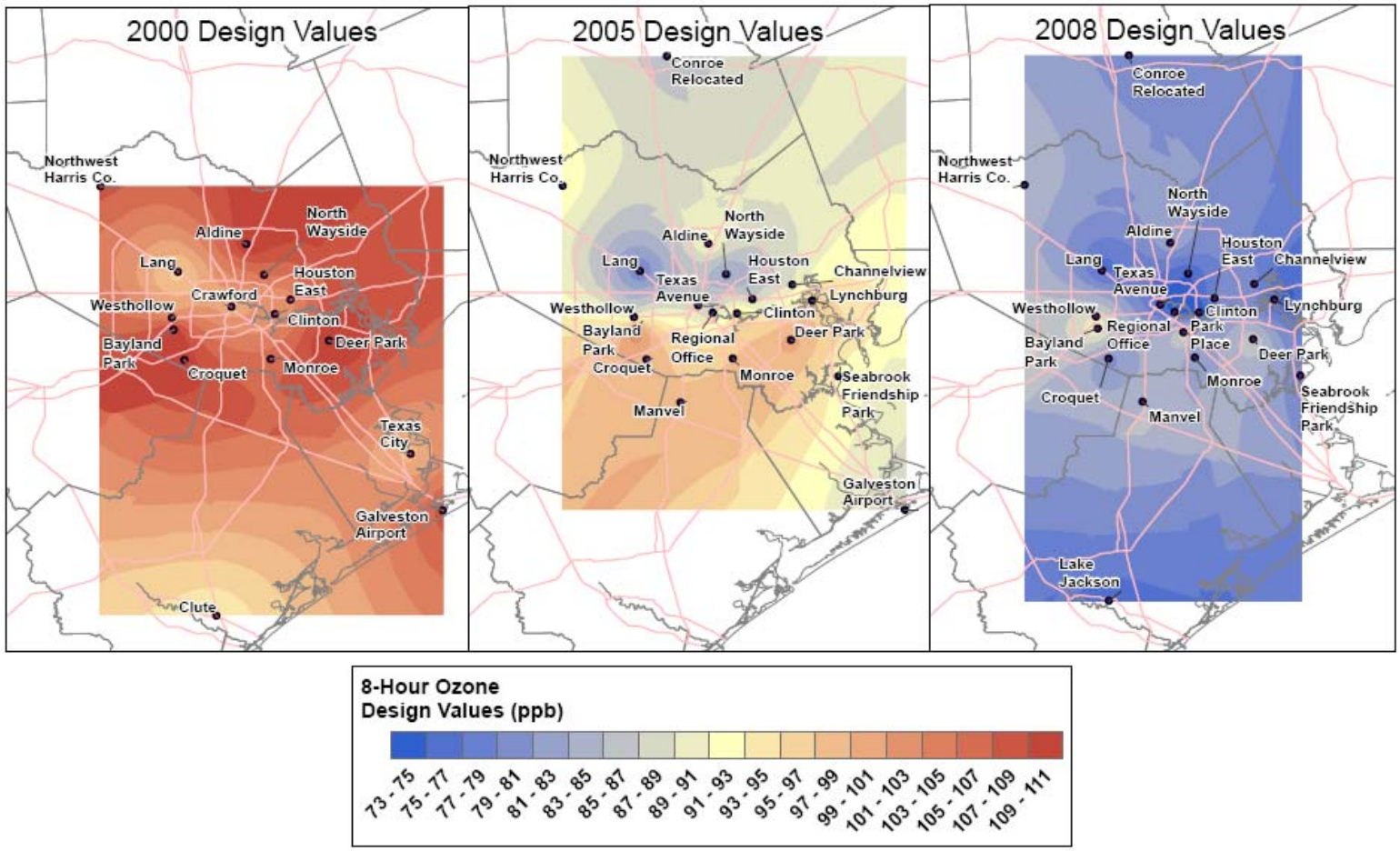

Figure 3-1: Eight-Hour Ozone Design Values for 2000, 2005, and 2008
Kriging interpolation was used to estimate design values in areas between monitors. Red represents higher ozone design values while blue represents lower ozone design values. The outermost monitors in each direction bound the area of interpolation. Note that as some monitors are shut down and others are opened, the interpolation domain changes.

In 2008, eight-hour ozone design values dropped even further. Ozone concentrations are substantially lower across a large part of the HGB area, with the kriging model predicting design values below the eight-hour ozone NAAQS at many locations. Maximum eight-hour ozone is now considerably lower, between 89 ppb and 91 ppb, and though it still occurs at Houston Bayland Park (CAMS 53) and Houston Deer Park (CAMS 35), a new monitor at Park Place (CAMS 416) also measured ozone in this range. The minimum eight-hour ozone in 2008 is much lower, and while there is still a minimum at Lang (CAMS 408), it is now much lower in the area surrounding Houston North Wayside (CAMS 405), Texas Avenue, Clinton (CAMS 403), and the Houston Regional Office (CAMS 81) of the TCEQ.

Notice that while the concentrations of eight-hour ozone are less severe, the areas that experience the highest and lowest ozone remain the same. Spatial interpolation shows that high ozone concentrations continue to occur south of downtown Houston, and stretch east from the Houston Ship Channel to west, near Houston Bayland Park (CAMS 53). The lowest ozone values are found to the south along the coast, north towards Conroe (CAMS 65), and to the northwest of downtown Houston, at Lang (CAMS 408).

The kriging method can also be employed to investigate the geographic origins of high ozone concentrations. Studies during the TexAQS 2000 field study reported that the highest ozone in the HGB area occurs in plumes emanating from industrial areas (Daum et al., 2004; Kleinman et al., 2005; Ryerson et al., 2003; Berkowitz et al., 2005). As these plumes are transported across the region, they can be tracked by the high ozone concentrations recorded at successive downwind monitors as the day progresses. An analysis of the time of day of maximum ozone at each monitoring site can confirm or challenge conclusions of the field study about these origins by revealing spatial patterns of ozone formation and movement.

Comparison of temporal patterns of ozone formation on days with high ozone concentrations to days with low ozone concentrations can identify unique features of high ozone days that may corroborate conclusions about sources of high ozone. Daily maximum ozone concentrations were divided into two groups: days with values exceeding the eight-hour ozone NAAQS, and days not exceeding the NAAQS. The time of day when peak ozone was recorded at each monitor was determined for each day, then averaged across the two groupings of days. Only monitors that report data to the EPA were included. Days were restricted to March through November to exclude months when few or no exceedance days occur in the HGB area.

Spatial interpolation with kriging was performed on the average time of day of peak ozone at each monitor, for both low and high ozone days, to identify when and where ozone peaks, on average, throughout Houston. Maps of the time of peak ozone in the HGB area are found in Figure 3-2. The left map shows that on days with low eight-hour ozone values, daily maximum values are recorded in the Galveston area early in the day, between 11:30 a.m. and 11:45 a.m. Inland monitors record their highest daily values at progressively later times of day, as monitors are located further inland from the Gulf Coast. On low ozone days, the earliest ozone maxima occur near the coast, and the latest occur in the Conroe (CAMS 65) area between 2:00 p.m. and 2:15 p.m. This pattern of ozone concentrations is consistent with the occurrence of the sea breeze, which, as mentioned in Chapter 1, often dominates local weather during the summer in the absence of synoptic, or large-scale, weather influences. After the plume is carried past a monitor, ozone levels often drop, reflecting the cleaner maritime air behind the sea breeze front.

By contrast, the right map of the daily pattern on high eight-hour ozone days looks quite different. Daily maximum ozone concentrations are observed earliest in the industrial areas, and successively later at sites that are progressively farther away from these areas. This pattern is consistent with high ozone forming first in the industrial areas, and being transported outward to suburban and rural sites later in the day. Maximum ozone occurs latest at Lake Jackson (CAMS 1016), Clute (CAMS 11), Northwest Harris Co. (CAMS 26), and Conroe (CAMS 65), the sites at the greatest distance from the industrial area.

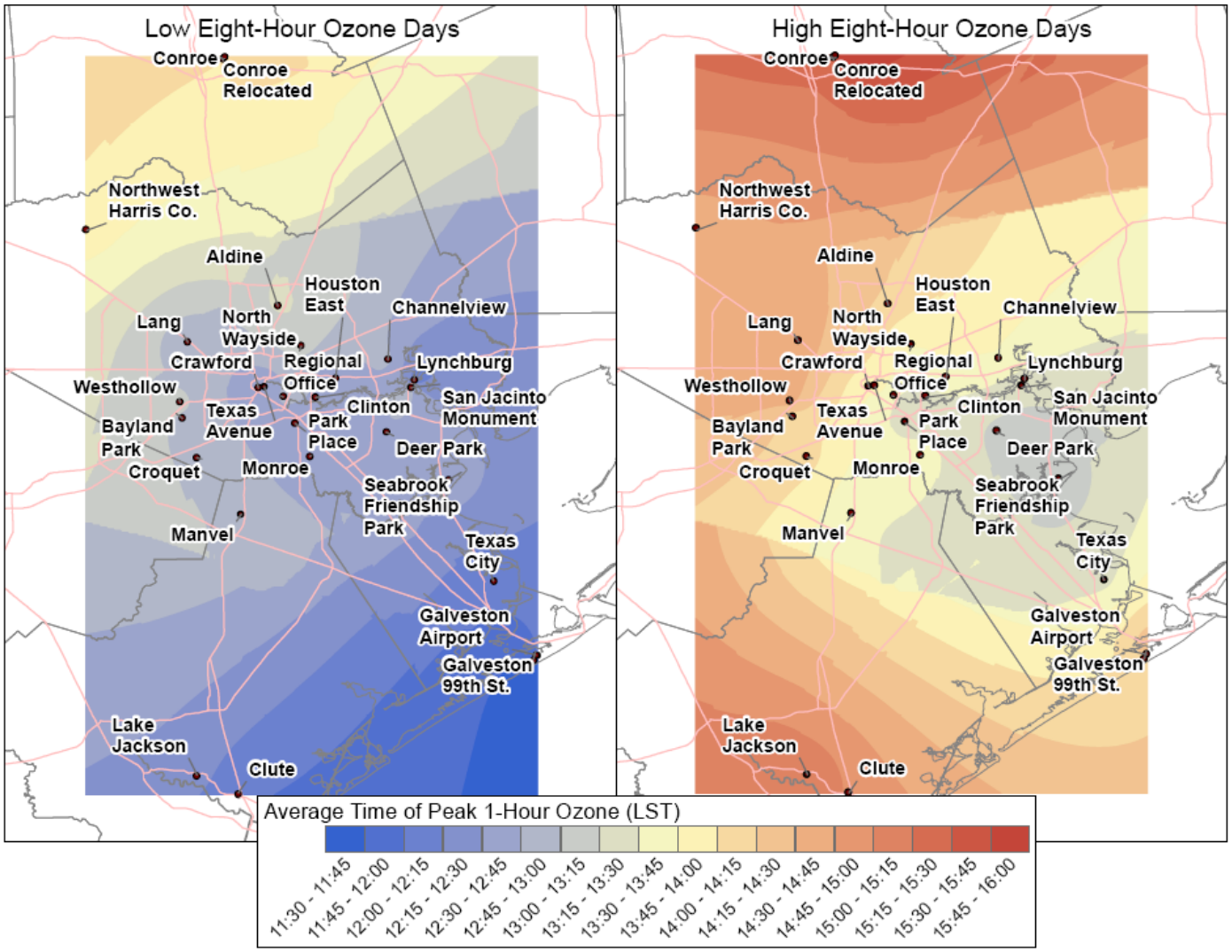

Figure 3-2: Time of Day of Peak Hourly Ozone

Spatial interpolation with kriging was used to determine the time of day of peak ozone in non-monitored areas. All available monitors satisfying regulatory criteria were used. Note reds represent times later in the day, while blues represent times earlier in the day. The left map shows days time of day of peak ozone on days when ozone was below 85 ppb, and the right map shows time of day of peak ozone on days when ozone was 85 ppb or greater. The time of peak ozone was averaged over the months of March to November, 1998 to 2008.

The time of day of maximum ozone on high eight-hour ozone days represents a composite pattern: high ozone formed in industrial areas is carried by winds to Conroe (CAMS 65) or Lake Jackson (CAMS 1016) on some days, and to western Houston on others. Combined with the earlier spatial design value analysis, it appears that the highest ozone concentrations are formed in the Houston Ship Channel, a heavily industrialized area, and are then transported to the west, where the highest ozone concentrations are routinely observed. To corroborate these findings, a careful analysis of ozone precursors, NO_X and VOC, along with meteorological patterns, follows.

3.2 SPATIAL VARIATION IN NITROGEN OXIDES

Like ozone, NO_X trends in Chapter 2 indicated that it varies both temporally and spatially. Table 3-1 shows a clear spatial trend in NO_X in the HGB area. Median NO_X concentrations from May to October 2008 in the HGB area range from 2 parts per billion (ppb) at the Lake Jackson (CAMS 1016) monitor to 14 ppb at the Texas Avenue monitor. Only active regulatory monitors with at least 75 percent data completeness for the period were included. Monitors with the lowest concentrations tend to be located in the southern portion of the HGB area, while monitors with higher concentrations tend to be located in eastern and central Houston.

Table 3-1: Median NO_X Concentrations in the HGB Area from May to October, 2008

Site	2008 median NO_X concentration (May-Oct)
	ppb
Houston Texas Avenue C411	14
Lang C408	11
Houston East C1	11
Houston Aldine C8/C108/C150	9
Park Place C416	8
Channelview C15/AH115	8
Houston Deer Park 2 C35/139	5
Northwest Harris Co. C26	4
Manvel Croix Park C84	4
Conroe Relocated C78	4
Seabrook Friendship Park C45	3
Houston Bayland Park C53	3
Lake Jackson C1016	2

The trend in spatial NO_X patterns is clearer when displayed on a map. While trends during the summer months are most relevant to ozone formation, NO_X trends in all months were used to assess spatial trends. All monitors with available data in each year were used in this analysis, despite the fact that some monitors were shut down and others were opened during that time. Similar to the ozone plots, ordinary kriging interpolation was used to determine the spatial variation of NO_X for each year, from 2000 to 2008, in the HGB area.

Figure 3-4 and Figure 3-5 illustrate the spatial variation of median NO_X in the HGB area. NO_X concentrations appear to be decreasing over space and time in areas such as in Lang (CAMS 408), Houston Aldine (CAMS 8) C8, Bayland C53, and Houston C1 East. Urban Houston, which is dominated by mobile source emissions, has the highest NO_X levels, but those levels have been decreasing from 2000 to 2008. As seen in the trend analysis, the lowest median NO_X values in 2008, which are found on the periphery of the HGB area, are 5 ppb at the Northwest Harris C26 site, and 4 ppb at the Seabrook Friendship Park C45 site.

NO_X concentrations at the Houston East (CAMS 1) monitor, which is adjacent to Interstate 10, have dropped from 22 ppb to 16 ppb over the 2000 to 2008 period. Because mobile source emissions are such a large source of NO_X, sites near major roadways might not always be

representative of NO_X in a larger area, which might be the case for Lang (CAMS 408), near Highway 290, and Houston Aldine (CAMS 8), near Highway 59. These sites, however, may be useful in examining trends of mobile source emissions, since the close proximity to the highways may allow the NOx to arrive at the monitor before substantial reaction has occurred.

The Houston Ship Channel area is heavily industrialized, with varying spatial densities of industries that emit both NO_X and VOC. Median NO_X in the Houston Ship Channel area appears to vary, depending on the location of the monitor within the Houston Ship Channel. Median NO_X concentrations in the Houston Ship Channel ranged from 10 to 42 ppb from 2000 to 2008, depending on the location of the monitor. For example, in 2008, the monitor at Houston East (CAMS 1), located on the west end of the Houston Ship Channel, recorded a median NO_X concentration of 16 ppb while the monitor at Lynchburg Ferry (CAMS 1015), located on the east end of the Houston Ship Channel, recorded a median NO_X of 10 ppb.

Because of the variety of NO_X sources, there can be a variety of reasons why NO_X concentrations in HGB have been decreasing. One potential cause for the decrease in NO_X over the entire HGB area is on-road vehicle fleet turnover, though this hypothesis has not yet been rigorously tested. Note that transport of industrial NO_X can obscure the patterns of mobile source emissions. The cause for the drop in NO_X in the urban HGB area may be due to regulatory controls on NO_X emissions imposed on industrial sources. Notice that, while the magnitude of median NO_X has decreased, the areas that experience the highest NO_X concentrations remain the same, with the exception of the area around the Houston Ship Channel, which appears to no longer show a peak in median NO_X in 2008. An investigation of other variables in ozone formation, such as VOC and meteorology, might help to explain not only the patterns in ozone, but also the patterns that we are seeing in NO_X concentration.

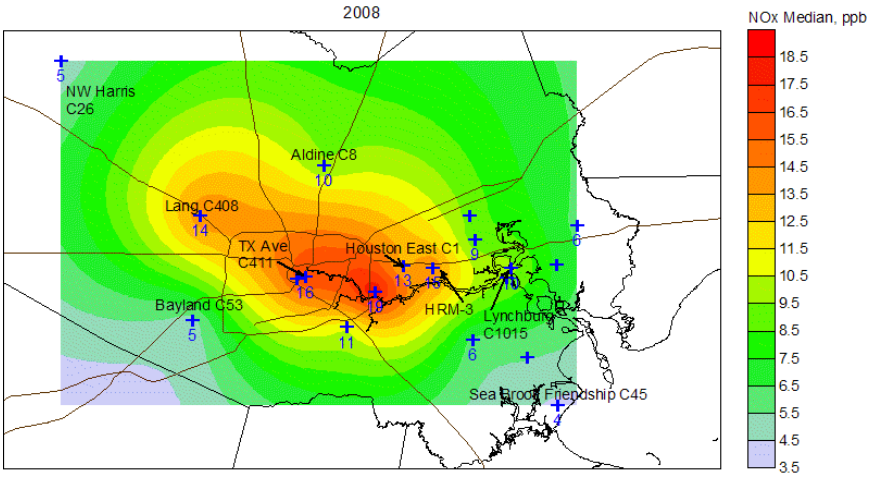

Figure 3-3: Median Hourly NO_X Concentrations in the HGB Area, 2008
Note that all monitors with data available in 2008 were used. The '+' represents the location of the monitor and the number below is the median NO_X concentration at that site. The red colors represent higher NO_X medians while the green and gray colors represent lower NO_X concentrations.

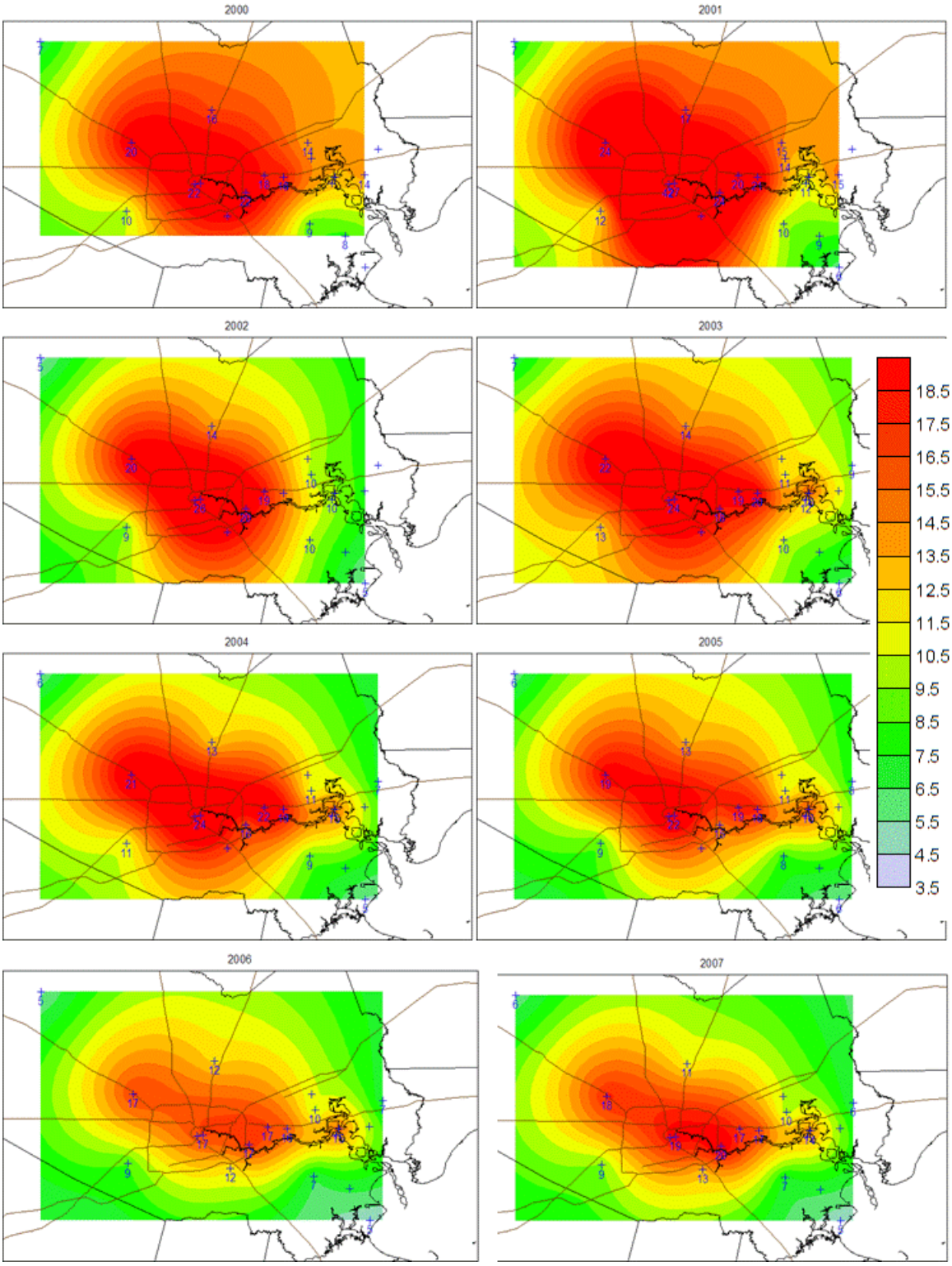

Figure 3-4: Median NO_X Concentrations (ppb) for the HGB Area, 2000 to 2007

Note that the maps from each year do not necessarily have the same number of monitors. Only sites with data for a particular year are represented on the maps; then NO_X concentrations ar those sites are representaed as a number beneath the '+' symbol. Depending on the number of sites, different spatial NO_X patters are possible. Some of the contours are extrapolated, for examonle, the far northeast corner of the contour domain.

3.3 RELATIONSHIP OF VOLATILE ORGNIC COMPOUNDS TO OZONE FORMATION

Ozone results from photolysis of nitrogen dioxide (NO_2) into nitric oxide (NO) and an oxygen atom (O), in the presence of sunlight. The oxygen atom quickly reacts with an oxygen molecule (O_2) to form ozone (O_3). Volatile organic compounds (VOC) enhance ozone formation via a series of reactions that result in NO ultimately becoming NO_2; this enables further formation of O_3 via photolysis. In the Houston-Galveston-Brazoria (HGB) area, emissions from numerous petrochemical plants result in downwind plumes that are typically rich in both NO and VOC, generating large amounts of NO_2 and enabling production of large amounts of ozone. More importantly, large amounts of highly reactive VOC (HRVOC), such as ethene (also known as ethylene) and propene (also known as propylene), which promote especially rapid formation of ozone, are emitted in the HGB area. In 2006, industrial sources in the area reported nearly 6,000 tons of HRVOC emissions (TCEQ, 2009).

In the 2000 Texas Air Quality Study (TexAQS 2000), in the highest-reactivity samples downwind of HGB petrochemical plants, scientists found that large HRVOC emissions led to VOC reactivities that were more than three-fold greater than those from comparable samples taken in Phoenix and Philadelphia (Daum et al, 2004). Moreover, in evaluating two key metrics, ozone production rate and ozone production efficiency, researchers found additional evidence of the differences between Houston and other cities. Ozone production rate, referred to as $P(O_3)$, is a measure of how quickly ozone is formed from available precursors; researchers in TXAQS 2000 found that $P(O_3)$ in the 10 percent of samples with the highest VOC reactivity ranged from 40 to 300 percent greater than the top 10 percent of the next-highest of four cities studied – the above two, plus Nashville, Tennessee, and New York City (Kleinman et al, 2005). Further, ozone production efficiency – the number of ozone molecules yielded per molecule of NO_X oxidized – in plumes downwind of three HGB area petrochemical plant clusters was found to range from ten to eighteen. By comparison, Ryerson, et al. (2003) found the urban plume from Nashville, yielded only one to four molecules of O_3 per oxidized molecule of NO_X, and plumes from rural power plants yielded zero to eight molecules.

The TCEQ has been collecting VOC measurements in the HGB area consistently for over a decade. This section examines implications of this long-term series of measurements, including temporal and geographic trends. Data from the TCEQ monitoring network from 1995 to 2008 are analyzed to identify trends in ambient concentrations of HRVOC, trends in emissions in specific source regions within the HGB area, and more detailed trends in overall VOC concentrations than those examined in Chapter 2. Findings from the two intense, though shorter-term, Texas Air Quality Studies in 2000 and 2005-2006 are also considered in the context of this longer temporal series to broaden understanding of the conclusions of the studies.

3.3.1 Ambient HRVOC Concentrations

Since the mid-1990s, the TCEQ has collected 40-minute measurements, on an hourly basis, of some 45 VOC compounds using automated gas chromatograph (auto-GC) instruments. Initially, measurements were collected at just one site (Clinton (CAMS 403)), but in subsequent years, auto-GC monitors have been added to new sites (see Figure 3-5). Currently, eight sites, listed in Table 3-2, along or near the Houston Ship Channel, along with three in Brazoria County and one in Texas City, are collecting VOC measurements with auto-GCs.

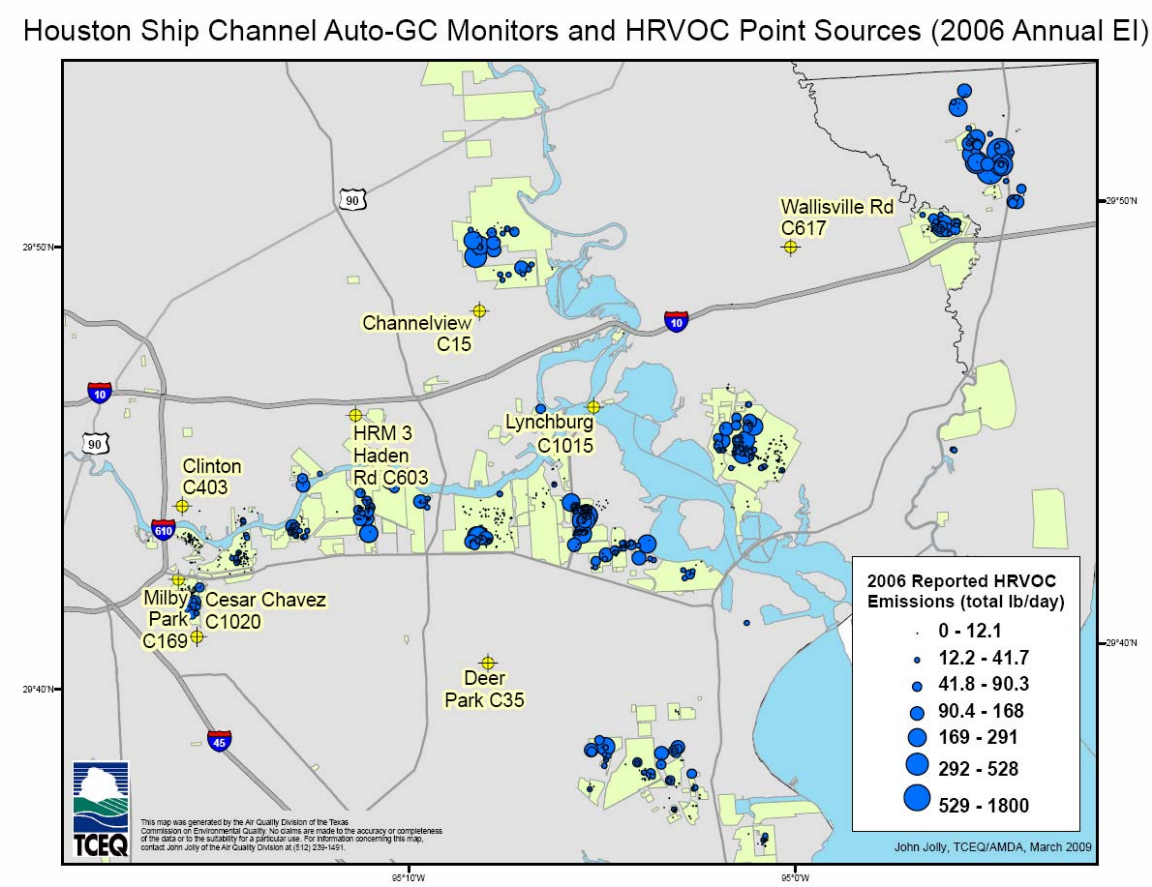

Figure 3-5: Houston Ship Channel Auto-GC Monitors
Locations of auto-GC monitors are noted (yellow circles with cross hairs), along with 206 reported point source HRVOC emissions points (blue circles) and plant boundaries (light green polygons).

Long-term monitoring of dozens of species at multiple monitors for multiple years has yielded hundreds of thousands of individual measurements, facilitating detailed analysis of long-term ambient VOC patterns in the HGB area. This surfeit of data was reduced to the following six compounds, from 1995 to 2008, for further analysis: ethene, propene, 1,3-butadiene, 1-butene, c-2-butene, and t-2-butene.

Table 3-2: Auto-GC Monitors in the Houston Ship Channel Area

site name	CAMS	AIRS code	latitude	longitude	city	start date
Channelview	C15/AH115		482010026		29.8025	-95.1256
	Channelview		8/3/2001			
Houston Milby Park	A169	482010069	29.7062	-95.2611	Houston	2/19/2005
HRM-3 Haden Road	C603/A114		482010803		29.7483	-95.1811
	Houston	8/20/2001				
Lynchburg Ferry	C1015	482011015	29.7646	-95.0780	Houston	5/24/2003
Clinton	C403/C304/AH113		482011035		29.7337	-95.2576
	Houston	7/1/1995				
Houston Deer Park 2	C35	482011039	29.6700	-95.1285	Deer Park	1/5/1997
Cesar Chavez	C1020	482016000	29.6844	-95.2536	Houston	4/13/2004
Wallisville Road	C617	482010617	29.8214	-94.99	Baytown	6/5/2003

Trends at each of the eight Houston Ship Channel monitors were examined. Data from the four other auto-GC monitors were analyzed only for trend slope and possible statistical significance of trends. Daily geometric means were computed from valid ambient hourly measurements for days with at least 18 valid hours of data. A geometric mean was calculated by taking the log of each

of the measurements, averaging these logs, then exponentiating (calculating the antilog) of this mean log value. The geometric mean is a preferable statistic to median or arithmetic (ordinary) mean for evaluating the central tendency of data when the data are skewed, that is, when the data are not symmetrically, or normally, distributed, but clustered around extreme high or low values. It is more robust than an ordinary average, meaning its value is not greatly influenced by one or a few very high or very low values. Many distributions of pollutant measurements in the HGB area are skewed. Monthly geometric means were also computed with a 75 percent data completeness criterion for valid days in a month.

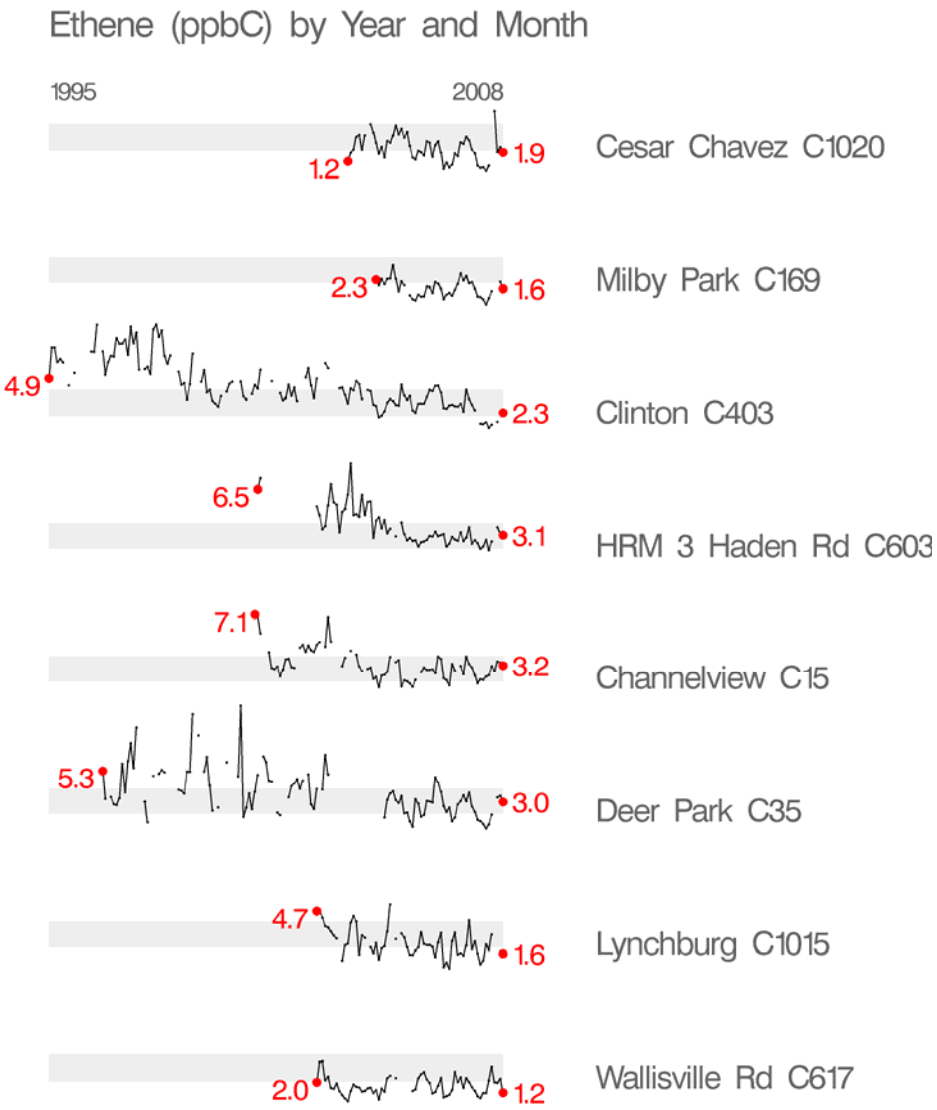

Figure 3-6: Monthly Geometric Mean Ethene Concentrations

Monthly geometric mean ethene concentrations at eight Houston Ship Channel monitors, July 1995 through December 2008. Monitors are sorted from west (top) to east (bottom). Grey bars denote 25th percentile (2.0 ppbC) through 75th percentile (4.0 ppbC) range, computed from the aggregation of valid data at all eight monitors. Months with incomplete data are excluded and appear as gaps in the data series.

Figure 3-6 shows monthly geometric mean ethene concentrations, ordered according to the monitor location from west to east. Grey bars denote the range of values from the 25th through 75th percentile concentrations, for all monitors. Noteworthy in this figure is the frequency of extremely high values recorded during the 1990s at Clinton (CAMS 403), at the western end of the Houston Ship Channel, and Houston Deer Park (CAMS 35), in south central Houston Ship Channel. These were the only monitors operating during the early years of this period; this pattern suggests that high ethene concentrations were not restricted to certain areas of the Houston Ship Channel, but were somewhat geographically widespread.

For four consecutive years, July 1995 through July 1999, valid monthly geometric mean concentrations at Clinton (CAMS 403) exceed the 75th percentile of the multi-decade series. Houston Deer Park (CAMS 35) also exhibited high concentrations in the first several years, including the highest mean value for any complete month, 10.2 parts per billion, carbon (ppbC) in March 2001. By contrast, few monthly mean concentrations exceeded the 75th percentile in the most recent four years, 2005 through 2008.

Though measured ethene and propene concentrations show a large degree of variability at all auto-GC monitors, downward trends are apparent at seven of the eight; only Wallisville Road (CAMS 617) appears to show no decrease. A statistical trend analysis, described below, provides further insight into this.

Peak monthly geometric mean ethene concentrations at all monitors, 6.9 ppbC and 8.4 ppbC in 2003 and 2004 respectively, decreased to 5.6 ppbC in 2005, 4.9 ppbC in 2006, and 4.5 ppbC in 2007, before climbing to 5.1 ppbC in 2008. This decline in ambient ethene concentrations suggests that ethene emissions in the Houston Ship Channel are declining, though meteorology, which will be discussed in a later chapter, could be responsible for some or all of this decline in mean concentrations.

Similar to Figure 3-6, Figure 3-7 displays monthly geometric mean concentrations of propene for the eight Houston Ship Channel area auto-GC monitors. Again, Clinton (CAMS 403) and Houston Deer Park (CAMS 35) show higher concentrations in earlier years compared to recent ones; however, the magnitude of concentrations at the two monitors are dissimilar, unlike ethene, suggesting elevated propene concentrations are more geographically limited than elevated ethene concentrations. Two other eastern Houston Ship Channel monitors, Channelview (CAMS 15) and Lynchburg Ferry (CAMS 1015), report concentrations well above the 75th percentile in 2003, and to a lesser extent in 2004 and subsequent years, suggesting there are greater propene emissions in the eastern Houston Ship Channel than the western Houston Ship Channel. Note, however, that the relatively fast reactivity of propene, compared to ethene, may explain part or all of the low concentrations seen in the western Houston Ship Channel.

Similar analyses were performed for 1,3-butadiene and the isomers of butene; however, trends in these pollutants can be difficult to interpret, as their relatively low concentrations are frequently within accepted measurement uncertainty. Further work is needed before trend estimation for these compounds can be considered accurate.

Though still quite variable from month to month, pervasive decreases, some of them relatively steep, suggest that overall industrial emissions of both ethene and propene have decreased considerably since 1995. This agrees with early findings reported from the 2005-2006 Texas Air Quality Study (TexAQS II) that ethene emissions along the Houston Ship Channel have decreased approximately 40 percent from 2000 to 2006, even after correcting for meteorological effects (Cowling et al, 2007).

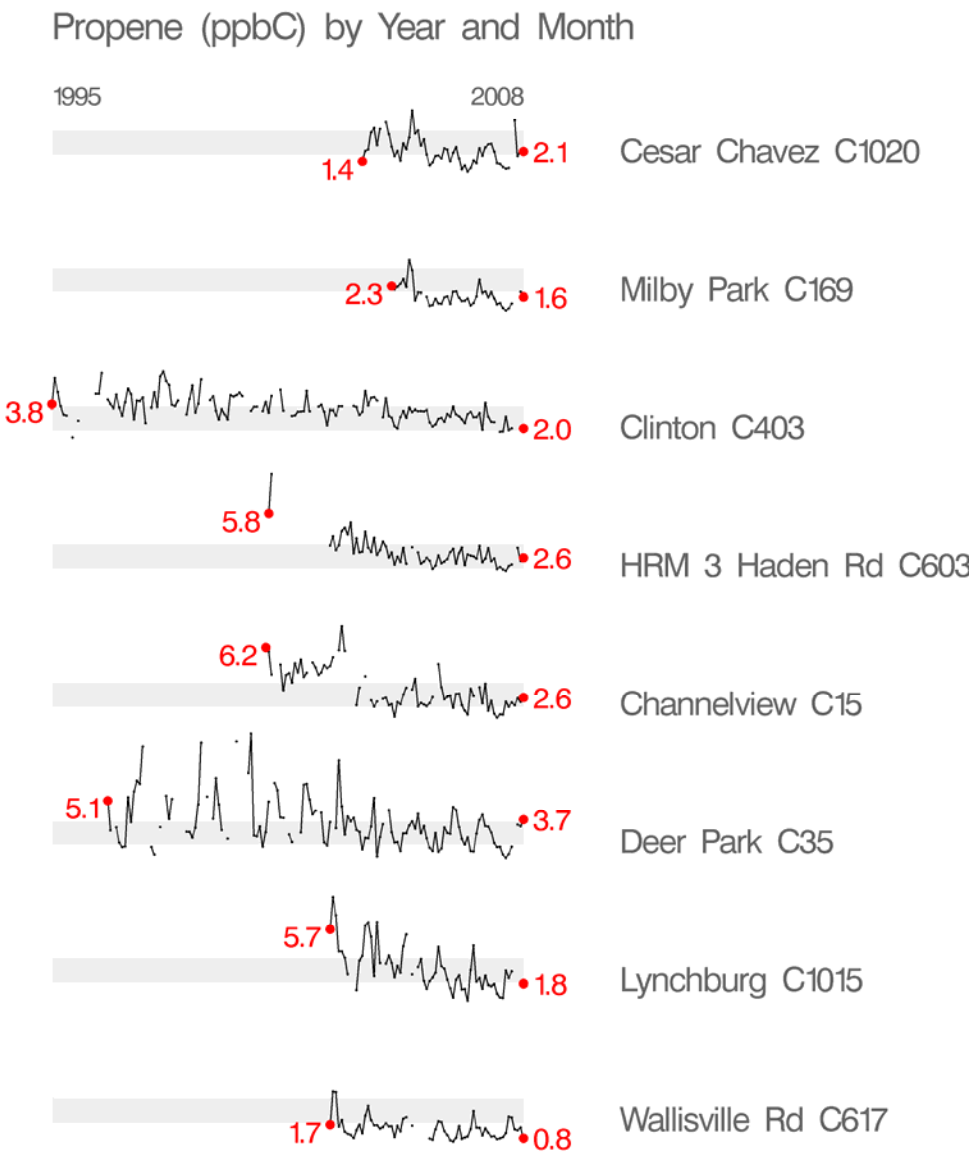

Figure 3-7: Monthly Geometric Mean Propene Concentrations

Monthly geometric mean propene concentrations at eight Houston Ship Channel monitors, July 1995 through December 2008. Monitors are sorted from west (top) to east (bottom). Grey bars denote 25th percentile (1.9 ppbC) through 75th percentile (3.6 ppbC) range, computed across all monitors. Months with incomplete data are excluded, and appear as gaps in data series.

A preliminary analysis was performed to verify whether decreases observed at 12 auto-GC monitors (eight near the Houston Ship Channel plus four others) were statistically supportable. Ordinary least squares regression lines were fit to the monthly geometric mean ethene and propene concentrations, using an index of month, where the first recorded month was given a value of zero. Results of these fits are reported in Table 3-4. In 23 of 24 combinations (2 compounds times 12 monitors), concentrations decreased across the respective study periods, with R^2 values ranging from 0.045 to 0.549. Eight of 12 monitors recorded statistically significant decreases for ethene, including six of eight Houston Ship Channel monitors. All 12 monitors recorded statistically significant decreases for propene. However, caution must be exercised when interpreting these results. First, some of the computed R^2 values are very low, confirming there is a substantial degree of variation in the measured values, with little of it explained by a simple linear model. Further statistical testing and verification, such as testing for and correcting possible autocorrelation, is necessary to fully validate these models.

Table 3-3: Parameter Estimates of Monthly Geometric Mean Concentrations Trends

	ethene				propene			
monitoring site	N	slope	intercept	R^2	N	slope	intercept	R^2
Houston Ship Channel-area auto GC monitors:								
Cesar Chavez C1020	52	-0.019*	2.74	0.09	52	-0.025*	2.86	0.16
Channelview C15/AH115	62	-0.017*	3.85	0.22	62	-0.039*	4.64	0.49
Clinton C403/C304/AH113	60	-0.032*	4.75	0.44	62	-0.018*	3.85	0.36
Houston Deer Park 2 C35	54	-0.033*	4.12	0.25	65	-0.026*	4.09	0.22
HRM-3 Haden Road C603/A11456			-0.051*	5.37	0.55	55	-0.026*	3.82
	0.42							
Houston Milby Park C1	39	-0.011	1.88	0.06	39	-0.021*	2.05	0.20
Lynchburg Ferry C1015	56	-0.029*	3.41	0.24	56	-0.059*	4.89	0.42
Wallisville Road C617	55	-0.002	1.79	0.00	55	-0.017*	2.08	0.17
Non-Houston Ship Channel-area auto-GC monitors:								
Mustang Bayou C619	53	-0.008*	0.72	0.20	53	-0.006*	0.83	0.13
Danciger C618	56	-0.003	0.57	0.05	56	-0.006*	0.78	0.16
Lake Jackson C1016	50	-0.006	1.00	0.05	50	-0.007*	0.77	0.18
Texas City 34th St. C620	59	-0.027*	2.43	0.50	59	-0.020*	2.19	0.37

*Significant at the 5 percent (0.05) level. Significance levels for intercepts are not reported. Parameter estimates from ordinary least squares fits of monthly geometric mean concentrations of ethene and propene on an index of month, by monitoring site and compound.

3.3.2 Geographic Patterns in HRVOC Measurements Near the Houston Ship Channel

The next analysis showed that, for some HRVOC, geographic patterns are apparent. Wind speed and wind direction measurements, collected in tandem with HRVOC concentrations at the Houston Ship Channel auto-GC monitors, were used not only to identify these patterns, but also to track their changes over time. Radar plots of geometric mean concentrations of ethene and propene, by wind direction, were plotted, superimposed on maps of the Houston Ship Channel, and displayed in Figures 3-8 through Figure 3-11.

These plots consist of jagged rings encircling a monitor. Each ring around a particular monitor represents the geometric mean concentration of the subject HRVOC at each of the 360 degrees surrounding the monitor, for a particular year. The distance from the origin to any point on the ring is proportional to the concentration of HRVOC arriving at the monitor from that direction. For example, Figure 3-9 shows that in 2003 at Houston Deer Park (CAMS 35), the highest mean ethene concentration, 16 ppbC, occurred when winds were blowing from the northeast, suggesting there may be large ethene emissions sources upwind of Houston Deer Park (CAMS 35) in that direction.

In order to help interpret these graphs, it is useful to describe a couple of hypothetical scenarios. In the first one, if HRVOC did not vary when winds arrived from different directions, the ring would be a smooth circle. Conversely, in the second scenario, if HRVOC were detected only when winds arrived from a single direction, the ring would simply be an elongated spike pointing in that direction.

It can be seen in Figures 3-8 through 3-11 that for the Houston Ship Channel monitors, there is typically a strong directional association with mean concentration. The directional spikes seen in these rings are referred to as “lobes” in this section.

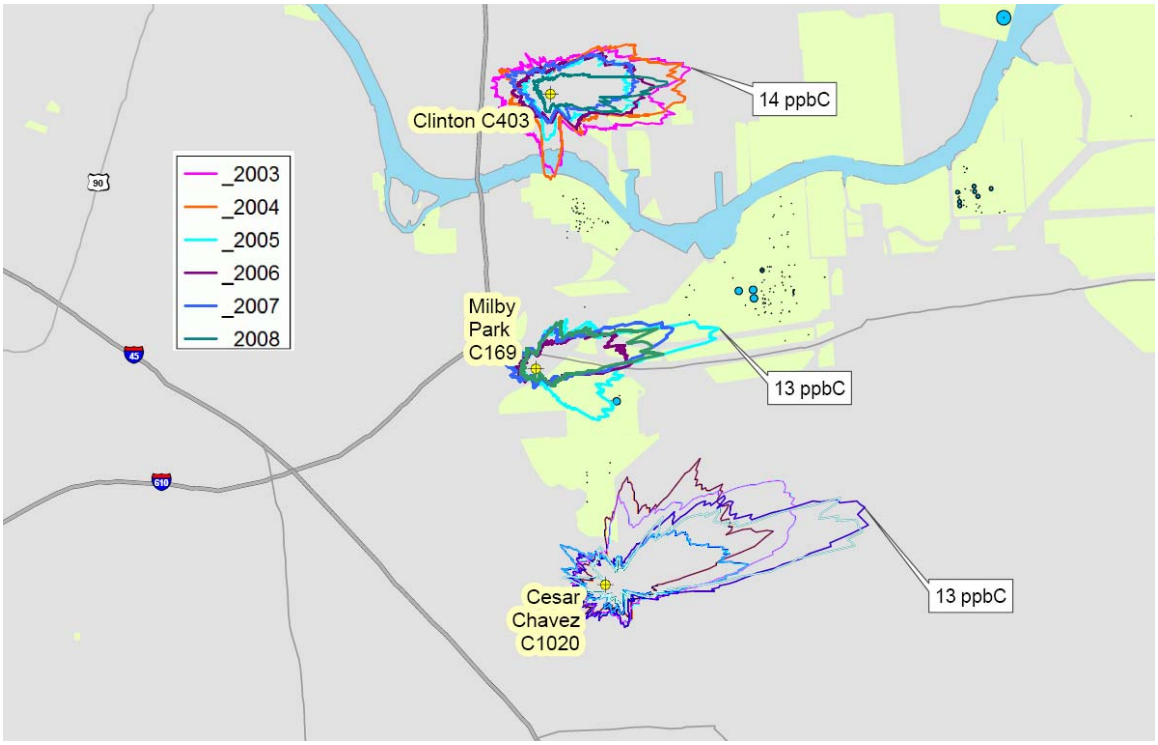

Figure 3-8: Geometric Mean Ethene Concentration at Western Houston Ship Channel Monitors
Reported ethene point source emissions are depicted as blue circles, with size of circle corresponding to mass of emissions reported. Valid hourly measurements from 2003 through 2008 were used; hours with hourly wind speed measurements less than two miles per hour (mph) were discarded, due to considerable error in wind direction measurements at low wind speeds. Air masses containing high mean ethene concentrations at Clinton (CAMS 403) largely arrive from easterly directions and due south, though moderate concentrations arrive from many directions. High mean ethene measured at Milby Park is traced to sources from the east-northeast and southeast, with more moderate mean concentrations from northeasterly directions. Air masses containing high mean ethene arriving at Cesar Chavez come from due north, north-northeast, northeast, and east-northeast, with the largest observations from the latter direction.

Sources of ethene (blue circles) and propene (brown circles) are also depicted on the map of the respective compound, with sizes proportional to values reported in the 2006 TCEQ Point Source emission inventory. Valid hourly measurements from 2002 through 2008 were used; hours with hourly wind speed measurements less than two miles per hour (mph) were discarded, due to considerable error in wind direction measurements at low wind speeds.

Crucially, note that while a compound's concentration for a particular wind direction at a particular monitor is proportional to the distance from the monitor to the ring at that direction, the scale differs across monitors. For example, peak 2003 ethene concentration (see Figure 3-9) at Lynchburg Ferry (CAMS 1015) is 24 ppbC, and 15 ppbC at Wallisville Road (CAMS 617), yet the length from each monitor to its respective peak (tip of sharp "point") is approximately the same. For this reason, peak concentration at each monitor, for each pollutant, is labeled.

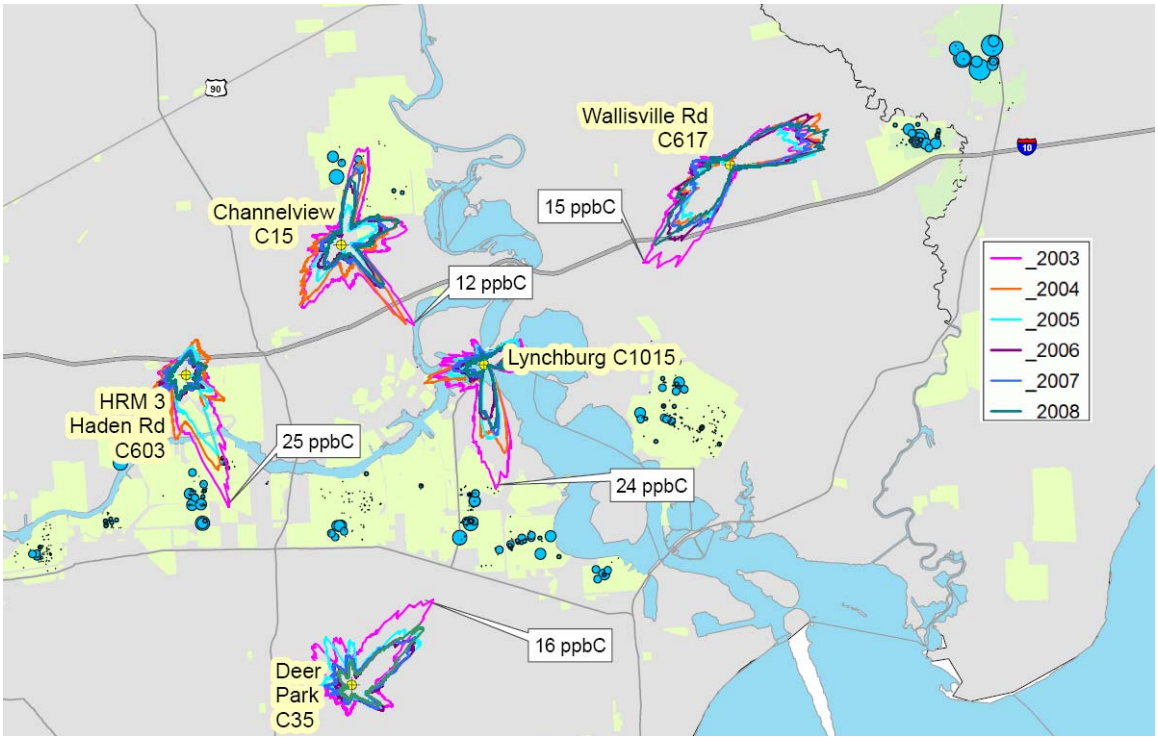

Figure 3-9: Geometric Mean Ethene Concentrations at Eastern Houston Ship Channel Monitors
Reported ethene point source emissions are depicted as blue circles, with size of circle corresponding to mass of emissions reported. Valid hourly measurements from 2002 through 2008 were used; hours with hourly wind speed measurements less than two miles per hour (mph) were discarded, due to considerable error in wind direction measurements at low wind speeds. Air masses containing high mean ethene concentrations typically arrive at Channelview (CAMS 15) from several directions: north, southeast, and southwest, with moderate concentrations from the east and south. The Wallisville Road (CAMS 617) monitor measures high mean ethene from the east-northeast and south-southwest. HRM-3 Haden Road (CAMS 603) measures high mean ethene arriving from the southeast, while the highest mean ethene concentrations measured at Lynchburg Ferry (CAMS 1015) originate from due south, with moderate concentrations from roughly due west. Houston Deer Park (CAMS 35) measures moderate mean ethene concentrations arriving from many directions, with the highest originating from the northeast.

Table 3-4: Geometric Mean Ethene for Key Wind Direction Lobes at Eastern Houston Ship Channel Monitors

Monitor	principal direction(s)	2003 *ppbC*	2004 *ppbC*	2005 *ppbC*	2006 *ppbC*	2007 *ppbC*	2008 *ppbC*	
lobes pointing to the same sources in the central Houston Ship Channel area:								
HRM-3 Haden Road C603/A114	ESE	**24.8**	**18.0**	**15.6**	5.0	4.7	5.2	
Channelview C15/AH115	SW	8.9	8.9	5.6	4.3	3.6	4.1	
lobes pointing to the same sources in the eastern Houston Ship Channel area:								
Houston Deer Park 2 C35	NE	16.6	missing	12.1	10.7	11.1	**13.0**	
Lynchburg Ferry C1015	SSE	24.3	17.7	14.5	10.8	**14.0**	12.6	
Channelview C15/C115	SE	12.5	11.9	6.6	6.9	7.1	6.8	
Wallisville Road C617	SW	15.0	9.8	8.4	**11.1**	9.9	12.8	
lobes pointing in other directions:								
Channelview C15/AH115	N	10.5	9.0	3.7	6.3	7.9	6.9	

Wallisville Road C617	ENE	9.7	11.5	9.6	10.8	9.2	11.6

Annual maxima are noted in boldface type.

Figure 3-8 shows mean ethene concentrations at the three western-most Houston Ship Channel auto-GC monitors. Sources of ethene having the greatest impact on these monitors are all located east of the monitors, as the greatest peaks for each monitor, across all years, point in this direction. The plot also shows trends across time at each monitor. At Clinton (CAMS 403), peak ethene occurred in 2003 from almost due east, as seen in the lobe labeled "14 ppbC." Following 2003 and 2004, peak concentrations from that direction have been somewhat lower. Also, note lobes pointing south, observed in 2003 and 2004, are markedly smaller in 2005 and subsequent years. An ExxonMobil olefins production plant located in the Milby Park area shut down in 2005; its emissions may be responsible for those lobes.

The plot also shows mean ethene concentrations for Cesar Chavez and Milby Park, which started operation in 2004 and 2005, respectively. While these monitors measured peak concentrations in different years from one another, both Milby Park (a large lobe to the southeast in 2005) and Cesar Chavez (a notable lobe to the north in 2004 and 2005) have peaks pointing in the direction of the ExxonMobil plant while it was in operation. This provides a stronger indication, when combined with the Clinton (CAMS 403) peak to the south, of the influence of emissions from that plant on local concentrations.

Figure 3-9 shows mean ethene concentrations at the five auto-GC monitors located in the eastern part of the Houston Ship Channel. Variation in mean concentrations by direction is even more pronounced here than in the western portion of the Houston Ship Channel. The pattern in mean concentrations at Lynchburg Ferry (CAMS 1015) suggests there is a large source of ethene emissions south-southeast of the monitor, near Battleground Road and Highway 225, and that emissions from this area have decreased. Table 3-5 shows that this lobe's mean 2003 concentration of 24.3 ppbC has halved in recent years.

The pattern observed at Houston Deer Park (CAMS 35) may provide additional evidence of suspected emission decreases in the same source area. The northeast lobe in Table 3-5 has dropped from a high of 16.6 ppbC in 2003 to a range of about 11 to 13 ppbC in recent years. Similarly, the southeast lobe at Channelview (CAMS 15), which points yet again to the same source area, peaked at 12.5 ppbC in 2003, dropped to 11.9 ppbC in 2004, and has not exceeded 7.1 ppbC since. While this monitor is farther from this source region than are the other two monitors, and therefore is more likely to be impacted by other emissions sources, consistent decreases observed at these three monitors across the six-year span of available data suggest ethene emissions have decreased in the subject source region.

HRM-3 Haden Road (CAMS 603) shows a peak of 24.8 ppbC to the southeast in 2003, which fell to 18 ppbC in 2004, then further to 15.6 ppbC in 2005. The mean concentration has dropped since then, not exceeding 5.2 ppbC. The magnitude of the decrease over 2006 to 2008, as compared to 2005 and earlier years, suggests a shut down of one or more major process units, or even entire plants, somewhere southeast of this monitor.

Peaks at the Wallisville Road (CAMS 617) monitor point southwest, toward the east Houston Ship Channel, and east-northeast, in the direction of the Mont Belvieu industrial area, where there is considerable ethene and propene storage in underground salt caverns. Table 3-5 shows that ethene originating to the southwest decreased from the six-year peak in 2003 (15 ppbC), to a range from 9.9 to 11.1 ppbC, before rising slightly to 12.8 ppbC in 2008. In contrast, the east-northeast lobe at this monitor shows relatively unvarying mean concentrations across the entire six-year period, ranging from 9.2 to 11.6 ppbC, with the six-year peak occurring in 2008.

These conclusions for five monitors and eight directional lobes show a nearly consistent pattern across these monitors. Seven of eight lobes witnessed their highest mean concentration in 2003.

Within one or two years of this peak, concentrations at all seven had dropped, from 27 to 65 percent, and have leveled off since; mean concentrations have not varied appreciably from 2006 to 2008. These findings suggest ethene emissions from source areas close to these monitors, especially Battleground Road, Highway 225 in La Porte, and the Lyondell-Equistar complex north of the Channelview (CAMS 15) monitor, have decreased considerably in recent years. Though further corroboration is warranted, this suggests that new TCEQ regulations specifically targeting HRVOC emissions in the HGB area (TCEQ, 2004), that required full compliance by early 2006, are proving effective in controlling point source HRVOC emissions. Caution is needed, however, since it has not been verified that 2003, and perhaps the one or two years following it, did not experience meteorology especially conducive to relatively high HRVOC concentrations.

Results for the lobe pointing east-northeast from the Wallisville Road (CAMS 617) monitor disagree with some key findings at other lobes. This Wallisville Road (CAMS 617) east-northeast lobe, unique among the eight, experienced an increase in mean concentration from 2003 (9.7 ppbC) to 2004 (11.5 ppbC). While 2006 to 2008 mean concentrations at Wallisville Road (CAMS 617), like those of other monitors and lobes, changed relatively little, mean concentrations of the east-northeast Wallisville Road (CAMS 617) lobe changed relatively little across the entire six-year period. The absence of recent decreases at this lobe compared to earlier years suggests that meteorology may not have caused high concentrations seen at most other lobes in earlier years.

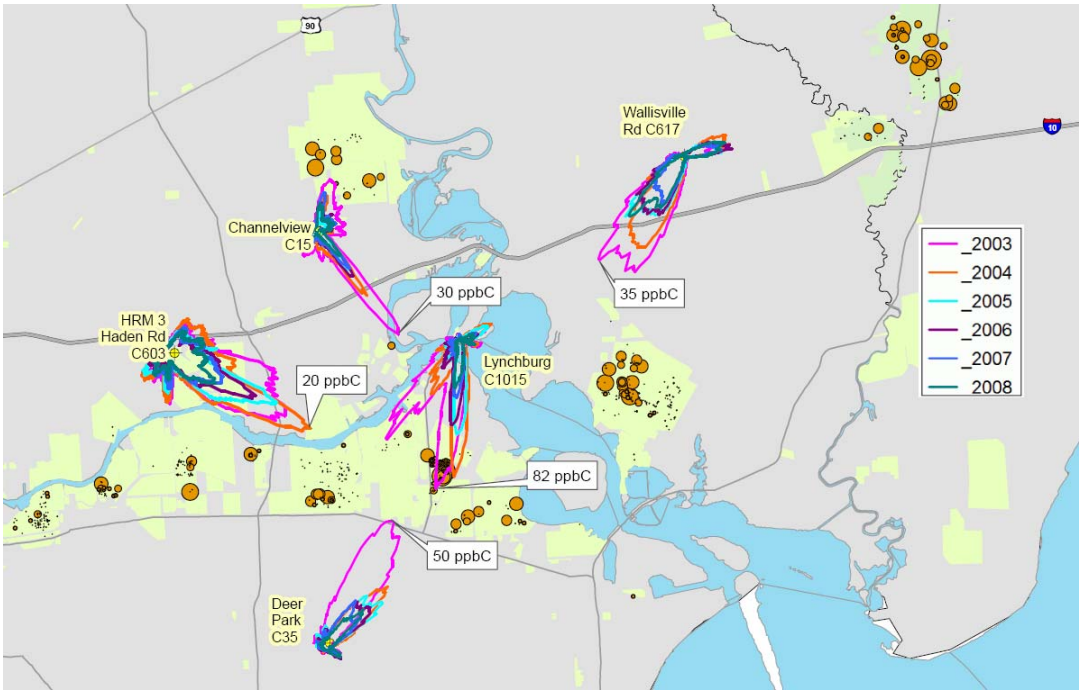

Figure 3-10: Geometric Mean Propene Concentration at Eastern Houston Ship Channel Monitors
Reported propene point source emissions are depicted as brown circles, with size of circle corresponding to mass of emissions reported. Valid hourly measurements from 2002 through 2008 were used; hours with hourly wind speed measurements less than two miles per hour (mph) were discarded, due to considerable error in wind direction measurements at low wind speeds. The highest mean propene concentrations typically arrive at Channelview (CAMS 15) from the southeast, with more moderate concentrations arriving from the north, northeast, east, south and southwest. The Wallisville Road (CAMS 617) monitor measures the highest mean propene from southwesterly directions, with moderate concentrations from the east-northeast. HRM-3 Haden Road (CAMS 603) measures high mean propene arriving from the east-southeast and southeast, while the highest mean propene concentrations measured at Lynchburg Ferry (CAMS 1015) originate from due south and southwest. Houston Deer Park (CAMS 35) measures the highest mean propene concentrations arriving from the north-northeast and northeast.

Figure 3-10 displays monthly geometric mean concentrations of propene in the same area of the eastern ship channel. As with ethene, Table 3-6 lists mean concentrations across the study period,

for each monitor and lobe. Similarities with ethene are evident. The seven lobes with consistent patterns in ethene concentrations exhibit similar patterns for propene. For propene, all seven lobes measured their highest concentrations in 2003 or 2004; five of the seven had their two lowest annual concentrations in 2007 and 2008. None of the seven lobes had concentrations in 2007 and 2008 that were greater than 60 percent of their respective six-year peaks.

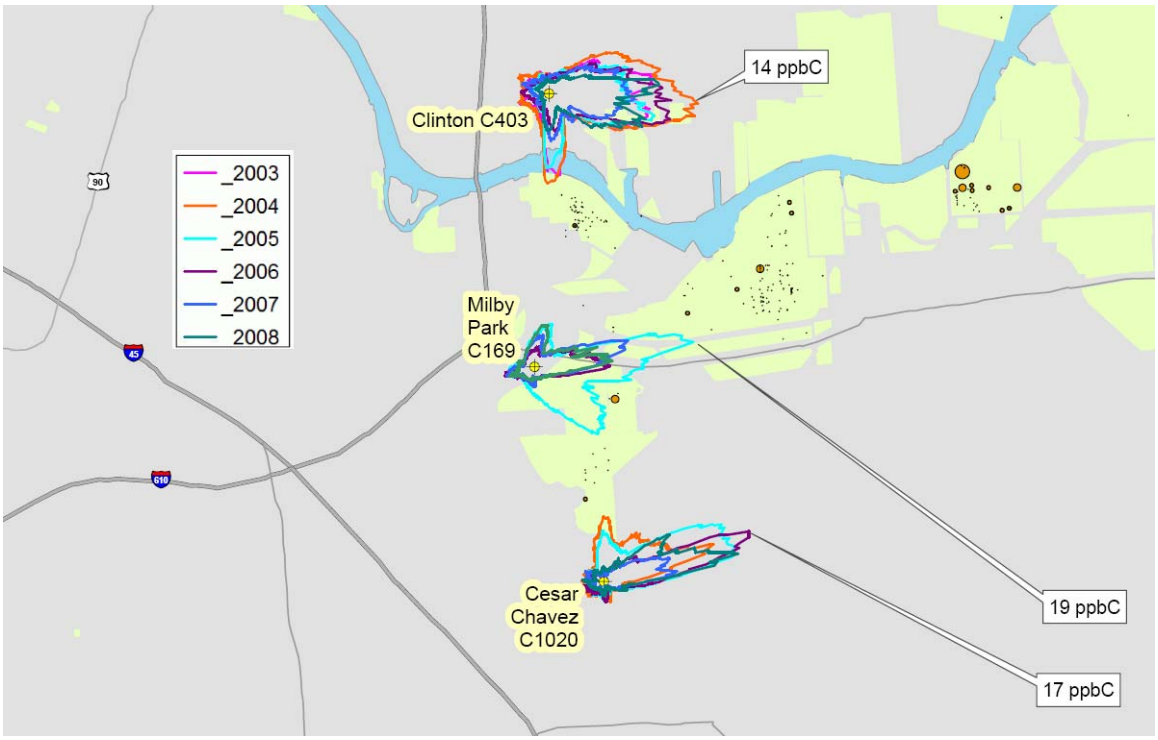

Figure 3-11: Geometric Mean Propene Concentration at Western Houston Ship Channel Monitors

Reported propene point source emissions are depicted as brown circles, with size of circle corresponding to mass of emissions reported. Valid hourly measurements from 2002 through 2008 were used; hours with hourly wind speed measurements less than two miles per hour (mph) were discarded, due to considerable error in wind direction measurements at low wind speeds. High mean propene concentrations at Clinton (CAMS 403) largely arrive from easterly directions and due south, though moderate concentrations arrive from many directions. High mean propene measured at Milby Park comes from the east-northeast and southeast, with more moderate mean concentrations from northeasterly directions. High mean ethene arriving at Cesar Chavez originates from due north, north-northeast, northeast, east-northeast, with the largest observations from the latter direction.

As with ethene, these results suggest that, at source regions near the monitors with large propene emissions, these emissions have dropped considerably in the six-year study period, and that the same HRVOC regulations cited above may be responsible for the decreases. As seen with ethene, patterns in geometric mean propene concentrations at the east-northeast Wallisville Road (CAMS 617) lobe differed considerably from the other seven. Propene concentrations varied relatively little across the six-year period, suggesting that, like ethene, Mont Belvieu propene emissions have changed little or not at all, on average, across the study period.

Figure 3-11 shows mean propene concentrations by wind direction at the three western Houston Ship Channel monitors. Patterns depicted here exhibit strong similarities to those seen with ethene in this area: the largest propene source areas are to the east, and judging from the disappearance of strong peaks from 2006 onward, emissions from the ExxonMobil plant located in the Milby Park area were probably affecting these monitors.

Table 3-5: Geometric Mean Propene Concentrations for Key Wind Directions at Eastern Houston Ship Channel Monitors

Monitor	principal direction(s)	2003	2004	2005	2006	2007	2008	
		ppbC	*ppbC*	*ppbC*	*ppbC*	*ppbC*	*ppbC*	
lobes pointing to the same source in the eastern Houston Ship Channel area:								
HRM-3 Haden Road C603/A114	SE	17.1	20.5	15.2	12.4	7.8	7.0	
Houston Deer Park 2 C35	NE	50.0	30.3	25.4	21.2	19.6	18.6	
Lynchburg Ferry C1015S		**82.8**	**75.4**	**51.5**	**46.2**	**31.5**	**26.3**	
Channelview C15/AH115	SE	30.1	19.0	11.7	13.8	11.7	8.2	
Wallisville Road C617SW		35.6	27.3	22.3	18.4	14.5	21.3	
lobes pointing to other sources:								
Lynchburg Ferry C1015SW		68.7	33.9	13.7	18.8	9.9	6.8	
Channelview C15/AH115	N	11.3	7.7	3.0	5.5	8.1	5.2	
Wallisville Road C617ENE		9.0	12.2	9.7	12.3	9.7	11.2	

Annual maxima are noted in boldface type.

3.3.3 Ambient Total VOC Concentrations

Considerable research has focused on patterns and trends in HRVOC concentrations in the HGB area (Henry et al., 1997; Brown and Hafner, 2002; Jolly and Schroeder, 2004). Less examined are patterns for other, less-reactive VOC. Similar to the VOC trends in Chapter 2, this section presents a detailed examination of patterns in total VOC concentrations in the HGB area, using concentrations of total nonmethane hydrocarbons (TNMHC) as a measure of total VOC. Each TNMHC measurement corresponds to the sum of all chromatogram peaks (identified and unidentified) from the start to the end of sample collection. TNMHC is a useful measure of total VOC because it has been calculated in a consistent manner over the entire study period, unlike other parameters, such as the sum of Photochemical Assessment Monitoring Stations (PAMS) target compounds, whose constituents have changed periodically.

Similar to the first HRVOC analysis presented in this section, geometric mean TNMHC concentrations, by monitor, year, and month, were calculated for valid months for all available data from each of the twelve HGB monitors. Further analysis of the four non-Houston Ship Channel-area monitors has not been completed at this time.

Figure 3-12 shows, for each of the eight Houston Ship Channel monitors, monthly geometric mean TNMHC concentration for all months with complete data, between the start of monitoring and December 2008. Monitors are sorted according to their location from west (top) to east (bottom); the grey bars denote the 25th through 75th percentile concentrations (85 ppbC and 149 ppbC respectively) of all valid months across all monitors.

As with ethene and propene, the two monitors with data before 2001, Clinton (CAMS 403) and Houston Deer Park (CAMS 35), recorded their highest monthly geometric mean values before 2001. It is apparent from Figure 3-12 that both monitors exhibited overall decreases across their respective data collection periods. A statistical analysis of possible trends, using ordinary least squares regression, is presented in Table 3-6. This statistical model indicates that all twelve monitors had decreasing monthly mean concentrations, from the beginning to the end of each monitor's respective data range. As well, this model indicates that eight of the twelve monitors' decreases were statistically significant at the 95 percent confidence level.

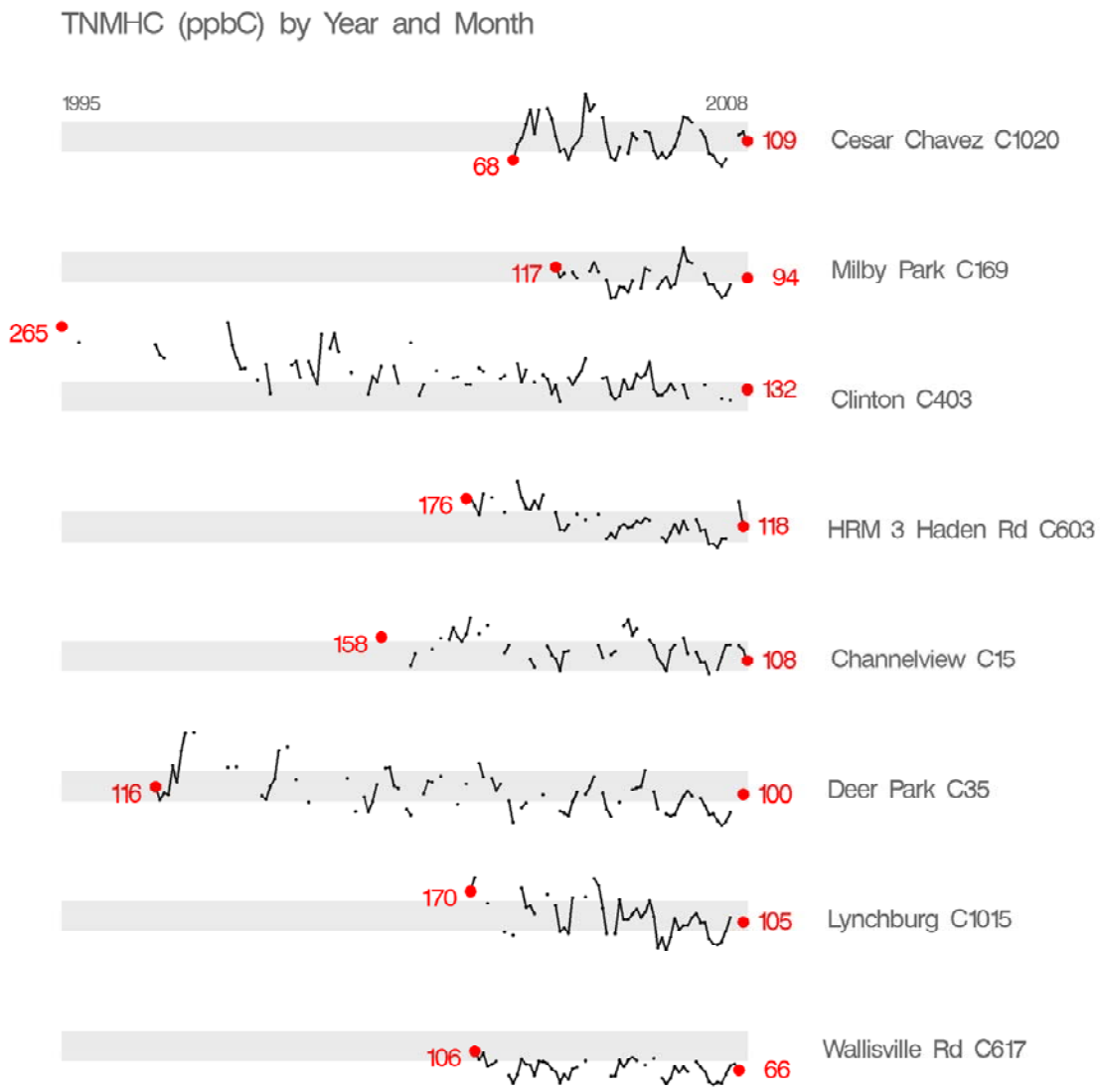

Figure 3-12: Monthly Geometric Mean TNMHC Concentrations
Monthly geometric mean TNMHC concentrations, by year and month, at 8 Houston Ship Channel monitors, July 1995 to December 2008. Monitors are sorted from west (top) to east (bottom). Grey bars denote 25th percentile (85 ppbC – bottom edge of bar) through 75th percentile (149 ppbC – top edge) concentrations, when valid monthly geometric mean measurements are aggregated across all monitors. Months with incomplete data are excluded, and appear as gaps in the data series.

Table 3-6: Parameter Estimates of Monthly Geometric Mean TNMHC Concentration Trends
Houston Ship Channel-area auto GC monitors:

Sitename	Slope of Trend	Intercept	Degrees of Freedom	R squared
Cesar Chavez C1020	-0.61	132	47	0.07
Channelview C15/AH115	-0.37*	153	49	0.10
Clinton C403/C304/AH113	-0.63*	225	78	0.46
Houston Deer Park 2 C35	-0.55*	148	80	0.31
Houston Milby Park C169	-0.33	99	33	0.03
HRM-3 Haden Road C603/A114	-1.22*	173	47	0.52
Lynchburg C1015	-1.14*	156	47	0.27
Wallisville Road C617	-0.31*	79	49	0.11

Non-Houston Ship Channel-area auto-GC monitors:

Sitename	Slope of Trend	Intercept	Degrees of Freedom	R squared
Danciger C618	-0.22*	44	47	0.12
Lake Jackson C1016	-0.18	34	43	0.04
Mustang Bayou C619	-0.11	61	43	0.01
Texas City 34th St. C620	-0.95*	102	57	0.46

*Significant at the 5 percent (0.05) level. Significance levels for intercepts are not reported. Parameter estimates from ordinary least squares fits of monthly geometric mean concentrations of TNMHC on an index of month, by monitoring site.

3.3.4 The Houston-Galveston-Brazoria Point Source Emission Inventory

A thorough understanding of ozone formation and transport in the HGB area requires an accurate, complete accounting of the amounts and locations of emissions of both NO_X and VOC. Toward this end, all companies in the HGB area that meet or exceed one or more emission criteria are required by Title 30 of the Texas Administrative Code (TAC), Section 101.10, to submit annual inventories of these emissions to the TCEQ. In these inventories, VOC must be speciated, that is, reported as individual organic compounds. The TCEQ records the amounts and locations of these emissions in a database.

These annual emissions inventories (EI) are a very important component of SIP control strategies, as they form a key input to photochemical modeling, which forecasts future ozone levels throughout the region. The 2003 through 2006 TCEQ annual point source emission inventories of VOC, by county, are shown in Figure 3-13. The figure shows that, while trends among individual counties vary, reported emissions have decreased area-wide by more than 20 percent over this period.

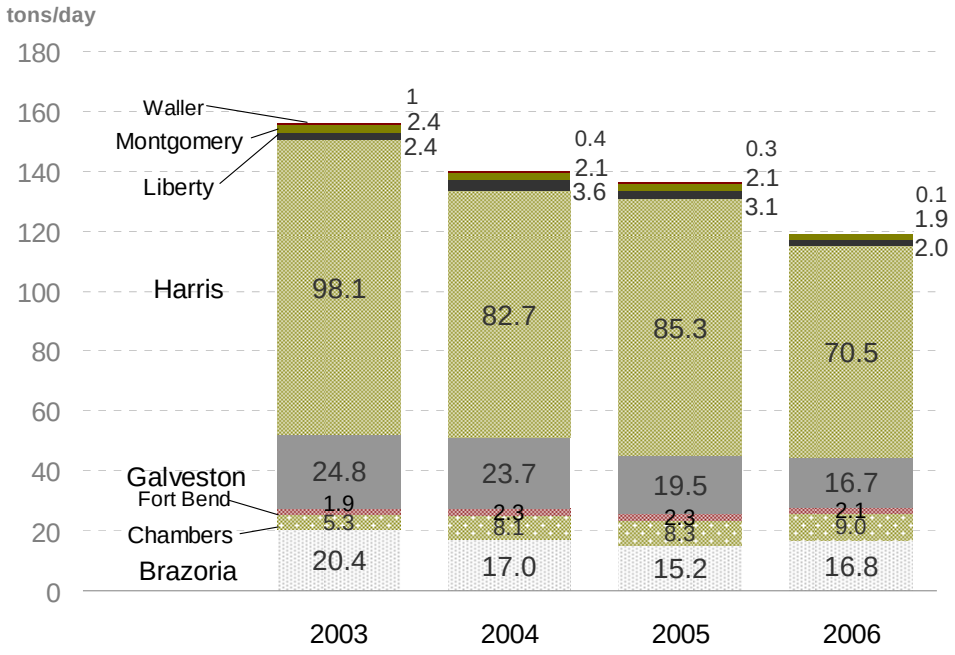

Figure 3-13: HGB Point Source VOC Emissions

HGB point source VOC emissions reported by county, 2003 to 2006. These values represent the sum of emissions reported by point sources to TCEQ in annual emission inventories.

It may appear that, given these decreases in reported emissions, it would be worthwhile to compare these decreases with those seen with ambient (monitor) data. However there is ample evidence that the HRVOC emissions reported by companies to the TCEQ in the Annual EI are profoundly underestimated, frequently by an order of magnitude or more (Ryerson et al, 2003; Cowling et al, 2007). If only a small percent of actual VOC emissions of many companies are

being reported, this introduces tremendous uncertainty in any comparison with ambient data, whose uncertainty (due to measurement error and allowable instrument bias) is tiny by comparison.

In addition to annual reporting of emissions, some plants in the HGB area submitted hourly emissions data, by FIN (Facility Identification Number) and EPN (Emission Point Number), for some of their process units during the period August 15 to September 15, 2006, corresponding to the intensive data collection period of the 2005-2006 Texas Air Quality Study. For this time period, these hourly emissions estimates can be compared to daily emissions figures taken from the 2006 Annual Emission Inventory.

Because this hourly data covered only a minority of sources within a minority of plants in the HGB area, its usefulness is limited for comparisons with the 2006 Annual EI, which covered all identified point sources in the 8-county area that have the potential to emit above applicable reporting standards. An informative tool for comparison can be constructed by substituting hourly EI data for existing data in the 2006 Annual EI, for FINs and EPNs in common to both the Hourly and Annual EIs, to create a 'hybrid' 2006 Annual/Hourly EI.

For the one-month period covered by the Hourly EI, a comparison of the 2006 hybrid EI to annual emission inventories from 2006 and earlier years, as well as comparison to ambient measurements taken during that period, provides a means of evaluating the relative accuracy of the various emission inventories. In Figure 3-14, propene emissions from a version of the 2004 Annual EI (red line) and the 2006 Hybrid EI (green line, identified as "Daily EI" in legend), are shown alongside the 2006 Hourly EI (blue line). Daily (24-hour) rates have been converted to kilograms per hour (kg/hr). Emissions figures are those reported by facilities to the east of Battleground Road. Propene measurements were collected in this area using a Solar Occultation Flux (SOF) instrument (Mellqvist et al, 2008), converted to identical units (kg/hr), and depicted as dotted black lines in the figure.

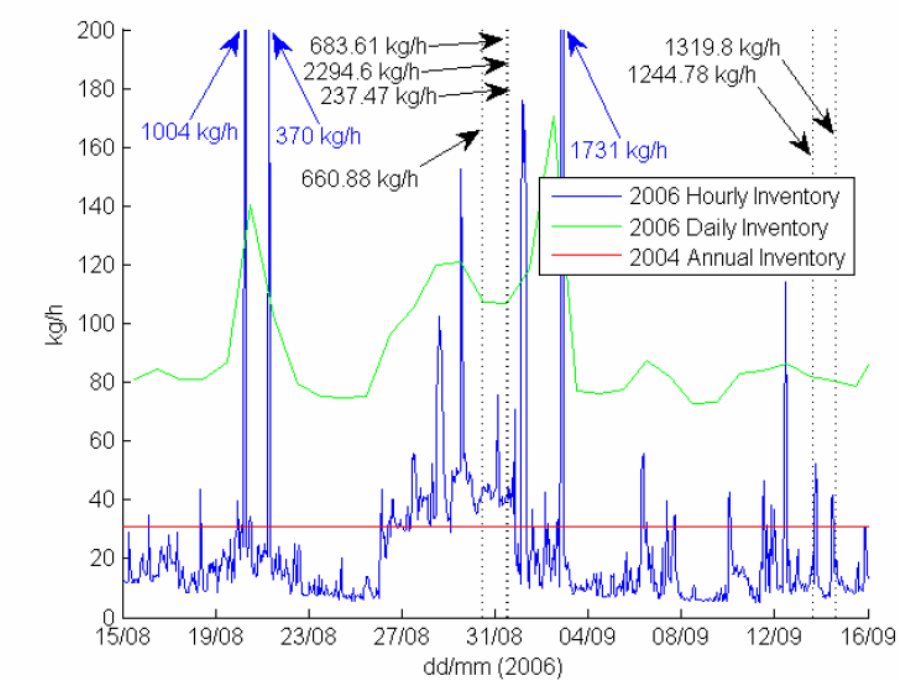

Figure 3-14: Propene Emissions and SOF Measurements East of Battleground Road

Time plots of total propene emissions and SOF measurements from sources east of Battleground Road. The 2004 annual EI is shown in red, the hourly inventory collected during the TexAQS II study is shown in blue, and the 'hybrid' inventory that contains both hourly and daily emissions estimates is shown in green. Measurements taken by the SOF instrument are noted as vertical dashed black lines, though actual values are not plotted. Three of these measurements were taken in rapid succession and so appear as a single line near August 31 (31/08) with 3 annotated values.

The figure depicts several noteworthy items. First, the reported 2004 emission rate (red) is considerably lower than the 2006 Hybrid EI (green). The hourly inventory (blue) shows tremendous variation, over two orders of magnitude, in this one-month period. Although the hourly data is a subset of the Hybrid EI and the hourly data has been converted to daily emission rates, which would be expected to suppress some of its variation, the 2006 Hybrid EI in the Battleground Road area still exhibits considerable variation, sufficient to double the baseline 2006 daily emission rate on one day. Finally, the three greatest hourly emissions rates (370 kg/hr; 1,004 kg/hr; and 1,731 kg/hr) are roughly comparable with the six SOF measurements taken in this area (ranging from 237 to 1,319 kg/hr), although they did not occur in close temporal proximity to one another. The six SOF measurements, all of which exceed the range of the y-axis in Figure 3-14, are displayed; however, three of these occurred nearly simultaneously and therefore appear as one line on the graph (see arrows noting measured values).

Figure 3-15 shows data from the same inventories, along with SOF measurements, for an area near Houston Deer Park (CAMS 35). This figure shows that the 2006 daily emissions rate (about 10 kg/hr), which does not vary from day to day, is approximately equal to the 2004 rate, but when the hourly data are included, the resulting Hybrid EI exhibits several days when the emissions rate is more than double the base rate. Even though there is considerable variation in the hourly emission rate, the highest hourly rate (180 kg/hr) is substantially less than the three emission rates measured by SOF (246 kg/hr; 710 kg/hr; and 895 kg/hr). Moreover, the hourly emission rates in the temporal vicinity of the SOF measurements are roughly twenty-fold less than the measurements. It is worth noting that the degree of "penetration" by the Hourly EI – that is, the percent of FINs and EPNs in a geographic area that reported hourly emissions, compared to the total number of normally-reporting FINs and EPNs in the same area – varied from area to area within the ship channel, therefore it cannot be determined from this graph if the poor agreement between the inventories and SOF measurements is attributable to misreported emissions, emissions from sources that did not report hourly emissions, or both.

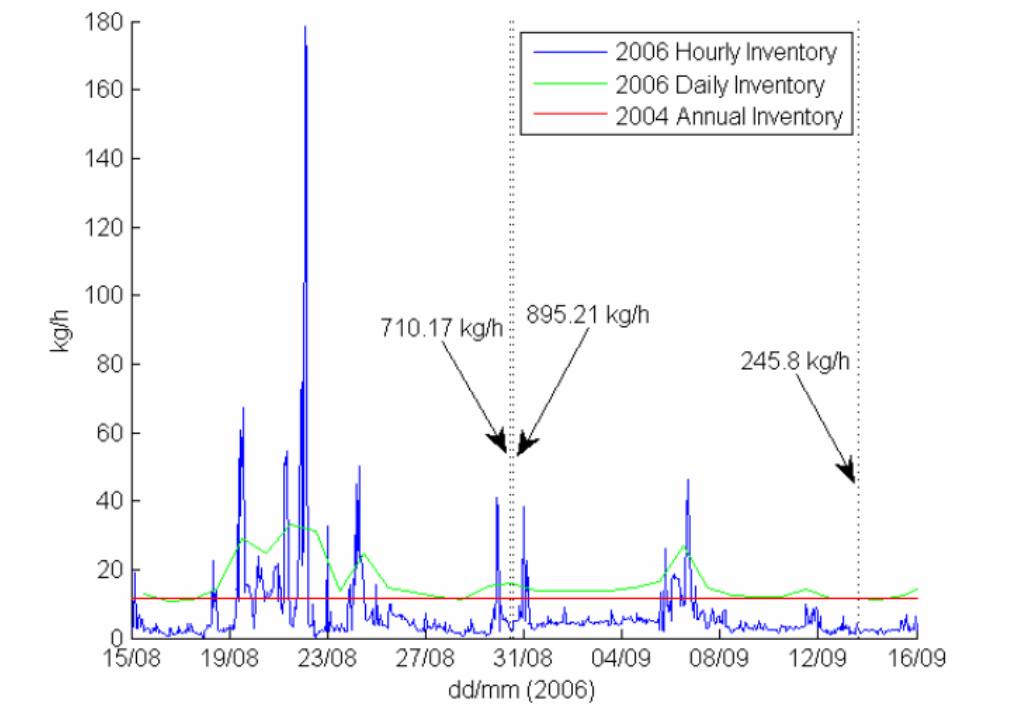

Figure 3-15: Propene Emissions and SOF Measurements Near Houston Deer Park C35
Time plots of total propene emissions and SOF measurements from sources near Houston Deer Park (CAMS 35). The 2004 annual EI is shown in red, the hourly inventory collected during the TexAQS II study is shown in blue, and the 'hybrid' inventory of hourly measurements aggregated to daily values is shown in green. Measurements taken by the SOF instrument are noted as vertical dashed black lines, though actual values are not plotted.

The analysis presented here of long-term ambient HRVOC measurements indicates that ethene and propene concentrations in the areas near the 12 HGB auto-GCs decreased across the six-year study period. The decrease seen for ethene qualitatively agrees with a key finding from the TexAQS II study: that ethene emissions near the Houston Ship Channel have decreased approximately 40 percent from 2000 to 2006 (Cowling et al, 2007). All 12 monitors showed statistically significant decreases for propene, and a majority showed this for ethene.

When the same long-term data are analyzed by wind direction, results suggest that ethene and propene emissions from important source areas near the Houston Ship Channel have decreased across the study period. Results seen at the Wallisville Road (CAMS 617) monitor, when winds were blowing from east-northeast, suggest that the relatively high concentrations observed from key wind directions at all other monitors in 2003 and 2004 were not attributable to meteorology that was unusually conducive to high HRVOC concentrations in either of those years.

Work was performed that compared emission flux measurements from the Solar Occultation Flux instrument to emissions reported in three EIs: the 2004 Annual EI, the 2006 Hourly EI, and a "hybrid" 2006 Annual/Hourly EI. This comparison found that in the vicinity of Battleground Road, reported emissions for most of the comparison period were much less than any of the six SOF measurements taken in this area, but at times the reported hourly emissions were greater than some of the SOF measurements. However, the reported emissions at the time of, and just preceding, the SOF measurements were considerably less than the fluxes measured by SOF.

The same comparison in the vicinity of Houston Deer Park (CAMS 35) shows, like Battleground Road, that the hourly reported emissions show tremendous variability, however the peak reported emissions do not come close to the emissions estimated from three SOF measurements taken there. As well, reported hourly emissions at and near the time of the SOF measurements are on the order of 20-fold less than the SOF estimates, but it cannot be determined how much this is attributable to the fact that the hourly EI did not cover all sources.

Several future analyses are suggested from this work. First, it would be valuable to see if HRVOC are contributing as strongly to total reactivity in recent years as they were in 2000, when scientists observed this. An analysis of relative contributions of different VOC classes to TNMHC concentration across the study period would be useful, since the TCEQ HRVOC regulations did not target other VOC classes, so those may not be decreasing as much. Also, nearly all the wind direction lobes showed relatively strong decreases, and thus high variance, in the 2003 through 2005 period, whereas the succeeding three years seem to show much less variance. These two periods may be statistically different from one another, which would suggest the effectiveness of the HRVOC regulations, but this needs to be quantitatively studied. Finally, the wind direction lobe analysis suggests that Mont Belvieu is distinct from other source areas studied; efforts are underway, using resources from several different work groups in the TCEQ, to investigate the causes of this.

Spatial patterns have been illustrated for not only VOC but also for ozone and NO_X. While all three pollutants have been shown to vary spatially, they exhibit temporal variations as well. The relationship between the temporal variations in ozone with that of NO_X and VOC will be discussed in the next section.

3.4 RECENT FINDINGS ON A DAY OF THE WEEK EFFECT

Studies (Croes et al., 2003; Fujita et al., 2003a; Fujita et al., 2003b; Heuss et al., 2003) have shown that ozone concentrations can exhibit not only annual and diurnal, but weekly patterns of variation. These studies have found that some cities exhibit substantially greater ozone concentrations on weekends, while others do not. Identification of a weekend effect can be valuable for guiding ozone photochemical modeling and control strategy development. Because a weekend effect is hypothesized to result from emissions from specific types of emitters, that is, mobile rather than point sources, its presence, if confirmed, can be used to tailor policies to target

specific sources. Even more importantly, a weekend effect can provide inferences as to whether an area is VOC-limited or NO_X-limited, hence providing clues to the efficacy of various candidate control strategies. A decrease in monitored ozone on weekends (compared to weekday levels) indicates NO_X-limitation, since weekend NO_X concentrations are generally lower compared to their weekday counterparts. Conversely, a weekend increase in ozone concentrations can indicate VOC-limitation. Finally, a weekend effect provides a natural laboratory for evaluating photochemical model response. If the model can reproduce observed weekend effects, then we will have greater confidence in its ability to correctly predict the effects of future emission changes.

Causes of weekly patterns in ozone concentrations have generally been related to changes in emissions during weekends compared to weekdays, and the sensitivity of ozone formation to those changes. Several hypotheses have been proposed to explain increased ozone concentrations on weekends (Croes *et al*., 2003; Lawson, 2003; Heuss *et al*., 2003). Generally, these tend to focus on variation in motor vehicle driving patterns and use of recreational and lawn and garden equipment: lower mobile source NO_X emissions are hypothesized to result in less ozone titration by NO, or fewer radical termination reactions, resulting in an increase in radical concentrations; weekend postponement of mobile source NO_X emissions until later in the day enhances ozone formation in aged, NO_X-depleted air; and increased weekend emissions from recreational and lawn and garden equipment enhance weekend ozone formation.

Following extensive investigation by the California Air Resources Board (CARB) and a host of researchers, several of the above hypotheses were discarded (Croes *et al*., 2003; Fujita *et al*., 2003a, 2003b; Blanchard *et al.* 2008, Blanchard and Tanenbaum, 2005; Heuss *et al*., 2003; Pun *et al*., 2003; Yarwood *et al*., 2003). Instead, the most likely explanations were attributed to lower mobile source NO_X emissions on weekends. Specifically, studies suggest the primary cause of increased ozone on weekends is a decrease in $NO + O_3$ titration reactions occurring on weekends due to lower NO_X emissions from heavy duty diesel vehicles. Furthermore, there is some indication that areas that see a pronounced weekend effect, with increasing ozone and decreasing NO_X, exhibit ozone formation in a VOC-limited regime. Areas for which a decrease in NO_X results in a decrease in ozone, however, are more likely to have NO_X-limited ozone formation (Murphy *et al*., 2007; Gao *et al*., 2005; Marr and Harley, 2002; Fujita *et al*., 2003b; Yarwood *et al*., 2003; Yarwood *et al*., 2008).

This section explores this observation to determine whether the HGB area exhibits a weekend effect. Ozone, ozone precursors (NO_X and VOC), carbon monoxide (CO), and "odd oxygen" (O_X) will be analyzed to identify weekly patterns and contributing source categories. Examining how ozone is generated in the HGB area on days with varied NO_X and VOC concentrations improves our understanding of how ozone would form if NO_X and VOC emissions changed from day to day within a week, or even from hour to hour within a day.

Figure 3-16 shows the number of days on which the HGB area experienced an exceedance of either the one-hour or eight-hour ozone NAAQS, grouped by day of the week, from 1997 to 2008. Chi-square tests were used to determine if there were significant changes in the number of one-hour (χ^2=0.8265, p-value=0.6615) and eight-hour (χ^2=0.9925, p-value=0.6088) ozone exceedance days from the weekdays to Saturdays and Sundays. Although it appears that the eight-hour ozone exceedances are higher towards the end of the week, the chi-square test revealed no significant difference in eight-hour ozone exceedance days on weekdays versus weekend. The test also demonstrates that the number of one-hour ozone exceedances that occur on weekdays is not significantly different from that on weekends.

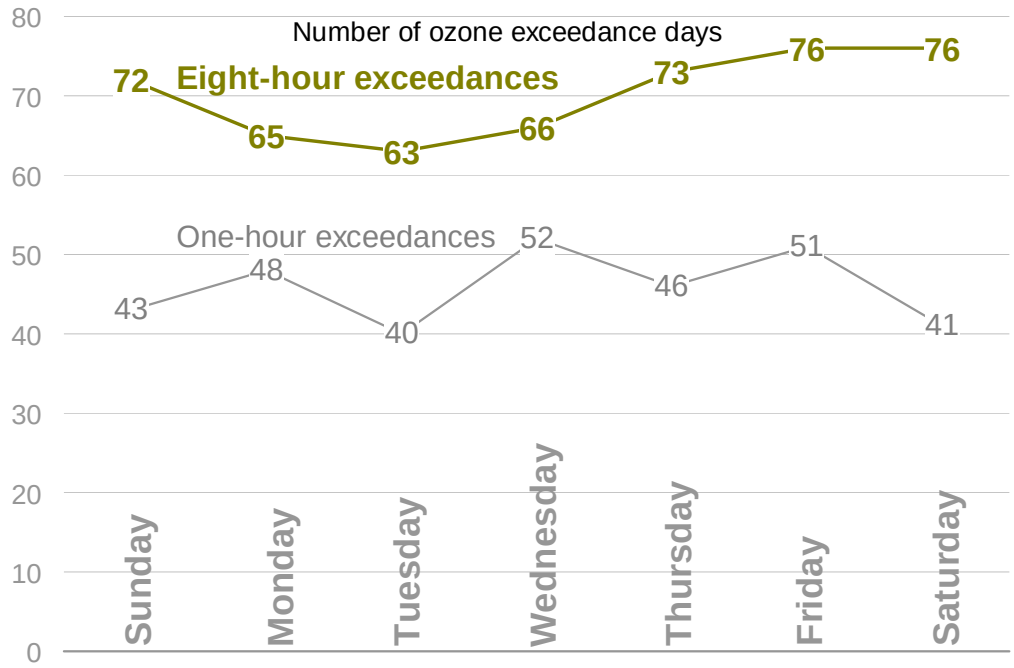

Figure 3-16: Number of Ozone Exceedance Days, 1997 to 2008
The number of one-hour and eight-hour ozone exceedance days, plotted by day of the week, in the HGB area from 1997 to 2008. No statistically significant difference was observed between weekdays and weekends, defined as Saturdays and Sundays.

To further investigate the change in ozone from weekday to weekend, weekly patterns in ozone precursors, NO_X and VOC, were also examined. Differences in median morning NO_X concentrations from Wednesdays to Sundays were calculated at regulatory sites for entire years, from 1997 to 2008. Morning hours are defined as 05:00 Local Standard Time (LST) to 10:00 LST. The presence of elevated levels of ozone precursors during morning hours increases the likelihood of recording elevated ozone concentrations later in the day.

The consistently positive values in Figure 3-17 signify that median morning NO_X concentrations consistently decrease from Wednesdays to Sundays at all sites. Lower morning NO_X on the weekend could result from the absence of rush hour motor vehicle traffic. Blanchard and Tannenbaum (2005) also found substantial differences between weekday and weekend NO_X in Houston, with 20-80% decreases observed.

Figure 3-18 shows differences in median total morning VOC concentrations from Wednesdays to Sundays at various VOC monitoring sites for entire years, from 1997 to 2008. In 2008, all sites except Clinton (CAMS 403) exhibited increases in median total morning VOC concentrations from Wednesdays to Sundays. Prior to 2008, however, all sites except Houston Deer Park (CAMS 35) exhibited decreases in median total morning VOC concentrations from Wednesdays to Sundays.

Carbon monoxide (CO), considered a tracer compound for mobile source emissions, was also examined for possible weekly patterns. A Wednesday-Sunday CO ratio was constructed as above, and is displayed in Figure 3-19. The figure exhibits generally decreasing (positive ratios) median morning CO concentrations from Wednesdays to Sundays, though there is considerable variation in the degree of decreases among sites.

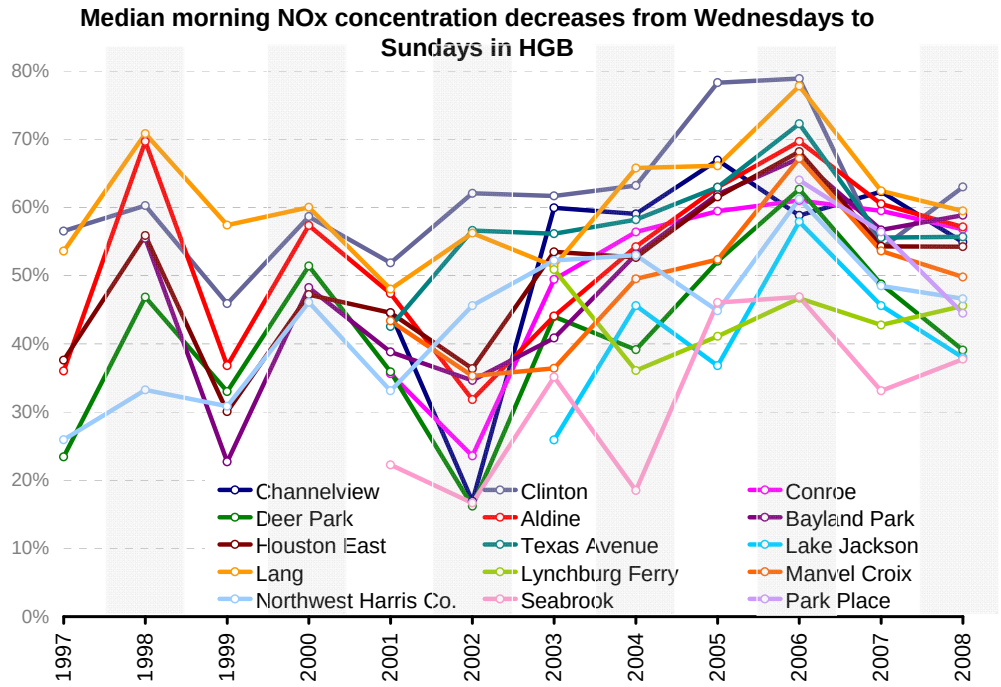

Figure 3-17: Ratio of Wednesday to Sunday Median Morning NO_X Concentrations
Median morning NO_X concentrations decrease from Wednesdays to Sundays at all sites in HGB from 1997 to 2008.

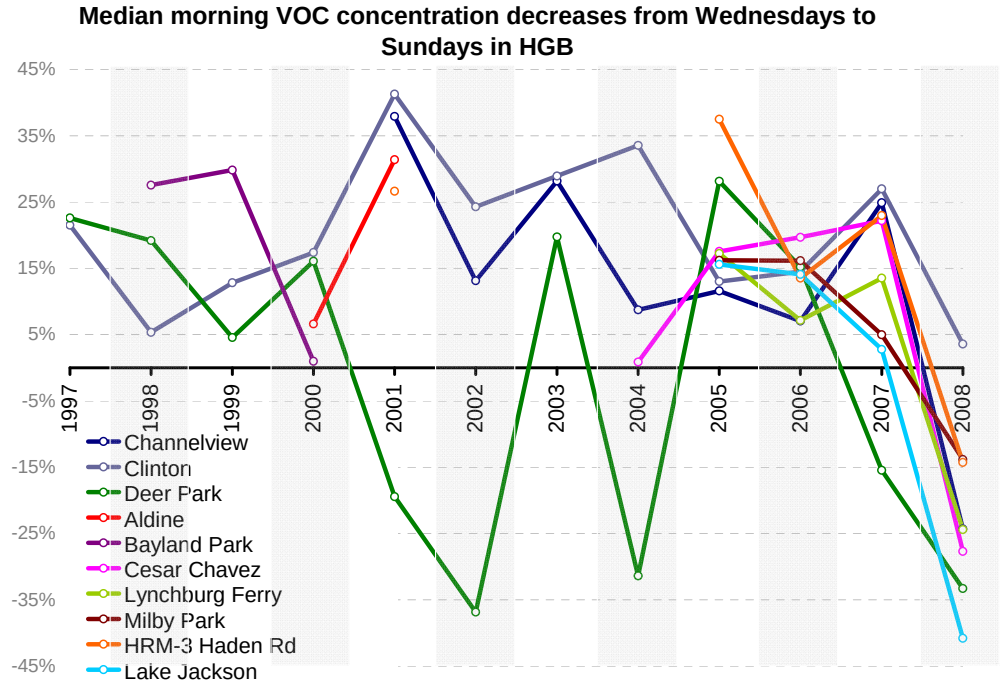

Figure 3-18: Ratio of Wednesday to Sunday Median Morning VOC Concentrations
Median morning VOC concentrations in HGB from 1997 to 2008 decrease from Wednesdays to Sundays at some sites and increase at others. The year 2008 is an anomaly as many monitors that previously recorded decreases (positive ratios) from Wednesdays to Sundays, instead recorded increases (negative).

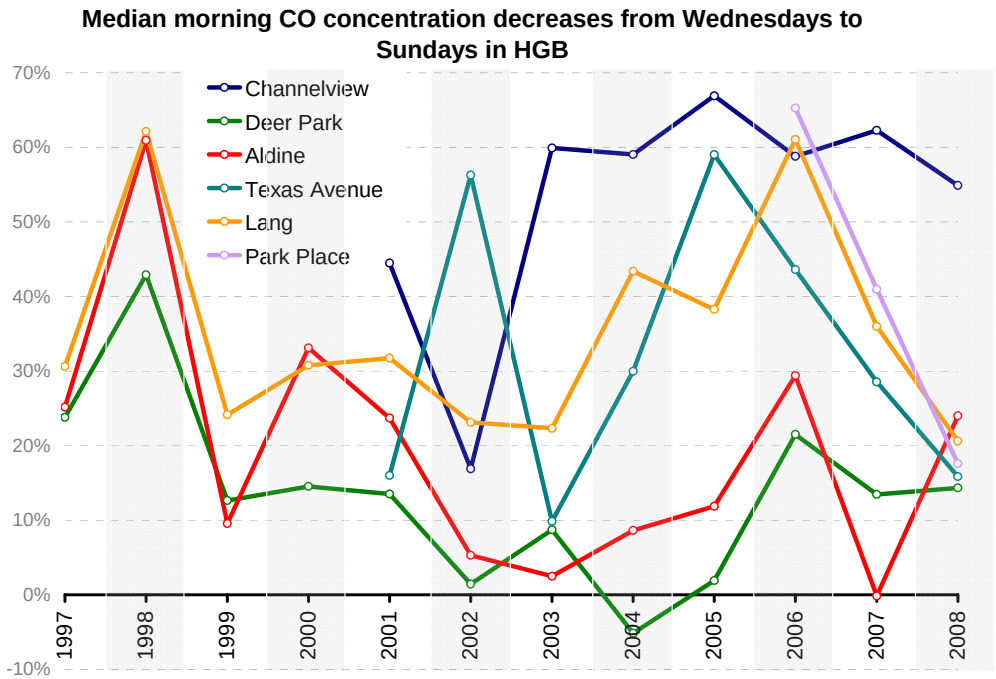

Figure 3-19: Ratio of Wednesday to Sunday Median Morning CO Concentrations
Median morning CO concentrations in HGB from 1997 to 2008 generally decreases (positive ratio) from Wednesdays to Sundays, though there is a great deal of variation in the magnitudes of decreases, and at least one increase (Houston Deer Park (CAMS 35), 2004).

Finally, odd oxygen (O_X) concentrations, defined as ozone plus NO_2, were compared between Wednesdays and Sundays in the HGB area at sites that have both ozone and NO_X data. Freshly emitted NO reacts with ozone, creating NO_2. As discussed in Chapter 1, ozone titration by NO can decrease ozone by delaying ozone accumulation, but since NO_2 can readily convert back to ozone through NO_2 photolysis, ozone can re-form and begin accumulating once an air mass consisting of fresh NO emissions moves out of the area. Examining O_X concentrations, in addition to O_3 and NO_X, makes it possible to distinguish between the two competing factors, titration and photolysis, affecting weekend ozone: interconversions of O_3, NO, and NO_2 (i.e., ozone titration), and differences in ozone production rates (Murphy *et al*., 2007).

Figure 3-20 shows ratios in median O_X concentrations from Wednesdays to Sundays in HGB at various sites. O_X concentrations in the early part of the period, 1997 to 2000, are fairly stable, with most sites exhibiting decreases (positive ratios) from Wednesdays to Sundays. A transition occurs in 2001 when ratios at all sites begin to turn negative, increasing in magnitude through 2005, with an anomalous turn positive in 2006. Though the ratios change from positive to negative across time, sites appear to be changing in concert, following a similar pattern. This generally indicates an area-wide effect, rather than something occurring at a small-scale in one or a few locations.

The apparent weekend effect in the O_X data suggests that titration by NO may not be the main source of a weekend effect in ozone in the HGB area. Were ozone titration the dominant effect, the odd oxygen concentrations would not be expected to exhibit noticeably different patterns on weekends relative to weekdays. Ratios would be fairly close to zero for all years, with no positive or negative tendency. Therefore, differences in ozone production rates as a source of a weekend effect remains a possibility in the HGB area. At low concentrations of NO_X, hydroperoxy (HO_2) and peroxy (RO_2) radicals are independent of NO_X, and ozone production increases linearly with increases in NO. High concentrations of NO_X relative to VOC reactivity, however, promotes reaction of OH with NO_2, suppressing the hydroxyl radical, which slows the production of HO_2+RO_2 and results in less ozone production.

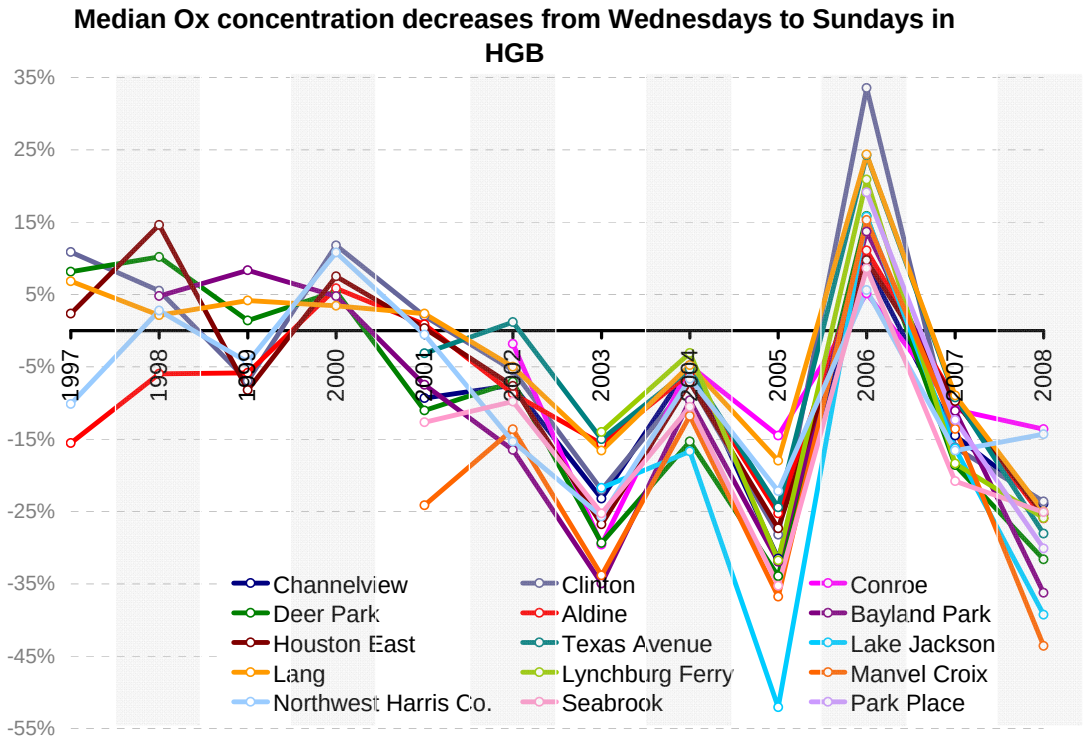

Figure 3-20: Median O_X Concentrations from Wednesdays to Sundays
This plot shows the temporal pattern of odd oxygen (OX) concentrations since 1997 for selected monitors in the HGB area. A clear downward trend is interrupted by an anomalous upward spike in 2006, followed by a return to trend.

This day of the week analysis shows that NO_X concentrations are lower on weekends in the HGB area. Furthermore, the weekend effect observed in O_X concentrations indicates that ozone titration cannot be considered the dominant reaction affecting weekend ozone in the HGB area and that differences in ozone production rates or radical termination can still be considered a source of the weekend effect in ozone.

The weekend effect helps to demonstrate the relationship between ozone and its precursors; however, all of these precursors can vary depending on meteorological conditions. Evaluating meteorological parameters which are correlated with ozone distinguishes trends resulting from a change in emissions from trends resulting from favorable meteorological conditions.

3.4 RECENT FINDINGS IN METEOROLOGY

2008 has been perceived as a unique year in the HGB area, in meteorological terms. Setting aside consideration of the most devastating hurricane to hit the region in over a century, the remainder of the year seemed, to many observers, to be less hot and less humid than recent years. Measured ambient ozone, NO_X, and VOC concentrations were also lower in 2008 than in recent years. This section will assess several meteorological parameters that have been shown to have an association with peak ozone in Houston to determine if lower ozone values are related to meteorology. Contrasting observations from recent years with 2008 values, and noting trends of interest will help determine if 2008 was unique meteorologically or if decreases seen in ozone were due to decreases in its precursors.

Ozone is created in a dynamic medium of sunlight, wind, temperature, humidity, and other meteorological factors that can affect ozone concentrations. It has been shown that a relationship exists between ozone and these meteorological parameters (Cox and Chu, 1993). For example, if there is a lack of sunlight, ozone production is not possible.

Meteorological parameters that explain most of the variability in daily ozone concentrations for an urban region have been found to be: daily maximum temperature, average morning wind speed, average afternoon wind speed, relative humidity, and cloud cover (Cox and Chu, 1993). While the present analysis applies similar methods used by Cox and Chu, this investigation of meteorological parameters includes only surface meteorological data that is available at TCEQ sites in the HGB area, and uses only the following meteorological parameters: temperature, morning and afternoon wind speeds, observed relative humidity, and solar radiation.

The maximum hourly ozone value was identified for each day from all HGB area monitors. Following Cox and Chu (1993), surface temperature is computed as the daily maximum of hourly average temperatures, restricted to hours starting from 7:00 through 10:00 LST (four hourly values), across all monitors. Maximum wind speed values are taken from hourly averages across all monitors, and restricted to 7:00 through 10:00 for morning wind, and 13:00 through 16:00 for afternoon wind. Relative humidity is constructed as the daily maximum of hourly average relative humidity, restricted to 10:00 through 16:00 Local Standard Time (LST), across all monitors. Maximum daily solar radiation is identified from all hourly averages across all monitors.

Scatter plots in Figure 3-21 demonstrate the association of each individual meteorological parameter with daily maximum ozone. Solar radiation and temperature exhibit positive association, although the association with temperature is rather weak. Relative humidity, morning wind speed, and afternoon wind speed show negative associations.

The following model was specified to fit all selected meteorological parameters to daily maximum hourly average ozone:

$$O_{3MAX} = SolarRadiation + Temperature + WindSpeed_{AM} + WindSpeed_{PM} + \mathrm{Re}lativeHumidity$$

where O_{3MAX} is daily maximum hourly average ozone in parts per billion (ppb), *SolarRadiation* is measured in langleys per meter-squared, *Temperature* is ambient outdoor temperature in Fahrenheit degrees, $WindSpeed_{AM}$ and $WindSpeed_{PM}$ are morning and afternoon wind speeds in miles per hour (mph), and *RelativeHumidity* is expressed in percent.

Table 3-7 shows coefficients estimated from a linear fit of the above model. All parameter estimates are significant at the 5 percent level ($\alpha = 0.05$), with the lowest t-value equal to -5.045. For a sufficiently large sample size, a t-value greater than 1.96 indicates statistical significance at the 5 percent level ($\alpha = 0.05$) for a two-tailed test and a t-value of 2.58 indicates significance at the 1 percent level ($\alpha = 0.01$). Although all the parameter estimates were found to be significant, there is a fair amount of unexplained variability in the model, as indicated by an adjusted R^2 of 0.43 (p-value < 0.0001).

In spite of these results, however, validation of the model resulted in rejection of the initial specification due to autocorrelation of some of the parameters. The Durbin-Watson test was positive for autocorrelation (DW = 1.0194; p-value < 2.2e-16) and the studentized Breusch-Pagan test identified heteroscedastic residuals (BP = 35.3902; degrees of freedom = 5; p-value = 1.258e-06). Finally, the RESET statistic reports that the functional form of the model may be incorrect (RESET = 45.424, $df_1 = 2$, $df_2 = 1363$, p-value < 2.2e-16).

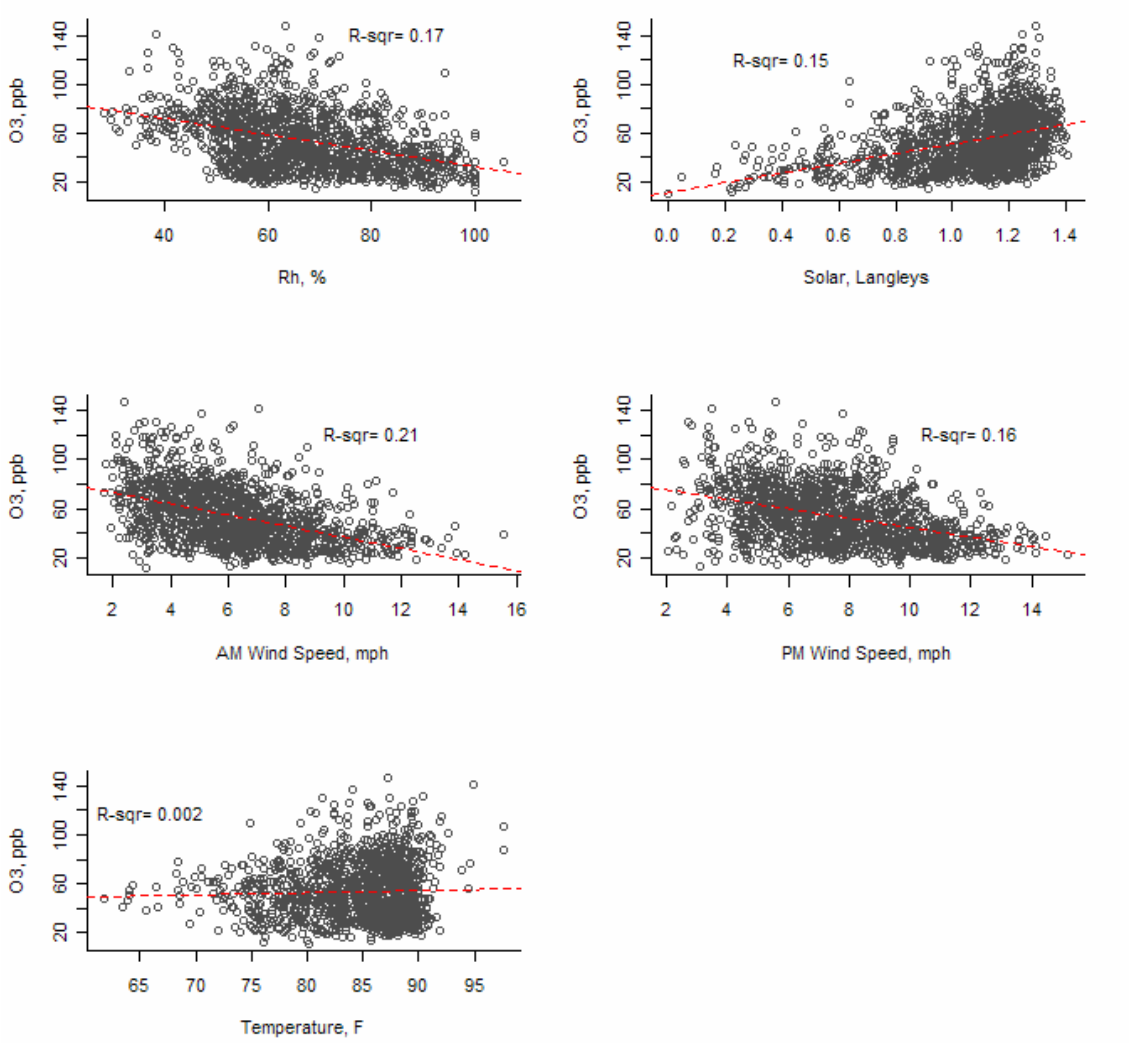

Figure 3-21: Scatter Plots of Selected Meteorological Parameters Versus Ozone

Scatter plots of daily maximum hourly average ozone with each of the selected meteorological parameters. Solar radiation and temperature exhibit positive associations with ozone, while relative humidity, and morning and afternoon wind speeds show negative associations. Dashed red lines are ordinary least squares fits.

Table 3-7: Model Results for Preliminary Meteorological Model

	Estimate	Standard Error	t value	Pr(>|t|)
Intercept	133.23997	9.90894	13.446*	< 2e-16
Relative Humidity	-0.40846	0.04406	-9.271*	< 2e-16
Temperature	-0.52444	0.10395	-5.045*	5.14e-07
Wind Speed AM	-3.52565	0.25857	-13.635*	< 2e-16
Wind Speed PM	-1.76503	0.24989	-7.063*	2.58e-12
Solar Radiation	25.88138	2.89001	8.955*	< 2e-16

*Significant at the 1 percent level ($\alpha = 0.01$). Residual standard error: 17.6 on 1,365 degrees of freedom (1 observation deleted due to missing values). Multiple $R^2 = 0.4316$, adjusted $R^2 = 0.4295$, F-statistic = 207.3 on 5 and 1,365 degrees of freedom, p-value = < 2.2e-16

An example residual plot is displayed in Figure 3-22. A possible trend is noticeable in this residual plot, though there is a large amount of scatter. This is indicative of heteroscedasticity, or non-constant variance in the data, which complicates estimation. Notice the points plotted on the left hand side are closely spaced and appear to exhibit a downward slope, while those on the right exhibit much wider spacing, more scatter, but no discernible trend. The red line demonstrates one possible fit to the residuals; if residuals can be well fit, they are unlikely to be randomly distributed and therefore caution should be exercised when interpreting model results.

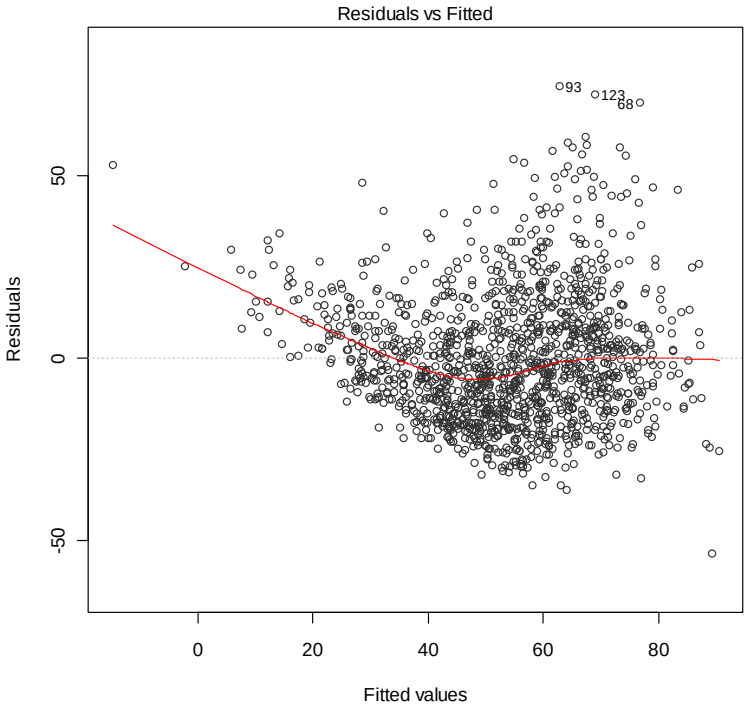

Figure 3-22: Residual Plot of Preliminary Model of Meteorological Parameters on Ozone
A possible trend is noticeable in this residual plot from the preliminary model, though there is a large amount of scatter. This is indicative of heteroscedasticity, or non-constant variance in the data, which complicates estimation.

The techniques necessary to correct for the shortcomings of the available data are beyond the scope of this analysis, which is to demonstrate the relationships between the selected meteorological parameters and daily maximum ozone in the HGB area. Studies have used measures similar to these meteorological parameters to predict daily maximum ozone (Cox and Chu, 1993; Seinfeld, et al., 1994; Camalier et al., 2007); therefore, the following analysis will be limited to identifying trends and mutivariate relationships of these meteorological parameters to ozone.

3.4.2 Meteorological Trends

Cox and Chu (1993) discuss the association of solar radiation, relative humidity, temperature and wind speed with anthropogenic ozone production (or destruction), provided sufficient precursor emissions are present. To determine whether meteorology observed in 2008 in the HGB area is similar to typical meteorology observed since 2000, trends in the selected meteorological parameters are investigated, and differences in those trends are highlighted. This analysis will focus on the peak ozone season, May through October.

The Tukey-Kramer multiple means comparison test was employed to compare the 2008 means of each meteorological parameter to the means from each of the years 2000 through 2008. This test compares means between two or more groups, controlling for unequal sample sizes, and is appropriate for this type of pair-wise comparisons. The procedure also detects when groups of years have means that are statistically indistinguishable from each other, because they fall within estimated confidence bounds.

Results presented in Table 3-8 show that both average morning wind speed and average afternoon wind speed in 2008 exceeded the nine-year average, and were among the highest recorded over that period. Although average 2008 morning wind speeds were not statistically different from any of the other group "A" years, 2000 through 2004, 2008 was different from the three immediately preceding years, 2005 through 2007. Years not sharing a letter code are significantly different at the $\alpha = 0.05$ level. Average 2008 afternoon wind speeds were

statistically indistinguishable from average morning wind speeds recorded in 2000 through 2002, the three other group "A" years.

Average morning wind speeds in 2008 were 0.9 mph faster than 2007. As discussed in Chapter 1, faster wind speeds can lead to more dilution of ozone concentrations and ozone precursors. It is noteworthy that in 2000, when wind speeds were comparable to those in 2008, ozone design values were high (112 ppb) compared to 2008 (91 ppb). While this analysis does not correct for possible changes in emissions between the two years, the difference in 2000 versus 2008 warrants greater scrutiny of meteorological influences on ozone.

Year 2008 recorded the lowest average relative humidity over the entire nine-year period at 59.7 percent. Though the 2008 average is not statistically different from averages for the other group "E" years, 2004 through 2006, it is still noteworthy that it was so low, especially since the average over the previous year, 67.0 percent in 2007, was over 7 percent higher. Perhaps even more notable is the 2001 average relative humidity of 77.2 percent, which stands alone in its own group, and is 5.4 percentage points higher than the next highest value. It is also 17.5 percentage points higher than the 2008 average. A longer time series would help determine whether relative humidity variation of this magnitude is truly an outlier, or is a common occurrence in the HGB area.

Relative humidity has been found to be negatively associated with peak hourly average ozone (Camalier, et al, 2007; Cox and Chu, 1993), although the lowest ozone over the period was recorded in 2008, the year with the lowest relative humidity. These results suggest humidity was not an important indicator in ozone formation in 2008 because higher ozone concentrations would be expected to be observed in a year that experienced lower relative humidity. Note that in the summer of 2008, Houston and much of central Texas experienced abnormal to extreme drought conditions (see e.g., the National Drought Mitigation Center: http://drought.unl.edu/monitor/monitor.htm), which are linked to low relative humidity.

Table 3-8: Tukey-Kramer Multiple Means Comparison Test Results

Morning wind speed

year	groups	mean
		mph
2002	A	6.7
2008	**A**	**6.7**
2000	A B	6.6
2004	A B C	6.4
2001	A B C	6.2
2003	A B C	6.1
2007	B C	5.8
2006	B C	5.8
2005	C	5.7
9-year mean		**6.2**

Afternoon wind speed

year	groups	mean
		mph
2000	A	8.4
2008	**A B**	**8.0**
2002	A B C	8.0
2001	A B C D	7.6
2006	B C D	7.4
2003	B C D	7.2
2005	B C D	7.2
2004	D	7.2
2007	D	7.1
9-year mean		**7.6**

Relative humidity

year	groups	mean
		%
2001	A	77.2
2003	B	71.8
2002	B	71.7
2000	B C	68.3
2007	C D	67.0
2006	D E	62.3
2004	E	62.1
2005	E	60.2
2008	**E**	**59.7**
9-year mean		**66.7**

Temperature

year	groups	mean
		^{o}F
2005	A	85.2
2000	A	85.0
2008	**A**	**84.9**
2004	A	84.8
2007	A	84.3
2002	A	84.3
2001	A	84.1

Solar radiation

year	groups	mean
		langleys
2000	A	1.12
2005	A B	1.10
2008	**A B C**	**1.08**
2006	A B C	1.07
2004	A B C	1.06
2003	A B C	1.05
2001	A B C	1.04

2003	A	84.1	2002	B	C	1.03
2006	A	84.1	2007		C	1.01
9-year mean		**84.5**				**1.06**

These tables compare means of various meteorological parameters for the HGB area, 2000 through 2008 using the Tukey-Kramer multiple means comparison test. Care should be exercised when reading these tables because they are sorted by means, in descending order, not by year. All values have been rounded. Years not sharing a letter code are significantly different at the $\alpha = 0.05$ level.

Average temperature in 2008 was not distinguishable from any other years over the period. Average solar radiation in 2008 was not statistically different from any other years over the period, noted by its presence in groups "A," "B," and "C," which include all other years.

Box plots in Figure 3-23 show annual distributions of the meteorological parameters, with annual means noted as red squares, medians as heavy lines, and the overall mean of the period as a dashed red line. Recall that each box encompasses the middle 50 percent of the data. It is clear from the plots that, while there is a great deal of spread in the data, some measures, notably temperature and solar radiation, have a large portion of values tightly clustered around their means.

In summary, examination of several meteorological measures proposed by Cox and Chu (1993) for the nine-year period of 2000 through 2008 revealed only weak correlations with both morning and afternoon wind speeds, and relative humidity. Temperature and solar radiation exhibited little variation useful for explaining ozone formation and transport. The meteorological variables examined in this analysis are insufficient to explain recent decreases in ambient ozone concentrations observed in the Houston area. Recent research from Sullivan (2009) shows that the ozone trends are significantly decreasing in the HGB area even with the removal of meteorological influences. Although ozone concentrations are somewhat higher in 2007-2008 once meteorological factors are removed, the trends are still downward, and are still statistically significant. These results are preliminary and further investigation may be warranted to more fully account for all meteorological factors in the HGB area.

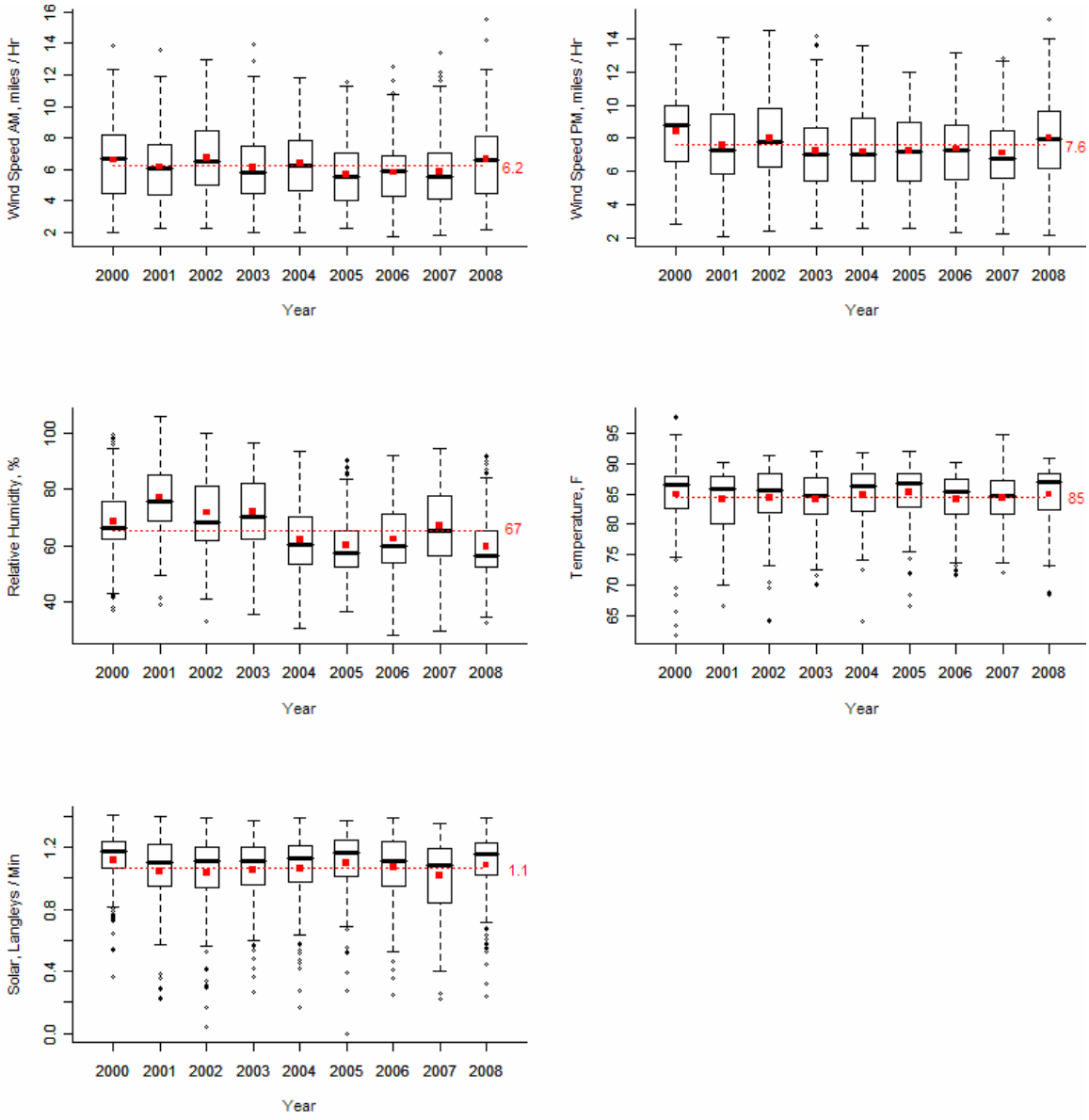

Figure 3-23: Annual Box Plots of Meteorological Parameters, 2000 to 2008
These box plots show annual means and distribution of meteorological parameters for years of 2000-2008. Note that the red reference line and number is the overall mean in ppb for the given 9-years of data. The red square within the box plot is the mean for a given year and the heavy black line is the median. Fifty percent of the data for each year falls within the box.

This section and the preceding one investigated local meteorological parameters to identify trends or anomalies that might account for lower ambient ozone concentrations observed in 2007 and 2008. Several approaches, including visual inspection, ordinary least squares regression, and the Tukey-Kramer Multiple Means Comparison test failed to detect significant meteorological trends. These results support the conclusion that no statistically significant variation in local meteorology occurred in recent years that would account for observed reduced ozone levels in the HGB area.

3.5 SUMMARY OF RECENT FINDINGS IN LOCAL OZONE DYNAMICS

An investigation of geographic patterns in ozone reveals that, while ozone concentrations in the HGB area have been decreasing, the same geographic areas tend to experience the highest ozone concentrations year after year. The highest levels of ozone typically occur in the area near the Houston Ship Channel to the east of downtown Houston, and in the area surrounding the Houston Bayland Park (CAMS 53) area to the west of downtown, and this pattern has been present for

many years. The geographic analyses have also shown that on high ozone days, ozone concentrations peak first in the vicinity of the Houston Ship Channel, then peak successively later at sites further and further from the Houston Ship Channel area. By contrast, on low ozone days, ozone concentrations peak first near the Gulf Coast, and successively later at sites that are further and further inland. These results suggest that the Houston Ship Channel and surrounding industrial areas are often the source of the highest ozone on exceedance days.

Similar to ozone, mean ambient NO_X concentrations have decreased, but the areas that experience the highest NO_X concentrations remain the same, with the exception of the area around the Houston Ship Channel. Peak NO_X typically occurs in the downtown area of Houston, which experiences high levels of automobile traffic, and in the Houston Ship Channel industrial zone. The area around the Houston Ship Channel no longer observed the peak in median NO_X in 2008. Because of the variety of NO_X sources, there are likely a variety of reasons why NO_X in the HGB area has generally declined. However, it is apparent that NO_X in the heavily industrialized areas of Houston has decreased, and that NO_X emissions in areas with heavy automobile traffic have also decreased, though to a lesser extent.

Analysis of long-term ambient HRVOC measurements indicates that ethene and propene concentrations in areas near the 12 HGB auto-GC monitors decreased across the six-year study period. The decrease seen for ethene agrees with a key finding from the TXAQS II study: that ethene emissions near the Houston Ship Channel have decreased approximately 40 percent from 2000 to 2006 (Cowling et al, 2007). While weak for individual monitors, and in need of further development, statistical evidence supporting ethene and propene trends described here is strong in that all 12 monitors showed statistically significant decreases for propene, and a majority showed this for ethene.

When the same long-term data are analyzed by wind direction, results suggest that ethene and propene emissions from important source areas within and near the Houston Ship Channel have decreased across the study period. Concentration decreases do not appear to be attributable to meteorological factors.

Emission flux measurements from the Solar Occultation Flux (SOF) instrument were compared to emissions reported in three EIs: the 2004 Annual EI, the 2006 Hourly EI, and a "hybrid" 2006 Annual/Hourly EI. This comparison found that in the vicinity of Battleground Road, reported emissions for most of the comparison period were much less than any of the six SOF measurements taken in this area, though at times reported hourly emissions were greater than some of the SOF measurements. However, reported emissions at the time of, and just preceding, the SOF measurements were considerably less than the fluxes measured by SOF.

The same comparison of emission fluxes in the vicinity of Houston Deer Park (CAMS 35), like Battleground Road, shows that reported hourly emissions exhibit tremendous variability. However, peak reported emissions do not come close to the emissions estimated from three SOF measurements taken there. As well, reported hourly emissions at and near the time of the SOF measurements are on the order of 20-fold less than the SOF estimates, but it cannot be determined how much this is attributable to the fact that the hourly EI did not cover all sources.

Various spatial analyses showed that most areas in HGB are experiencing decreases in not only ozone, but also VOC and NO_X. Monitors near the Houston Ship Channel have measured large decreases in both NO_X and VOC, which appears have contributed, to some degree, to the decreases in ozone in the HGB area.

To determine if ozone formation is more sensitive to decreases in NO_X or to decreases in VOC, an analysis of variability by day of the week was performed. This day of the week analysis showed that NO_X concentrations are lower on weekends in the HGB area. Furthermore, the weekend effect observed in "odd oxygen" (O_X) concentrations indicates that ozone titration

cannot be considered the dominant reaction affecting weekend ozone in the HGB area and that differences in ozone production rates or radical termination can still be considered a source of the weekend effect in ozone.

Because recent observed decreases in ozone, NO_X, and VOC could be, in large part, explained by variations in meteorology that occurs in the HGB area from year to year, meteorological parameters were examined in detail. This examination revealed that while high levels of sunlight and temperature lead to ozone formation, these two parameters do not exhibit high levels of variation from year to year, and temperature and solar radiation observed in 2008 were not statistically different from any other year back to 2000. Further, no trends in morning wind speed, afternoon wind speed, and relative humidity were identified. If trends in meteorological parameters existed, these should correlate with observed downward trends in ozone and precursors. Detailed investigation led to rejection of this conjecture for the HGB area.

Higher wind speeds were shown generally to correlate with lower ozone concentrations, due to resulting dilution. Average morning wind speeds in 2008 were 0.9 mph faster than 2007; these higher wind speeds in 2008 may have contributed to lower levels of ozone and its precursors, despite low relative humidity of 59.7 percent (the lowest observed for all years back to 2000), which usually signifies higher ozone. Wind speeds comparable to 2008 occurred in 2000, a year that saw a relatively high ozone design value, 112 ppb, compared to the 2008 design value of 91 ppb. While higher wind speeds appeared to contribute to recent decreases in ozone, it does not appear that the decreasing trend in ozone and its precursors is due only, or even largely, to local meteorological influences.

Although local emissions and meteorology act in tandem to generate elevated ozone concentrations in the HGB area, ozone transported into the area can contribute sufficiently high concentrations to elevate monitored ozone levels well above the federal NAAQS. To fully explain patterns of ozone formation and conveyance in the HGB area, the next section investigates patterns in background ozone transported into the area.

CHAPTER 4: RECENT FINDINGS IN BACKGROUND OZONE AND OZONE TRANSPORT INTO THE HOUSTON-GALVESTON-BRAZORIA AREA

This chapter discusses background ozone and ozone precursor concentrations that are transported into the HGB area from sources outside the region and the state. A better understanding of the background and transport phenomenon will guide selection of appropriate approaches to state and local control strategy development. Background ozone, defined as ozone that is not produced locally, has been found to vary considerably by geographic region, by season of the year, across years, and by direction of transport (Nielson-Gammon et al., 2005a). Further, background ozone is a substantial contributor to overall ozone levels in the Houston-Galveston-Brazoria (HGB) area, accounting for over half of the total ozone during periods when peak ozone levels are observed. When high concentrations of background ozone are transported into the HGB area, local ozone production exacerbates an already high baseline concentration, resulting in greater likelihood of violating the National Ambient Air Quality Standards (NAAQS).

In this chapter, we examine background ozone concentrations at selected monitoring sites, under specific meteorological restrictions, to determine whether a trend across time is apparent. This approach builds on work by Nielson-Gammon (2005a) and others (Camalier 2007, Draxler 2003) and determines that there is no discernible trend in background ozone. An apparent trend in background ozone, either increasing or decreasing, would have ramifications for local ozone control strategies adopted in the HGB area. Rising background ozone concentrations could overwhelm improvements made through local emission reductions, while falling background ozone concentrations could moderate the amount of local control needed to attain the NAAQS. Further, temporal changes in background ozone complicate modeling by introducing additional complexity in identifying appropriate model input values.

Next, we investigate larger scale, extra-regional, meteorological parameters to determine whether ozone and precursors are being transported into Texas and the HGB area, and, if so, from which other regions and under what conditions this transport is generally observed. An approach using HYSPLIT back trajectories identifies ozone being transported into the state from the Ohio River Valley region and possibly other regions to the northeast.

4.1 BACKGROUND OZONE IN TEXAS

Research on the meteorology of the HGB area has found that the highest background ozone transported into the HGB area predominately originates from the north and northeast (Nielson-Gammon et al., 2005a). In the present analysis, two techniques are used to examine the background ozone concentrations in Texas since 2000. The first technique examines the trend in ozone concentrations at four sites that can be considered background sites under certain flow conditions. The second technique examines ozone concentrations associated with different patterns of long-term back trajectories.

Identifying appropriate background ozone monitoring sites from which to ascertain trends is complicated by local ozone, complex wind patterns, and natural variability in background ozone itself. To estimate background ozone, Nielson-Gammon et al. evaluated all monitors in the region to identify those that could be considered to be recording background ozone values. They proposed a modification of a TCEQ procedure to identify such sites.

The TCEQ procedure involves determining the direction of transport winds, then selecting a rural monitor upwind of the area in that direction. Nielson-Gammon et al. simply select as the background value the lowest of the peak eight-hour ozone values from all monitors. Unlike the Nielson-Gammon procedure, which used gridded output of a meteorological model, this analysis follows the TCEQ approach using direct measurements of surface winds and tracking background ozone concentrations over time at selected monitors. Modifying the Nielson-Gammon procedure, the approach presented here identifies the 90^{th} percentile values recorded at the selected monitors

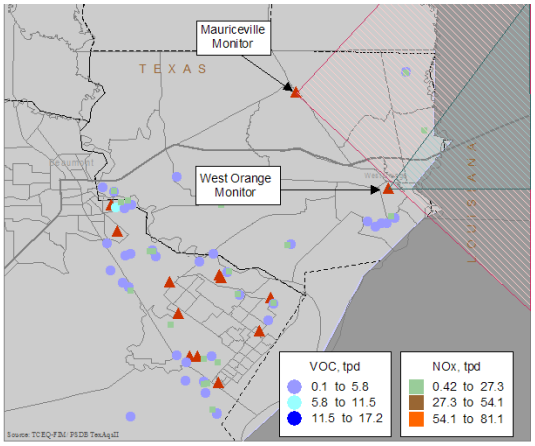

Figure 4-1: SETPRC Mauriceville 42 C642/C311/C665 and West Orange C9/A141 Monitors

Locations of SETPRC Mauriceville 42 C642/C311/C665 and West Orange C9/A141 monitors east of Beaumont-Port Arthur, including directions used for analysis, and VOC and NO_X point sources reported to the TCEQ. Note that the shaded areas are approximately drawn. The SETPRC Mauriceville 42 C642/C311/C665 monitor shaded area, in light red, contains VOC and NO_X point sources. The West Orange C9/A141 monitor has a much smaller shaded area in green, which avoids the point sources. These two monitors observe ozone transported into Texas.

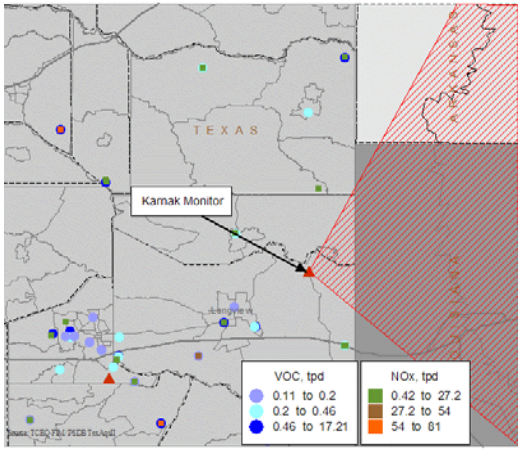

Figure 4-2: Karnack C85/AFHP303 Monitor

Location of Karnack C85/AFHP303 monitor near the Louisiana border, including range of directions used for analysis. This site observes ozone transported into Texas when winds are from the east and northeast. Several large point sources are west of the monitor. The red shaded area constitutes the directions considered in this analysis.

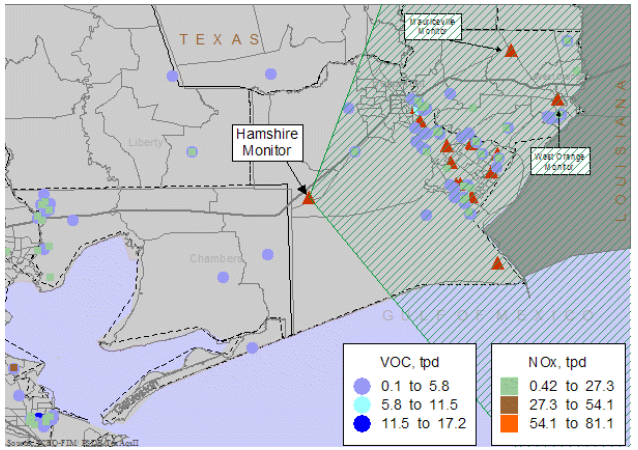

Figure 4-3: Hamshire C64/C654 Monitor

Location of the Hamshire C64/C654 monitor between Houston and Louisiana, including range of directions used for analysis. This site observes ozone transported into Houston when winds are from the east. The green shaded area represents directions considered in this analysis.

and examines the distribution of daily maximum ozone concentration over time to determine whether these supposed background concentrations have increased or decreased. Note that both the Nielson-Gammon methods and the TCEQ methods may not strictly estimate background ozone, as defined above, because they do not remove any potential recirculation of pollutants generated via local emissions. Also, background ozone alone may not tell the complete story, since ozone precursors, which can react with each other and with local emissions to produce ozone, may also be present in transported air.

Four candidate monitors were selected for this analysis and are listed in Table 4-1. Two monitors, West Orange (CAMS 9) and SETPRC Mauriceville 42 (CAMS 642), are located east of the HGB area, adjacent to the Texas-Louisiana border, east of the Beaumont-Port Arthur (BPA) area; one, Karnack (CAMS 85), is located in northeast Texas near the Texas-Louisiana-Arkansas border and the Tyler-Longview-Marshall (TLM) area; and one, Hamshire (CAMS 64), is located east of the HGB area, between the HGB area and the BPA area. Each of these monitors was selected for specific purposes. West Orange (CAMS 9) and SETPRC Mauriceville 42 (CAMS 642) were chosen because they are as close as possible to the Texas border and, thus, are useful for isolating background ozone being transported into the state from the east. Karnack (CAMS 85), in northeast Texas, is also very near the Texas border, and was selected to provide an assessment of background ozone transport from more northerly regions. The final site, Hamshire (CAMS 64), was selected to aid stratification of background ozone being transported into the HGB area into a component originating outside the state, and a component contributed by the BPA area.

Table 4-1: Monitors Selected for Background Transport Analysis

Monitor	metro area	location	years
West Orange C9/A141	BPA	TX-LA border	2000-2008
SETPRC Mauriceville 42 C642/C311/C665	BPA	TX-LA border	2000-2008
Karnack C85/AFHP303	TLM	TX-LA-AR border	2001-2008
Hamshire C64/C654	HGB	between BPA and HGB	2000-2008

Source: TCEQ/LEADS database. Data with wind speeds less than 3 miles per hour were excluded to minimize influences from periods of stagnation which may result in over estimation of background concentrations

To isolate ozone being transported into the state, measurements at the selected monitors were restricted by wind direction. The West Orange (CAMS 9) monitor is located less than 3 miles from the Louisiana border but is near several industrial sites. Only ozone measurements taken when winds originated from directions ranging from 30° to 90° (Figure 4-1) were considered, to minimize possible influence from these sources. Thirty degrees corresponds to a north-northeast direction and 90^{o} is due east. The SETPRC Mauriceville 42 (CAMS 642) monitor is located ten miles from the Louisiana border, north of the West Orange (CAMS 9) monitor. This site may have some minor influence from relatively small NO_X and VOC sources. Nevertheless, data from this monitor was restricted to wind directions originating from 30° to 90°, similarly to West Orange (CAMS 9), to minimize any possible influence of point sources.

The Karnack (CAMS 85) monitor in the Tyler/Longview/Marshall area is located eight miles from the Texas-Louisiana border, and roughly 20 miles from Arkansas. Measurements from Karnack (CAMS 85) were restricted to wind directions originating from 30° to 135° (Figure 4-2), that is, from north-northeast clockwise to southeast. Though this site is not near Houston, it records large influxes of continental air transported from the Midwestern U.S. into Texas, which ultimately may raise background ozone concentrations throughout the state. Also, estimates of background ozone concentrations from Karnack (CAMS 85) can be compared to background estimates from West Orange (CAMS 9) and SETPRC Mauriceville 42 (CAMS 642), which is useful for corroborating estimates at these two sites, and determining the range of background ozone entering the state.

The final site under consideration is Hamshire (CAMS 64), located between the HGB area and the BPA area. Ozone measurements from this site can be used to estimate background ozone concentrations transported to Houston when winds are from the east. These background ozone measurements will be a combination of pollution transported into Texas, as well as the contribution of pollution from the Beaumont-Port Arthur area. To avoid undue influence of nearby industrial sites, similar to Karnack (CAMS 85), data from Hamshire (CAMS 64) are restricted to measurements obtained when winds originate from directions ranging from 30° to 135°. For the four monitors, monthly 10th, 25th, 50th, 75th and 90th percentiles of hourly ozone concentrations were calculated for the spring and summer ozone season, May through September, 2000 through 2008, except Karnack (CAMS 85) which only has data since 2001. These values are plotted in Figures 4-4 through 4-7. Ninetieth percentile values are reported in Table 4-2.

Table 4-2: Range of Monthly 90th Percentile Daily Peak One-Hour Ozone Concentrations, for Subject Wind Directions

	Hamshire C64/C654		Karnack C85/AFHP303		SETPRC Mauriceville 42 C642/C311/C665		West Orange C9/A141	
year	min	max	min	max	min	max	min	max
	ppb	*ppb*	*ppb*	*ppb*	*ppb*	*ppb*	*ppb*	*ppb*
2000	38	74	.	.	56	81	43	**83**
2001	50	**71**	.	54	45	69	57	68
2002	51	62	58	**84**	40	68	53	69
2003	30	**68**	60	64	39	61	38	66
2004	43	**71**	39	66	30	61	41	66
2005	55	**79**	62	75	43	76	52	75
2006	45	76	42	**78**	32	63	43	75
2007	37	62	55	67	40	62	47	**69**
2008	40	62	.	65	47	**70**	50	60
9-year period	30	79	39	**84**	30	81	38	83

Note: Though data has been restricted by wind direction to mitigate influences from nearby pollution sources, there may be unknown influences that are unaccounted for. Maximum values for each year are highlighted in boldface type.

To statistically verify whether a trend across time exists in the data, an index of date was fit to the daily peak values using ordinary least squares regression. Additional regressions were performed using an index of month against the selected percentiles of the monthly distributions. The resulting parameter estimates from these models revealed no statistically significant trend at the 5 percent significance level ($\alpha = 0.05$); however, it is important to note that the data likely suffers from autocorrelation, a problem common to time series data. Time series data are often correlated with themselves across time, which complicates formal statistical estimation by biasing parameter estimates.

Rather than performing the tedious procedures necessary to detect, measure, and correct for autocorrelation, a careful visual inspection of time series plots, presented in Figures 4-4 through 4-7, satisfies that no time trend is perceptible. These four figures plot the five selected percentiles of the monthly distributions at each monitor. While no trend is detectable, what is apparent is that ozone concentrations measured at these monitors, which have been restricted in such a way as to proxy background levels, vary substantially. Background ozone at these monitors varies as much as 35 parts per billion (ppb), due to meteorological effects and ozone dynamics occurring in upwind regions.

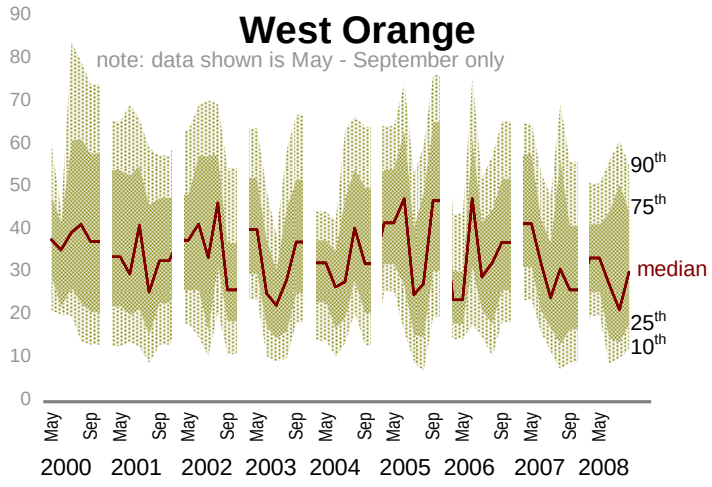

Figure 4-4: Selected Statistics for the West Orange C9/A141 Monitor

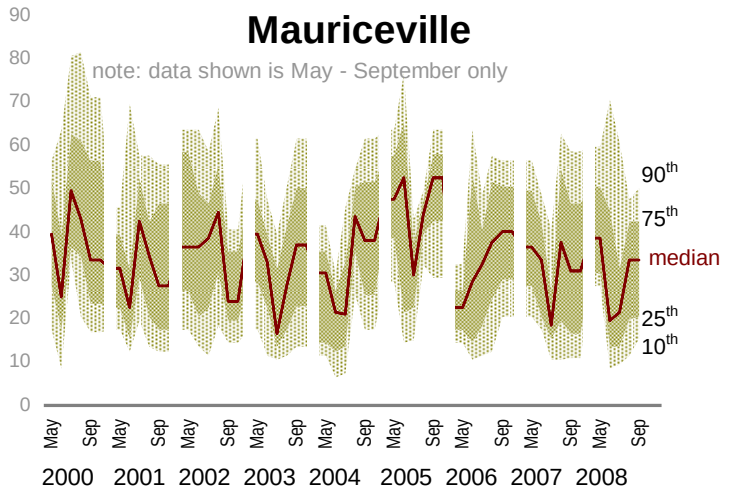

Figure 4-5: Selected Statistics for the SETPRC Mauriceville 42 C642/C311/C665 Monitor

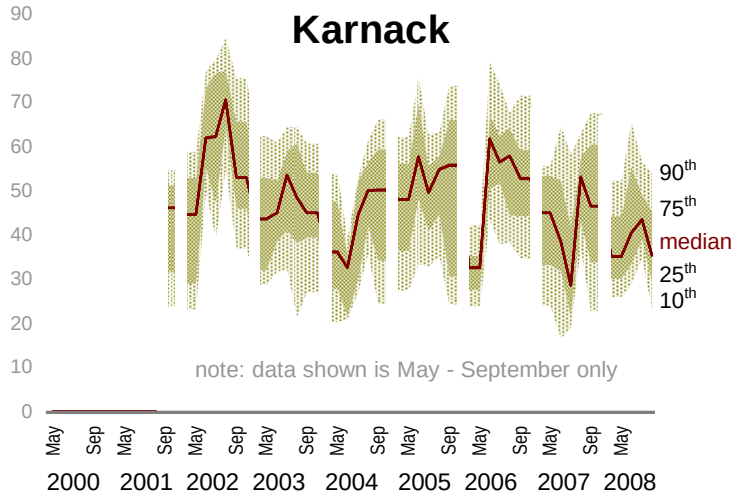

Figure 4-6: Selected Statistics for the Karnack C85/AFHP303 Monitor

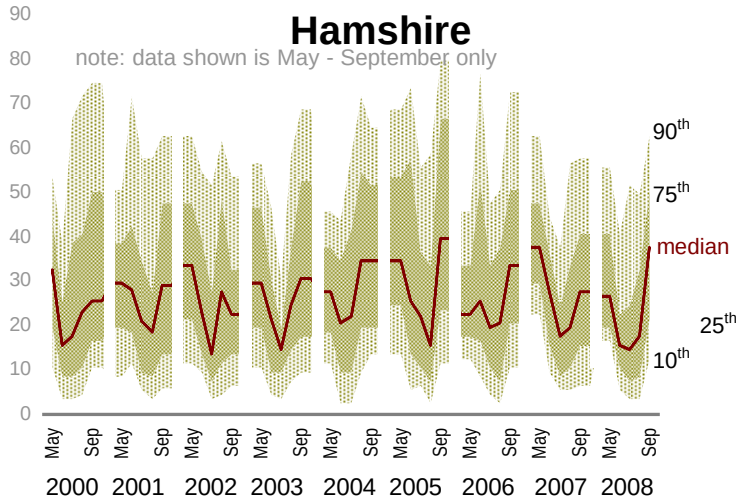

Figure 4-7: Selected Statistics for the Hamshire C64/C654 Monitor

Notable in Figure 4-7, one-hour ozone concentrations at Hamshire (CAMS 64) behave similarly to West Orange (CAMS 9) and Karnack (CAMS 85), in that there is no observable or statistically significant trend of the median or 90th percentile values. The 90th percentile at Hamshire (CAMS 64), considering directionally restricted data for May to September, 2000 through 2008, is 59 ppb. This value is in the range of values computed by Nielson-Gammon using different procedures; however, the 90th percentile can exceed 80 ppb at any of the sites, and even exceeded 90 ppb at SETPRC Mauriceville 42 (CAMS 642) in 2000. The 2006 Texas Air Quality study also found background ozone concentrations exceeding the NAAQS (TexAQS II Rapid Science Synthesis Team 2006).

Table 4-3: Parameter Estimates for Regression of West Orange C9/A141 on SETPRC Mauriceville 42 C642/C311/C665

	intercept	slope
β estimate	4.95706	1.01251
Std. Error	0.55480	0.01421
t-statistic	8.935	71.278
Pr(>|t|)	<2e-16	<2e-16
R^2	0.78	

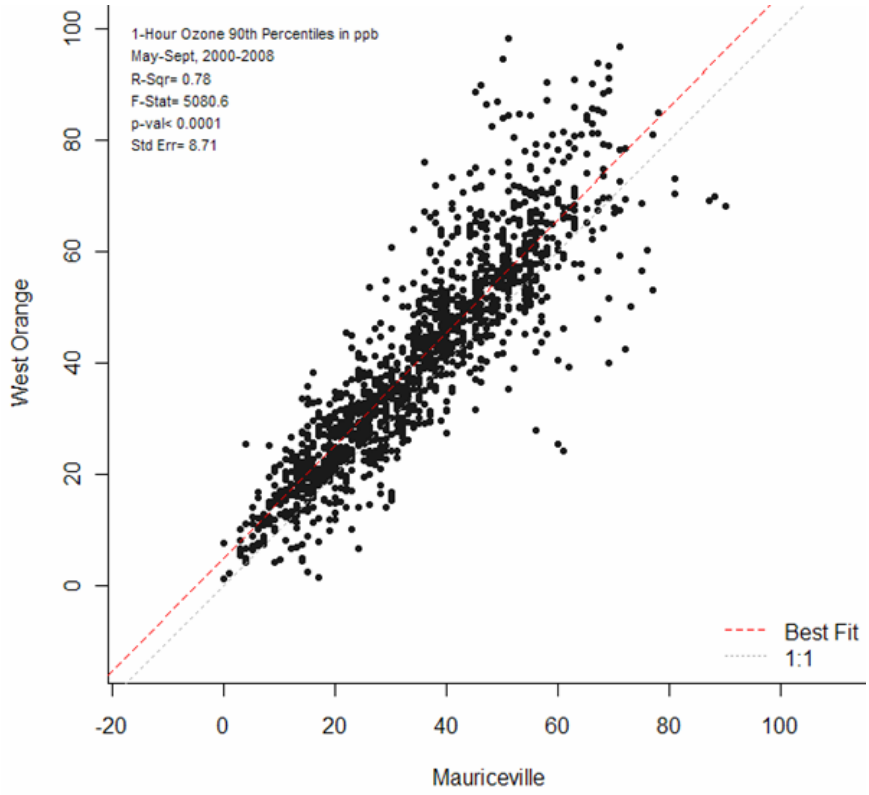

Figure 4-8: Scatter-plot of 90th Percentile Hourly Values at West Orange C9/A141 and SETPRC Mauriceville 42 C642/C311/C665
Note that the values are from May to September, 2000 to 2008. This plot supports the contention that these two monitors are measuring roughly the same phenomena, under wind-restricted regimes.

Over the period 2000 through 2008, the maximum 90th percentile one-hour ozone concentrations at West Orange (CAMS 9) and SETPRC Mauriceville 42 (CAMS 642) are 79 and 92, respectively. The maximum 90th percentile for Karnack (CAMS 85) over the period 2001 through 2008 is 81. Karnack (CAMS 85) appears to consistently measure a higher background than either West Orange (CAMS 9) or SETPRC Mauriceville 42 (CAMS 642). These results are consistent with estimates reported by Nielson-Gammon, et al. (2005a), which also found higher

background ozone concentrations during the ozone season in northeast Texas than in the HGB area.

Regression analysis was used to determine whether the 90th percentile values at West Orange (CAMS 9) and SETPRC Mauriceville 42 (CAMS 642) track one another, which suggests they are measuring roughly equivalent phenomena. The resulting R^2 of 0.78, which is significant at a probability level less than 0.1 percent (Table 4-3), indicates very strong correlation between measurements at the two sites. The scatter plot of the data is illustrated in Figure 4-8.

In summary, none of the four sites used for estimating background ozone concentrations recorded a statistically significant trend. The 90th percentiles of hourly ozone concentrations for the entire 9-year period of available data is 63 ppb for West Orange (CAMS 9), 58 ppb for SETPRC Mauriceville 429 (CAMS 642), 60 ppb for Hamshire (CAMS 64), and 72 ppb for Karnack (CAMS 85). It was expected that the Hamshire (CAMS 64) site would record higher ozone in the Houston area, being downwind of the Beaumont-Port Arthur industrialized area. Karnack (CAMS 85), having less influence from Texas industry, recorded the highest 90th percentile measurement with background ozone reaching as high as 63 ppb, but is furthest from Houston. The West Orange (CAMS 9) and SETPRC Mauriceville 42 (CAMS 642) sites behave similarly, where West Orange (CAMS 9) records higher ozone than SETPRC Mauriceville 42 (CAMS 642).

4.2 LONG RANGE TRANSPORT TRENDS

This section investigates patterns in continental transport of ozone into Texas. The EPA AIRNow website reports daily national ozone levels. Eight-hour daily ozone concentrations from AIRNow, for May through September, 2004 through 2008, were used to identify days on which transport of ozone into Texas was likely. Candidate days were selected by examining AIRNow ozone plots for days when ozone over 85 ppb occurred in multiple states upwind of Texas, generally as far east as the Midwestern U.S. For these days, back trajectories were created using the National Oceanic and Atmospheric Administration (NOAA) HYSPLIT (Hybrid Single Particle Lagrangian Integrated Trajectory) (Draxler, et. al, 2003) model and EDAS (Eta Data Assimilation System) (Rolph, 2003) data for each identified day, to verify whether transport was indeed possible from the Midwest.

For example, if AIRNow showed ozone concentrations above 85 ppb from the Ohio River Valley down into Texas, which is a common transport path on a nation-wide scale, the associated back trajectory would have to traverse Texas to the Ohio River Valley region to be considered a possible transport day. Frequencies of identified transport days, by year, were computed; however, an unknown degree of uncertainty accompanies this approach, due to the visual identification procedure for identifying transport events from AIRNow plots. Examples of HYSPLIT backward trajectories are presented in Figure 4-9 and Figure 4-10 for an eastern transport trajectory and a Gulf trajectory, respectively.

Each day was further categorized as either an eastern transport day, a Gulf transport day, or a Texas transport day, depending on which states recorded high ozone and the direction of the back trajectory. An eastern transport day indicates that the HYSPLIT trajectory model predicted air fetches from any state east and northeast of Texas. Similarly, Gulf transport indicates fetches from the Gulf of Mexico, and Texas transport indicates fetches from within Texas all in combination with elevated ozone. The length of the back-trajectories, or fetches, is 48 hours, with trajectories arriving at 1,500 meters altitude. Table 4-4 reports results of trajectory frequency computations.

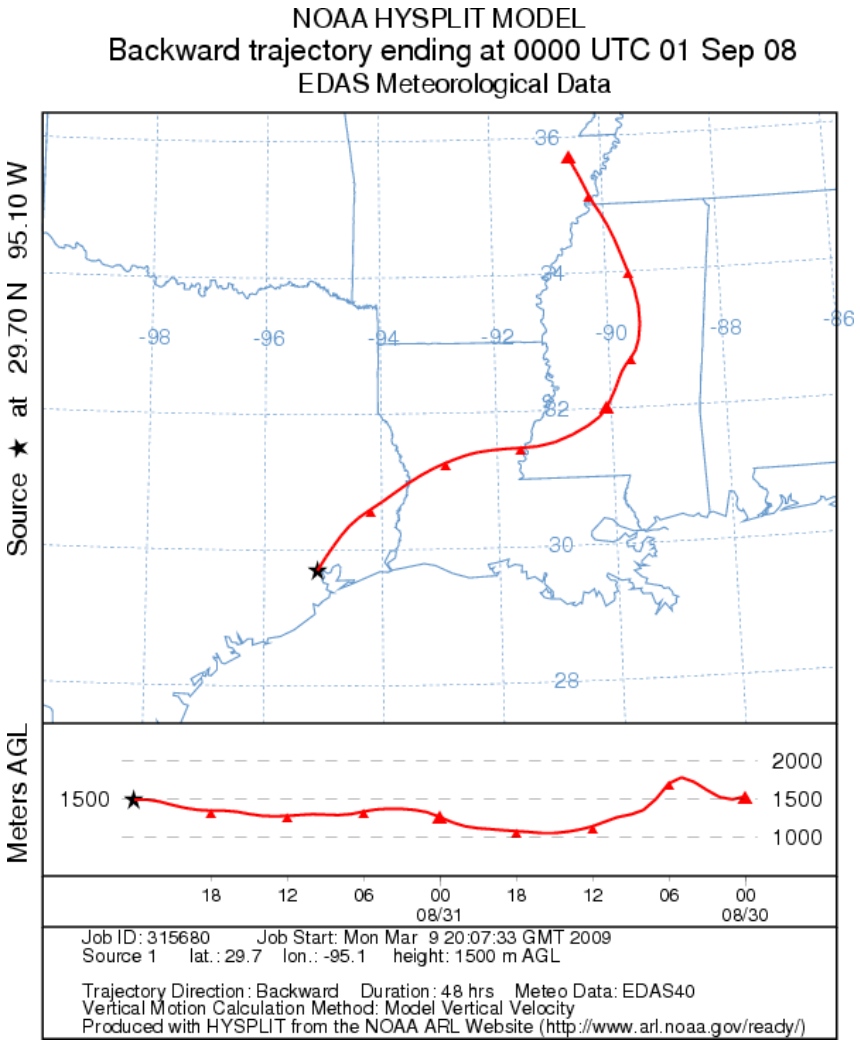

Figure 4-9: HYSPLIT Backward Trajectory from Eastern Source
Typical output from NOAA HYSPLIT backward trajectory computation showing transport elevation winds deriving from eastern sources. Source winds originate at 1,500 meters altitude. Trajectory is 48 hours long, ending at 00:00 hours on September 1, 2008.

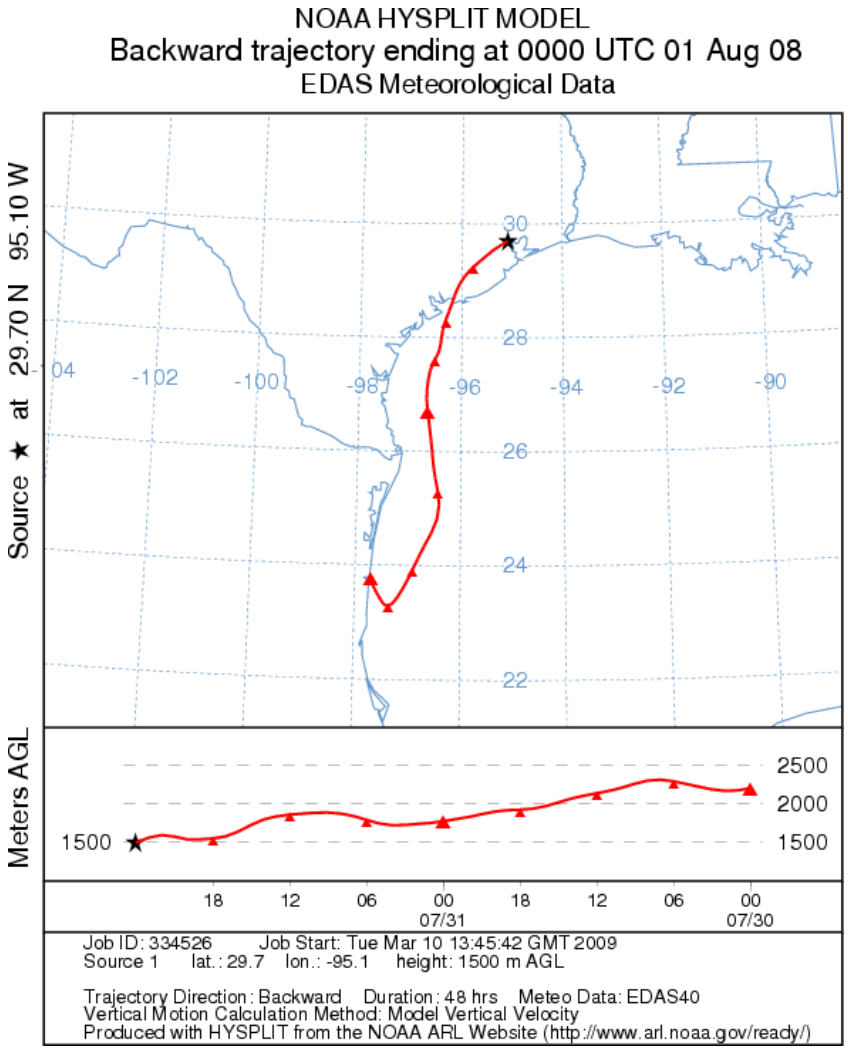

Figure 4-10: HYSPLIT Backward Trajectory from Gulf Source
Typical output from NOAA HYSPLIT backward trajectory computation showing transport elevation winds deriving from a Gulf sources. Source winds originate at 1,500 meters altitude. Trajectory is 48 hours long, ending at 00:00 hours on August 1, 2008

As shown in Table 4-4, eastern transport frequency totals in 2004, 2007, and 2008 are similar, with 11, 8 and 10 days, respectively. Years 2005 and 2006, however, recorded higher frequencies of high ozone back trajectories, with 22 and 34 days, respectively. Identified transport days are fewer in 2004, 2007 and 2008, suggesting that background ozone levels transported from Eastern states were lower, which would also be expected to reduce Texas's ozone levels in those years.

Table 4-4: Frequency of Eastern Ozone Transport Events

	May	June	July	August	September	Total
2004	0	0	1	6	4	11
2005	6	3	4	8	13	34
2006	0	8	6	8	0	22
2007	1	3	0	0	4	8
2008	1	5	2	2	0	10
Total	8	19	13	24	21	85

Monthly frequencies (May through September) of eastern transport days were regressed against monthly 50th percentile ozone concentrations recorded at both the West Orange (CAMS 9) and Karnack (CAMS 85) monitors. Correlations at both monitors were noted, with R^2=0.3 and p-value=0.0037 at West Orange (CAMS 9), and R^2=0.4 and p-value<0.001 at Karnack (CAMS 85) (Figure 4-12). It appears that in months when more ozone transport events occur, the corresponding monthly 50th percentile of ozone is larger in magnitude. Table 4-5 provides additional information on the regression coefficients.

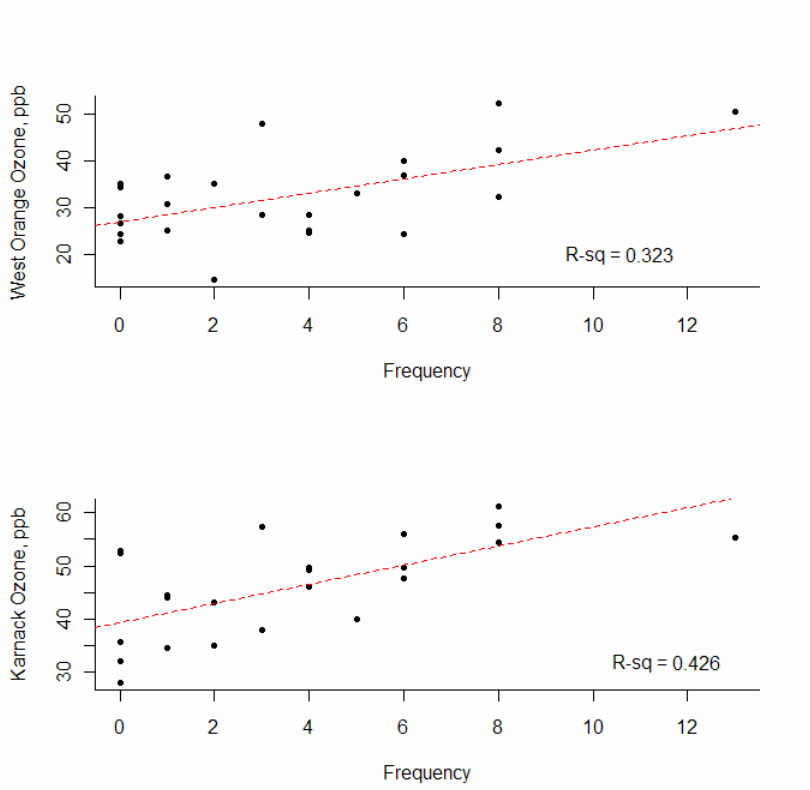

Figure 4-11: Monthly Median Ozone and Frequency of Eastern Transport Events
Top plot illustrates West Orange C9/A141 and bottom plot is Karnack C85/AFHP303. Note that as the frequency of identified transport events increases, median (50th percentile) ozone measurements also increase at both monitors.

Table 4-5: Parameter Estimates from Regression of Ozone on Transport Frequency

	West Orange C9/A141		Karnack C85/AFHP303	
	intercept	slope of Transport Frequency	intercept	slope of Transport Frequency
β estimate	26.969	1.532	39.339	1.7948
t-statistic	11.699	3.241	18.161	4.041
Pr(>|t|)	6.47e-11	0.00375	9.9e-15	0.000545
R^2	0.323		0.426	

The resulting explanatory power of the model is not large, but it reinforces the idea that there is a positive association between days indicative of transported ozone and ambient ozone measured at the West Orange (CAMS 9) and Karnack (CAMS 85) monitors. Though states in the eastern part of the U.S. are reporting lower design values (discussed below), ozone concentrations during transport from the east at Karnack (CAMS 85) and West Orange (CAMS 9) did not demonstrate any trend.

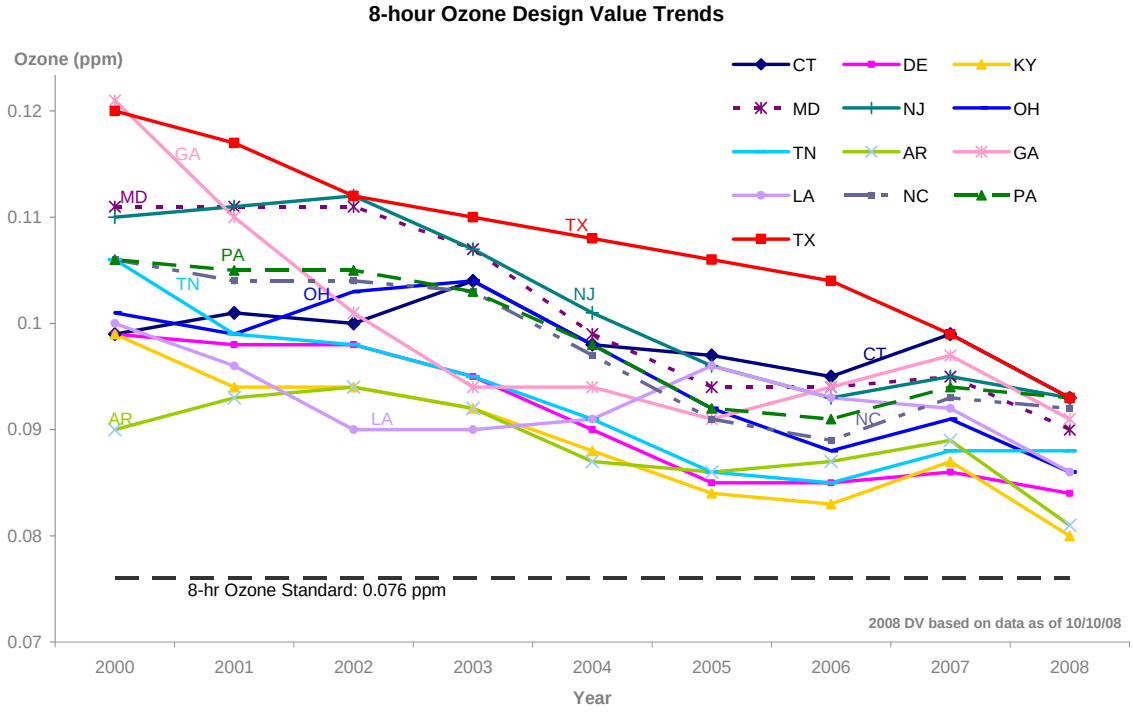

Figure 4-12: State-Wide Eight-Hour Ozone Design Values
Design Values have not been adjusted for meteorological effects. Most states shown exhibit a downward trend in state-wide Design Values. Data were obtained from EPA's AIRData Monitoring Reports with annual ozone values summarized by each state.

Another way to examine background ozone trends is to examine the ozone trends at states upwind of Texas. In Figure 4-12, eight-hour ozone design values (ppm) are plotted for 2000 through 2008 for Texas and selected eastern states. Chosen states were origination points of the back trajectories computed with HYSPLIT. Note that the eight-hour ozone design values shown are state-wide and are different from non-attainment area-specific ozone design value estimates. State-wide eight-hour ozone design values are derived using the highest fourth maximum eight-hour ozone value reported during the year by all monitoring sites in a state.

A steady downward trend in the state-wide eight-hour ozone design values for Texas is clear in Figure 4-12. State-wide ozone design values in the selected eastern states shown are also trending downward, although perhaps to a lesser degree. The statistical significance of these trends has not been calculated here. If the apparent overall decreasing trends in state-wide ozone design values in eastern states continue, they would be expected to reduce background ozone levels being transported into Texas.

While design values in many eastern states appear to be declining, design values in states adjacent to Texas, namely Arkansas and Louisiana, do not appear to be exhibiting a clear trend over the past decade. This suggests that control strategies adopted in eastern states may be having the desired effect, though previously these have been primarily oriented to addressing one-hour, rather than eight-hour, ozone violations. However, ozone transported from more easterly states must traverse the adjacent states before entering Texas, complicating source attribution efforts. Dispersion, dilution, vertical mixing and other phenomena all affect, and obscure analysis of, transport of ozone from eastern and northeastern sources into Texas. This further corroborates earlier findings that background ozone concentrations transported into Texas are not exhibiting a clear trend, either upward or downward, and are unlikely to be sufficient to explain reductions in ambient ozone concentrations observed in the HGB area.

4.3 SINUOSITY OF TRAJECTORIES

Measures of sinuosity, or "curviness," of the trajectory of an air parcel can be used to determine its original source (Nielson-Gammon, et al, 2005). When winds are straighter, or less sinuous, source identification is enhanced because there is less variability, and thus less uncertainty, in computations of originating directions. This section investigates the sinuosity of winds, specifically transport winds, traveling into the HGB area to determine whether these winds varied from year to year. Variability in transport winds across years could complicate determination of regions contributing background ozone to the HGB area, and, thus obscure selection of appropriate model input values for background ozone.

For purposes of this analysis, transport winds are defined as high elevation winds capable of moving air masses over long distances. These winds can carry pollutants from one area to another and affect local ozone concentrations (Cooper et al., 2006). A measure of sinuosity used by Xie and Berkowitz (2005) can be computed for a trajectory using wind speeds and directions. Sinuosity of transport winds (S) is calculated as the tip-to-tip (start point and end point) length (D_{t2t}) of a 48-hour trajectory – i.e., the distance from one tip to the other, "as the crow flies" – divided by the sum of intra-distances between adjacent hourly endpoints for the same trajectory (sum of D_i, for i hours):

$$S = \frac{D_{t2t}}{\sum D_i}$$

When D_{t2t} equals D_i , the trajectory is straight and the sinuosity equals one, the highest possible value. As a trajectory becomes less straight, that is, as ΣD_i increases with respect to D_{t2t}, the sinuosity increases and S becomes smaller. This is depicted in Figure 4-13 which compares a trajectory with sinuosity equal to 1.0 (the straight trajectory) with one with a sinuosity equal to 0.8 (the curved trajectory). For the straight trajectory, the numerator and denominator of the above equation are the same. For the curved trajectory, the numerator is the total distance of the straight trajectory, while the denominator is the total distance of the curved trajectory, summing the lengths of all intermediate segments. Higher sinuosity values, therefore, correspond to straighter winds.

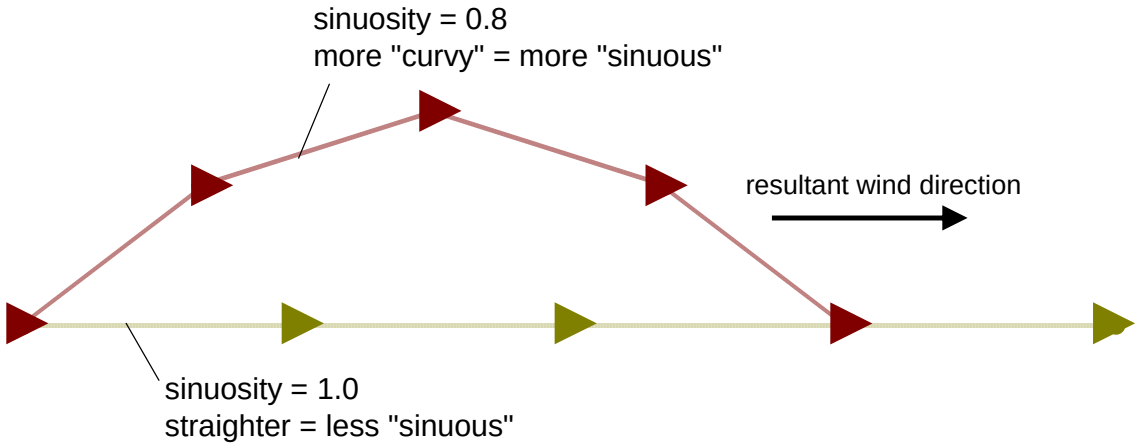

Figure 4-13: Comparison of Two Trajectories, One More and One Less Sinuous
The jagged trajectory (red line) is more sinuous, S is smaller (S = 0.85), than the straight trajectory (khaki line) where S is larger (S = 1.0).

Transport winds are modeled in this analysis with HYSPLIT 48-hour back-trajectories at 1500 meters altitude, for May through September, 2000 to 2008. HYSPLIT performs forward and backward trajectory modeling, and is available on the web site of the National Oceanic and Atmospheric Administration (NOAA). HYSPLIT computations report coordinates of the end points of trajectory segments, from which sinuosities can be calculated. Average sinuosity, S, was computed for each year and compared using the Tukey-Kramer multiple means comparison test, illustrated in Figure 4-14. Calculated sinuosities of the HGB trajectories for 2000 through 2008 are not statistically different at the 5 percent level ($\alpha = 0.05$); however, years 2005 and 2008 did show lower means, which suggests that those years observed more sinuous transport winds.

Further work is necessary to properly link these results to observed ozone concentrations. The complexities of the effects of sinuosity on ozone concentrations are copious. Regarding local ozone production, it is not entirely clear from the available research that straighter winds correspond to higher ozone concentrations, due to the absence of dilution from sources of ozone precursors, or whether the reverse is true, that more sinuous winds cause greater mixing of ozone precursors and thus dilution. This analysis focuses on large scale sinuosities, which would not necessarily apply to ozone production on a local level. A cursory examination of results for the two years with high sinuosity (i.e., straighter winds), 2000 and 2008, is inconclusive. Results for 2000, when ozone was high and wind sinuosity was also high, supports the first hypothesis, whereas results for 2008, when winds were also sinuous, but ozone was low, support the second.

Total wind trajectory length (D_{t2t}) was examined and no statistical difference was found in the means at a confidence level of 5 percent ($\alpha = 0.05$). The year with the longest median trajectory length was 2004, implying more dilution for that year. However, the Tukey-Kramer multiple means comparison test detected to no statistical difference among the years (Figure 4-16).

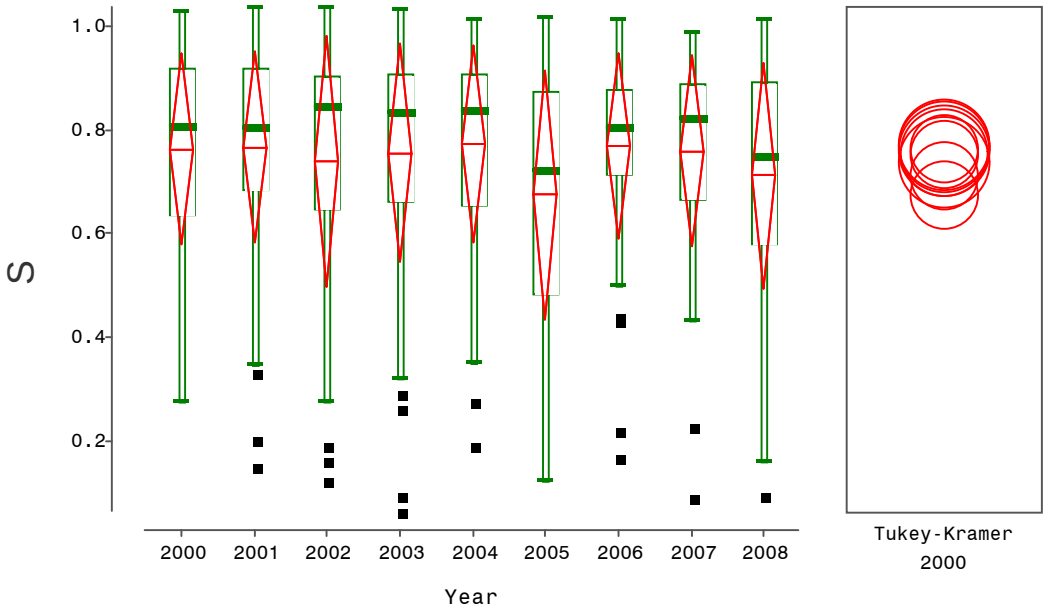

Figure 4-14: Box Plots and Tukey-Kramer Test Results for Sinuosity

Annual box plots (left) and graphical results of Tukey-Kramer means comparison test for sinuosity (S), for years 2000-2008 (right). Red lines on box plots represent means and heavy green likes represent medians. Red circles (right) represent confidence bounds computed from Tukey-Kramer. Because all cicles overlap each other, means are statistically indistinguishable from each other, at the $\alpha = 0.05$ level. Maxima may exceed one due to measurement error.

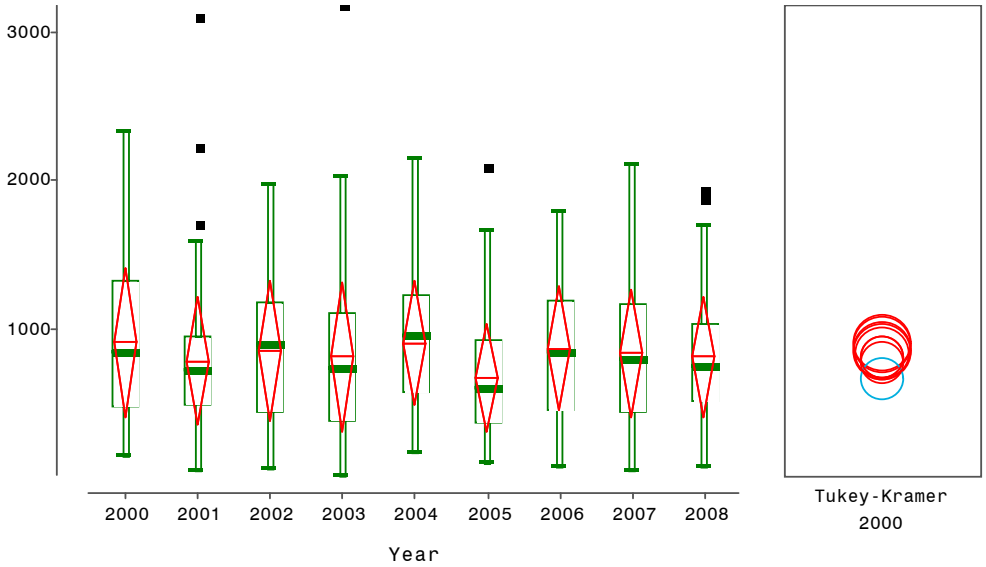

Figure 4-15: Box plots and Tukey-Kramer Test Results for Tip-to-Tip Trajectory Length

Annual box-plots (left) and graphical results of Tukey-Kramer mean comparison test of tip-to-tip length (D_{t2t}), for years of 2000-2008 (right). Red lines on box plots represent means and heavy green lines represent medians. Red circles (right) represent confidence bounds computed from Tukey-Kramer. Because all cicles overlap each pther, means are statistically indistinguishable from each other, at the $\alpha = 0.05$ level. The blue circle represents the year associated with the lowest mean, 2005.

Sinuosity of transport winds during 2008 were found to be statistically indistinguishable from other recent years using the Tukey-Kramer multiple means comparison test. The Tukey-Kramer method also confirmed that average 2008 wind trajectory length did not deviate from the typical sinuosity profile of transport winds traversing the HGB area.

4.4 TRANSPORT INTO THE HOUSTON-GALVESTON-BRAZORIA AREA

Previous sections have identified that, while transport plays a role in elevated ozone levels in the HGB area, the level of transport may not significantly change from year to year. It is important to be able to estimate the levels of ozone transported into the HGB area so that the amount of ozone than can be controlled (locally produced ozone) is identified. Studies done for the TCEQ (Sullivan, 2009) used HYSPLIT back trajectories along with EDAS to estimate the amount of ozone entering into the HGB area.

Numerous 72-hour back trajectories were run starting at 12:00 CST in central Houston, at 300 meters above ground level, during the peak of ozone season in the HGB area (May 1 to October 31, 2000 to 2007). Use of multiple trajectories can distinguish between source areas, or paths, that lead to higher than average, or lower than average ozone concentrations (Sullivan, 2009). A clustering algorithm was used to group multiple trajectories based on trajectory size and shape. Six identified clusters appear in Figure 4-16. Forty back trajectories that did not end up in any of the six clusters, illustrated in Figure 4-17, were grouped and assigned a cluster number of zero. Note that all but one of the back trajectories in cluster zero originate from the south and that these trajectories appear to extend beyond the EDAS modeling domain, which is the only difference between cluster zero and cluster two.

Figure 4-16 shows that cluster one and cluster two represent days in which winds originated from the Gulf of Mexico; these trajectories typically represent cleaner air coming from the Gulf and hence lower observed ozone concentrations in the HGB area. Cluster three represents long trajectories which come into the HGB area from the north as far away as Canada; this type of trajectory can also bring clean air from northern states and Canada into the HGB area. Cluster four represents stagnant air conditions, a frequent cause of ozone accumulation. Cluster five shows trajectories that originate from the northeast, in the Ohio River Valley, that bring polluted air from more populated areas into the HGB area. Cluster six illustrates trajectories from the east, some of which cross over Louisiana and the Beaumont-Port Author (BPA) area, and some of which cross over the Gulf. The mean centerline from each of the six clusters is shown in Figure 4-18. To quantify how these trajectories are related to ozone in the HGB area, trajectories were compared to ozone concentrations in the HGB area.

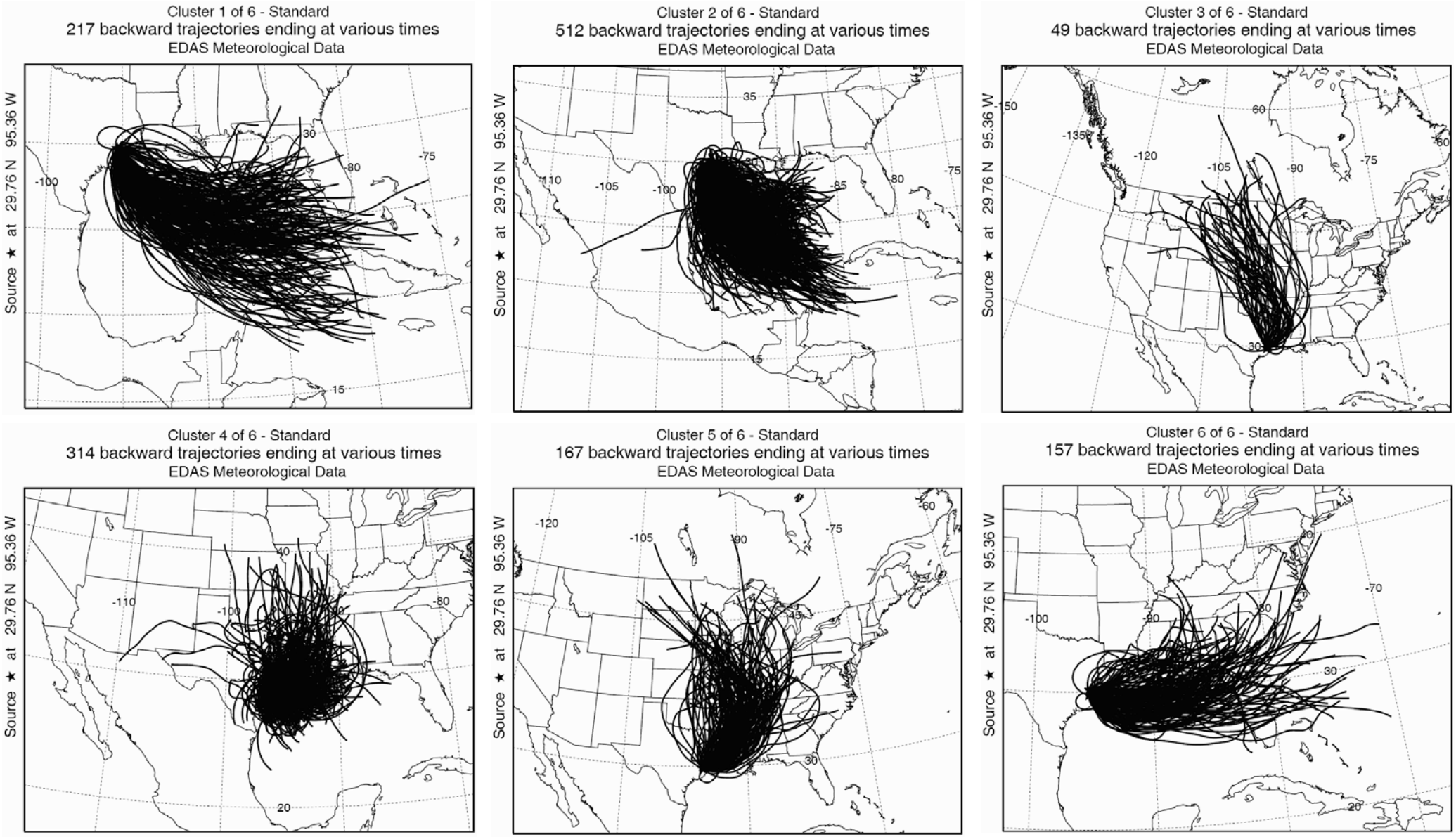

Figure 4-16: Six Clusters Found Using HYSPLIT Back Trajectory Clustering Algorithm

Back trajectories starting at 18:00 UTC were created for each day from May 1 to October 31, 2000 to 2007. The number of back trajectories in each cluster is found at the top of each map.

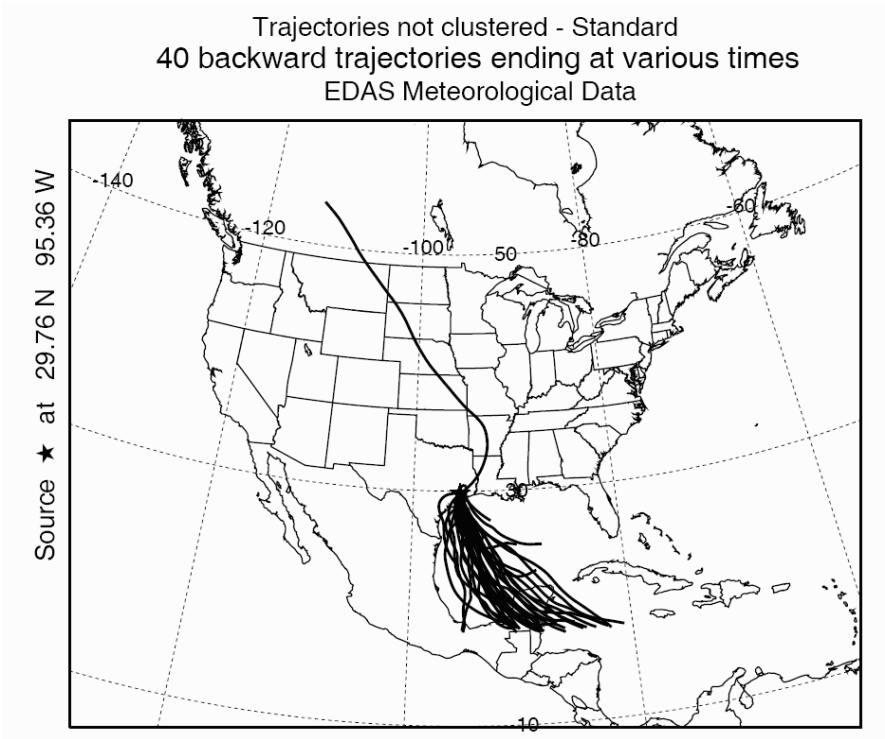

Figure 4-17: Cluster 0 Back Trajectories
These trajectories did not end up in any of the other six clusters. Note all but one of the back trajectories are from the south. One outlier back trajectory is from the northwest.

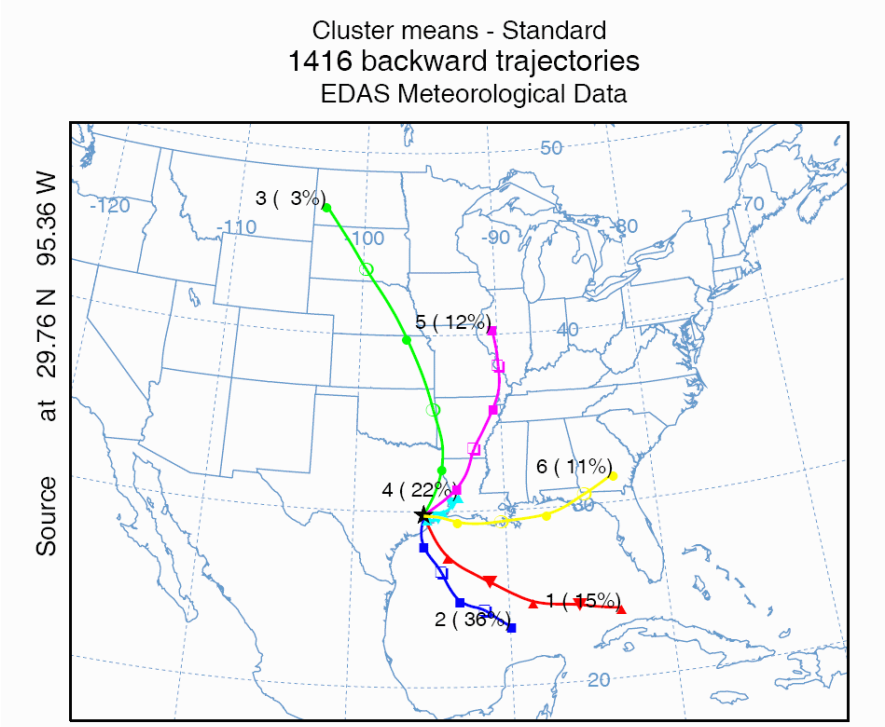

Figure 4-18: Means of Six 60-hour Back Trajectory Clusters
May-October 2000 – 2007, Houston origin 300 m AGL, 18 UTC: 0. (not shown) far southerly fetch; 1. red, SE fetch; 2. blue, SSE fetch; 3. green, northerly fetch; 4. cyan, short fetch; 5. magenta, NE fetch; 6. yellow, easterly fetch.

Twelve ozone sites, shown in Figure 4-19, that had near continuous operation from 2000 to 2007 in the HGB area were selected to compare with trajectory clusters. In an effort to use measurements from a consistent, long-term set of monitors, data from sites that were shut down

was combined with data from sites that began collecting data near the sites that were taken off-line. Examples of sites where data was combined are Lake Jackson (CAMS 1016) and Clute (CAMS 11), and Galveston Airport (CAMS 34) and Galveston 99th St. (CAMS 1034) Sites were selected based on locations as either a site upwind of the HGB area, or a site downwind of the HGB area. Northwest Harris Co. (CAMS 26), the Lake Jackson (CAMS 1016) / Clute (CAMS 11) combined site pair, and the Galveston Airport (CAMS 34)/ Galveston 99th St. (CAMS 1034) combined site pair generally represent sites measuring background ozone concentrations. Sites on the downwind side of downtown Houston and the Houston Ship Channel generally represent sites measuring maximum ozone concentrations in the HGB area. Maximum peak and minimum peak eight-hour ozone concentrations from the twelve monitors were found for each day, then merged with the cluster classification from each day. Following Nielson-Gammon et al. (2005a), that minimum peak eight-hour average ozone concentration was used to represent the "background" ozone level in the HGB Area.

Figure 4-19: Sites Used in Ozone Area Maximum and Background Determination
Note that data from Lake Jackson C1016 and Clute C11 and data from Galveston 99th St. C1034/A320/X183 and Galveston Airport C34/C109/X152 were combined to create two long term data sets, one for the Galveston monitors and one for the Lake Jackson C1016 monitors.

Table 4-6 summarizes average maximum and average minimum, or background, ozone concentrations for each cluster. Average maximum peak daily eight-hour ozone among the clusters ranges from 40.6 ppb to 73.3 ppb, while average minimum peak daily eight-hour ozone, considered a proxy for background ozone concentrations, ranges from 21.4 ppb to 45.1 ppb. The difference between these two means can be used as a surrogate for locally produced ozone. Cluster four and cluster five, which represent the short fetch and the northeast fetch, have the highest average maximum ozone concentrations, 71.6 ppb and 73.3 ppb, respectively, and, perhaps not coincidentally, the highest average background, 40.8 ppb and 45.1 ppb. These two clusters also exhibit some of the largest average differences, or local contributions. Cluster zero, the far southeast cluster, cluster one, the east southeast cluster, and cluster two, the southeast cluster, exhibited some of the smallest average background and average peak ozone; these clusters are expected to have a lower background ozone due to their origins over the Gulf of Mexico.

Table 4-6: Ozone Statistics for HYSPLIT Back Trajectory Clusters

Cluster	Fetch	Number of back trajec-tories	Average maximum peak daily eight-hour ozone	Average minimum peak daily eight-hour ozone	Average difference, minimum and maximum ozone*
		#	*ppb*	*ppb*	*ppb*
5	NE	166	73.3	45.1	28.1
4	Short	312	71.6	40.8	30.8
6	East	151	61.1	35.6	25.5
3	North	49	59.1	37.2	21.9
2	SE	506	48.5	24.8	23.7
0	far SE	40	45.0	23.8	21.1
1	ESE	217	40.6	21.4	19.1

* May not sum due to rounding. Note: Data is May through October, 2000 to 2007. Fetch represents the main direction of the cluster, count is the number of back trajectories in each cluster, and average minimum peak daily eight-hour ozone is taken as the background ozone concentration. Clusters are sorted in descending order by average maximum peak daily eight-hour ozone.

Table 4-7: Average Maximum Ozone and 95 Percent Confidence Intervals

Cluster ranked by maximum average	Fetch	Count	Average maximum peak daily eight-hour ozone	Average maximum + 2 standard errors	Average maximum - 2 standard errors
		#	*ppb*	*ppb*	*ppb*
5	NE	166	73.3	76.7	69.8
4	Short	312	71.6	74.3	68.9
6	East	151	61.1	64.5	57.8
3	North	49	59.1	65.2	53.0
2	SE	506	48.5	50.3	46.6
0	far SE	40	45.0	51.5	38.4
1	ESE	217	40.6	42.7	38.5

Note: Confidence intervals were constructed using two standard errors. Clusters are sorted in descending order by average maximum peak daily eight-hour ozone. Confidence intervals for differences between the area ozone maximums generally do not overlap beyond one or two rows.

The 95 percent confidence intervals for the mean eight-hour ozone maximum for each cluster are shown in Table 4-7. Two standard errors were used for the confidence intervals in each row. The confidence intervals in the table show that the differences between means are statistically significant for most of the pair-wise comparison. This is shown graphically in Figure 4-20.

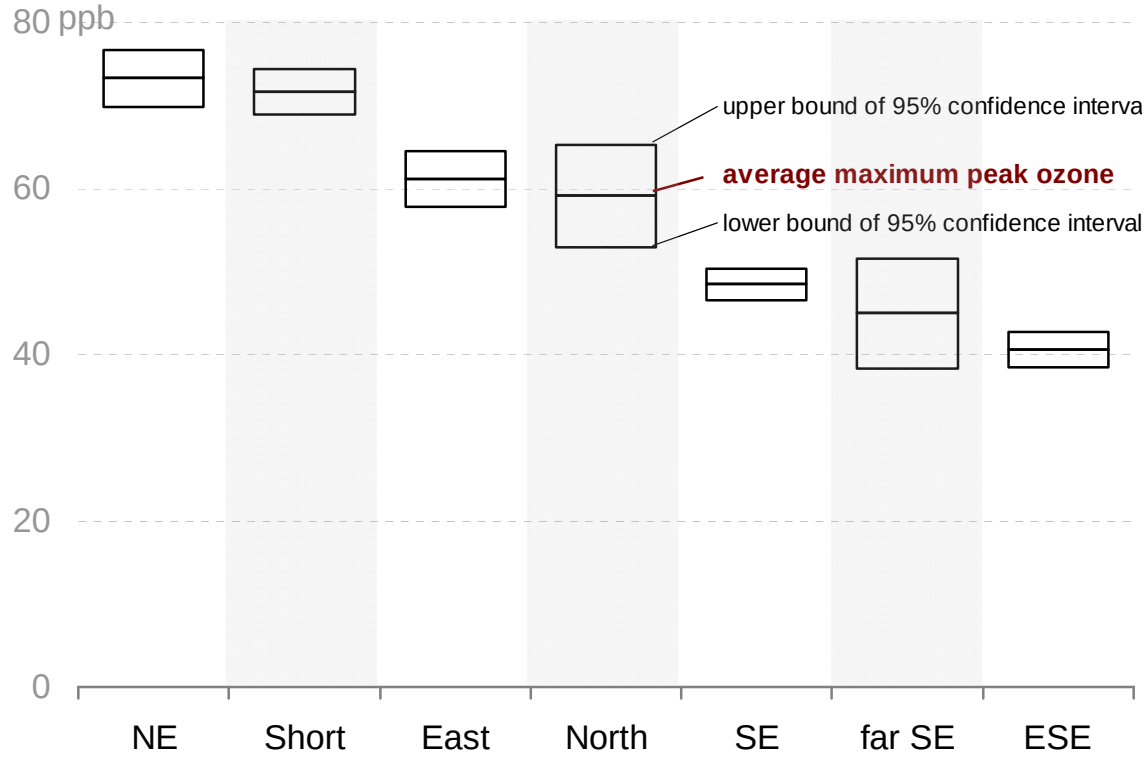

Figure 4-20: Average Maximum Ozone and 95 Percent Confidence Intervals
Average maximum peak daily eight-hour ozone concentrations by directional cluster, with upper and lower bounds of the 95 percent confidence intervals. Note that fetches originating from the northeast and east, as well as the "short" fetch, have the highest average peak daily ozone values, and they are tightly clustered. Clusters originating from the north and far southeast have noticeably wider confidence intervals, indicating more variability, but with lower average peak daily ozone concentrations than the northeast and east clusters.

Although many of the selected sites were intended to represent background and maximum ozone in the HGB area, note that, on many days, true "background" ozone concentrations may be observed farther away, in more rural areas, and the true maximum ozone concentration may also be underestimated. Despite uncertainty in estimates of true background and maximum ozone concentrations, the large number of observations used in this analysis, as well as evidence presented earlier, provides clear evidence that ozone in the HGB area is affected by transport of ozone from external sources.

Figure 4-21, recreated from Sullivan (2009), shows there is a significant linear relationship between mean HGB area minimum and maximum eight-hour average ozone concentrations by trajectory cluster ($p<0.01$). The relationship between maximum and minimum ozone by cluster suggests that trajectory cluster is a factor determining severity of both HGB area maximum and background ozone concentrations (Sullivan, 2009). The estimated slope parameter ($\beta=1.36$) of the ordinary least squares regression of average minimum ozone concentration against average maximum ozone concentration shows that maximum ozone concentration increases at a greater rate with trajectory cluster when compared to minimum ozone.

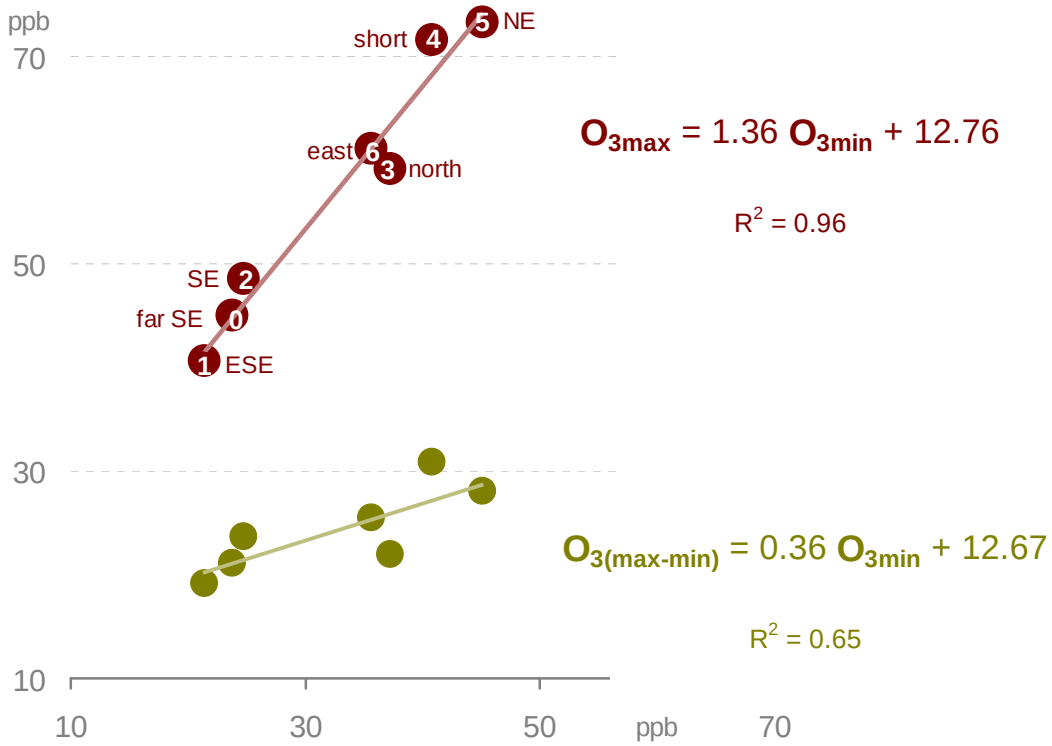

Figure 4-21: Relationship Between Minimum and Maximum Ozone Concentrations
Dark red points and estimated regression line represent the relationship between mean maximum ozone and mean minimum (background) ozone concentrations by cluster. Olive points and estimated regression line represent the relationship between "local contribution" (difference between maximum and minimum) and mean minimum ozone concentrations by cluster.

Figure 4-21 also shows that the difference between mean HGB area maximum and minimum ozone concentrations is also roughly linear with area minimum, but with a lower slope (β=0.36) and less statistical significance (p-value=0.03) (Sullivan, 2009). The linear relationship between the difference and mean HGB area minimum ozone suggests the local contribution may also be related to transport. The slower air movement of cluster four, which is the "short" cluster, allows greater accumulation in the area under lower local surface wind speeds. Note that winds originating from the directions of cluster six, the "east" cluster, and cluster five, the "northeast" cluster, help to move surface air along the area around the Houston Ship Channel and across the downtown Houston area, which, as noted, contain large amounts of ozone precursors. Overall, this analysis shows that directions of back trajectories can account for up to 24 ppb of variation in background ozone concentrations, and up to 35 ppb of variation in maximum ozone concentrations.

4.5 TRANSPORT AND SURFACE WIND TRAJECTORIES

While still incomplete, a preliminary analysis of upper level, or transport, wind trajectories was conducted to confirm and extend findings from the above directional analysis. Additional HYSPLIT modeling of 48-hour back trajectories at 1500 meters for May through August, 2000 to 2008, was used to detect difference in trajectories across years that may have influenced ozone concentrations in the HGB area.

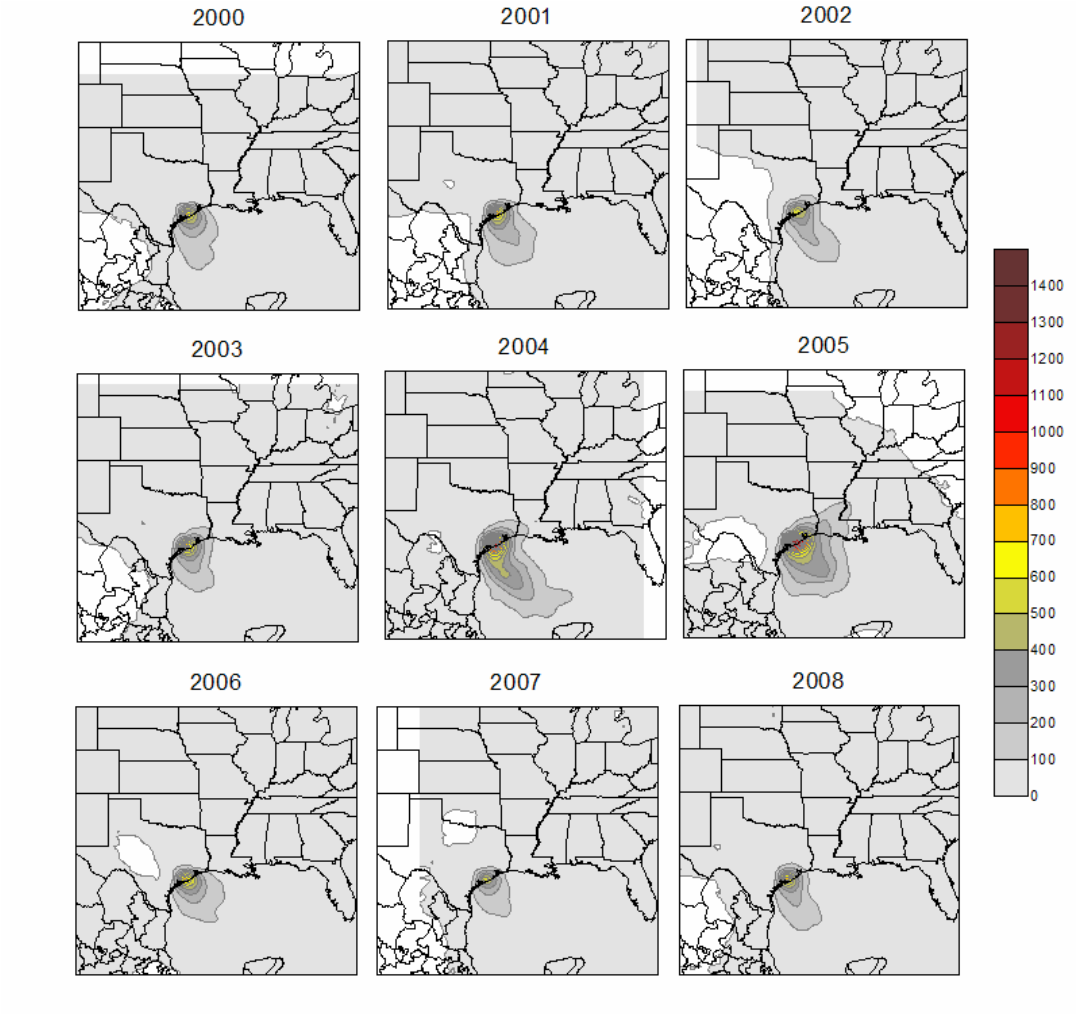

Figure 4-22: Distributions of End Points from HYSPLIT 48-hour Back Trajectories
This matrix compares distributions of 48-hour trajectory end points computed with HYSPLIT for 2000 to 2008. Notice that 2000 and 2008 have similar distributions, though each recorded substantially different magnitudes of ozone concentrations.

A simple visual inspection of the densities of distributions of trajectory end points presented in Figure 4-22 shows that upper elevation wind patterns for 2008, a year that observed relatively low ozone concentrations, do not noticeably differ from patterns in other years. Of the years analyzed, the pattern for 2000, a year with relatively high levels of ozone, is perhaps the most similar to 2008. The spatial distribution is similar among years and wind speeds are also similar. Higher wind speeds are evident in 2004 and 2005, as implied by trajectories with longer fetches.

Further preliminary analysis was conducted on surface level winds. Figure 4-23 displays 14-hour duration, 10 meter surface wind back-trajectories for May to September, at start hour 13:00 back to the previous midnight (hour 0:00). These trajectories were derived from surface winds using an inverse squared weighted model, similar to the model used by Xie and Berkowitz (2005). This time period was selected to facilitate tracing of observed peaks in eight-hour ozone concentrations back to their origins from the preceding morning. Though these observations have not yet been quantified, visual inspection of the figure reveals that 2008 did not exhibit noticeable deviation from other years. Spatial distributions, though different, were not different enough to suggest a departure from typical patterns.

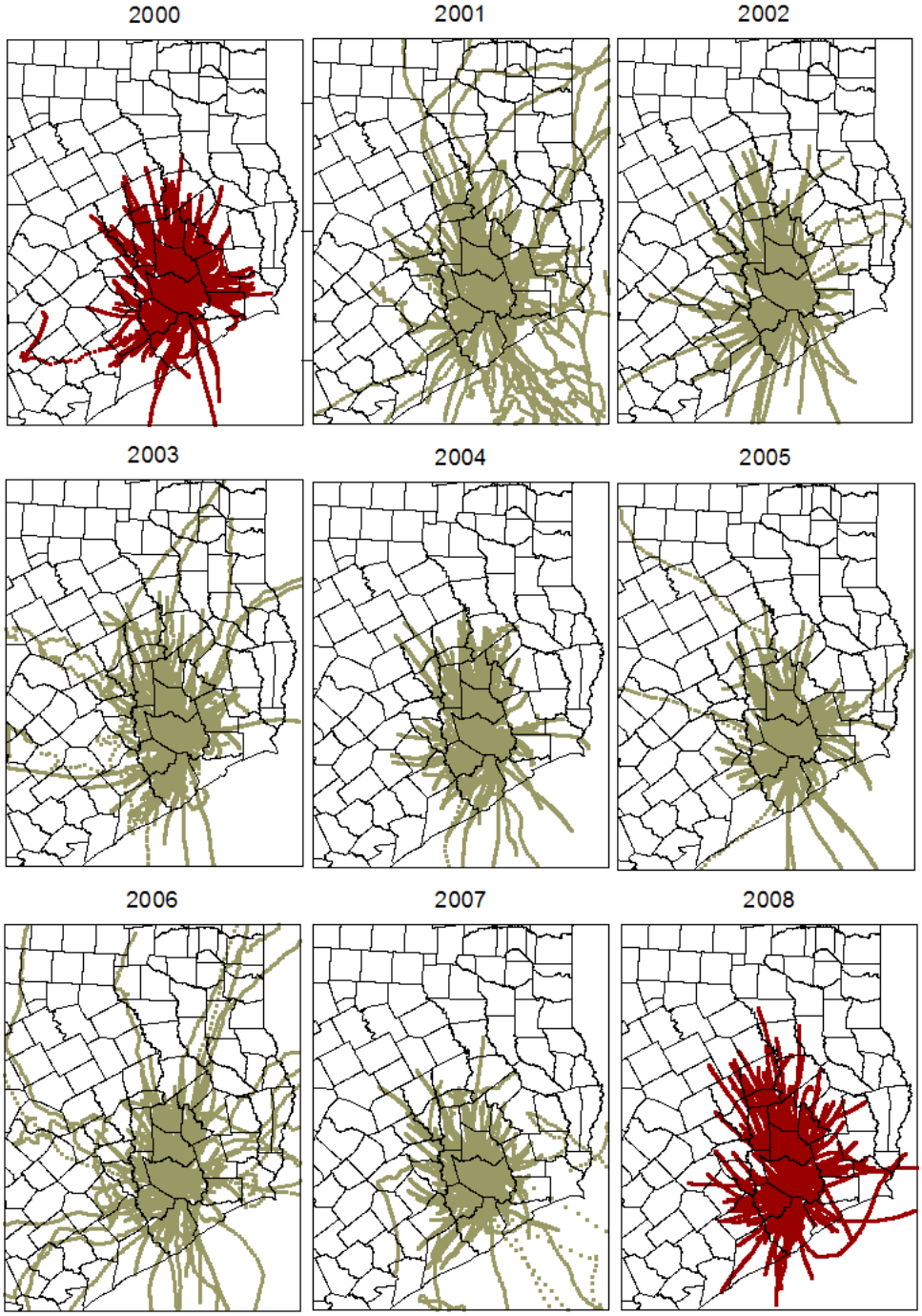

Figure 4-23: 14-Hour Surface Wind Back Trajectories
Surface wind backward trajectories computed with HYSPLIT for May through Spetember, 2000 to 2008. Start hour was 13:00 and trajectories are 14 hours in duration.

Caution must be used when interpreting these results as they are preliminary. Future work is planned to quantify and rigorously validate these findings supporting the contention that differences in meteorological conditions cannot be considered determinative of reductions in observed ozone concentrations in 2008.

4.6 SUMMARY OF RECENT FINDINGS IN BACKGROUND OZONE AND OZONE TRANSPORT

The need to quantify background ozone, or ozone transported from outside the HGB area, in addition to quantifying local ozone production, is essential given that a large city, such as Houston, regularly generates enough local ozone to exceed the standard when starting from a high background. Modifying procedures developed by TCEQ and Nielson-Gammon, et al.

(2005a), this chapter has demonstrated that background ozone levels traveling into Texas are regularly as high as 60 ppb, and often higher.

Examination of 90th percentile ozone concentrations at selected upwind monitors from 2000 to 2008, with data restricted by wind direction and season of the year, revealed no discernible trend in background ozone over the nine-year period observed. The absence of a trend simplifies interpretation of influences from background and local components of ambient ozone, as well as computation of benefits of local control strategies.

Investigation of HYSPLIT back trajectories identified likely transport of ozone into Texas on days following elevated ozone episodes in eastern U.S. states. Further examination of state-wide design values for Texas, and eastern states where high ozone likely originates, revealed clear downward trends from 2000 to 2008. This may lead to lower background levels of ozone being transported into Texas from eastern states, but there was insufficient evidence to support this conclusion based on the lack of trend in background ozone values.

Sinuosity of transport winds during 2008 were found to be statistically indistinguishable from other recent years using the Tukey-Kramer multiple means comparison test. The Tukey-Kramer method also confirmed that average 2008 wind trajectory length did not deviate from the typical sinuosity profile of transport winds traversing the HGB area. These analyses showed that transport into Texas, and subsequently the HGB area, was not changing, which allows for an analysis over multiple years to determine background ozone concentrations that enter into the HGB area.

Clustering daily back trajectories from May to October, 2000 to 2007, revealed six distinct trajectory clusters in the HGB area. Clusters from the northeast, and those that were shorter in length, were found to account for not only the highest background ozone concentrations entering into the HGB area, but also the highest maximum ozone concentrations. Clusters that were from the south and southeast occurred on days with the lowest background ozone due to the clean air blowing into the HGB area from the Gulf. A regression analysis showed that back trajectories can account for around 24 ppb of variation in background concentrations, and around 30 ppb in variation in maximum ozone concentrations.

These background and transport analyses show that efforts focused solely on controlling local emissions may be insufficient to bring Houston into ozone attainment, particularly with regard to the revised 2008 ozone standard of 75 ppb, given that, on many days, background estimates are well over half the eight-hour ozone NAAQS of 85 ppb.

CHAPTER 5: LOCAL WIND PATTERNS DURING HGB AREA OZONE EVENTS, 2003-2006

5.1 PREVIOUS STUDIES OF OZONE-CONDUCIVE METEOROLOGY IN THE HGB AREA

Davis et al. (1998) performed a cluster analysis on observational data from National Weather Service meteorological stations from April through October, 1981-1992 to determine which met conditions were most conducive to ozone formation. For the seven clusters he found (see Table 4, p. 2516), the highest ozone concentrations were observed in the HGB area on the back side of migrating anticyclones, which tend to occur in April, May, September, and October, and the front side of migrating anticyclones, which also occur during the spring and fall. Days that are dominated by a stationary anticyclone (the Bermuda High, for example) tend to have lower ozone, in part because this circulatory pattern brings steady southeast winds from the Gulf of Mexico. Davis et al. also found that high ozone is associated with relatively lower humidity and lower temperatures in the HGB area. This study investigated flow patterns on the synoptic scale rather than local scale, though the synoptic patterns Davis et al. identified can interact with local land-sea breeze patterns, and these interactions play a large role in whether or not conditions are conducive to ozone formation and accumulation.

Breitenbach et al. (2002) examined the wind speed and direction data from the TCEQ monitoring network in the HGB area to determine if there was a difference between area-wide average winds during ozone episode days and non-episode days. The study found that, on average, winds varied in a clockwise direction during ozone episode days, resulting in a degree of recirculation of emissions within the HGB area. During non-episode days, on average, winds were steady from the southeast. This finding is consistent with Davis et al. in that Davis showed that when the Bermuda High was dominant, ozone was relatively low in the HGB area. Usually, winds are from the southeast when the Bermuda High is in its usual location during mid-summer. Seasonal ozone data also shows that in months during which the Bermuda High dominates (late June to early August), ozone is generally lower than during late spring and early autumn.

Berkowitz et al. (2004) sampled near the top of a tall building in the HGB area during TexAQS 2000. They sampled ozone and ozone precursors, and related these observations to trajectories calculated from local radar profiler measurements, which were more finely resolved than HYSPLIT trajectories. They found that the highest ozone concentrations were closely associated with trajectories from industrial areas of the HGB area. They also found that trajectories showing stagnation or flow reversal were also closely associated with high ozone. Berkowitz et al. (2005) showed that the highest ozone concentrations, observed in west Houston, were associated with high concentrations of light alkenes, an indication of industrial emissions, but they also showed that relatively high ozone can be observed in air parcels that do not appear to originate in industrial areas of the HGB area.

Banta et al. (2005) presented a definitive study of an ozone episode day in the HGB area. The analysis combined data from the TCEQ monitoring network, NOAA downward-looking ozone lidar, and NOAA ground-based Doppler lidar. The study found that the ozone episode on August 30, 2000, proceeded in three phases: a period of offshore flow in the morning hours; a period of stagnation in the early afternoon, as the bay breeze struggled to push against the offshore flow, and a period of easterly and southerly flow, as the bay breeze pushed inland, followed by the Gulf breeze. The period of highest ozone occurred during the stagnation period, and the following period, as the bay breeze pushed inland from the coast of Galveston Bay. The highest ozone observations were due in part to the onshore intrusion of highly polluted and photochemically-aged air; the emissions from industry had been carried over Galveston Bay by the morning offshore winds, and had formed high concentrations of ozone over the Bay. As the photochemically-aged air was pushed inland, it encountered fresh urban and industrial emissions from the HGB area, allowing additional ozone formation to occur. One-hour ozone concentrations of 199 ppb were observed in the convergence zone where air containing aged

plumes encountered fresh emissions. Banta et al. concluded that several factors contributed to the severity of the pollution episode: (1) the timing of the bay breeze allowed a period of stagnation during midday; (2) the location of the bay breeze convergence zone, over the area of abundant industrial emissions; (3) the direction of the morning wind flow, i.e., nearly opposite in direction to the bay and Gulf breeze, thus creating a period of stagnation, allowing aged air to return to the areas of high industrial and urban emissions for a second dose of fresh emissions. These findings form the basis for the extended analysis below, which shows that these three local-scale phenomena occur in most of the episodes of elevated ozone in the HGB area.

Darby (2005) performed a cluster analysis on hourly wind speeds and directions collected at TCEQ monitoring stations during 27 days during August and September 2000. A total of 16 one-hour wind patterns were discerned; several of these were more often associated with high ozone in the HGB area than others. Specifically, four clusters of winds identified as bay breeze or Gulf breeze winds were present 27 percent of the time, but were associated with 47 percent of the one-hour ozone exceedances. These winds were from the south or southeast, but occurred preferentially in the afternoon, when the thermally-driven bay/Gulf breeze is expected to occur. Using this analysis, the study showed three different sequences of local one-hour winds resulted in ozone exceedances in the HGB area, with an an example of each pattern: Aug 30, 2000, Aug 25, 2000, and Sept 6, 2000. The Banta et al. and Darby analyses form the basis for the current analysis.

Nielsen-Gammon et al. (2005) examined wind patterns from an offshore meteorological buoy to study these patterns in an environment not influenced by local wind effects or by decoupling of the nocturnal boundary layer. That study concluded that wind patterns in this area of Texas are influenced by a coastal oscillation, in which the wind direction gradually shifts 360° over 24 hours. This oscillation is due to the diurnally-varying coastal temperature gradient, and to inertial oscillation associated with the Coriolis force. Near 30° latitude, the inertial oscillation is synchronous with the diurnal heating, and therefore the sea breeze is at its maximum amplitude. The result is a relatively large-scale sea breeze that can affect inland areas as well as coastal areas, and can play a large role in local flow patterns.

Allen et al. (2006) examined HYSPLIT trajectories for days with high ozone during the TexAQS 2000 field study, and for days with particularly high ozone from 2002 to 2005. The study found that the highest ozone days for the monitoring sites tended to have trajectories that brought emissions from industrial and urban areas of Harris County to the monitoring sites. HYSPLIT is not necessarily the best tool to distinguish between flows from different parts of the same county, so it is difficult to determine, from this analysis alone, whether industrial areas or urban core areas are primarily linked to the highest ozone concentrations. Allen (2006) examined days with the highest ozone concentrations at the Houston Bayland Park (CAMS 53) monitor, which had the highest design value from 2003 to 2005. Wind patterns on these days consistently brought plumes from the industrial areas of east Harris County to the Houston Bayland Park (CAMS 53) site. Photochemical modeling analysis of similar days during 2000 showed that industrial emissions played a particularly large role in creating ozone observed at Houston Bayland Park (CAMS 53) on the highest ozone days. The researchers concluded that wind patterns that bring industrial plumes from east Harris County to west Harris County are a necessary condition for the highest ozone episodes to occur there. However, relatively high ozone can still occur at Houston Bayland Park (CAMS 53) without transport of industrial plumes to west Houston.

Ngan and Byun (2008) and Rappenglueck et al. (2008) discuss a combined principal components analysis/cluster analysis of 850 millibar (mb) wind fields determined from 12 km meteorological modeling of the ozone seasons in the HGB area during 2005 to 2006. These studies concluded that three synoptic situations were most closely associated with high ozone: easterly synoptic-scale flow due to a high pressure center located northeast of the HGB area; near-stagnant synoptic-scale flow due to high pressure located north of the HGA area; and post-frontal northerly flow due to a high pressure center located northwest of the HGB area. This finding

appears to be consistent with the Davis et al. finding, which indicated that migrating high pressure systems were associated with ozone-conducive conditions.

Langford et al. (2009) examined which ozone monitors in the HGB area tend to experience high ozone simultaneously, in an effort to identify common patterns of ozone formation, accumulation, and transport. Using principal components analysis, they found that the largest principal component increased all ozone monitors in the city together, suggesting that background ozone or stagnant conditions were responsible. A second factor showed monitors along the Harris-Brazoria county line and in west Houston preferentially affected by high ozone, suggesting transport from industrial areas in east Harris County to areas south, southwest, and west of the urban core. A third factor showed monitors north of the Houston Ship Channel and east of the urban core affected by high ozone, along with monitors north and west of the urban core. This factor is consistent with transport of ozone and precursors from industrial areas to areas north, northwest and west.

Sullivan et al (2009) performed cluster analysis on daily 72-hour HYSPLIT back trajectories for 2000 to 2007 to determine which transport patterns were associated with high ozone in the HGB area. They examined historical ozone data for a selected group of TCEQ ozone monitors with data records back to 2000, and determined the maximum and minimum ("background") ozone for each day. They found statistically significant differences in maximum ozone concentrations between most pairs of transport clusters, with the highest concentrations found for trajectories that were particularly short, and for those from the northeast. The lowest concentrations were observed for the trajectory cluster with a long fetch from the Gulf of Mexico. They also found that mean daily minimum and mean daily maximum ozone for different clusters were well-correlated, which is consistent with findings of Langford et al. (2009), who found that the strongest tendency among ozone monitors in the HGB area was to rise or fall together, implying that background ozone plays a major role in eight-hour average ozone behavior in the HGB area.

As described above, a number of researchers have examined the effect of synoptic-scale wind patterns on the frequency of high ozone occurrences (Davis et al., 1998; Ngan and Byun 2008; Sullivan et al., 2009). Long-range transport and "background" ozone concentrations clearly do play a major role in eight-hour ozone in the HGB area. However, local wind patterns appear to play a substantial role in the location, intensity and duration of the highest ozone in the HGB area, and so local flow patterns must be examined as well (Breitenbach, 2002; Banta et al., 2005; Nielsen-Gammon et al., 2005; Darby, 2005, Langford et al., 2009).

Local dynamic phenomena interact with synoptic-scale pressure gradients to create wind conditions experienced in the HGB area on any given day. On days with very light synoptic forcing, winds in the HGB area are not stagnant, because of land-sea breeze and coastal oscillation effects. On days when synoptic forcing balances local forcing, there is greater chance for ozone formation and accumulation, because the balance of forces can create a period of stagnation. Direction and strength of the synoptic forcing determine when and where stagnation occurs. High ozone tends to occur if emissions that pool during the period of stagnation are exposed to strong sunlight before they disperse. (Nielsen-Gammon et al., 2005; Banta et al., 2006)

The most important findings from the studies above can be summarized as follows:

- Both local-scale and regional-scale wind patterns determine whether high ozone concentrations occur in the HGB area, and their interaction determines the location, timing and intensity of the highest ozone concentrations;
- Regional-scale offshore winds, i.e., winds with a northerly and/or westerly component, are likely to interact with the early-afternoon bay breeze and late-afternoon Gulf breeze to create stagnation, flow reversals, and convergence zones that accentuate ozone formation;

- The coastal oscillation described by Nielsen-Gammon et al. (2005) can result in continually veering winds during the day, which often carry high ozone plumes from industrial areas into southern and western Harris County and neighboring counties;
- Coastal oscillation can cause winds to shift from offshore to onshore flow throughout southeast Texas nearly simultaneously, and hence can result in winds that never stagnate during the day;
- Regional-scale winds from the northeast are often associated with high ozone in the HGB area, because of transport of ozone from the southeastern and central U.S., and because of the interaction of northeast winds with bay and Gulf breezes;
- Stagnation often plays a crucial role in high ozone, particularly if it occurs during midday, when solar radiation and temperature peak;
- Synoptic weather features most closely associated with high ozone are migrating high pressure centers, which can bring regional-scale offshore winds, flow from the southeast and central U.S., light winds, low humidity and high insolation;
- Regional-scale flow from the Gulf of Mexico is usually not associated with high ozone, and therefore the presence of the persistent Bermuda High to the east of the HGB area is generally not conducive to high ozone.

Given these findings, the following analysis elucidates which local-scale flow patterns are associated with ozone exceedances in the HGB area from 2003 to 2006. This analysis is a work in progress, so it will be refined further in the future.

5.2 METHODS AND DATA

These classifications are based upon wind speed and direction data from TCEQ monitoring stations. TCEQ meteorologists have summarized these data into "plumes." Each map shows the location of theoretical plumes of emissions at the given time, with each endpoint representing the location of a theoretical puff that was "emitted" for each hour since midnight. For example, at 6:00 am, each emission point will have a plume emanating from it that contains six endpoints. The plumes are created from interpolated wind speed and direction data measured by the monitoring network. Many of these trajectories can be seen at the TCEQ Significant Air Pollution Event web site: http://www.tceq.state.tx.us/compliance/monitoring/air/monops/sigevents09.html. An example of these trajectories is presented in Figure 5-1. For most episode days, these trajectory maps are available for each hour from 0900 to 1800 CST. In addition, the radar profiler data collected at Ellington Field or La Porte Airport were sometimes also reviewed to help determine the wind patterns prevailing on a particular day. The ozone days were sorted in a subjective manner, a technique which was simple to employ on some days, and much more difficult on others. In particular, some days experienced stagnation over much of the area. At low wind speeds, the wind direction data becomes less reliable, and hence the distinctions can become more difficult to discern. Most days with substantial stagnation have been classified in a single category (i.e., flow reversals), because stagnation appears to be an essential feature of those days, in addition to the wind flow patterns present on those days. While this technique of classification is not as objective as cluster analysis, the examples provided below should make it clear that the patterns are obvious much of the time.

Presented below are descriptions of different types of ozone events. These descriptions do not attempt to explain in depth the dynamic balance of forces underlying observed wind fields; rather, they simply describe some common patterns of surface winds associated with ozone episodes. They also do not discuss synoptic weather patterns present during each episode day, though synoptic patterns found by others to be ozone-conducive appear to be consistent with the descriptions below.

5.3 RESULTS OF LOCALIZED FLOW ANALYSIS

5.3.1 Typical Veering Episodes

A typical veering episode day begins with winds from the northeast, which gradually shift clockwise to the east, southeast, and south. These winds slowly carry emissions from industrial and urban areas of the HGB area during early morning hours (0000-0800) into southeast Harris County. On some typical veering days, ozone begins to form rapidly, triggering ozone exceedances at Houston Deer Park (CAMS 35), Milby Park, Houston Monroe (CAMS 406), and Park Place (CAMS 416) monitoring sites. As the wind continues veering to the east and southeast, ozone plumes are then carried across the city.

Although pollutants that trigger the highest ozone in the HGB area are emitted in eastern Harris County, ozone often reaches its highest area-wide concentrations in southwestern or western Harris County, at the Houston Bayland Park (CAMS 53), Tom Bass (CAMS 558), West Houston (CAMS 554), and Houston Westhollow (CAMS 410) sites. High ozone is often observed at Manvel Croix Park (CAMS 84) Park in northern Brazoria County as well, and if monitor density in Brazoria and Fort Bend Counties were greater, maximum area-wide ozone might be observed occasionally in those counties rather than Harris. On some typical veering days, winds veer to south or southwest, and ozone plumes are carried northerly or northeasterly, where they can affect the Northwest Harris monitor. Figures 5-1 and 5-2 show maps of ozone concentrations and winds on August 31, 2006, a typical veering day during the TexAQS II study. Figures 5-3 and 5-4 show plume trajectories for that day.

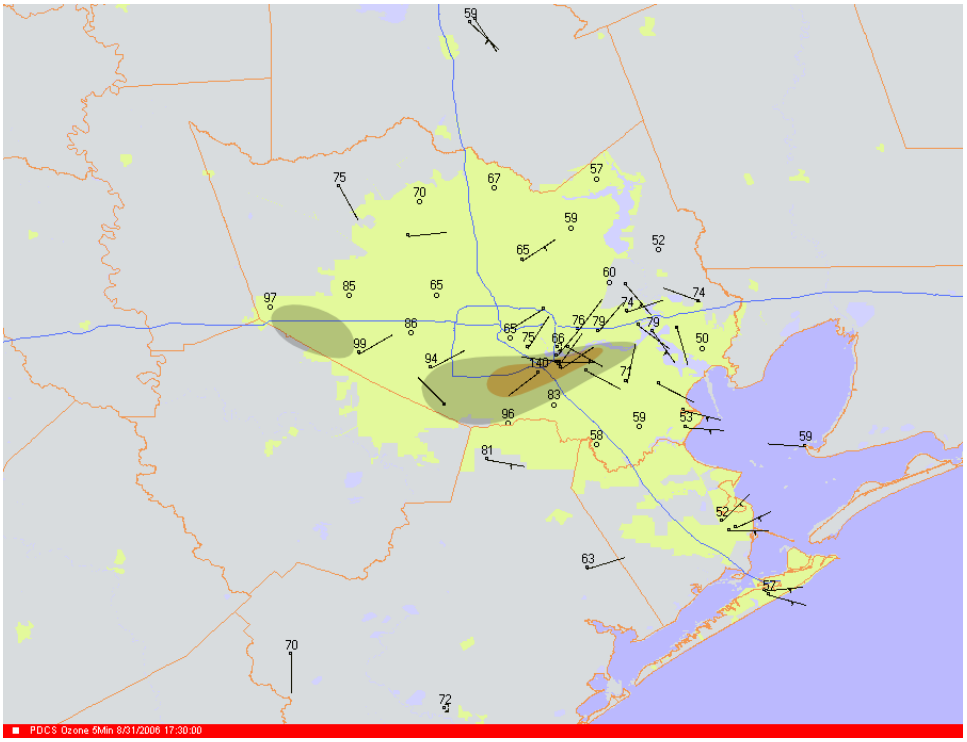

Figure 5-1: Early Stages of a Typical Veering Episode: August 31, 2006
Plumes from industrial sources have been carried south of the urban core by the light ENE winds. Interpolated ozone concentrations are depicted by isopleths; wind barbs indicate wind speed and direction; numbers at each monitoring site show 15-minute average ozone concentrations, shown for 11:30 am CST, 31 August 2006.

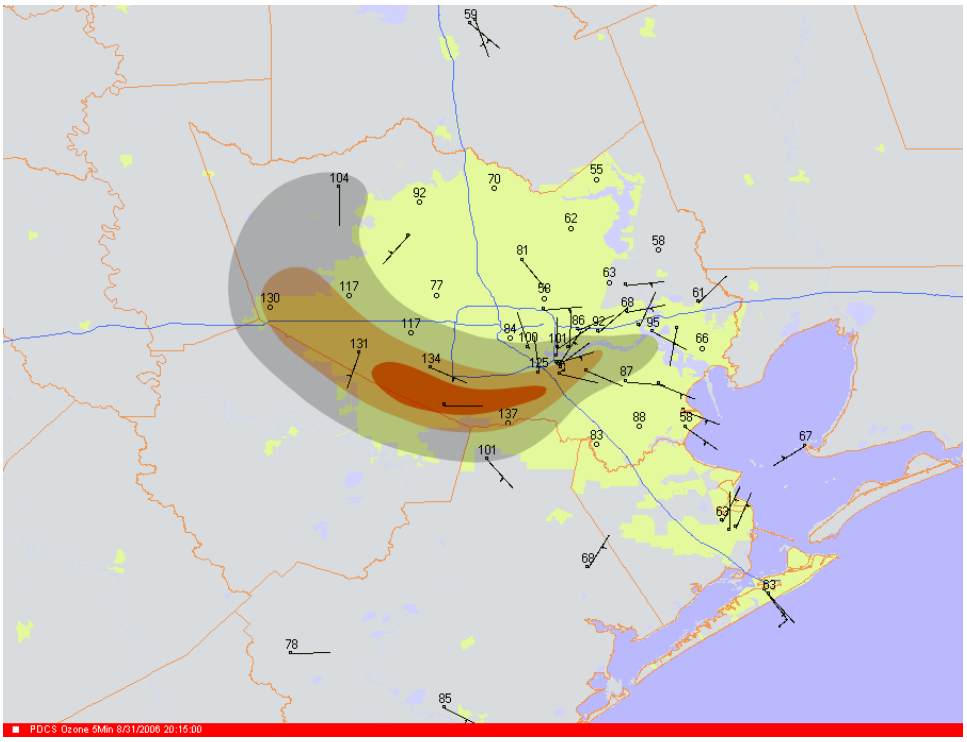

Figure 5-2: Later Stages of a Typical Veering Episode: August 31, 2006
By 2:15 pm, winds have veered to the southeast and south, carrying plumes from industrial areas over the city.

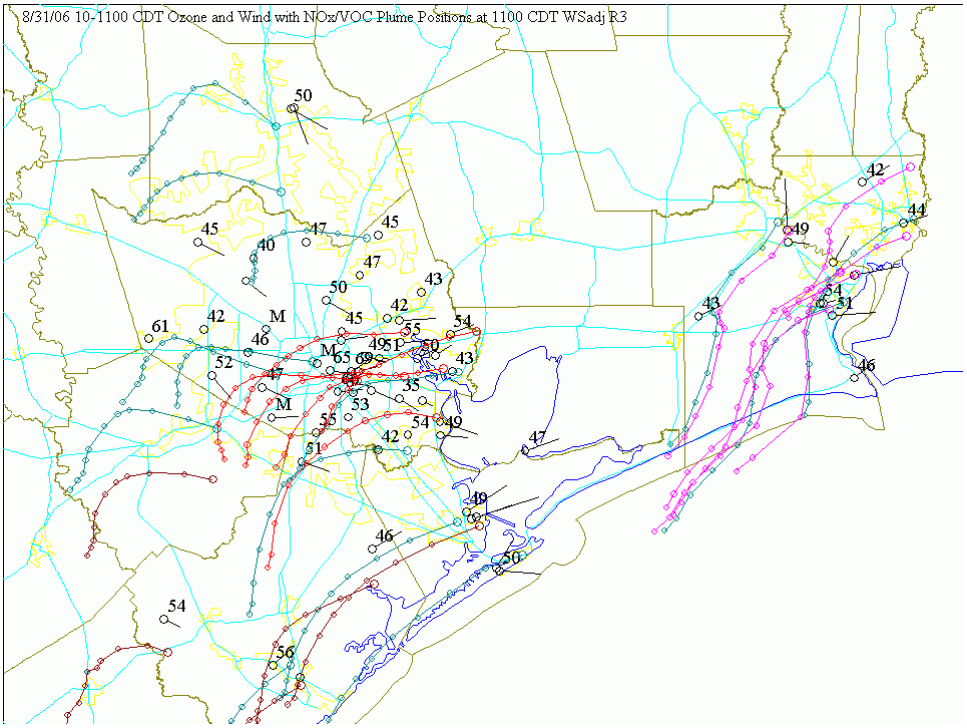

Figure 5-3: Early Stages of a Typical Veering Episode: August 31, 2006
Theoretical plumes are presented for selected emission areas, as derived from wind data collected at TCEQ monitoring sites, for 0000-1100 CDT on August 31, 2006. Numbers at each monitoring site represent one-hour average ozone concentrations from 1000-1100. Wind barbs depict wind speed and direction at each site for 1000-1100. For a typical veering episode, winds push industrial plumes to the west southwest, towards Houston.

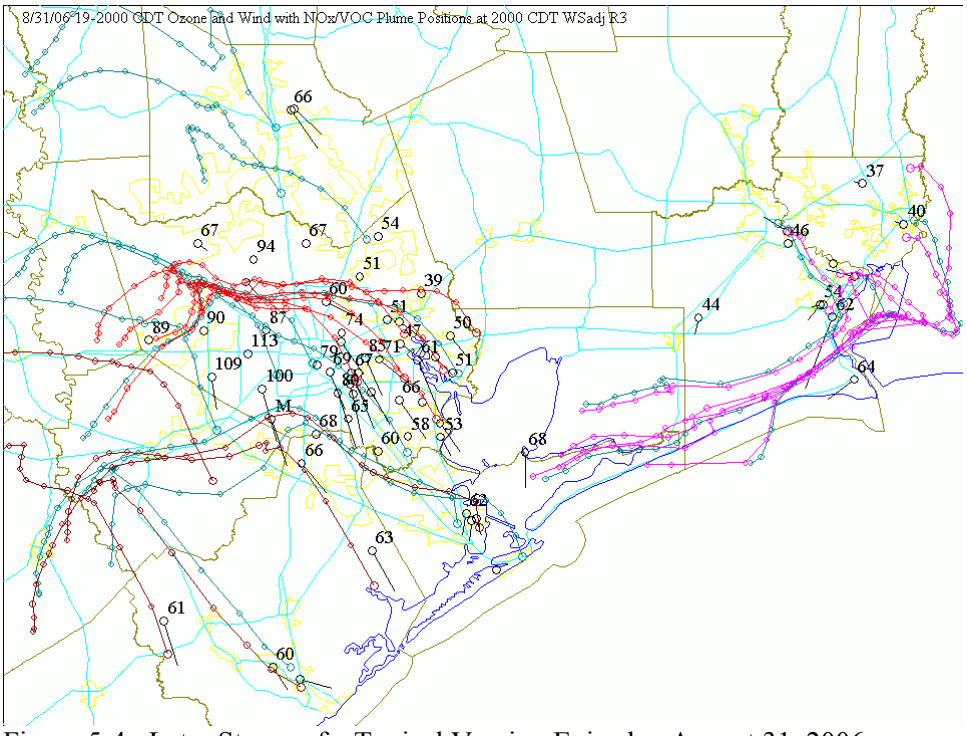

Figure 5-4: Later Stages of a Typical Veering Episode: August 31, 2006
These forward trajectories show that by 2000 CDT, winds shift from east northeast to east to southeast to south southeast, carrying industrial plumes into south Houston, and then into west Houston.

Table 5-1 lists event days that match this pattern. Note that this list is not comprehensive for the 2003-2006 period; 49 event days have not yet been categorized for this period. However, 155 episode days have been classified, including the most severe ozone episodes for each year. It should also be noted that the maximum observed eight-hour ozone concentrations might not represent the actual maximum. Observations are limited by locations of monitoring sites. For a number of events, the highest ozone was observed on the edge of the monitoring network, suggesting the peak concentration may not yet have been reached.

Table 5-1: Typical Veering Events Observed in the HGB Area from 2003 to 2006

Ozone Episode Dates with Typical Veering Flow	8-hr maximum ozone concentration	Monitoring site with highest value
	ppb	
April 26, 2003	124	Houston Bayland Park C53/A146
August 22, 2003	129	Houston Bayland Park C53/A146
September 16, 2003	81	Houston Bayland Park C53/A146
September 25, 2003	106	Houston Croquet C409
October 4, 2003	103	Northwest Harris Co. C26/A110/X154
October 20, 2003	105	Clinton C403/C304/AH113
April 4, 2004	89	Northwest Harris Co. C26/A110/X154
July 20, 2004	110	Houston Bayland Park C53/A146
August 7, 2004	104	Danciger C618
August 8, 2004	107	Houston Croquet C409
August 9, 2004	92	West Houston C554
August 10, 2004	103	Mustang Bayou C619
August 17, 2004	104	Houston Bayland Park C53/A146
September 9, 2004	116	Manvel Croix Park C84
September 20, 2004	93	West Houston C554
September 30, 2004	125	Houston East C1/G316
October 3, 2004	101	Houston Bayland Park C53/A146

May 6, 2005	97	Northwest Harris Co. C26/A110/X154
May 27, 2005	116	Northwest Harris Co. C26/A110/X154
June 21, 2005	101	Houston Bayland Park C53/A146
June 22, 2005	103	Houston Westhollow C410
June 23, 2005	96	Northwest Harris Co. C26/A110/X154
June 24, 2005	91	Northwest Harris Co. C26/A110/X154
June 25, 2005	82	West Houston C554
June 26, 2005	88	Northwest Harris Co. C26/A110/X154
June 27, 2005	88	Northwest Harris Co. C26/A110/X154
June 28, 2005	103	Katy Park C559
June 29, 2005	82	Northwest Harris Co. C26/A110/X154
July 8, 2005	104	Hou.DeerPrk2 C35/235/1001/AFH139FP239
September 4, 2005	104	Houston Monroe C406
September 5, 2005	109	Houston Croquet C409
September 20, 2005	102	Houston Monroe C406
October 9, 2005	107	Houston Monroe C406
October 16, 2005	89	Houston Bayland Park C53/A146
April 13, 2006	90	Northwest Harris Co. C26/A110/X154
April 22, 2006	107	Houston Westhollow C410
May 5, 2006	94	Houston Westhollow C410
June 3, 2006	84	Houston Bayland Park C53/A146
June 14, 2006	112	Manvel Croix Park C84
June 28, 2006	106	Houston Bayland Park C53/A146
June 29, 2006	121	Manvel Croix Park C84
August 4, 2006	68	Houston Bayland Park C53/A146
August 17, 2006	105	Houston Bayland Park C53/A146
August 18, 2006	89	Katy Park C559
August 31, 2006	126	Houston Westhollow C410
September 7, 2006	110	Houston Bayland Park C53/A146
September 14, 2006	97	Northwest Harris Co. C26/A110/X154
September 20, 2006	86	Houston Bayland Park C53/A146
October 4, 2006	81	Katy Park C559

5.3.2 Flow Reversal Episodes

A second common pattern is the "flow reversal" pattern. In this case, morning winds are more directly opposed to the directions of the bay breeze and Gulf breeze. Consequently, stagnation is a key aspect of this pattern. At the beginning of a flow reversal day, winds are light, with a westerly component. Next, a period of stagnation ensues, which allows emissions to build up in industrial and urban areas. Wind flow then reverses direction, shifting to the east or southeast. The reversal can carry aged, NO_X-depleted plumes into areas where fresh NO_X has accumulated during the stagnation period. The result is often substantial ozone formation. Finally, flow reversal days usually end with winds shifting to the south, which can carry ozone plumes to northern Harris County and Montgomery County. Darby (2005) analyzed a flow reversal day with very severe ozone, August 30, 2000. That study interpreted the sequence of wind shifts as (1) synoptic flow from the west, followed by (2) slow intrusion of the bay breeze from the east, and then (3) arrival of the Gulf breeze from the south; these conventions are followed in this analysis.

Several characteristics distinguish flow reversal events from typical veering events. First, at the start of the day, winds often have a westerly component for flow reversal conditions, but they also have an easterly component for typical veering conditions. Second, winds usually do not stagnate on typical veering days—in spite of the continuous winds, however, ozone forms, accumulates, and is transported across the city. By contrast, flow reversal days have a period of light winds or complete stagnation. Third, typical veering events usually affect monitoring sites along the southern boundary of Harris County, and areas west of the urban core. Flow reversal episodes,

however, often affect monitoring sites to the east of the urban core, and sometimes result in exceedances at sites in eastern Harris County (e.g., Houston Aldine (CAMS 8), Atascocita (CAMS 560), Kingwood Library (CAMS 555), Crosby Library (CAMS 553), Sheldon (CAMS 551), Channelview (CAMS 15), Wallisville Road (C617), Baytown Wetlands Center (CAMS 552)) or Conroe (CAMS 65) in Montgomery County.

For about 50 percent of flow reversal days, these wind shifts occur virtually simultaneously all over the 8-county area. These ubiquitous wind shifts are characteristic of the coastal oscillation described by Nielsen-Gammon et al. (2005), i.e., the combined effects of the land-sea breeze and inertial oscillation occurring due to the Coriolis force. These days can begin with morning winds from the west or northwest, then winds usually slow to near stagnation, followed by a shift to the south. In some cases, morning winds are virtually stagnant, then southerly winds from the Gulf breeze push ozone that has formed to the north.

For the other 50 percent of flow reversal days, easterly and southerly wind shifts due to the bay breeze and Gulf breeze, respectively, only occur near the coastlines. This subset is characterized by northwest flow all day at sites in northern and western Harris County. For example, on these days, winds at the Northwest Harris Co. (CAMS 26) monitoring site remain from the northwest for the entire day. In the afternoon, however, along the coast of Galveston Bay, winds become stagnant, then shift to the east, and then to the south. On a few occasions, ozone is trapped in southern Harris County, between the northwest flow and the coastal flow. All these cases have been grouped together in the flow reversal category, because they all experience some degree of flow reversal, which can have profound effects on ozone formation. On flow reversal days, wind shifts can proceed as clockwise (veering) or counter-clockwise (backing), or the wind may shift directions so abruptly that neither designation is appropriate.

Monitoring sites most often affected by this pattern are along Galveston Bay in southeastern Harris County, along the Houston Ship Channel, and to the north and northeast of the Houston Ship Channel, e.g., Baytown Wetland Center (CAMS 552), Lynchburg Ferry (CAMS 1015), Houston Aldine (CAMS 8), Kingwood Library (CAMS 555), and Conroe (CAMS 65). Sometimes, ozone can push more westerly, deep into the urban core, so that sites such as Clinton (CAMS 403), Houston East (CAMS 1), and the Houston Regional Office (CAMS 81) of TCEQ are affected. On other occasions, sites near the northern coast of Galveston Bay (Baytown Wetlands Center (CAMS 552), Wallisville Road (CAMS 617), HRM-10 Mont Belvieu (CAMS 610) and HRM-11 E Baytown (CAMS 611)) experience high ozone. August 21, 2000, and August 30-31, 2000 exhibited this pattern. Figures 5-5 and 5-6 show the evolution of spatial ozone patterns during a September 1, 2006 flow reversal event. Figures 5-7 and 5-8 display plume trajectories that show how winds evolved during this day. A second example of flow reversal leading to high ozone is presented in Figures 5-9 and 5-10, which show the events of June 2, 2005. Table 5-2 lists high ozone days with the characteristic signs of flow reversal.

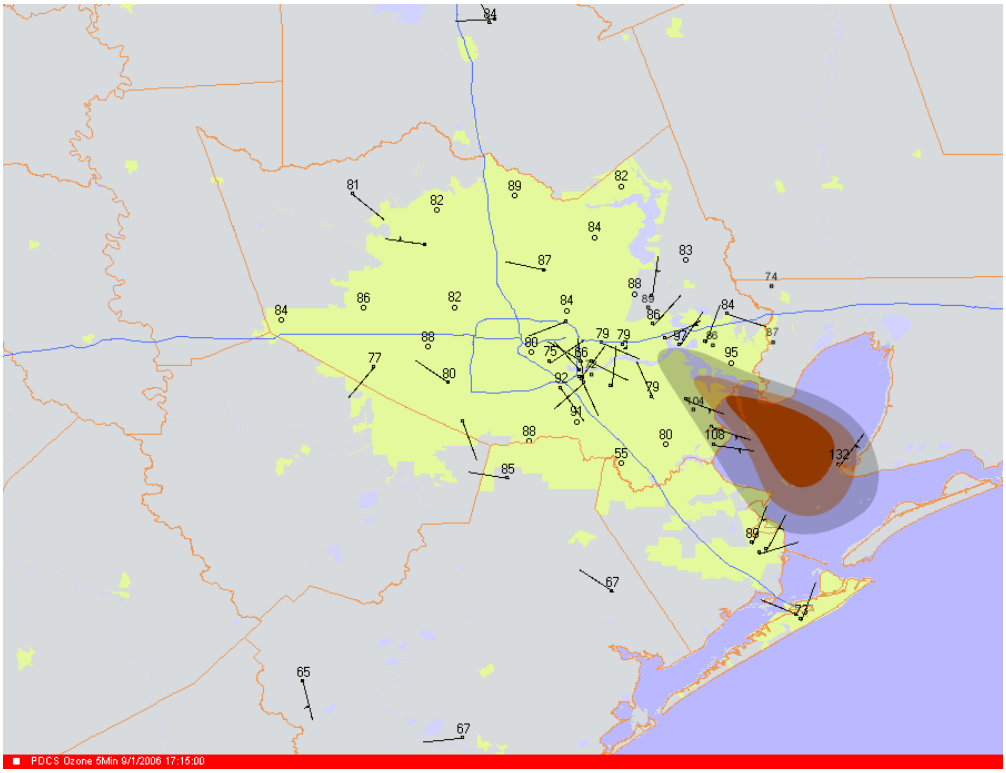

Figure 5-5: Early Stages of Flow Reversal, September 1, 2006

In the early stages of a flow reversal, winds are light, with a northwesterly component, pushing emissions from industrial areas over Galveston Bay. The NOAA ship Ronald H. Brown observed ozone concentrations near 200 ppb in Galveston Bay at about this time.

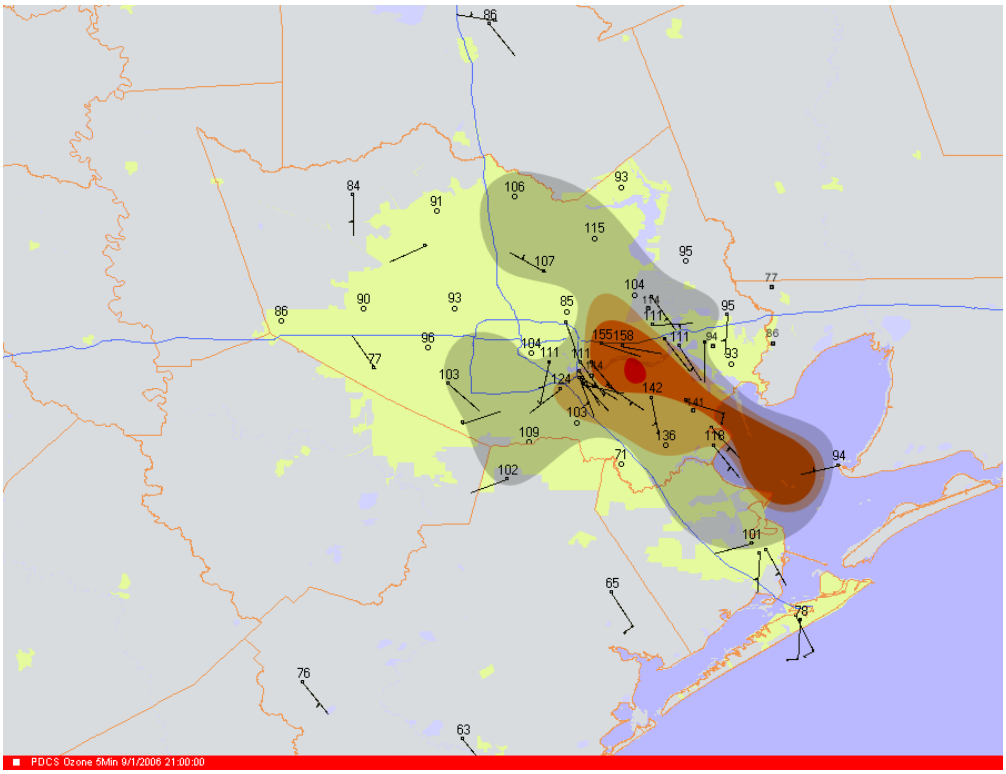

Figure 5-6: Later Stage of a Flow Reversal, September 1, 2006

In the later stages of a flow reversal, the bay and Gulf breezes have pushed into a nearly-stagnant air mass, bringing aged air from Galveston Bay into industrial and urban areas of eastern Harris County.

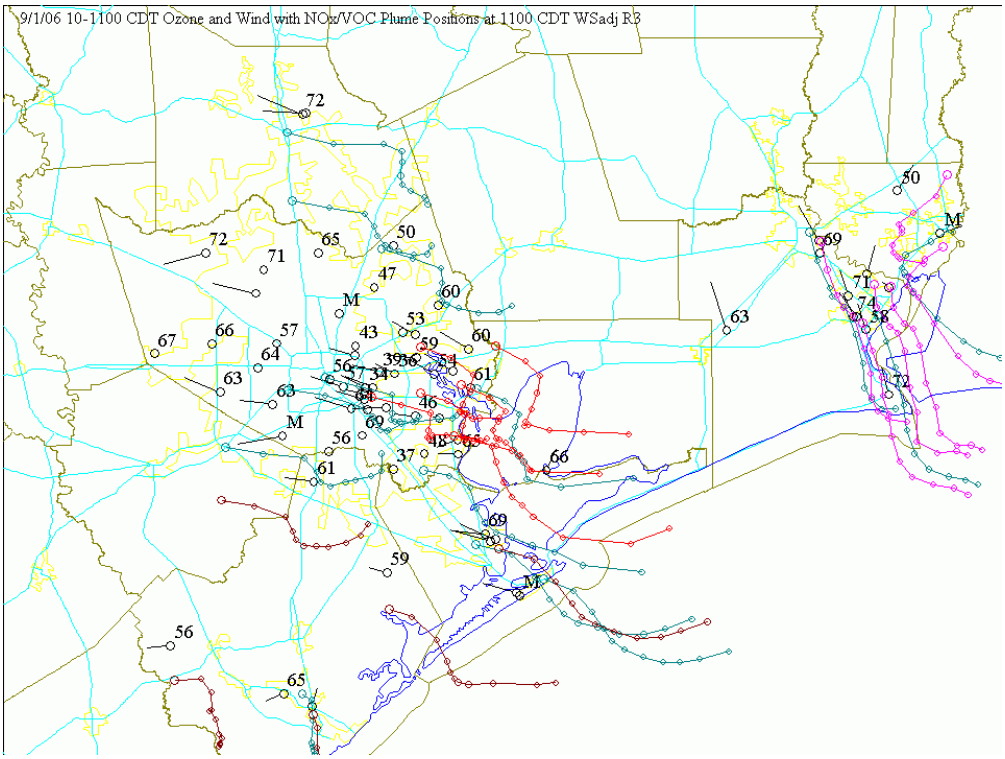

Figure 5-7: Forward Plume Trajectories for September 1, 2006, Showing Transport of Emissions from Midnight to 11:00 am CDT

Monitoring sites in Montgomery, Brazoria, Galveston, and Harris Counties show flow from the west-northwest.

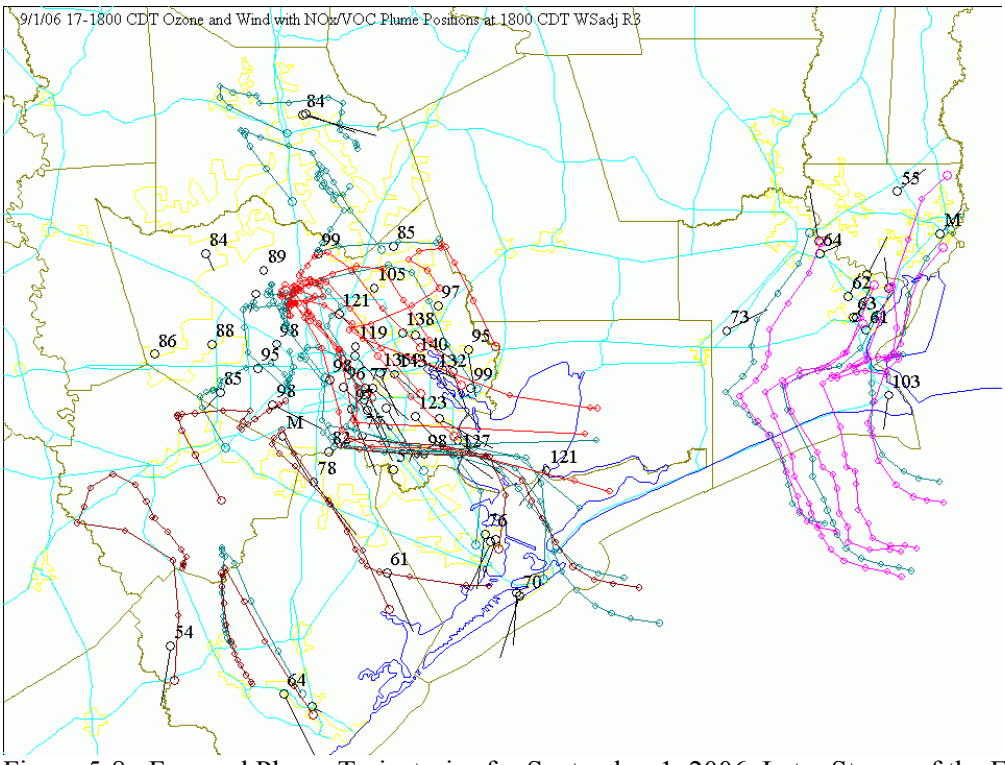

Figure 5-8: Forward Plume Trajectories for September 1, 2006, Later Stages of the Episode

Note that both the bay breeze (in eastern Harris County) and the Gulf breeze (in Brazoria and Galveston Counties) have begun. In eastern Harris County, one-hour ozone concentrations exceed 120 ppb at eight locations.

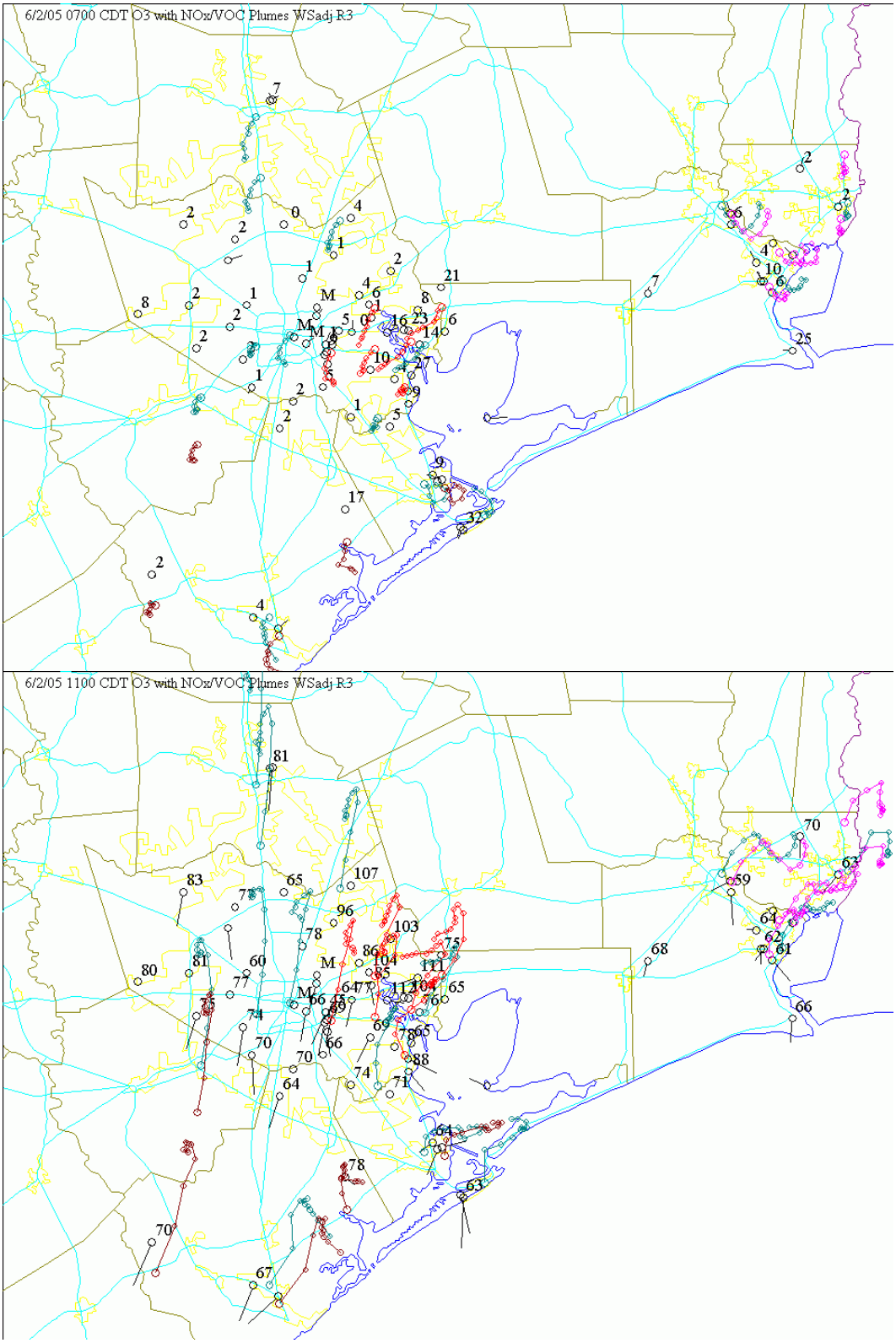

Figure 5-9: Early Stages of a Flow Reversal Event: June 2, 2005
(a) These forward trajectories represent transport of emissions from 0000-0700 CDT; winds are virtually stagnant at all sites. (b) Forward trajectories from 0000-1100 show winds switching direction from northeast to south-southwest.

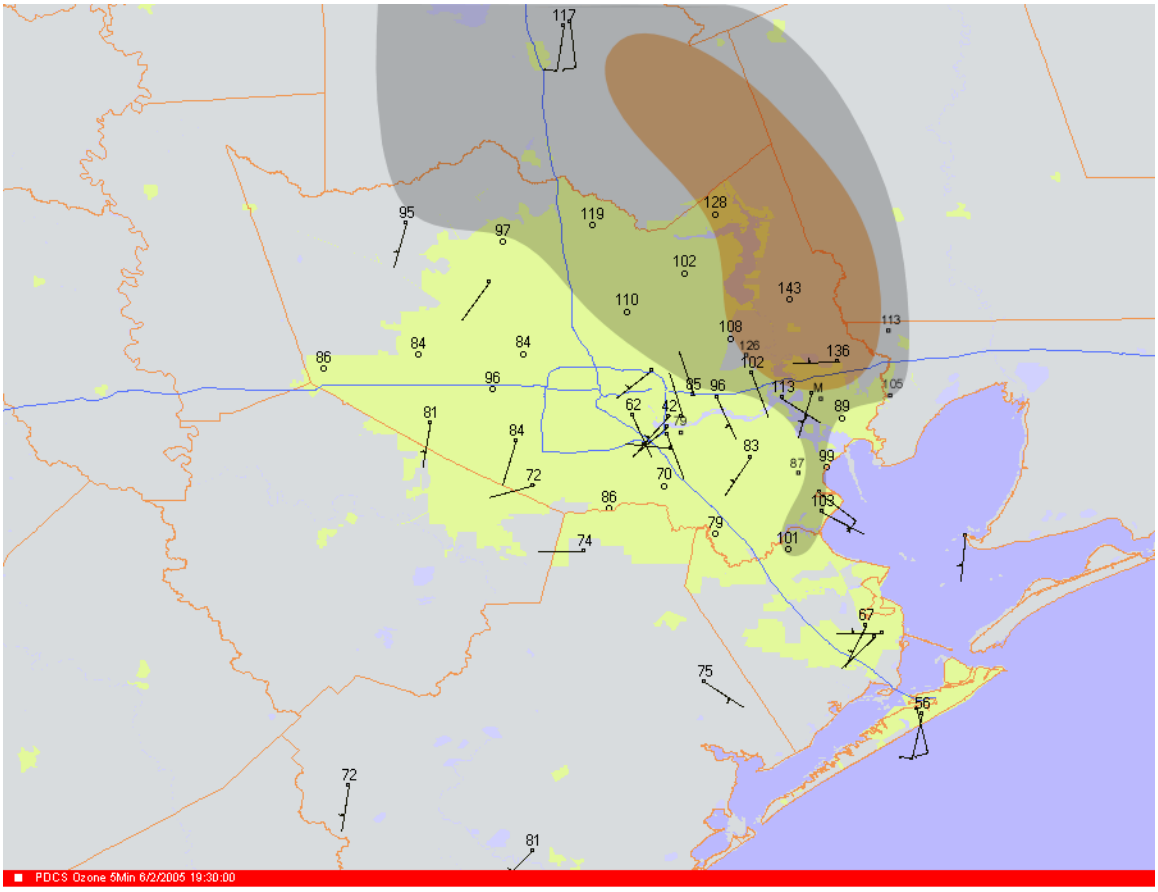

Figure 5-10: Flow Reversal Episode: June 2, 2005
Winds switch direction from northeast to south southwest, pushing aged plumes back over the industrial areas, triggering high ozone that spreads through eastern Harris and Montgomery Counties.

Table 5-2: Flow Reversal Event Days, 2003-2006

Ozone Episode Dates with Flow Reversal	8-hr maximum ozone concentration	Monitoring site with highest value
	ppb	
May 19, 2003	121	Northwest Harris Co. C26/A110/X154
May 29, 2003	126	Hou.DeerPrk2 C35/235/1001/AFH139FP239
July 17, 2003	105	HRM-3 Haden Road C603/A114
August 8, 2003	108	Lynchburg Ferry C1015/A165
August 23, 2003	130	Seabrook Friendship Park C45
August 24, 2003	141	Galveston Airport C34/A109/X152
September 8, 2003	126	Clinton C403/C304/AH113
September 13, 2003	108	Lynchburg Ferry C1015/A165
September 23, 2003	103	Houston Texas Avenue C411
September 26, 2003	92	Clear Brook High School C570
October 23, 2003	120	Houston Aldine C8/AF108/X150
March 31, 2004	92	Houston Monroe C406
April 9, 2004	104	Conroe Relocated C78/A321
May 4, 2004	79	Wallisville Road C617
June 4, 2004	94	Wallisville Road C617
June 19, 2004	101	Houston Monroe C406
July 13, 2004	118	Hou.DeerPrk2 C35/235/1001/AFH139FP239
July 14, 2004	87	Texas City 34th St. C620
July 15, 2004	94	Houston Bayland Park C53/A146
July 16, 2004	86	Wallisville Road C617

July 24, 2004	90	Texas City 34th St. C620
July 25, 2004	105	Texas City 34th St. C620
July 27, 2004	113	Houston Croquet C409
July 31, 2004	91	Seabrook Friendship Park C45
August 2, 2004	87	Manvel Croix Park C84
August 3, 2004	112	Manvel Croix Park C84
August 5, 2004	97	Hou.DeerPrk2 C35/235/1001/AFH139FP239
August 11, 2004	97	Houston Aldine C8/AF108/X150
September 6, 2004	114	Texas City 34th St. C620
September 11, 2004	103	Manvel Croix Park C84
September 17, 2004	111	Galveston Airport C34/A109/X152
September 18, 2004	100	Houston Aldine C8/AF108/X150
September 28, 2004	100	Mustang Bayou C619
September 29, 2004	116	Lynchburg Ferry C1015/A165
November 6, 2004	94	Wallisville Road C617
March 20, 2005	88	Wallisville Road C617
March 25, 2005	75	Houston Bayland Park C53/A146
March 28, 2005	72	Baytown Wetlands Center C552
April 8, 2005	92	Texas City 34th St. C620
May 14, 2005	98	Houston Aldine C8/AF108/X150
May 21, 2005	91	La Porte Sylvan Beach C556
May 22, 2005	97	Baytown Wetlands Center C552
May 25, 2005	91	Wallisville Road C617
May 31, 2005	90	Houston Croquet C409
June 2, 2005	123	Conroe Relocated C78/A321
July 11, 2005	94	Wallisville Road C617
July 28, 2005	95	Seabrook Friendship Park C45
August 1, 2005	92	Clinton C403/C304/AH113
August 2, 2005	103	Houston Bayland Park C53/A146
August 3, 2005	87	Northwest Harris Co. C26/A110/X154
August 6, 2005	91	Houston Monroe C406
August 7, 2005	88	Wallisville Road C617
August 8, 2005	84	Wallisville Road C617
August 21, 2005	118	Lynchburg Ferry C1015/A165
August 22, 2005	107	Seabrook Friendship Park C45
August 23, 2005	92	Wallisville Road C617
August 26, 2005	90	Houston Bayland Park C53/A146
August 30, 2005	118	Seabrook Friendship Park C45
October 17, 2005	100	Houston Monroe C406
October 18, 2005	104	Wallisville Road C617
April 30, 2006	90	Wallisville Road C617
May 12, 2006	93	Conroe Relocated C78/A321
May 18, 2006	87	Wallisville Road C617
June 2, 2006	94	Hou.DeerPrk2 C35/235/1001/AFH139FP239
June 4, 2006	102	Seabrook Friendship Park C45
June 5, 2006	103	Houston East C1/G316
June 6, 2006	110	Conroe Relocated C78/A321
June 7, 2006	83	Atascocita C560
June 8, 2006	111	Hou.DeerPrk2 C35/235/1001/AFH139FP239
June 9, 2006	101	Manvel Croix Park C84
June 10, 2006	93	Wallisville Road C617
June 12, 2006	101	Hou.DeerPrk2 C35/235/1001/AFH139FP239
June 13, 2006	90	Mustang Bayou C619
June 24, 2006	88	La Porte Sylvan Beach C556
July 16, 2006	89	HRM-3 Haden Road C603/A114

July 17, 2006	87	Baytown Wetlands Center C552
July 23, 2006	88	Wallisville Road C617
August 16, 2006	88	Conroe Relocated C78/A321
September 1, 2006	121	Hou.DeerPrk2 C35/235/1001/AFH139FP239
September 6, 2006	87	Clear Lake High School C571
September 13, 2006	88	Manvel Croix Park C84
September 26, 2006	87	Danciger C618
October 11, 2006	86	Texas City 34th St. C620

5.3.3 Steady Flow episodes

A third common pattern of ozone event is the "steady flow" pattern. In this pattern, winds often blow from virtually the same direction most of the day, with only minor fluctuations. Steady winds that cause ozone events usually have winds with northerly and easterly components, though on rare occasions, winds with strong westerly or southerly components can also create this type of episode.

Several examples are presented below: October 6, 2006; September 6, 2000; May 5, 2004; and July 26, 2004. On October 6, 2006 (Figure 5-11) and September 6, 2000 (Figure 5-12), steady winds from the northeast were observed, resulting in a long plume of high ozone from southeast Harris County, across the southern suburbs of the HGB area and into rural areas southwest of the HGB area. However, on May 5, 2004 (Figure 5-13), steady winds with south southeast flow were observed, a situation which leads to ozone exceedances very rarely, but in this case it led to an 85 ppb eight-hour average ozone at Conroe (CAMS 65). Note that upwind concentrations of ozone coming ashore are greater than 60 ppb, which is higher than is usually seen for flow from the Gulf. The northerly flow event of July 26, 2004 is presented in Figure 5-14, which resulted in an ozone exceedance at Mustang Bayou (CAMS 619), in southern Brazoria County.

An ozone exceedance on a day with relatively steady winds of moderate velocity is unusual. On some days, such as May 5, 2004, background ozone may be elevated, making it easier for the ozone standard to be exceeded. On other days, a period of stagnation or recirculation has occurred during the night, allowing emissions to build up to high concentrations. Even though winds during the next day are steady and sometimes even brisk, ozone still forms in high enough concentrations to cause exceedances. Even days with moderate southerly winds can experience high ozone if preceded by late evening and early morning stagnation before sunrise. A third possible explanation is a particularly large emission event; TexAQS II data and modeling sensitivity analyses (not presented here) suggest that the October 6, 2006 event is probably associated with a prolonged emission event that lasted several days.

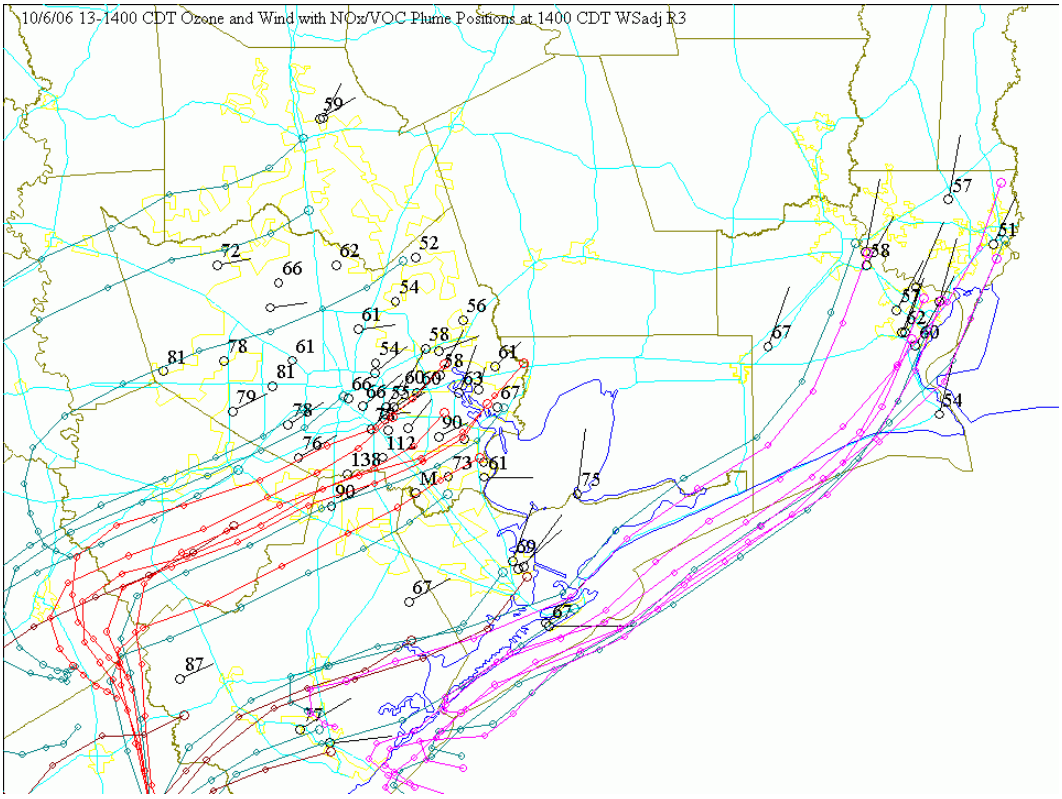

Figure 5-11: Steady Northeast Flow, October 6, 2006

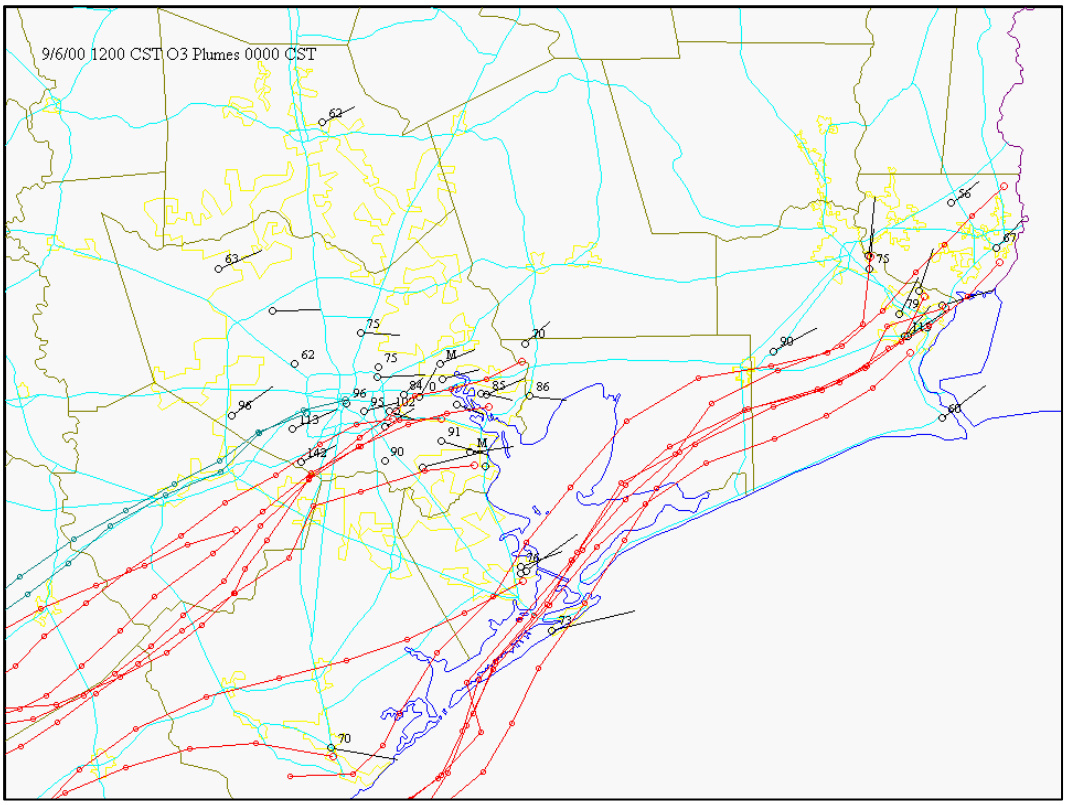

Figure 5-12: Steady Northeast Flow, September 6, 2000

Steady northeast winds carried Houston plumes to the southwest, resulting in an exceedance in southwest Houston.

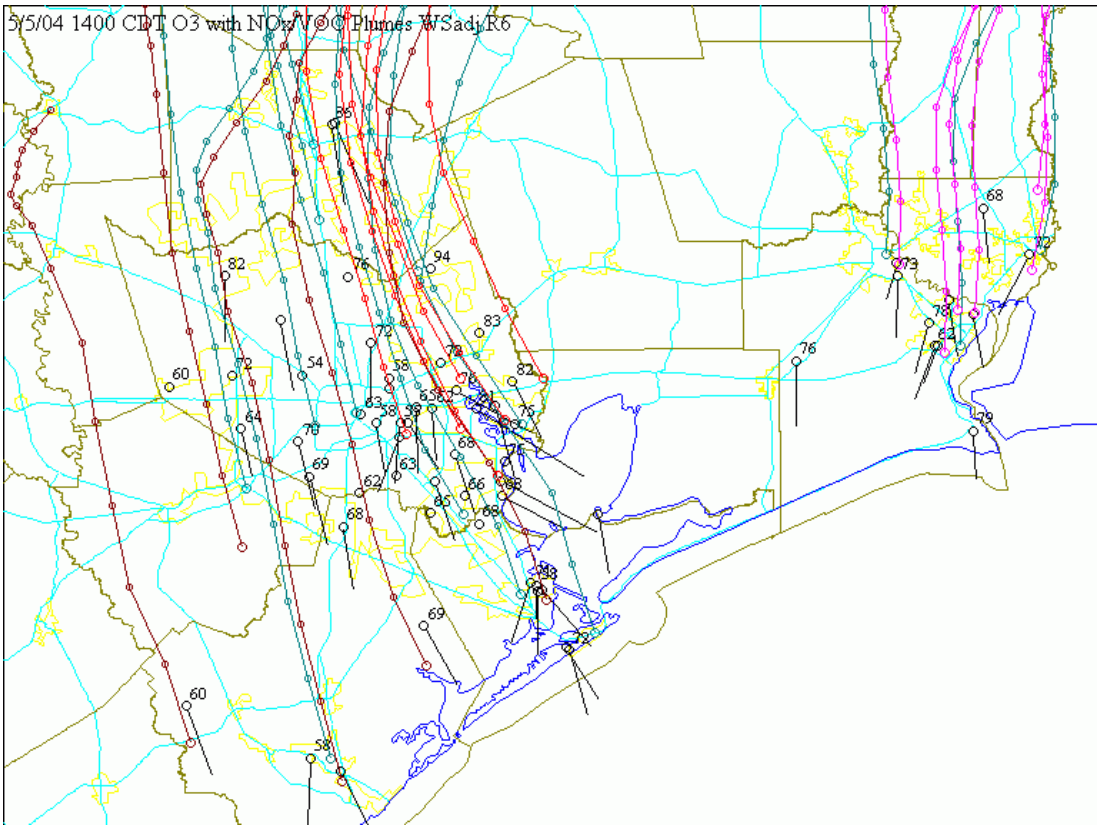

Figure 5-13: Steady South Southeast Flow: May 5, 2004, with an Exceedance at Conroe (CAMS 65)

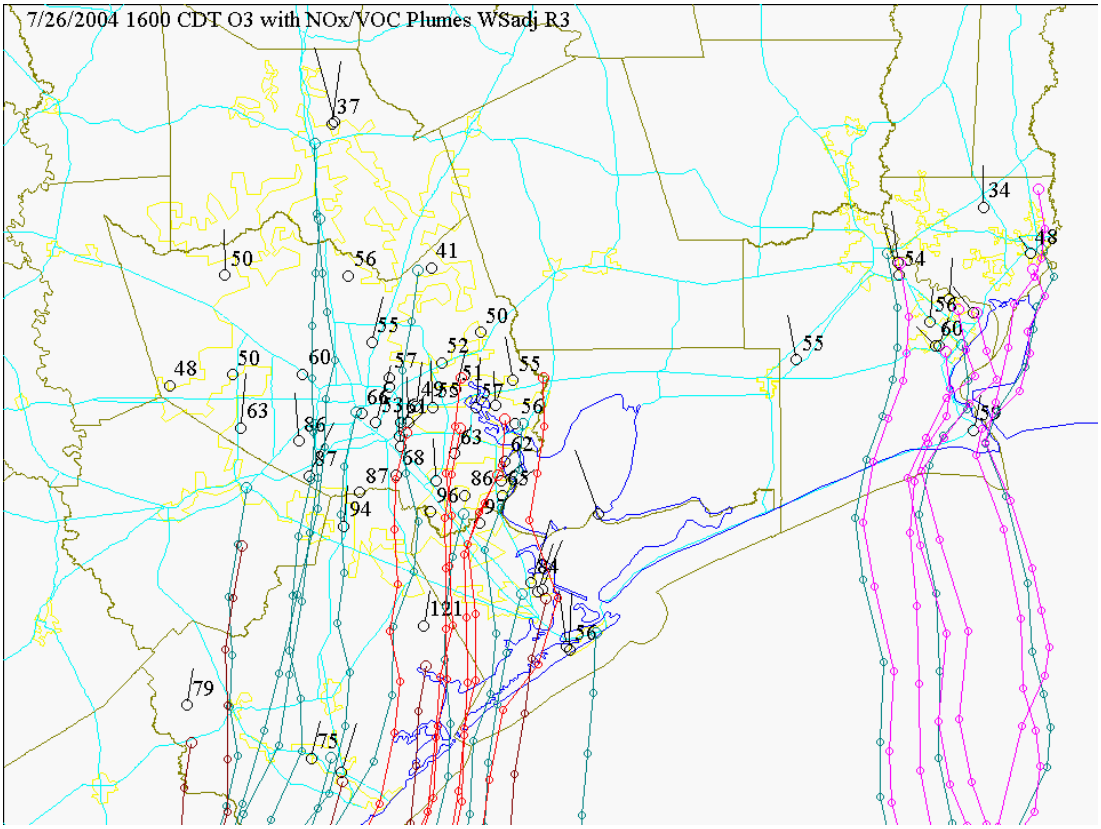

Figure 5-14: Steady North Northeast Flow: July 26, 2004, with an Exceedance at Mustang Bayou (CAMS 619)

Table 5-3: Steady Wind Event Days, 2003-2006

Ozone Episode Dates with Steady Flow	8-hr maximum ozone concentration	Monitoring site with highest value
	ppb	
September 27, 2003	109	Mustang Bayou C619
May 5, 2004	85	Conroe Relocated C78/A321
July 19, 2004	89	Houston Bayland Park C53/A146
July 26, 2004	103	Mustang Bayou C619
September 16, 2004	93	Texas City 34th St. C620
September 27, 2004	90	Mustang Bayou C619
April 16, 2005	90	Conroe Relocated C78/A321
May 26, 2005	87	Tom Bass C558
June 1, 2005	91	Texas City 34th St. C620
June 19, 2005	90	Houston Westhollow C410
July 29, 2005	89	Houston Monroe C406
July 30, 2005	84	Lake Jackson C1016
September 30, 2005	104	Houston Monroe C406
October 12, 2005	101	Houston Croquet C409
June 15, 2006	93	Conroe Relocated C78/A321
June 27, 2006	94	Manvel Croix Park C84
June 30, 2006	85	Conroe Relocated C78/A321
September 2, 2006	83	Smith Point Hawkins Camp
September 3, 2006	88	Manvel Croix Park C84
September 4, 2006	79	Tom Bass C558
October 5, 2006	82	Danciger C618
October 6, 2006	93	Manvel Croix Park C84
October 7, 2006	86	Manvel Croix Park C84

*Flow was from the northeast unless otherwise noted.

Table 5-4 shows a summary of episode days classified by local flow patterns. Flow reversal and typical veering episode days have similar 75th and 95th percentile values, but the medians are substantially different. Steady flow events are notably lower than the other two categories, and occur less frequently. Note that 49 high ozone days during 2003 to 2006 were not analyzed, due to lack of trajectory analyses for these days. Future work will expand the number of events analyzed, including episode days from earlier and later years.

Table 5-4: Summary Statistics for Daily Maximum Eight-Hour Ozone Concentrations for Each Flow Regime Classification

Local flow regime during ozone episode	Number of episode days	Percentage of classified episode days	Mean AreaWide Peak 8-Hr O_3 (ppb)	25th percentile	Median	75th percentile	95th percentile
	#	%	*ppb*	*ppb*	*ppb*	*ppb*	*ppb*
Flow reversal	83	53.5	98.9	89.5	94.0	106.0	122.8
Steady flow	23	14.8	90.8	85.5	90.0	93.0	103.9
Typical veering	49	31.6	100.6	90.0	103.0	107.0	124.6
Total for classified events	155		98.3	89.0	94.0	105.0	123.3
Unclassified episode days	49		95.3	88.0	93.0	100.0	113.4

Table 5-5: High Ozone Days Selected for Photochemical Grid Modeling, 2005-2006

Date	8-hr maximum ozone concentration	Site of maximum ozone	Flow regime	Number of sites exceeding
	ppb			#
21-May-05	92.6	LPSB		1
22-May-05	98.3	BYWC		2
25-May-05	92.2	WALV		2
26-May-05	88	TOMB		1
27-May-05	116.8	HNWA		10
31-May-05	98.5	FWCB		7
1-Jun-05	92.2	TXCT		3
2-Jun-05	125.8	CRBL		20
19-Jun-05	90.1	SHWH		3
20-Jun-05	96.8	DNCG		4
21-Jun-05	102.4	TOMB		12
22-Jun-05	104.4	KATP		17
23-Jun-05	96.4	HNWA		4
24-Jun-05	91.2	HNWA		2
26-Jun-05	90	MEYE		3
27-Jun-05	88.2	HNWA		1
28-Jun-05	104.2	KATP		3
28-Jul-05	95.4	SBFP		3
29-Jul-05	89	HSMA		1
30-Jul-05	85.2	MSTG		1
1-Aug-05	93.7	KATP		6
2-Aug-05	104.6	WHOU		10
3-Aug-05	92	MEYE		2
6-Aug-05	91.6	HSMA		4
7-Aug-05	89.3	WALV		1
2-Jun-06	94.7	DRPK		8
3-Jun-06	85	BAYP		1
4-Jun-06	111.7	H07H		13
5-Jun-06	109.1	H04H		16
6-Jun-06	110.5	CNR2		9
7-Jun-06	86.4	H10H		1
8-Jun-06	122.9	BYWC		19
9-Jun-06	106.5	BUHV		13
10-Jun-06	94.1	CRBL		7
12-Jun-06	101.8	DRPK		9
13-Jun-06	91.2	MSTG		3
14-Jun-06	120.4	TOMB		17
15-Jun-06	93.6	CNR2		2
16-Aug-06	95.5	MERC		6
17-Aug-06	113.6	TOMB		14
18-Aug-06	89.7	KATP		1
31-Aug-06	127.1	SHWH		14
1-Sep-06	121.8	DRPK		27
3-Sep-06	88.7	MACP		1
7-Sep-06	110.5	BAYP		12
13-Sep-06	89	MACP		1
14-Sep-06	118.9	WHOU		8
20-Sep-06	86.7	BAYP		1
26-Sep-06	87.8	DNCG		1

27-Sep-06	90.5	MEYE	2
6-Oct-06	95.3	TOMB	3
7-Oct-06	87	MACP	1
11-Oct-06	90.4	ANAH	3

The three event types can be viewed as a continuum rather than three distinct categories. The steady wind case sometimes begins with a stagnation event, and sometimes ends with a slight veering, progressing from northeast to east to southeast flow. The typical veering case sometimes includes periods of several hours with relatively steady flow. Flow reversals can occur with either veering or backing winds, or abrupt shifts in wind direction. If veering winds are the cause, often the veering occurs very quickly or with light winds, resulting in little dispersion of aged air masses before they pass back over source regions.

Table 5-6: Eight-Hour Ozone Days, 2003-2006

Date	8-hour maximum ozone concentration	Monitoring site with highest value	Start time of 8-hour maximum ozone average
	ppb		*hour*
2003			
April 12, 2003	100	Houston East C1/G316	09:00
April 26, 2003	124	Houston Bayland Park C53/A146	11:00
April 27, 2003	91	Northwest Harris Co. C26/A110/X154	11:00
August 10, 2003	86	Mustang Bayou C619	11:00
August 17, 2003	92	Seabrook Friendship Park C45	09:00
August 22, 2003	129	Houston Bayland Park C53/A146	11:00
August 23, 2003	130	Seabrook Friendship Park C45	11:00
August 24, 2003	141	Galveston Airport C34/A109/X152	10:00
August 25, 2003	95	Mustang Bayou C619	12:00
August 26, 2003	91	Houston Bayland Park C53/A146	11:00
August 8, 2003	108	Lynchburg Ferry C1015/A165	11:00
July 17, 2003	105	HRM-3 Haden Road C603/A114	10:00
July 18, 2003	102	Wallisville Road C617	11:00
June 18, 2003	94	Lynchburg Ferry C1015/A165	11:00
June 19, 2003	95	Houston Croquet C409	10:00
June 21, 2003	91	Hou.DeerPrk2 C35/235/1001/ AFH139FP239	10:00
June 7, 2003	103	Clute C11/A111	13:00
June 8, 2003	105	Clute C11/A111	11:00
June 9, 2003	117	Conroe Relocated C78/A321	11:00
March 23, 2003	111	Galveston Airport C34/A109/X152	13:00
May 17, 2003	95	Texas City C10	11:00
May 18, 2003	115	Hou.DeerPrk2 C35/235/1001/ AFH139FP239	09:00
May 19, 2003	121	Northwest Harris Co. C26/A110/X154	11:00
May 23, 2003	111	Manvel Croix Park C84	11:00
May 24, 2003	117	Lynchburg Ferry C1015/A165	09:00
May 28, 2003	99	Manvel Croix Park C84	11:00
May 29, 2003	126	Hou.DeerPrk2 C35/235/1001/ AFH139FP239	10:00
May 30, 2003	94	Houston Aldine C8/AF108/X150	10:00
May 31, 2003	99	Conroe Relocated C78/A321	11:00
October 20, 2003	105	Clinton C403/C304/AH113	10:00
October 21, 2003	103	Galveston Airport C34/A109/X152	09:00
October 23, 2003	120	Houston Aldine C8/AF108/X150	11:00

October 4, 2003	103	Northwest Harris Co. C26/A110/X154	11:00
September 13, 2003	108	Lynchburg Ferry C1015/A165	10:00
September 17, 2003	86	Northwest Harris Co. C26/A110/X154	10:00
September 23, 2003	103	Houston Texas Avenue C411	10:00
September 24, 2003	91	Houston Aldine C8/AF108/X150	10:00
September 25, 2003	106	Houston Croquet C409	10:00
September 27, 2003	109	Mustang Bayou C619	09:00
September 6, 2003	102	Mustang Bayou C619	10:00
September 7, 2003	109	Mustang Bayou C619	10:00
September 8, 2003	126	Clinton C403/C304/AH113	10:00
September 9, 2003	87	Northwest Harris Co. C26/A110/X154	10:00

2004

April 4 2004	89	Northwest Harris Co. C26/A110/X154	10:00
April 9 2004	104	Conroe Relocated C78/A321	12:00
August 10 2004	103	Mustang Bayou C619	11:00
August 11 2004	97	Houston Aldine C8/AF108/X150	11:00
August 13 2004	89	Manvel Croix Park C84	11:00
August 16 2004	96	Houston Bayland Park C53/A146	10:00
August 17 2004	104	Houston Bayland Park C53/A146	11:00
August 2 2004	87	Manvel Croix Park C84	09:00
August 29 2004	93	Seabrook Friendship Park C45	09:00
August 3 2004	112	Manvel Croix Park C84	12:00
August 30 2004	86	Mustang Bayou C619	11:00
August 4 2004	98	Wallisville Road C617	11:00
August 5 2004	97	Hou.DeerPrk2 C35/235/1001/ AFH139FP239	10:00
August 7 2004	104	Danciger C618	12:00
August 8 2004	107	Houston Croquet C409	09:00
July 13 2004	118	Hou.DeerPrk2 C35/235/1001/AFH139FP239	11:00
July 14 2004	87	Texas City 34th St. C620	12:00
July 15 2004	94	Houston Bayland Park C53/A146	11:00
July 16 2004	86	Wallisville Road C617	10:00
July 19 2004	89	Houston Bayland Park C53/A146	10:00
July 20 2004	110	Houston Bayland Park C53/A146	10:00
July 24 2004	90	Texas City 34th St. C620	11:00
July 25 2004	105	Texas City 34th St. C620	09:00
July 26 2004	103	Mustang Bayou C619	11:00
July 27 2004	113	Houston Croquet C409	10:00
July 31 2004	91	Seabrook Friendship Park C45	11:00
June 15 2004	89	Hou.DeerPrk2 C35/235/1001/ AFH139FP239	11:00
June 19 2004	101	Houston Monroe C406	12:00
June 20 2004	87	Wallisville Road C617	10:00
June 3 2004	85	Channelview C15/AH115	10:00
June 4 2004	94	Wallisville Road C617	09:00
March 31 2004	92	Houston Monroe C406	10:00
May 5 2004	85	Conroe Relocated C78/A321	11:00
November 6 2004	94	Wallisville Road C617	10:00
October 3 2004	101	Houston Bayland Park C53/A146	11:00
October 4 2004	88	HRM-3 Haden Road C603/A114	09:00
September 1 2004	86	Manvel Croix Park C84	10:00
September 10 2004	91	Houston Bayland Park C53/A146	11:00
September 11 2004	103	Manvel Croix Park C84	09:00

September 12 2004	86	Manvel Croix Park C84	09:00
September 16 2004	93	Texas City 34th St. C620	12:00
September 17 2004	111	Galveston Airport C34/A109/X152	13:00
September 18 2004	100	Houston Aldine C8/AF108/X150	09:00
September 19 2004	100	Manvel Croix Park C84	10:00
September 27 2004	90	Mustang Bayou C619	11:00
September 28 2004	100	Mustang Bayou C619	11:00
September 29 2004	116	Lynchburg Ferry C1015/A165	11:00
September 30 2004	125	Houston East C1/G316	10:00
September 6 2004	114	Texas City 34th St. C620	09:00
September 9 2004	116	Manvel Croix Park C84	10:00

2005

April 12 2005	88	Galveston Airport C34/A109/X152	15:00
April 16 2005	90	Conroe Relocated C78/A321	11:00
April 8 2005	92	Texas City 34th St. C620	13:00
August 1 2005	92	Clinton C403/C304/AH113	08:00
August 2 2005	103	Houston Bayland Park C53/A146	11:00
August 21 2005	118	Lynchburg Ferry C1015/A165	10:00
August 22 2005	107	Seabrook Friendship Park C45	10:00
August 23 2005	92	Wallisville Road C617	10:00
August 26 2005	90	Houston Bayland Park C53/A146	12:00
August 27 2005	88	Houston Monroe C406	10:00
August 3 2005	87	Northwest Harris Co. C26/A110/X154	13:00
August 30 2005	118	Seabrook Friendship Park C45	11:00
August 6 2005	91	Houston Monroe C406	10:00
August 7 2005	88	Wallisville Road C617	10:00
July 11 2005	94	Wallisville Road C617	09:00
July 28 2005	95	Seabrook Friendship Park C45	11:00
July 29 2005	89	Houston Monroe C406	10:00
July 8 2005	104	Hou.DeerPrk2 C35/235/1001/ AFH139FP239	10:00
June 1 2005	91	Texas City 34th St. C620	13:00
June 15 2005	88	Lynchburg Ferry C1015/A165	10:00
June 19 2005	90	Houston Westhollow C410	10:00
June 2 2005	123	Conroe Relocated C78/A321	12:00
June 20 2005	96	Danciger C618	11:00
June 21 2005	101	Houston Bayland Park C53/A146	11:00
June 22 2005	103	Houston Westhollow C410	10:00
June 23 2005	96	Northwest Harris Co. C26/A110/X154	10:00
June 24 2005	91	Northwest Harris Co. C26/A110/X154	10:00
June 26 2005	88	Northwest Harris Co. C26/A110/X154	10:00
June 27 2005	88	Northwest Harris Co. C26/A110/X154	10:00
March 20 2005	88	Wallisville Road C617	11:00
May 14 2005	98	Houston Aldine C8/AF108/X150	11:00
May 25 2005	91	Wallisville Road C617	09:00
May 27 2005	116	Northwest Harris Co. C26/A110/X154	11:00
May 31 2005	90	Houston Croquet C409	10:00
May 5 2005	93	Manvel Croix Park C84	11:00
May 6 2005	97	Northwest Harris Co. C26/A110/X154	10:00
October 12 2005	101	Houston Croquet C409	10:00
October 15 2005	86	Manvel Croix Park C84	10:00
October 16 2005	89	Houston Bayland Park C53/A146	10:00
October 17 2005	100	Houston Monroe C406	10:00
October 18 2005	104	Wallisville Road C617	10:00

October 9 2005	107	Houston Monroe C406	09:00
September 20 2005	102	Houston Monroe C406	11:00
September 30 2005	104	Houston Monroe C406	08:00
September 4 2005	104	Houston Monroe C406	09:00
September 5 2005	109	Houston Croquet C409	10:00
September 8 2005	88	Houston Croquet C409	10:00
September 9	90	Houston Westhollow C410	11:00
2006			
April 13 2006	90	Northwest Harris Co. C26/A110/X154	11:00
April 22 2006	107	Houston Westhollow C410	10:00
April 30 2006	90	Wallisville Road C617	09:00
August 16 2006	88	Conroe Relocated C78/A321	14:00
August 17 2006	105	Houston Bayland Park C53/A146	13:00
August 31 2006	126	Houston Westhollow C410	11:00
July 16 2006	89	HRM-3 Haden Road C603/A114	11:00
July 23 2006	88	Wallisville Road C617	09:00
June 10 2006	93	Wallisville Road C617	10:00
June 12 2006	101	Hou.DeerPrk2 C35/235/1001/ AFH139FP239	12:00
June 13 2006	90	Mustang Bayou C619	11:00
June 14 2006	112	Manvel Croix Park C84	11:00
June 15 2006	93	Conroe Relocated C78/A321	09:00
June 2 2006	94	Hou.DeerPrk2 C35/235/1001/AFH139FP239	11:00
June 27 2006	94	Manvel Croix Park C84	10:00
June 28 2006	106	Houston Bayland Park C53/A146	10:00
June 29 2006	121	Manvel Croix Park C84	08:00
June 30 2006	85	Conroe Relocated C78/A321	09:00
June 4 2006	102	Seabrook Friendship Park C45	09:00
June 5 2006	103	Houston East C1/G316	11:00
June 6 2006	110	Conroe Relocated C78/A321	11:00
June 8 2006	111	Hou.DeerPrk2 C35/235/1001/ AFH139FP239	10:00
June 9 2006	101	Manvel Croix Park C84	11:00
May 12 2006	93	Conroe Relocated C78/A321	12:00
May 18 2006	87	Wallisville Road C617	10:00
May 5 2006	94	Houston Westhollow C410	10:00
October 11 2006	86	Texas City 34th St. C620	13:00
October 6 2006	93	Manvel Croix Park C84	10:00
October 7 2006	86	Manvel Croix Park C84	10:00
September 1 2006	121	Hou.DeerPrk2 C35/235/1001/ AFH139FP239	11:00
September 13 2006	88	Manvel Croix Park C84	12:00
September 14 2006	97	Northwest Harris Co. C26/A110/X154	11:00
September 20 2006	86	Houston Bayland Park C53/A146	10:00
September 26 2006	87	Danciger C618	11:00
September 27 2006	97	Conroe Relocated C78/A321	10:00
September 3 2006	88	Manvel Croix Park C84	09:00
September 7 2006	110	Houston Bayland Park C53/A146	10:00

5.4 SUMMARY OF LOCAL WIND PATTERNS DURING HGB AREA OZONE EVENTS, 2003-2006

The following are the most important finings from the analysis of local wind patterns duing ozone events in the HGB area:

- Flow reversals tend to occur with regional-scale winds with westerly and northerly components, i.e., regional winds that are opposed in direction to the bay breeze and Gulf breeze.
- Flow reversals can proceed in two ways: as a clash between the northwesterly regional-scale winds and the bay/Gulf breezes, or as a manifestation of the coastal oscillation phenomenon described by Nielsen-Gammon et al. and Banta et al., whereby the diurnal land-sea breeze cycles are in synch with the inertial oscillations driven by the Coriolis effect. In the former case, breeze fronts can form, and convergence zones may trap ozone in the HGB area for several hours. In the latter case, stagnation occurs, and then the ozone formed is advected northward.
- Typical veering days tend to occur with regional-scale winds with northerly and easterly components. When combined with the bay breeze and then the Gulf breeze, the wind directions veer, and spread ozone and precursors from the industrial emission areas in southeast Harris County across the HGB area.
- Ozone episodes can occur even on days with relatively steady winds during most of the day; however, these episodes tend to be less frequent and less severe than days with flow reversals or typical veering.
- The flow regimes described above can be seen as end-members of a continuum. Each pattern appears to arise from the interactions of the regional-scale flow and the local diurnal patterns that arise due to the land/bay/Gulf breeze and the coastal oscillation that occurs at 30° N latitude.
- The ozone episode days chosen for photochemical grid modeling during 2005-2006 appear to adequately represent the relative abundance of the three different flow regimes for the 2003-2006 period.

This analysis is a work in progress, and a partial explanation of ozone formation in the HGB area, at best. Efforts to refine this analysis may include better quantification of the flow regimes, use of radar profiler data and ozonesonde data, and coupling with background ozone and long-range transport analyses.

CHAPTER 6: CONCLUSIONS AND FUTURE RESEARCH

The HGB area has made considerable progress in controlling its ozone pollution problem. This conceptual model provides a detailed explanation of how, where, and why ozone forms in the Houston-Galveston-Brazoria area. Beyond that, it identifies and quantifies large decreases in ozone and its precursors recorded at monitors throughout the region, then corroborates these findings through trend analyses, detailed investigations of emissions patterns across time and space, and extensive examination of background and transport phenomena. While much has been accomplished in pursuit of attainment of the NAAQS of 0.08 ppm, much work remains to achieve this standard, as well as the more stringent 2008 standard of 0.075 ppm. This conceptual model has provided comprehensive insight into ozone dynamics in the Houston-Galveston-Brazoria area. However, much more research will be necessary in the future to complete this task and prepare for attainment of the revised standard.

Chapter 1 presented the fundamentals of ozone formation photochemistry and meteorology, followed by a more specific treatment of the HGB area, especially the unique combination of emissions and local meteorology that influence when and how ozone is formed in the region. The chapter concluded with a summary of the most salient findings of the 2005-2006 Texas Air Quality field study.

Tropospheric, or ground-level, ozone pollution is a public health concern in many metropolitan areas throughout the United States (National Academy of Sciences, 1991; Bell, 2004, EPA, 2006). Ozone is generally associated with relatively clear skies, light winds, abundant sunshine, and temperatures above 80 to 85 degrees Fahrenheit. Typically, these meteorological conditions are associated with high pressure areas that migrate across the U.S. during the summer season.

Though ozone in the HGB area peaks at roughly the same time of year as other areas of Texas and the U.S., the ozone season in Houston is of longer duration than most other areas, effectively spanning the entire year (Davis et al., 1998). During summer, especially in late summer, Houston experiences relatively light winds and persistent hot, humid, and sunny conditions. Late summer peak ozone concentrations in the HGB area also tend to be higher than other areas. While the basic factors that contribute to ozone formation are abundant in the HGB area, the area is unique in its large population, the types of emissions from local industry, and its meteorology.

Large urban areas are prone to generating elevated levels of ozone in the ambient air because of a confluence of contributing factors: the presence of millions of people, the presence of a vast multitude of emissions sources that serve and employ that population, and meteorological conditions favorable to formation of ozone from those emissions. Substantial amounts of precursor compounds, chiefly nitrogen oxides (NO_X) and volatile organic compounds (VOC), are emitted by mobile sources, such as on-road and off-road vehicles and equipment; area sources, such as commercial facilities; and point sources, such as industrial equipment. Other sources include biogenic emitters, such as vegetation, ozone and precursor compounds transported into an urban area from external locations, and the continental background of ozone and precursors.

Certain types of highly-reactive VOC (HRVOC), the light alkenes, have been found to play a major role in forming ozone. HRVOC react more quickly with sunlight to form radicals that contain unpaired electrons, which accelerate the ozone formation process (Ryerson et al., 2003; Daum et al., 2003, 2004; Kleinman et al., 2002, 2005; Wert et al., 2003; Czader et al., 2008). HRVOC recycle NO_X, while ordinary VOC recycle radicals. NO_X recycling speeds up the process of ozone formation and accumulation.

Elevated emissions of ozone precursor compounds emanate from industrial and petrochemical facilities located throughout the region, but predominately along the Houston Ship Channel. In this region, distinctive photochemistry is observed. Elevated concentrations of HRVOC are co-emitted with NO_X from industrial facilities. This combination leads to substantial and rapid

ozone production in periods as short as a few hours. Furthermore, ozone production in the HGB area can vary significantly over spatial scales smaller than other urban areas. Specifically, ozone concentrations may vary by 50 ppb or more over distances as small as a few kilometers (Kleinman et al., 2002; Ryerson et al., 2003). The unique ozone formation chemistry of the HGB area atmosphere, specifically in the Houston Ship Channel region, places demands on chemical mechanisms not encountered in other regions.

In the absence of accidental releases or spills, whether high concentrations of pollutants form on a given day is controlled mostly by meteorological processes, which may transport the pollutants and either dilute pollutant emissions or allow them to accumulate. Meteorology also affects other key processes, such as chemical reaction rates (Banta, et al., 2005). High ozone concentrations are observed most frequently in the HGB area on days lacking strong synoptic, or large-scale, pressure gradients. Absent dominant synoptic weather systems, smaller-scale local wind patterns govern ozone formation, most notably the complex local coastal and sea breeze oscillations (Rao et al., 1997; Banta et al., 2005; Nielsen-Gammon et al., 2005b). Light to moderate synoptic-scale winds originating from the northeast oppose the direction of the bay breeze arising in the late morning or early afternoon (Banta et al., 2005; Ngan et al., 2008; Darby, 2005). Local wind components, including persistent sea breezes along the coast of the Gulf of Mexico, land-sea breeze flow reversals, and a shoreline convergence zone combine to form a rotational wind pattern that often re-circulates emissions over ozone precursor sources, amplifying ozone formation dynamics (Banta, et al., 2005; Nielson-Gammon et al., 2005b).

As precursor emissions are advected across the region, they mix with other local emissions, as well as compounds transported into the region, to generate elevated amounts of ozone. The rotational wind pattern accumulates precursors generated in the morning, or left over from the previous day, which then react during the warmest and sunniest portion of the day. Ozone rich air masses typically begin to form in the center and south of the city. Later in the afternoon, southerly Gulf breezes and the rotational pattern can advect, or horizontally transport, the pool of high ozone over the city toward the west and northwest (Darby, 2005; Banta et al., 2005). When large-scale weather systems move through the region, ozone and precursor emissions tend to be diluted and carried out of the city, rather than concentrated in still, stagnating air, to be heated, reacted and turned into ozone. Days dominated by strong synoptic weather systems tend to experience low ozone levels (Banta, et al., 2005).

Wind directions on days when eight-hour ozone levels in the HGB area exceed the National Ambient Air Quality Standards (NAAQS) typically show a circular movement throughout the day, rotating continuously over a twenty-four hour period. Very early in the morning, the wind originates from the west, with directions gradually shifting to the northwest to north soon after sunrise. During the morning hours, winds shift gradually to come from the northeast, then from the east a little after noon. Finally, directions shift to come from the southeast a little before sunset, after which the winds begin to calm while shifting to coming from due south about midnight.

Examination of ozone trends shows that ozone design values, the statistics used to compare observed ambient ozone levels to the NAAQS regulatory standard, have decreased markedly in the HGB area over the past seventeen years. The 2008 eight-hour ozone design value of 91 ppb is approaching the ozone NAAQS of 85 ppb (0.080 ppm) and represents a 24 percent decrease from the 1991 design value of 119 ppb. A regression analysis of design value on year estimated that eight-hour ozone design values decreased at the rate of 1.2 ppb per year and that this decrease was statistically significant. Although the one-hour ozone NAAQS of 125 ppb (0.12 ppm) was revoked as a regulatory standard in 2005, the value in 2008 was 147 ppb, a 33 percent decrease from the 1991 design value of 220 ppb. Regression of one-hour design values on year showed they decreased at the rate of 3.6 ppb per year, which is even faster than the eight-hour ozone design value decreased.
Examination of design values at individual monitors corroborates these decreases, with over half

of those monitors at levels below both the eight-hour standard and the vacated one-hour standard by 2008. Since 1999, the number of eight-hour and one-hour ozone exceedance days, another useful, but imperfect, statistic for comparing ozone trends, occurring in the HGB area have fallen 83 percent and 96 percent, or 18 percent and 30 percent per year, respectively. In just the last three years, the number of eight-hour and one-hour ozone exceedance days have fallen 76 percent and 92 percent, or 37 percent and 57 percent per year, respectively.

The total number of eight-hour exceedance days, including double counting of days when more than one monitor may have exceeded the standard, fell from a high of 340 in 1995 to 39 in 2007 and just 19 in 2008. Prior to 2007, that number was never below 100, except for one year, 1993, when it was 94. The number of monitors recording an exceedance of the eight-hour ozone standard has fallen by half, from a maximum of 23 in 2003 to only 12 in 2008.

A similar pattern is apparent with the number of exceedances of the one-hour ozone NAAQS. The total number of one-hour ozone exceedance days, including double counting of days when more than one monitor may have exceeded the standard, fell from a high of 165 in 1995 to just three in 2008. Those three exceedances occurred at only two monitors. Prior to 2005, the number was never below 50. As recently as 2006, a total of 15 monitors recorded at least one exceedance.

Decreases in exceedance days are apparent despite an increase in the number of monitors located throughout the HGB area. Examination of exceedances by year and month revealed that the ozone season was also less severe and peaks at a later date in recent years. In 2008, Hurricane Ike hit the HGB area, causing many monitors to shut down for several weeks in September. More work needs to be done to determine whether and how this missing data affected the trends in both the ozone design values and the number of exceedance days.

The variety of methods used to assess ozone trends in the HGB area generally agree that ozone concentrations have been decreasing. Decreases seen in both ozone design values and ozone exceedances represent the remarkable progress that has occurred in a fairly short amount of time in an area well known for its air quality challenges. However, the area still faces challenges in achieving attainment of the 1997 ozone NAAQS.

Similar to ozone, NO_X concentrations in the HGB area appear to be decreasing over time. NO_X concentrations have shown larger decreases in recent years, especially 2008, a year that also recorded some of the lowest ozone concentrations. Since 1991, the NO_2 design value has been well below the NO_2 NAAQS of 53 ppb, computed as an annual average, recording its maximum value, 28 ppb, in 1994. Since then, the NO_2 design value has fallen 51 percent, or over 4 percent per year, to 14 ppb, its lowest value yet, in 2008. The decrease in the NO_2 design value just since 1998, 43 percent, is even more pronounced, at over 6 percent per year.

Though highly variable from season to season, daily peak hourly NO_X also shows a general decreasing trend since 1991. Maximum NO_X concentrations typically occur in winter, and, while erratic, have decreased overall by 41 percent, to 409 ppb, since 1999, though one anomalous extreme value, 809 ppb, occurred in 2003. This is an average of roughly 32 ppb per year, or nearly 6 percent. The drop since the 1991 high of 880 ppb is 54 percent, or over 4 percent annually.

Average daily peak hourly NO_X has dropped even more precipitously, falling 53 percent, or 8 percent per year, from 75 ppb to 35 ppb, since 1999. Since 1991, average NO_X has dropped 68 percent, or over 6 percent per year, from the series high of 110 ppb. Daily peak hourly NO_X also demonstrates a general decreasing trend since 1991. The maximum NO_X concentration typically occurs in the winter, and, while variable, has shown large decreases, especially since 2003. In 2008, both the NO_2 design value and maximum daily peak NO_X recorded the lowest values of any previous year back to 1991.

Among individual monitors, favorable trends were noted at Houston East (CAMS 1), where the 90th percentile NO_X concentration decreased 34 percent, and the median decreased 42 percent, between 1998 and 2008. The Clinton (CAMS 403) monitor experienced a drop of 16 percent in the 90th percentile, with a 21 percent decrease in the median between 1998 and 2007 (2008 had incomplete data).

To further corroborate these decreases in NO_X, more work will need to be done to investigate the effects of Hurricane Ike on the trends for 2008. Another useful analysis to substantiate the causes of the NO_X trends would be to compare the NO_X trends in HGB to the NO_X trends from other areas, particularly those that have more mobile source oriented NO_X emissions. If NO_X trends in the HGB area are similar to those in areas where NO_X emissions are dominated by mobile sources, then mobile sources could at least partly explain decreases observed in NO_X. If trends in the HGB area are different from other areas, industrial source controls and shut downs would more likely explain the change in NO_X emissions. Another analysis to examine the effects of mobile sources on NO_X emissions would be to look at NO_2/NO_X ratios during pre-rush hour, rush hour, and post-rush hour. Variation in the slopes of these ratios would provide some insight into the decreases observed when mobile emissions should be at their greatest.

Regarding VOC, the 90th percentile total non-methane hydrocarbons (TNMHC) has exhibited a sizeable decrease, from 433 ppbC to 258 ppbC, or roughly 5 percent annually, over the 1997 to 2008 period, but the decline is even sharper, over 8 percent annually, after 2001. Interestingly, in 2008 both median and 90th percentile TNMHC are lowest compared to all other years. Future examination of trends in data collected at VOC canister sites would help validate decreasing trends observed in TNMHC.

NO_X trends from 1991 to 2008, and VOC trends from 1997 to 2008, show most monitors in the HGB area experienced decreases in both median and 90th percentile concentrations. Most strikingly, 2008 experienced not only some of the lowest ozone design values in seventeen years, but also some of the lowest NO_X and VOC values.

An investigation of geographic patterns in ozone revealed that, while ozone concentrations in the HGB area have been decreasing, areas of HGB that experience the highest ozone concentrations remain the same. The highest levels of ozone typically occur in the area near the Houston Ship Channel to the east, and in the area surrounding the Houston Bayland Park (CAMS 53) area to the west. Examining the time of day of peak ozone revealed that the highest ozone concentrations appear to form first in the Houston Ship Channel area, a heavily industrialized area, then are transported to the west, where some of the highest ozone design values occur.

To corroborate these spatial patterns, data from other ozone monitors in the HGB area, those that are not regulatory monitors, should be analyzed. However, before data at these sites can be used, thorough quality assurance methods must be implemented to ensure data is appropriate for technical analysis. To verify that values interpolated between monitors are correct, more robust kriging methods must be investigated. Another informative investigation of ozone trends might also include exploration of transient high ozone events (THOES). Analysis of THOES would corroborate trends observed in spatial ozone gradients.

Similar to ozone, the magnitude of median NO_X has decreased, but areas that experience the highest NO_X concentrations remain the same, with the exception of the area around the Houston Ship Channel. Peak NO_X typically occurs in the downtown area of Houston, which experiences high levels of automobile traffic, and in the Houston Ship Channel industrial zone. The area around the Houston Ship Channel no longer recorded peak median NO_X in 2008. Because of the variety of NO_X sources, there are likely a variety of reasons why NO_X in the HGB area has generally declined. However, it is apparent that NO_X in the heavily industrialized areas of Houston has decreased, and that NO_X emissions in areas with heavy automobile traffic has also

decreased, though to a lesser extent.

Analysis of long-term ambient HRVOC measurements indicated that ethene and propene concentrations in the areas near the 12 HGB auto-GCs decreased across the six-year study period, 2003 – 2008. The decrease seen for ethene agrees with a key finding from the TXAQS II study: that ethene emissions near the Houston Ship Channel have decreased approximately 40 percent from 2000 to 2006 (Cowling et al, 2007). All 12 monitors showed statistically-significant decreases in propene concentrations across the 2003-08 study period, as did seven of 12 for ethene.

When the same long-term data were analyzed by wind direction, decreases in ambient ethene and propene concentrations from certain directions suggest that emissions of these two compounds from important source areas within and near the Houston Ship Channel have decreased across the study period. While meteorology cannot be ruled out as a cause of this trend, the lack of a decrease at the Wallisville Road (CAMS 617) monitor supports the hypothesis that emissions reductions are causing the concentration trends.

Ambient total VOC concentrations have decreased at all twelve study monitors; at eight of these, decreases are statistically significant. Reported point source VOC emissions in the TCEQ annual emission inventory decreased between 2003 and 2006; however, evidence suggests that VOC emissions are so underreported that this cannot realistically be used as evidence of any emissions decrease.

Work was performed that compared emission flux measurements from the Solar Occultation Flux instrument to emissions reported in three EIs: the 2004 Annual EI, the 2006 Hourly EI, and a "hybrid" 2006 Annual/Hourly EI. This comparison found that in the vicinity of Battleground Road, reported emissions for most of the comparison period were much less than any of the six SOF measurements taken in this area, but at times the reported hourly emissions were greater than some of the SOF measurements. However, the reported emissions at the time of, and just preceding, the SOF measurements were considerably less than the fluxes measured by SOF.

The same comparison of emission fluxes in the vicinity of Houston Deer Park (CAMS 35) showed, like Battleground Road, that the hourly reported emissions show tremendous variability, however the peak reported emissions do not come close to the emissions estimated from three SOF measurements taken there. As well, reported hourly emissions at and near the time of the SOF measurements are on the order of 20-fold less than the SOF estimates, but it cannot be determined how much this is attributable to the fact that the hourly EI did not cover all sources.

Several compelling next steps are apparent, following this work. First, it would be valuable to see if HRVOC are contributing as strongly to total reactivity in recent years as they were in 2000, when scientists observed this during the field study. Information on relative contributions of different VOC classes to TNMHC concentration across the study period would be valuable, since the TCEQ HRVOC regulations did not target other VOC classes, and therefore the latter might not be decreasing as much if at all. Also, nearly all wind direction lobes showed relatively strong decreases, and thus high variance, in the 2003 through 2005 period, whereas the succeeding three years seem to show much less variance. These two periods may be statistically different from one another, which would suggest the effectiveness of the HRVOC regulations, but this needs to be quantitatively studied. Finally, the wind direction lobe analysis suggests that Mont Belvieu is distinct from other source areas studied; efforts are currently underway, using resources from several different work groups in the TCEQ, to investigate the causes of this.

Various spatial analyses showed that most areas in HGB are experiencing decreases in not only ozone, but also VOC and NO_X. The Houston Ship Channel, a heavily industrial area which has been shown to be the origin of high ozone, has seen large decreases in both NO_X and VOC, that have undoubtedly contributed largely to the decreases in ozone in the HGB area.

To determine if ozone formation is more sensitive to decreases in NO_X or to decreases in VOC, an analysis of variability by day of the week was performed. This day of the week analysis showed that NO_X concentrations are lower on weekends in the HGB area. Furthermore, the weekend effect observed in "odd oxygen" (O_X) concentrations indicates that ozone titration cannot be considered the dominant reaction affecting weekend ozone in the HGB area and that differences in ozone production rates or radical termination can still be considered a source of the weekend effect in ozone.

Because observed decreases in ozone, NO_X, and VOC could potentially be explained by variations in meteorology that occur in the HGB area from year to year, meteorological parameters were examined in detail. This examination revealed that, while high levels of sunlight and temperature lead to ozone formation, these two parameters do not exhibit high levels of variation from year to year, and temperature and solar radiation observed in 2008 were not statistically different from any other year back to 2000. Further, no trends in morning wind speed, afternoon wind speed, and relative humidity were identified. If trends in meteorological parameters existed, these trends would be expected to correlate with observed downward trends in ozone and precursors; however, this was not the observed scenario in the HGB area.

Higher wind speeds were shown generally to correlate with lower ozone concentrations, due to resulting dilution. Average morning wind speeds in 2008 were 0.9 mph faster than 2007; these higher wind speeds in 2008 may have contributed to lower levels of ozone and its precursors, despite low relative humidity of 59.7 percent (the lowest observed for all years back to 2000); low relative humidity usually signifies higher ozone. Wind speeds comparable to 2008 occurred in 2000, a year that saw a higher ozone design value of 112 ppb, compared to the design value of 91 ppb in 2008. While higher wind speeds appeared to contribute to recent decreases in ozone, it does not appear that the decreasing trend in ozone and its precursors is due only to local meteorological influences.

To substantiate trends observed in ozone and its precursors, more meteorological research will need to be done. Hodograms, which combine wind speeds and wind directions, would be useful for looking at local wind patterns in the HGB area on high ozone days. New methods for removing meteorological variables from ozone trends must be examined in detail to determine if ozone decreases are truly due to emissions or due to changes in meteorology.

Although local emissions and meteorology contribute greatly to elevated ozone concentrations in the HGB area, ozone transported into the area can contribute enough to elevate ozone concentrations well above the federal NAAQS. The need to quantify background ozone, or ozone transported from outside the HGB area, in addition to quantifying local ozone production, is essential given that a large city, such as Houston, regularly generates enough local ozone to exceed the standard when starting from a high background. Background ozone levels traveling into Texas are regularly as high as 60 ppb, and often higher.

Examination of 90^{th} percentile ozone concentrations at selected upwind monitors from 2000 to 2008, with data restricted by wind direction and season of the year, revealed no discernible trend in background ozone over the nine year period observed. Absence of trend simplifies interpretation of influences from background and local components of ambient ozone, as well as computation of benefits of local control strategies. Future investigation into the correlations of ozone concentrations among the selected monitors, and other monitors possibly measuring background ozone in other regions of Texas, would provide further evidence of the stability of background ozone concentrations. Further, such an analysis could isolate the contribution of the Beaumont-Port Arthur area from the contributions of other source regions, to ozone concentrations in the HGB area. Additional investigation into the characteristics of background ozone in East Texas will utilize data collected during the TexAQS II field study.

Investigation of HYSPLIT back trajectories identified likely transport of ozone into Texas on days following elevated ozone episodes in eastern U.S. states. Further examination of state-wide design values for Texas, and eastern states where high ozone likely originates, revealed clear downward trends from 2000 to 2008. This may lead to lower background levels of ozone being transported into Texas from eastern states, but there was insufficient evidence to support this conclusion based on the lack of trend in background ozone values.

Sinuosity of transport winds during 2008 was found to be statistically indistinguishable from other recent years using the Tukey-Kramer multiple means comparison test. The Tukey-Kramer method also confirmed that average 2008 wind trajectory length did not deviate from the typical sinuosity profile of transport winds traversing the HGB area. These analyses showed that transport into Texas, and subsequently the HGB area, was not changing. Further work on sinuosity, however, is necessary to properly link these results to observed ozone concentrations. Additional areas for exploration include a time series investigation of sinuosity by month, and a direct comparison of ozone to sinuosity by year.

Clustering daily back trajectories from May to October, 2000 to 2007, revealed six distinct trajectory clusters in the HGB area. Clusters from the northeast or those which were shorter in length were found to account for not only the highest background ozone concentrations entering into the HGB area, but also the highest maximum ozone concentrations. Clusters that were from the south and southeast occurred on days with the lowest background ozone due to clean air blowing into the HGB area from the Gulf. A regression analysis showed that back trajectories can account for around 24 ppb of variation in background concentrations, and around 30 ppb in variation in maximum ozone concentrations.

These background and transport analyses show that efforts focused solely on controlling local emissions may be insufficient to bring Houston into ozone attainment, given that, on many days, background estimates are well over half the eight-hour ozone NAAQS of 85 ppb.

Taken together, the components of this Houston Conceptual Model lay the theoretical foundation for development, testing and implementation of the Houston photochemical model. Improvements to theoretical understanding provide a basis for evaluating and improving the photochemical model, with the ultimate goal of predicting and reducing ozone pollution in the HGB area. Evidence presented throughout this document supports the conclusion that decreasing trends in measured ozone concentrations are largely a result of real, quantifiable reductions in precursor emissions, and, although meteorology might have accounted for the lower values observed in 2008, the decreases are not solely due to anomalous meteorological conditions that are unlikely to recur.

CHAPTER 7: REFERENCES

Allen, D., T. Thompson, and E. McDonald-Butler. 2005. Analyses of Emission Reduction Strategies for Attaining the National Ambient Air Quality Standard for Ozone (with concentrations averaged over 8 hours) in the Perimeter Counties of the Houston-Galveston Brazoria Area: Phase I Report, 9/20/2005.

Allen, D., E. McDonald-Butler, T. Thompson, and A. Webb. 2006. Analyses of Emission Reduction Strategies for Attaining the National Ambient Air Quality Standard for Ozone (with concentrations averaged over 8 hours) in the Perimeter Counties of the Houston-Galveston Brazoria Area: Phase II Report, 2/1/2006.

Allen, D. 2006. Analyses of Emission Reduction Strategies for Attaining the National Ambient Air Quality Standard for Ozone (with concentrations averaged over 8 hours) in the Perimeter Counties of the Houston-Galveston Brazoria Area: Phase III Report, 7/10/2006.

Banta, R.M., C.J. Senff, J. Nielson-Gammon, L.S. Darby, T.B. Ryerson, R.J. Alvarez, S.P. Sandberg, E.J. Williams, and M. Trainer. 2005. A Bad Air Day in Houston. *Bulletin of the American Meteorological Society*, 86(5): 657-669.

Bell, M. L., A. McDermott, S. L. Zeger, J. M. Samet, and F. Domenici. 2004: Ozone and short-term mortality in 95 US urban communities. *J. Amer. Med. Assoc.,* **292,** 2372-2378.

Berkowitz, C. M., C. W. Spicer, and P. V. Doskey. 2005. Hydrocarbon observations and ozone production rates in Western Houston during the Texas 2000 Air Quality Study. *Atmospheric Environment,* **39**, 3383–3396.

Berkowitz, C. M., T. Jobson, G. Jiang, C. W. Spicer, and P. V. Doskey. 2004. Chemical and meteorological characteristics associated with rapid increases of O3 in Houston, Texas. *J. of Geophysical Research*, **109**, doi:10.1029/2004JD004141, 2004.

Blanchard, C., S. Tanenbaum, and D. Lawson. 2008. Differences between weekday and weekend air pollutant levels in Atlanta; Baltimore; Chicago; Dallas-Fort Worth; Denver; Houston; New York; Phoenix; Washington, DC; and surrounding areas. J. Air & Waste Manage. Assoc., 58: 1598-1615.

Blanchard, C. and S. Tanenbaum. 2005. Weekday/weekend differences in ambient concentrations of primary and secondary air pollutants in Atlanta, Baltimore, Chicago, Dallas-Fort Worth, Denver, Houston, New York, Phoenix, Washington, and surrounding areas, Final Report, NREL Project ES04-1, May 16, 2005.

Breitenbach et al. 2002. *Conceptual Model for Ozone Formation in the Houston-Galveston Area*, Appendix A to Phase I of the Mid Course Review Modeling Protocol and Technical Support Document, Technical Analysis Division, TCEQ, December 13, 2002.

Brown et al. 2002. *Preliminary characterization of 2001 event-triggered VOC and carbonyl samples*. STI-900680-2188-IR. Prepared by Steven G. Brown, Paul T. Roberts, Jason A. Roney of Sonoma Technology, Inc. Prepared for Erik Gribbin, Texas Natural Resources Conservation Commission, July 17, 2002.

Brown, S., and H. Hafner Main. 2002. Acquisition, review and analysis of auto-GC VOC data in the Houston area, 1998-2001: Final report. STI-900670-2224-FR. Prepared by Steven G. Brown and Hilary Hafner Main, Sonoma Technology, Inc, for Texas Natural Resource Conservation Commission, July 31, 2002.

Buzcu-Guven, B., M. P. Fraser. 2008. Comparison of VOC emissions inventory data with source apportionment results for Houston, TX, *Atmos. Environ.*, **42**, 5032-5043.

Buzcu, B., and M. P. Fraser. 2006. Source identification and apportionment of volatile organic compounds in Houston, TX, *Atmos. Environ.*, **40**, 2385-2400.

Brown, S., and H. Hafner Main. 2002. Acquisition, review and analysis of auto-GC VOC data in the Houston area, 1998-2001: Final report. STI-900670-2224-FR. Prepared by Steven G. Brown and Hilary Hafner Main, Sonoma Technology, Inc, for Texas Natural Resource Conservation Commission, July 31, 2002.

Camalier, L., W. Cox, and P. Dolwick. 2007. The effects of meteorology on ozone in urban areas and their use in assessing ozone trends. *Atmos. Environ.*, **41**, 7127–7137.

Cooper, O. R., et al. 2006. Large upper tropospheric ozone enhancements above midlatitude North America during summer: In situ evidence from the IONS and MOZAIC ozone measurement network, J. Geophys. Research, 111: D24S05, doi:10.1029/2006JD007306.

Cowling, E. B., C. Furiness, B. Dimitriades, and D. Parrish. 2007. Final Rapid Science Synthesis Report: Findings from the Second Texas Air Quality Study (TexAQS II). TCEQ Contract No. 582-4-65614, 31 August 2007. Accessed January 6, 2009, at http://www.tceq.state.tx.us/assets/public/implementation/air/am/texaqs/rsst_final_report.pdf

Cox, W. M., and S.-H. Chu. 1993. Meteorologically Adjusted Ozone Trends in Urban Areas: A Probabilistic Approach, *Atmos. Environ*., **27B**, 425-434.

Croes, B. et al. (2003), The O3 "weekend effect" and NOx control strategies: Scientific and public health findings and their regulatory implications. EM, pp. 27-35, July 2003.

Davis, J.M., B.K. Eder, D. Nychka, and Q. Yang. 1998. Modeling the Effects of Meteorology on Ozone in Houston Using Cluster Analysis and Generalized Additive Models. *Atmos. Environ*., **32**, 2505-2520.

Darby, L.S. 2005. Cluster Analysis of Surface Winds in Houston, Texas, and the Impact of Wind Patterns on Ozone. *J. Appl. Meteor.*, **44**, 1788–1806.

Daum, P.H., L. I. Kleinman, S. R. Springston, L. J. Nunnermacker, Y.-N. Lee, J. Weinstein-Lloyd, J. Zheng, and C. M. Berkowitz. 2003. A comparative study of O3 formation in the Houston urban and industrial plumes during the 2000 Texas Air Quality Study. *J. of Geophys. Res.*, **108**, 4715, doi:10.1029/2003JD003552.

Daum, P.H., L. I. Kleinman, S. R. Springston, L. J. Nunnermacker, Y.-N. Lee, J. Weinstein-Lloyd, J. Zheng, and C. M. Berkowitz. 2004a. Origin and properties of plumes of high ozone observed during the Texas 2000 Air Quality Study (TexAQS 2000). *J. of Geophys. Res.*, **109**, D17306, doi:10.1029/2003JD004311.

Daum, P.H., and L. I. Kleinman. 2004b. Ambient Hydrocarbons in the Houston Metropolitan Area During TexAQS 2000: An Identification of Unusual Features. Prepared for Houston Advanced Research Center for project H20, December 5, 2004.

Davis, J. M., B. K. Eder, D. Nychka, Q. Yang. 1998. Modeling the effects of meteorology on ozone in Houston using cluster analysis and generalized additive models, *Atmospheric Environment*, Volume 32, Issues 14-15, August 1998, Pages 2505-2520.

Draxler, R. 2000. Meteorological Factors of Ozone Predictability at Houston, Texas. *J. Air. and Waste Manage. Assoc*., **50**, 259-271.

Estes, M., S. Wharton, D. Boyer, Z. Fang, J. Smith, S. McDowell, F. Mercado, J. Neece, E. Gribbin, and J. Price. 2002. *Analysis of Automated Gas Chromatograph Data from 1996-2001 to determine VOCs with largest ozone formation potential.* Houston-Galveston-Brazoria Ozone SIP Revision Technical Support Document, Attachment 6, adopted by the TCEQ on December 12, 2002. pp. 50. http://www.tceq.state.tx.us/assets/public/implementation/air/am/docs/hgb/tsd1/attachment6-agc_voc.pdf .

Fang, Z., and S. McDowell. 2003. Analysis of canister data for the Houston-Galveston and Beaumont-Port Arthur areas. Houston-Galveston-Brazoria Ozone Mid-Course Review SIP Revision, Appendix CC of Chapter 4, pp. 15. http://www.tceq.state.tx.us/assets/public/implementation/air/sip/sipdocs/2004-05-HGB/04042sipapcc.pdf . Figures for Appendix CC: http://www.tceq.state.tx.us/assets/public/implementation/air/sip/sipdocs/2004-05-HGB/04042sipapccfigs.zip .

Faraji, M., Y. Kimura, E. McDonald-Buller, and D.T. Allen. 2008. Comparison of the Carbon Bond and SAPRC photochemical mechanisms under conditions relevant to southeast Texas. *Atmos. Environ.*, **42**, 5821-5836.

Fujita, E., et al. 2003a. Evolution of the magnitude and spatial extent of the weekend ozone effect in California's South Coast Air Basin, 1981-2000. *J. Air & Waste Manage. Assoc*., **53**, 802-815.

Fujita, E., et al. 2003b. Diurnal and weekly variations in the source contributions of ozone precursors in California's South Coast Air Basin. *J. Air & Waste Manage. Assoc*., **53**, 844-863.

Gao, O. H., B. A. Holmen, D. A. Niemeier. 2005. Nonparametric factorial analysis of daily weigh-in-motion traffic: implications for the ozone 'weekend effect' in Southern California, *Atmos. Environ*., **39**, 1669-1682.

Hafner Main, H., T. O'Brien, C. Hardy, S. Wharton, D. Sullivan. 2001. *Characterization of auto-GC data in Houston*, prepared for Jim Price of the Texas Natural Resource Conservation Commission, August 31, 2001, pp. 81. http://www.tceq.state.tx.us/assets/public/implementation/air/am/contracts/reports/da/CharacterizationAutoGCdata.pdf

Hafner, H., and Brown. 2003. *Exploratory Source Apportionment of Houston's Clinton Drive Auto-GC 1998-2001 Data*. Prepared for Erik Gribbin, Texas Commission on Environmental Quality, May 15, 2003, pp. 144. http://www.tceq.state.tx.us/assets/public/implementation/air/am/contracts/reports/da/Source_Apportionment_of_AutoGC_Data.pdf

Heck, W.W., W.W. Cure, J.O. Rawlings, L.J. Zaragosa, A.S. Heagle, H.E. Heggestad, R.J. Kohut, L.W. Kress, and P.J. Temple. 1984. Assessing impacts of ozone on agricultural crops: crop yield functions and alternative exposure statistics. *J. Air Pollut. Control Ass*., **34**, 810-817.

Henry, R.C., C.H. Spiegelman, J.F. Collins, and E. Park. 1997. Reported emissions of organic gases are not consistent with observations. *Proc. Natl. Acad. Sci. USA*, **94**, 6596–6599.

Heuss et al. 2003. Weekday/weekend ozone differences: What can we learn from them? *J. Air & Waste Manage. Assoc.*, **53**, 772-788.

Jobson et al., 2004. Hydrocarbon source signatures in Houston, Texas: Influence of the petrochemical industry. 2004. *J. Geophys. Res*. **109**, D24305, doi:10.1029/2004JD004887.

Jolly, J., and E. Schroeder. 2004. Analysis of Houston-Galveston Area Enhanced Industry-Sponsored Monitoring (EISM) data. Presentation at EISM Network Stakeholders meeting, Houston, Texas, February 19, 2004.

Jolly, J., S. McDowell, B. Kurka, F. Mercado, J. Neece, and G. Cantú. 2003. *Analyzing VOC reactivity in Houston*. December 13, 2003. Houston-Galveston-Brazoria Ozone Mid-Course Review SIP Revision, Appendix GG of Chapter 4, adopted December 1, 2004, pp. 36. http://www.tceq.state.tx.us/assets/public/implementation/air/sip/sipdocs/2004-05-HGB/04042sipapgg_pro.pdf .

Jolly, J. 2003. Assessing the importance of carbonyl compounds in ozone formation in Houston-Galveston: Relative reactivities of carbonyl and hydrocarbon species. May 2003, updated May 3, 2004. Houston-Galveston-Brazoria Ozone Mid-Course Review SIP Revision, Appendix EE of Chapter 4, pp. 13. http://www.tceq.state.tx.us/assets/public/implementation/air/sip/sipdocs/2004-05-HGB/04042sipapee_pro.pdf . See also the figures for Appendix EE.

Karl et al., 2004

Karl, T., T. Jobson, W. C. Kuster, E. Williams, J. Stutz, R. Shetter, S. R. Hall, P. Goldan, F. Fehsenfeld, and W. Lindinger. 2003. Use of proton transfer-reaction mass spectrometry to characterize volatile organic compound sources at the La Porte super site during the Texas Air Quality Study 2000. *J. of Geophys. Res.*, **108**, 4508, doi:10.1029/2002JD003333, 2003.

Kim, E., S. G. Brown, H. R. Hafner, P. K. Hopke. 2005. Characterization of non-methane volatile organic compounds sources in Houston during 2001 using positive matrix factorization, *Atmos. Environ.*, **39**, 5934-5946.

Kleinman, L. I., P. H. Daum, Y.-N. Lee, L. J. Nunnermacker, S. R. Springston, J. Weinstein-Lloyd, and J. Rudolph. 2005. A comparative study of ozone production in five U.S. metropolitan areas, *J. Geophys. Res*., **110**, D02301, doi:10.1029/2004JD005096.

Kleinman, L. I., P.H. Daum, D. Imre, Y. Lee, L.J. Nunnermacker, and S.R. Springston. 2002. Ozone production and hydrocarbon reactivity in 5 urban areas: A cause of high ozone concentration in Houston. *Geophysical Research Letters*, **30**, 1639-1642.

Langford, A. O., C. J. Senff, R.M. Banta, R.M. Hardesty, R.J. Alvarez II, S. P. Sandberg, and L. S. Darby. 2009. Regional and local background ozone in Houston during TexAQS 2006, *J. Geophys. Res.,* doi:10.1029/2008JD011687, in press. (accepted 24 April 2009).

Lawson, D. R. 2003. The weekend ozone effect—The weekly ambient emissions control experiment, EM, pp. 17-25, July 2003.

Marr, L., and R. Harley. 2002. Modeling the effect of weekday-weekend differences in motor vehicle emissions on photochemical air pollution in central California, **Environ. Sci. Technol**., **36**, 4099-4106.

Mellqvist, J., J. Johansson, J. Samuelsson, C. Rivera, B. Lefer, and S. Alvarez. 2008. Comparison of Solar Occultation Flux Measurements to the 2006 TCEQ Emission Inventory and Airborne Measurements for the TexAQS II. TCEQ Grant No. 2008-24.

Melqvist, J., J. Samuelsson, C. Rivera, B. Lefer, and M. Patel. 2007. *Measurements of industrial emissions of VOCs, NH3, NO2 and SO2 in Texas using the Solar Occultation Flux method and mobile DOAS*, Final Report HARC project H-53, August 20, 2007. http://www.tercairquality.org/AQR/Projects/H053.2005

Morris G. A., et al. 2006. Alaskan and Canadian forest fires exacerbate ozone pollution over Houston, Texas, on 19 and 20 July 2004, *J. Geophys. Res.*, 111, D24S03, doi:10.1029/2006JD007090.

Murphy, et al. 2007. The weekend effect within and downwind of Sacramento—Part 1: Observations of ozone, nitrogen oxides, and VOC reactivity. *Atmos. Chem. Phys*., **7**, 5327-5339.

National Academy of Sciences. 1991. *Rethinking the Ozone Problem in Urban and Regional Air Pollution.* National Academies Press, 524 pp.

Ngan, F. and D. Byun. 2008. *The analysis of ozone dependence on synoptic weather patterns*, presented at the 7th Annual Community Model and Analysis System Conference, October 6, 2008. http://www.cmascenter.org/conference/2008/slides/ngan_analysis_ozone_cmas08.ppt

Nielsen-Gammon, J.W., J. Tobin, and A. McNeel. 2005. A Conceptual Model for Eight-Hour Ozone Exceedances in Houston, Texas, Part II: Eight-Hour Ozone Exceedances in the Houston-Galveston Metropolitan Area, January 29, 2005. http://files.harc.edu/Projects/AirQuality/Projects/H012.2004/8HRA/H12-8HRA-FinalReport2.pdf

Nielsen-Gammon, J.W., C.L. Powell, M.J. Mahoney, W.M. Angevine, C. Senff, A. White C. Berkowitz, C. Doran, and K. Knupp. 2007. Multisensor Estimation of Mixing Heights over a Coastal City. J. Applied Meteorology and Climatology, **47**, 27–43.

Pitchford, M.L., et al. 2004. Big Bend Regional Aerosol and Visibility Observational (BRAVO) Study. NPS, EPA, TCEQ, NOAA, and EPRI.

Pun, B. K., et al. 2003. Day-of-week behavior of atmospheric ozone in three U.S. cities, *J. Air & Waste Manage. Assoc.*, **53**, 789-801.

Rao, S.T., I.G. Zurbenko, R. Neagu, P.S. Porter, J.Y. Ku, and R.F. Henry. 1997. Space and Time Scales in Ambient Ozone Data. *Bull. Amer. Meteorological Soc*., **78**, 2153-2166.

Rapid Science Synthesis Team. 2006. Final Rapid Science Synthesis Report: Findings from the Second Texas Air Quality Study (TexAQS II), A Report to the Texas Commission on Environmental Quality, *2006 Texas Air Quality Study*.

Rappenglück B., R. Perna, S. Zhong, G. A. Morris. 2008. An analysis of the vertical structure of the atmosphere and the upper-level meteorology and their impact on surface ozone levels in Houston, Texas, *J. Geophys. Res*., 113, D17315, doi:10.1029/2007JD009745.

Robinson, R., T. Gardiner, and B. Lipscombe. 2008. *Measurements of VOC emissions from petrochemical industry sites in the Houston area using Differential Absorption Lidar*

(DIAL) during summer 2007, Draft. Submitted to Russell Nettles, TCEQ, by Rod Robinson, Tom Gardiner, and Bob Lipscombe of the National Physical Laboratory, Teddington, Middlesex UK TW11 0LW, February 8, 2008, pp. 86.

Ryerson, T.B.; M. Trainer, W.M. Angevine, C.A. Brock, R.W. Dissly, F.C. Fehsenfeld, G.J. Frost, P.D. Goldan, J.S. Holloway, G. Hu¨bler, R.O. Jakoubek, W.C. Kuster, J.A. Neuman, D.K. Nicks Jr., D.D. Parrish, J.M. Roberts, D.T. Sueper, E.L. Atlas, S.G. Donnelly, F. Flocke, A. Fried, W.T. Potter, S. Schauffler, V. Stroud, A.J. Weinheimer, B.P. Wert, C. Wiedinmyer, R.J. Alvarez, R.M. Banta, L.S. Darby, and C.J. Senff. 2003. Effect of petrochemical industrial emissions of reactive alkenes and NOx on tropospheric ozone formation in Houston, Texas. *J. Geophys. Res*., **108**(D8), 4249, doi:10.1029/2002JD003070.

Savanich, K., and N. George. 2007. Day of the Week Patterns in Ambient Ozone and NO_X in HGB and DFW. Presentation at EPA Region 6 Quality Assurance Conference, Dallas, Texas, October, 2007.

Savanich, K. 2006. Ozone Exceedance Days as a Function of the Number of Monitors, TCEQ, February, 2006.

Seinfeld, J., 1994. Rethinking the Ozone Problem in Urban and Regional Air Pollution, National Research Council.

Senff, C.J.; R.M. Banta, L. Darby, W. Angevine, A. White, C. Berkowitz, and C. Doran. 2002. Spatial and Temporal Variations in Mixing Height in Houston. TNRCC Project F-20. http://www.tceq.state.tx.us/assets/public/implementation/air/am/contracts/reports/mm/Mixing_Height_Variations_Houston.pdf .

Smith, J. and J. Jarvie, 2008, Reconciling reported VOC emissions with ambient measurements, continued. Presented at Southeast Texas Photochemical Modeling Technical Committee Meeting, February 12, 2008, http://www.tceq.state.tx.us/assets/public/implementation/air/am/committees/pmt_set/20080212/20080212-smith-voc_emissions_ambient_measurements.pdf .

Sullivan, D. 2009. Effects of Meteorology on Pollutant Trends. Final Report to TCEQ. Grant Activities No. 582-5-86245-FY08-01. Prepared by Dave Sullivan, University of Texas at Austin Center for Energy and Environmental Resources, Prepared for Kasey Savanich, for the Texas Commission on Environmental Quality, March 16, 2009. http://www.tceq.state.tx.us/assets/public/implementation/air/am/contracts/reports/da/582058624 5FY0801-20090316-ut-met_effects_on_pollutant_trends.pdf

Texas Commission on Environmental Quality. 2009. 2006 Annual Emission Inventory, extracted from STARS database February 27, 2009.

Texas Commission on Environmental Quality. 2006. Houston-Galveston-Brazoria Nonattainment Area Ozone Conceptual Model, Chapter 4 § Mean, Time Resolved Surface Winds, pp. 4-6f.

Texas Commission on Environmental Quality. 2004. Subchapter H: Highly-Reactive Volatile Organic Compounds, 30 TAC § 115.720, 115.722, 115.725 – 115.727, 115.729, adopted December 23, 2004.

Texas Commission on Environmental Quality. 1999. Emission Inventory Requirements, Texas Register §101.10, adopted March 30, 1999.

U.S. Environmental Protection Agency. 2008. National Ambient Air Quality Standards for Ozone, Title 40 Code of Federal Regulations, Parts 50 and 58.

U.S. Environmental Protection Agency. 2006. Air Quality Criteria for Ozone and Related Photochemical Oxidants, EPA 600/R-05/004aF.

U.S. Environmental Protection Agency. 2005. Identification of Areas for Which the 1-Hour Standard Has Been Revoked and Technical Correction to Phase 1 Rule, Title 40 Code of Federal Regulations, Parts 50 and 81.

Wert et al., 2003. Signatures of terminal alkene oxidation in airborne formaldehyde measurements during TexAQS 2000. Journal of Geophysical Research, VOL. 108, NO. D3, 4104, doi:10.1029/2002JD002502, 2003.

Westenbarger, D.A., and G. B. Frisvold. 1994. Agricultural exposure to ozone and acid precipitation. *Atmos. Environ*., **28**, 2895-2908.

Wittig, A. E., and D. T. Allen. 2007. Improvement of chemical mass balance model for apportioning ambient sources of non-methane hydrocarbons using composite aged source profiles, *Atmos. Environ.*. doi:10.1016/j.atmosenv.2007.10.072

Xie, Y., and C. M. Berkowitz. 2007. The use of conditional probability functions and potential source contribution functions to identify source regions and advection pathways of hydrocarbon emissions in Houston, Texas, *Atmos. Environ.*, **41**, 5831-5847.

Xie, Y., and C. M. Berkowitz. 2006. The use of positive matrix factorization with conditional probability functions in air quality studies: An application to hydrocarbon emissions in Houston, Texas, *Atmos. Environ.*, **40**, 3070-3091.

Xie, Y., and C. M. Berkowitz. 2005. Source attribution and emission adjustment study: Task 1. Back trajectory climatology and identification of key source regions. 10 January 2005. http://www.tceq.state.tx.us/assets/public/implementation/air/am/contracts/reports/ei/Source_Attribution_and_Emission_Adjustment_Study_Task1.pdf

Yarwood, G., et al. 2003. Modeling weekday/weekend ozone differences in the Los Angeles region for 1997, *J. Air & Waste Manage. Assoc*., 53, 864-875.

Yarwood, G., J. Grant, B. Koo, A. M. Dunker. 2008. Modeling weekday to weekend changes in emissions and ozone in the Los Angeles basin for 1997 and 2010, *Atmos. Environ*., **42**, 3765-3779.

Zhang, J., and S.T. Rao. 1999. The Role of Vertical Mixing in the Temporal Evolution of Ground-Level Ozone Concentrations. *J. Applied Meteorology*, **38**, 1674-1691.

Zhao W., P. Hopke, and T. Karl. 2003. Source identification of volatile organic compounds in Houston, Texas. *Environ. Sci. Technol.* **38**, 1338-1347.